Nonnegative Dynamics in Nonlocal Models
Reaction Networks and Spatial Extensions

PhD Dissertation

Author:

Mihály András Vághy

Thesis Supervisor:

Dr. Mihály Kovács, DSc

Thesis Co-supervisor:

Dr. Gábor Szederkényi, DSc

Pázmány Péter Catholic University

Faculty of Information Technology and Bionics

Roska Tamás Doctoral School of Sciences and Technology

2025

Abstract

In this dissertation we investigate the interplay between structure, dynamics, and stability in nonnegative and kinetic systems, with a particular focus on chemical reaction networks (CRNs), nonlocal conservation laws, and quantum graph models.

In the first part, we study delayed CRNs beyond mass-action kinetics, focusing on complex balanced systems. We show that, under suitable conditions, these networks retain asymptotic stability w.r.t. the positive stoichiometric compatibility classes.

Then we analyze a class of multidimensional nonlocal pair-interaction models, proving well-posedness via semigroup theory. This contributes to the mathematical foundation of nonlocal conservation laws, generalizing earlier one-dimensional results.

Subsequent chapters investigate how these nonlocal models give rise to discrete CRNs through finite volume discretization. We examine ribosome flow models (RFMs) and their generalizations, establishing persistence and stability properties under broad assumptions. We also analyze a nonlocal partial integro-differential equation modeling gene regulatory networks, showing how discretization aids not only in efficient simulation but also in qualitative analysis.

Finally, we consider quantum graphs as a spatially refined extension of compartmental models, where transitions are governed by partial differential equations along edges. We design an efficient simulation strategy based on a nonoverlapping domain decomposition method, enabling scalable numerical solutions and setting the stage for future control and inverse problems.

Acknowledgements

I am deeply grateful to my thesis advisors, Prof. Mihály Kovács and Prof. Gábor Szederkényi, for their support and guidance throughout my studies. Their insights have shaped my thinking in essential ways, and I especially thank them for allowing my own curiosity to guide the direction and development of this dissertation.

I am thankful to Balázs Kulcsár, Stig Larsson, Adam Andersson, Annika Lang, Irene Otero-Muras, Balázs Farkas and Maria López-Fernández for generously inviting me to their respective universities. These visits sparked insightful conversations and helped broaden my research perspectives.

I thank my family and friends for their encouragement troughout the years. I thank my doctoral fellows, especially Máté Geng, for the stimulating discussions. I thank Péter Polcz and Gergely Szlobodnyik for their careful supervision at the beginning of my academic journey. I thank many other academics for the fruitful discourses. I thank Gergely Kiss, Csongor Loránd Laczkó, Ágoston Paless, Máté András Száraz and several other students I had the privilege to supervise. Their questions, insights, and enthusiasm contributed in many small but meaningful ways to my work.

Last but not least, I would like to thank the reviewers for their insightful comments.

Finally, I acknowledge the support of the following grants:

1. Grants no. 131545 and 145934 of the Hungarian National Research, Development and Innovation Office (NKFIH).

2. ÚNKP-21-3-I-PPKE-60, ÚNKP-22-3-I-PPKE-72 and ÚNKP-23-3-II-PPKE-81 National Excellence Programs of the Ministry for Innovation and Technology from the source of the National Research, Development and Innovation Fund.

3. EKÖP-24-3-II-PPKE-134 University Research Scholarship Program of the Ministry for Culture and Innovation from the source of the National Research, Development and Innovation Fund.

Contents

List of Acronyms

Acronym	Meaning	First occurrence
ODE	Ordinary Differential Equation	p. 1
CRN	Chemical Reaction Network	p. 2
CRNT	Chemical Reaction Network Theory	p. 2
RFM	Ribosome Flow Model	p. 2
PIDE	Partial Integro-Differential Equation	p. 4
PDE	Partial Differential Equation	p. 59
RFMLK	Ribosome Flow Model with Langmuir Kinetics	p. 60
TASEP	Totally Asymmetric Simple Exclusion Process	p. 64
LWR	Lighthill-Whitham-Richards	p. 67
CFL	Courant-Friedrichs-Lewy	p. 69
TVD	Total Variation Diminishing	p. 69
RFMR	Ribosome Flow Model on a Ring	p. 79
ISS	Input-to-State Stable	p. 89
LTV	Linear Time-Varying	p. 91
GRFM	Generalized Ribosome Flow Model	p. 100
GRN	Gene Regulatory Networks	p. 103
FVM	Finite Volume Method	p. 104
PDF	Probability Density Function	p. 106
CME	Chemical Master Equation	p. 122
PID	Proportional-Integral-Derivative	p. 125
FETI	Finite Element Tearing and Interconnecting	p. 133
FEM	Finite Element Method	p. 133
PCG	Preconditioned Conjugate Gradient	p. 143

Chapter 1

Introduction

1.1 Nonnegative and kinetic systems

Nonnegative systems form an important subclass within dynamical systems, characterized by the invariance of the nonnegative orthant with respect to the dynamics. Their theoretical development is motivated by applications in chemistry, biology, population and disease dynamics, where state variables in their original physical coordinates are naturally nonnegative [1].

Compartmental models describe the distribution and transport of entities (for example molecules, particles, vehicles, people, or information) among distinct storage compartments over time [1, 2]. These compartments may represent physically separate subsystems, such as interconnected containers, or conceptual states, such as different stages of a disease in epidemiological models [3]. Accordingly, the applicability of compartmental systems is rather wide including (bio)chemistry, pharmacokinetics, ecological, epidemiological and transportation modeling [4]. Since the state variables in compartmental systems correspond to amounts, concentrations, or numbers of molecules, these models inherently belong to the nonnegative system class [5, 6].

The fundamental properties of compartmental models have been extensively studied, particularly regarding observability, controllability, realizability, and identifiability [7]. Linear compartmental ODEs and their analytic solutions have been analyzed in kinetic contexts [8], while qualitative properties of general nonlinear compartmental models, including equilibrium structures and stability, are discussed in [9]. The strong descriptive power of compartmental models allows them to represent numerous complex dynamical phenomena [10, 7]. Their associated directed graph structures (compartmental graphs) provide insights into dynamical properties [9, 11]. The mathematical theory of compart-

mental matrices and their dynamics is detailed in [2, 12, 13, 14].

An important related family of models is the class of chemical reaction networks (CRNs) or kinetic systems. CRNs are dynamical models formally represented by transformations (reactions) between abstract chemical complexes [15, 16]. While originating in physical chemistry, CRNs have been mathematically generalized [17, 18, 19], broadening their applicability to non-chemical processes. The scope of reaction networks reaches far beyond the (bio)chemical application field, since they can be considered as general descriptors of nonlinear dynamics capable of producing complex dynamical phenomena such as multiple equilibria, nonlinear oscillations, limit cycles, and even chaos [20]. Many compartmental models, such as those used in population dynamics or epidemiology, can naturally be represented in kinetic form, and other non-chemically motivated models can often be algorithmically transformed into reaction networks [21, 22].

Chemical reaction network theory (CRNT) provides deep results on the relationship between network structure and qualitative dynamics [23]. A central problem in CRNT is persistence analysis, which is crucial for proving the global asymptotic stability of complex balanced networks in which, at equilibrium, the total rate of reactions entering each complex equals the total rate leaving it [24, 25, 26]. Stability in mass-action CRNs is typically analyzed using entropy-like logarithmic Lyapunov functions [27]. A major conjecture in CRNT, the "Global Attractor Conjecture," asserts that complex balanced kinetic systems are globally stable within the nonnegative orthant [26]. This was proven for networks with a single connected reaction graph component [24]. Related stability results for zero-deficiency networks extend beyond mass-action kinetics, allowing time-varying rate coefficients and generalized Lyapunov functions [28]. The stability analysis of ribosome flow models (RFMs) via CRN representation has also been identified as an important research direction [29, 30].

1.2 Conservation laws

Local conservation and balance laws have been widely applied in aerodynamics, Eulerian gas dynamics [31], traffic modeling [32, 33], pedestrian flows [34], and ribosome flows [35]. Recently, nonlocality has been incorporated into these models to capture more realistic dynamics. A common approach is to define a nonlocal velocity using a spatial convolution, which has been applied to supply chain modeling [36, 37, 38] and traffic flows [39]. However, some nonlocal models fail to preserve monotonicity or violate the maximum principle. Alternative formulations using integral kernels have been explored

to address these issues [40, 41, 42]. Peridynamics and other spatial nonlocal models have also been developed [43, 44, 45]. A key advantage of nonlocal pair-interaction models is their reduction to local counterparts as the nonlocal horizon vanishes [46], which is not always true for other nonlocal models [47]. Due to these advantages, nonlocal models are widely applied in peridynamics [48, 49] and in the formulation of the nonlocal Allen-Cahn equation [50].

1.3 Quantum graphs

In recent decades differential operators on metric graphs, often called quantum graphs, have found a myriad of applications when describing quasi-one-dimensional phenomena in a broad range of fields, such as superconductivity in granular materials [51], classical wave propagation in wave guide networks [52, 53], membrane potential of neurons [54], cell differentiation [55], and optimal control [56, 57, 58, 59]. These applications can be seen, from a modelling point of view, as compartmental models, where the transitions are explicitly described by partial differential equations.

1.4 Aims and scope of the dissertation

Based on the above, the aims of my doctoral research are:

- Investigate the stability of delayed complex balanced CRNs with non-mass action kinetics. Our hypothesis was that asymptotic stability w.r.t. the positive stoichiometric compatibility classes can be derived, as in the mass action case. The results are presented in Chapter 2.

- Prove the well-posedness of the multidimensional nonlocal pair-interaction via semigroup theory. While well-posedness in one-dimension was proved in [60] with a different method, the existence of an underlying operator semigroup is an important advancement, as well as the generalization to multiple dimensions. The results are presented in Chapter 3.

- Investigate the persistence and stability of ribosome flows, obtained through finite volume discretization of the nonlocal pair-interaction model, as well as their generalizations. We generalize both in terms of structure and transition rate functions. The results are presented in Chapter 4.

- Investigate the finite volume discretization of the partial integro-differential equation (PIDE) model of gene regulatory networks, another nonnegative nonlocal conservation law. While the main motivation was an efficient simulation technique, the discretization turns out to be benefitial for qualitative analysis too. The results are presented in Chapter 5.

- Design an efficient simulation for quantum graphs in the form of a nonoverlapping domain decomposition method. The results are presented in Chapter 6.

Chapter 2

Asymptotic stability of delayed complex balanced reaction networks with non-mass action kinetics

In this chapter we consider delayed chemical reaction networks with non-mass action monotone kinetics and show that complex balancing implies that within each positive stoichiometric compatibility class there is a unique positive equilibrium that is locally asymptotically stable relative to its compatibility class. The main tools of the proofs are respectively a version of the well-known classical logarithmic Lyapunov function applied to kinetic systems and its generalization to the delayed case as a Lyapunov-Krasovskii functional. Finally, we demonstrate our results through illustrative examples.

2.1 Introduction

Stability is a key qualitative property of dynamical models and their equilibria. In [27], the local stability of complex balanced equilibria of kinetic systems was shown using an entropy-like logarithmic Lyapunov function. The most well-known stability-related result in CRNT is probably the Deficiency Zero Theorem which states that weakly reversible deficiency zero CRNs are complex balanced independently of the (positive) values of reaction rate coefficients [61]. According to the Global Attractor Conjecture, the stability of complex balanced networks is actually global within the nonnegative orthant [26, 24]. The stability of a wide class of CRNs with more general kinetics than mass action was shown in [62]. These results were further extended in [28] for time-varying reaction rates using the notion of input-to-state stability.

The explicit modeling of time delays is often necessary to understand complex dynamical phenomena in nature or technology, and to build models having sufficient level of reliability [63]. Various phenomena may justify the inclusion of time delays into dynamical models such as protein expression time in systems biology [64], hatching or maturation time in population dynamics [65], driver reaction times in traffic flow models [66], latent periods in epidemic modeling [67], or communication and feedback delays in complex networks [68]. The most commonly used approach in the stability analysis of time-delay systems is the construction of appropriate Lyapunov-Krasovskii functionals which is generally a challenging problem [69].

The main motivation for introducing delayed chemical reactions was to focus on the most important species and chemical transformations, and to avoid the detailed description of mechanisms of less interest [70]. In delayed reactions, the consumption of reactant species is immediate, while the formation of products is delayed either through discrete or distributed delays. The notion of stoichiometric compatibility classes was generalized for delayed mass action CRNs in [71], and it was proved using a logarithmic Lyapunov-Krasovskii functional that complex balanced networks are at least locally stable for arbitrary finite delays. An analogous result for kinetic systems with distributed delays was given in [72]. In [73] the authors introduced the notion of stoichiometric compatibility classes for arbitrary delayed CRNs and proved the generalization of well-known persistence results [74, 75] to the delayed case. In [76] the authors prove a delayed version of the deficiency zero theorem and discuss global asymptotic stability. In [77] the authors provide several sufficient conditions for the persistence of delayed complex balanced CRNs with mass action kinetics, and they improve the practical applicability of these results via semilocking set decomposition in [78].

Using the achievements outlined above, the purpose of the present chapter is to further extend stability results for delayed complex balanced kinetic systems with general (non-mass action) kinetics. For this, an appropriate Lyapunov-Krasovskii functional is proposed through which the local asymptotic stability of positive equilibria can be shown.

The structure of the chapter is as follows. Section 2.2 introduces the basic notions related to kinetic systems. In Section 2.3 we study the set of positive equilibria in the context of complex balancing and the quasi-thermodynamic/thermostatic properties for non-mass action kinetics, our first main contribution. The other main contribution can be found in Section 2.4, where the local asymptotic stability of positive complex balanced equilibria is shown. Section 2.6 contains three computational examples to illustrate the

theory. Finally, conclusions of the chapter are given in Section 2.7.

Throughout the chapter $\mathbb{R}^N$, $\mathbb{R}^N_+$ and $\overline{\mathbb{R}}^N_+$ denote the N-dimensional space of real, positive and nonnegative column vectors, respectively, and the Euclidean norm is denoted by $|.|$. For $x, y, \in \mathbb{R}^N_+$ the vector exponential x^y is defined as $x^y = \prod_{k=1}^N x_k^{y_k}$ and the inner product $x \cdot y$ is defined as $x \cdot y = \sum_{k=1}^N x_i y_i$. For $x \in \mathbb{R}^N_+$ the vector logarithm $\log(x)$ is defined element-wise. For every $\tau \geq 0$ we denote the Banach space of continuous functions mapping the interval $[-\tau, 0]$ into $\mathbb{R}^N$, into $\mathbb{R}^N_+$ and into $\overline{\mathbb{R}}^N_+$ by $\mathcal{C}_\tau = C\big([-\tau, 0], \mathbb{R}^N\big)$, $\mathcal{C}_{+,\tau}$ and $\overline{\mathcal{C}}_{+,\tau}$, respectively. We equip the spaces $\mathcal{C}_\tau$, $\mathcal{C}_{+,\tau}$ and $\overline{\mathcal{C}}_{+,\tau}$ with the standard norm $\|\psi\| = \sup_{s\in[-\tau,0]} \big|\psi(s)\big|$, and the open ball around ψ with radius $\epsilon > 0$ is denoted by $\mathcal{B}_\epsilon(\psi)$. The space of continuously differentiable functions on $\mathbb{R}$ is denoted by $C^1(\mathbb{R})$.

2.2 Preliminaries

In this section we introduce of kinetic systems (also called chemical reaction networks) based on [15, 27]. A kinetic model contains N species denoted by $\mathcal{X} = \{X_1, X_2, \ldots, X_N\}$, and the corresponding species vector is given as $X = [X_1 \ X_2 \ \ldots \ X_N]^\top$. Species are transformed into each other through elementary reaction steps of the form

$$C_k \xrightarrow{\mathcal{K}_k} C_{k'}, \quad k = 1, 2, \ldots, M, \tag{2.1}$$

where $C_k = y_k^\top X$ and $C_{k'} = y_{k'}^\top X$ are the complexes with the stoichiometric coefficient vectors $y_k, y_{k'} \in \overline{\mathbb{Z}}^N_+$ for $k = 1, 2, \ldots, M$. The transformation shown in Eq. (2.1) means that during an elementary reaction step between the C_k reactant complex and $C_{k'}$ product complex $[y_k]_i$ molecules of species X_i are consumed, and $[y_{k'}]_i$ molecules of X_i are produced for $i = 1, 2, \ldots, N$. The reaction (2.1) is called an input (output) reaction of species X_i if $[y_{k'}]_i > 0$ ($[y_k]_i > 0$). From now on we say that $i \in \mathrm{supp}(y_k)$ if $[y_k]_i > 0$.

The directed graph containing the complexes as vertices and reactions as directed edges is called the reaction graph of a CRN. A directed graph is strongly connected if there exists a directed path between any pair of its vertices in both directions. A strong component (also called linkage classes in the theory of CRNs) of a directed graph is a maximal strongly connected subgraph. A weakly connected component of a directed graph is a subgraph where all vertices are connected to each other by some (not necessarily directed) path. A reaction graph is called weakly reversible if each weakly connected component of it is a strong component. Weak reversibility is equivalent to the property that each directed edge (reaction) is a part of a directed cycle in the reaction graph.

Let $x(t) \in \overline{\mathbb{R}}^N_+$ denote the state vector corresponding to X for any $t \geq 0$ (in a chemical

context, the state x is the vector of concentrations of the species in X). Then the ODEs describing the evolution of x in the kinetic system containing the reactions (2.1) are given by

$$\dot{x} = \sum_{k=1}^{M} \mathcal{K}_k(x)[y_{k'} - y_k], \quad x(0) \in \overline{\mathbb{R}}_+^N, \tag{2.2}$$

where $\mathcal{K}_k : \overline{\mathbb{R}}_+^N \longrightarrow \overline{\mathbb{R}}_+$ is the rate function corresponding to reaction step k, determining the velocity of the transformation [15]. For the rate functions, we assume the following for $k = 1, 2, \ldots, M$:

(A1) $\mathcal{K}_k$ is differentiable,

(A2) $\dfrac{\partial \mathcal{K}_k(x)}{\partial x_i} \geq 0$ if $i \in \operatorname{supp}(y_k)$, and $\dfrac{\partial \mathcal{K}_k(x)}{\partial x_i} = 0$ if $i \notin \operatorname{supp}(y_k)$,

(A3) $\mathcal{K}_k(x) = 0$ whenever $x_i = 0$ such that $i \in \operatorname{supp}(y_k)$.

The above properties guarantee the local existence and uniqueness of the solutions as well as the invariance of the nonnegative orthant for the dynamics in Eq. (2.2). The dynamics of a kinetic system (2.2) is called persistent if no trajectory that starts in the positive orthant has an omega-limit point on the boundary of $\mathbb{R}_+^N$. A positive linear conserved quantity (or positive linear first integral) for a CRN is defined as $c^\top x$ for which $c^\top \dot{x}(t) = 0$ for $t \geq 0$, where $c \in \overline{\mathbb{R}}_+^M$ and $c \neq 0$.

The set of stoichiometric vectors is denoted with $\mathcal{K}$. In some cases we will use the complex matrix Y that has the stoichiometric vectors as columns. The reaction vector of reaction k is defined as $y_{k'} - y_k$. The linear span of the reaction vectors is called the stoichiometric subspace $\mathcal{S}$ of (2.5), defined as

$$\mathcal{S} = \operatorname{span}\{y_{k'} - y_k \,|\, k = 1, 2, \ldots, M\}$$

and for $p \in \mathbb{R}_+^N$ the corresponding positive stoichiometric compatibility class $\mathcal{S}_p$ is defined by

$$\mathcal{S}_p = \{x \in \mathbb{R}_+^N \,|\, x - p \in \mathcal{S}\}.$$

It is well-known that the positive stoichiometric compatibility classes are positively invariant under (2.3); that is, we have that $x(t) \in \mathcal{S}_p$ for $t \geq 0$ if $x(0) \in \mathcal{S}_p$.

The deficiency of a CRN is defined as $\delta = m - \ell - s$, where m is the number of complexes, ℓ is the number of linkage classes and s is the dimension of $\mathcal{S}$.

An important special case in the theory of CRNs is mass action kinetics when the rate function is given in the following monomial form

$$\mathcal{K}_k(x) = \kappa_k \prod_{i=1}^{N} x_i^{[y_k]_i}, \quad k = 1, 2, \ldots, M$$

where $\kappa_i > 0$ for $i = 1, 2, \dots, M$ are the reaction rate coefficients; that is, the dynamics of mass action kinetic systems can be given as

$$\dot{x}(t) = \sum_{k=1}^{M} \kappa_k x^{y_k}(t)\big(y_{k'} - y_k\big). \tag{2.3}$$

Stability of systems of the form (2.3) can be investigated through the entropy-like logarithmic Lyapunov function

$$V(x, \overline{x}) = \sum_{i=1}^{N} \big(x_i(\log x_i - \log \overline{x}_i - 1) + \overline{x}_i\big) = \sum_{i=1}^{N} \left(x_i \log \frac{x_i}{\overline{x}_i} + \overline{x}_i - x_i\right), \tag{2.4}$$

where $\overline{x}$ is a positive equilibrium. We aim to generalize certain stability results to include non-mass action cases like the Michaelis-Menten kinetics or general Hill-type kinetics, while still relying on a similar Lyapunov function. In order to do so, we consider kinetic systems of the form

$$\dot{x}(t) = \sum_{k=1}^{M} \kappa_k \gamma^{y_k}\big(x(t)\big)\big(y_{k'} - y_k\big), \tag{2.5}$$

where the function $\gamma : \overline{\mathbb{R}}_+^N \mapsto \overline{\mathbb{R}}_+^N$ is defined element-wise by the increasing functions $\gamma_i \in C^1(\mathbb{R})$. We recall that in this case the vector exponential $\gamma^{y_k}\big(x(t)\big)$ expands to $\prod_{i=1}^{N} \gamma_i^{y_{k,i}}\big(x_i(t)\big)$. This class of systems include a wide variety of interesing and relevant kinetics, while the product structure of $\gamma^{y_k}(x)$ allows us to rely on logarithmic identities in the calculations. In particular, the Michaelis-Menten kinetics can be given by $\gamma_i(s) = \frac{s}{c_i + s}$ for $c_i > 0$, and more general Hill kinetics can be given by $\gamma_i(s) = \frac{s^{n_i}}{c_i + s^{n_i}}$ for $c_i > 0$ and $n_i > 0$.

We impose the following assumptions on the γ_i functions. First of all, if the concentration of any reactant is zero, the reaction should not take place; that is, we assume that $\gamma_i(0) = 0$. A fundamental case for the choice of the γ_i transformations is $\gamma_i(s) = s$, which corresponds to mass action kinetics. For regularity, in particular for the existence of nontrivial equilibria, we usually assume that the γ_i functions further satisfy $\int_0^1 |\log \gamma_i(s)| \, \mathrm{d}s < \infty$ and that $\gamma_i : \overline{\mathbb{R}}_+ \mapsto \overline{\mathbb{R}}_+$ are onto. In this case the inverse of $\gamma_i^{-1}(s)$ is strictly increasing from $\overline{\mathbb{R}}_+$ onto $\overline{\mathbb{R}}_+$, and thus

$$\lim_{x \to \infty} \left(\int_a^x \gamma_i^{-1}(e^s) \, \mathrm{d}s - bx\right) = \infty \tag{2.6}$$

holds for any $0 \leq a < \infty$ and any b. While the $\gamma_i(s) = s$ mass action case satisfies the above assumptions, many fundamental examples from biochemistry do not; in particular, the Michaelis-Menten kinetics and the Hill kinetics fail to do so, since they are not onto $\overline{\mathbb{R}}_+$ and they do not meet assumption (2.6). However, as we will show, a slightly relaxed

condition still ensures the existence of nontrivial equilibria. Instead of assuming that the γ_i function are onto $\overline{\mathbb{R}}_+$, we only require that they are onto $[0, \sigma_i)$, where $0 < \sigma_i \leq \infty$ can be finite. Then instead of (2.6) we will require that

$$\lim_{x \uparrow \log \sigma_i} \left(\int_a^x \gamma_i^{-1}(e^s)\, \mathrm{d}s - bx \right) = \infty \tag{2.7}$$

holds for any $0 \leq a < \infty$ and any b. For more details we refer to [62, Section IV.B].

We note that (2.5) can be rewritten in matrix form as follows. Assume that the number of distinct complexes is L and define κ_{ij} as κ_k if there is a reaction k such that $y_{k'} = y_j$ and $y_k = y_i$, and zero otherwise. Denoting by K the matrix defined element-wise as $[K]_{ij} = \kappa_{ij}$, the system (2.5) takes the form

$$\dot{x}(t) = Y\big(K - \mathrm{diag}(1_L^\top K)\big)\Gamma(x) =: Y\tilde{K}\Gamma(x), \tag{2.8}$$

where $1_L \in \mathbb{R}^L$ denotes a column vector with all of its coordinates equal to one and $\Gamma : \overline{\mathbb{R}}_+^N \mapsto \overline{\mathbb{R}}_+^N$ is defined as

$$\Gamma(x) = \big[\gamma^{y_1}(x)\ \gamma^{y_2}(x)\ \cdots\ \gamma^{y_L}(x)\big].$$

Note, that $\tilde{K}$ is the weighted negative Laplacian of the reaction graph of the system.

We also consider the delayed version of (2.5), having the form

$$\dot{x}(t) = \sum_{k=1}^{M} \kappa_k \Big(\gamma^{y_k}\big(x(t-\tau_k)\big) y_{k'} - \gamma^{y_k}\big(x(t)\big) y_k \Big), \tag{2.9}$$

where $\tau_k \geq 0$ are discrete constant time delays. The solution corresponding to an initial function $\psi \in \overline{\mathcal{C}}_{+,\tau}$ at time $t \geq 0$ is denoted by $x^\psi(t) \in \overline{\mathbb{R}}_+^N$ or by $x_t^\psi \in \overline{\mathcal{C}}_{+,\tau}$ when we use it as a function. A positive vector $\overline{x} \in \mathbb{R}_+^N$ is called a positive equilibrium of (2.9) if $x(t) \equiv \overline{x}$ is a solution of (2.9); that is, the equilibria of (2.9) and (2.5) coincide. The Lyapunov-Krasovskii approach for such delayed systems is formally very similar to the Lyapunov approach of ODEs [69, 1]. Let $\tau = \max_k \tau_k$ and $\overline{x}$ be an equilibrium of (2.9). If the functional $V : \mathcal{C}_{+,\tau} \to \mathbb{R}$ is such that $V(\overline{x}) = 0$ and

$$V(\psi) \geq \alpha\big(|\psi(0) - \overline{x}|\big),$$
$$\dot{V}(\psi) \leq 0,$$

holds for $\psi \in \mathcal{C}_{+,\tau}$, where $\alpha : \overline{\mathbb{R}}_+ \mapsto \overline{\mathbb{R}}_+$ is a continuous and strictly increasing function with $\alpha(0) = 0$, then $\overline{x}$ is Lyapunov stable. If there exists a $\gamma : \overline{\mathbb{R}}_+ \mapsto \overline{\mathbb{R}}_+$ is a continuous and strictly increasing function with $\gamma(0) = 0$ such that

$$\dot{V}(\psi) \leq -\gamma\big(|\psi(0) - \overline{x}|\big)$$

then the system is locally asymptotically stable. Finally, if $\alpha(s) \to \infty$ as $s \to \infty$, then the system is globally asymptotically stable.

2.3 Quasi-thermodynamic property and complex balancing

In this section, we restate some of the stability results described in [62] under milder conditions using the computational approach of [15]. Here we consider nondelayed kinetic systems of the form (2.5). First, let us recall some definitions. A positive vector $\overline{x} \in \mathbb{R}^N_+$ is called a positive equilibrium of (2.5) if $x(t) \equiv \overline{x}$ is a solution of (2.5); that is, the equilibria of (2.5) satisfy the equation

$$f(\overline{x}) := \sum_{k=1}^{M} \kappa_k \gamma^{y_k}(\overline{x})\big(y_{k'} - y_k\big) = 0,$$

where $f : \overline{\mathbb{R}}^N_+ \mapsto \mathcal{S}$ denotes the species formation rate function of the kinetic system (2.5). In the classical terminology of [27, 15] a kinetic system is called quasi-thermostatic if there exists a positive vector $\overline{x} \in \mathbb{R}^N_+$ such that the set of positive equilibria is identical to the set

$$\mathcal{E} = \big\{\tilde{x} \in \mathbb{R}^N_+ \big| \log(\tilde{x}) - \log(\overline{x}) \in \mathcal{S}^\perp\big\}.$$

In this case we say that the kinetic system is *quasi-thermostatic* with respect to $\overline{x}$. Standard arguments show that then the system is quasi-thermostatic with respect to any element of $\mathcal{E}$. The distribution of positive equilibria of quasi-thermostatic systems can be efficiently characterized, namely, each positive stoichiometric compatibility class contains precisely one positive equilibrium [27].

Furthermore, a kinetic system is called *quasi-thermodynamic* if there exists an $\overline{x} \in \mathbb{R}^N_+$ such that the system is quasi-thermostatic with respect to $\overline{x}$, and

$$\big(\log(x) - \log(\overline{x})\big) \cdot f(x) \leq 0 \tag{2.10}$$

holds for $x \in \mathbb{R}^N_+$, with equality holding only if $f(x) = 0$ or, equivalently, if $\log(x) - \log(\overline{x}) \in \mathcal{S}^\perp$. In this case we say that the kinetic system is quasi-thermodynamic with respect to $\overline{x}$. Similarly to quasi-thermostaticity, a system is quasi-thermodynamic with respect to any element of $\mathcal{E}$. The main consequence of quasi-thermodynamicity is that the unique positive equilibrium of each positive stoichiometric compatibility class is locally asymptotically stable relative to its class. This arises from the fact that the gradient of the function

$$H(x, \overline{x}) = \sum_{i=1}^{N} x_i(\log x_i - \log \overline{x}_i - 1)$$

is given by $\log(x) - \log(\overline{x})$ which is a term in Eq. (2.10). Thus, the function (2.4) is a Lyapunov function for quasi-thermodynamic kinetic models. The short physical

background of this is that H was used to describe the Helmholtz free energy density of the system, and its gradient is the chemical potential function.

As noted in [27], while the above definition is physically associated with mass action kinetics and ideal gas mixtures, it could apply to any kinetic system. In some cases the definitions can be extended without voiding their consequences. In order to do so, following [62], we define for $x \in \mathbb{R}^N_+$ the function

$$\rho(x) = \log\big(\gamma(x)\big),$$

where γ is defined as in Eq. (2.5). A kinetic system of the form (2.5) is called *quasi-thermostatic in the generalized sense* if there exists an $\overline{x} \in \mathbb{R}^N_+$ such that the set of positive equilibria is identical to the set

$$\mathcal{E} = \big\{\tilde{x} \in \mathbb{R}^N_+ \big| \rho(\tilde{x}) - \rho(\overline{x}) \in \mathcal{S}^\perp\big\}. \tag{2.11}$$

For brevity, we simply say that the kinetic system is quasi-thermostatic with respect to $\overline{x}$. Again, similarly to classical quasi-thermostaticity, standard arguments show that then the system is quasi-thermostatic with respect to any element of $\mathcal{E}$. Furthermore, the distribution of the positive equilibria of quasi-thermostatic kinetic systems across positive stoichiometric compatibility classes can be characterized. We describe that distribution in the following proposition.

Proposition 2.3.1. *Assume that the kinetic system* (2.5) *is quasi-thermostatic. Then, for every $p \in \mathbb{R}^N_+$ the corresponding positive stoichiometric compatibility class $\mathcal{S}_p$ contains precisely one positive equilibrium.*

Proof. We first show the existence of a point in $\mathcal{S}_p \cap \mathcal{E}$. Let $\overline{x}$ be an element of $\mathcal{E}$. By [79, Proposition B.1] there exists a (unique) vector $\mu \in \mathcal{S}^\perp$ such that

$$\gamma(\overline{x})e^\mu - p \in \mathcal{S}.$$

Let $\tilde{x}$ be defined by

$$\gamma(\tilde{x}) := \gamma(\overline{x})e^\mu.$$

Then $\tilde{x} \in \mathcal{S}_p$ and taking logarithm shows that

$$\rho(\tilde{x}) - \rho(\overline{x}) = \mu \in \mathcal{S}^\perp;$$

that is, we have that $\tilde{x} \in \mathcal{E}$ as well.

In order to show uniqueness, let us assume by contradiction that $\tilde{x}$ and $\overline{x}$ are distinct positive equilibria in $\mathcal{S}_p$. Then $\tilde{x} - \overline{x} \in \mathcal{S}$ and $\rho(\tilde{x}) - \rho(\overline{x}) \in \mathcal{S}^\perp$, and thus

$$0 = \big(\rho(\tilde{x}) - \rho(\overline{x})\big) \cdot (\tilde{x} - \overline{x}) = \sum_{i=1}^{N} \big(\log \gamma_i(\tilde{x}_i) - \log \gamma_i(\overline{x}_i)\big)(\tilde{x}_i - \overline{x}_i).$$

Since the functions γ_i and the logarithm are strictly increasing, the above expression is zero if and only if $\tilde{x} = \overline{x}$. □

Remark 2.3.2. *Note that we implicitly used assumption* (2.7)*, see [62, Lemma IV.1] and Proposition 2.4.2 for more details.*

A kinetic system of the form (2.5) is called *quasi-thermodynamic in the generalized sense* if there exists an $\overline{x} \in \mathbb{R}^N_+$ such that the system is quasi-thermostatic with respect to $\overline{x}$ and

$$\big(\rho(x) - \rho(\overline{x})\big) \cdot f(x) \leq 0$$

holds for $x \in \mathbb{R}^N_+$, where equality holds only if $f(x) = 0$ or, equivalently, if $\rho(x) - \rho(\overline{x}) \in \mathcal{S}^\perp$. Again, for brevity, we simply say that the kinetic system is quasi-thermodynamic with respect to $\overline{x}$, however, similarly to quasi-thermostaticity, a system is quasi-thermodynamic with respect to any element of $\mathcal{E}$.

The following proposition and its proof shows that the underlying function

$$V(x, \overline{x}) = \sum_{i=1}^{N} \int_{\overline{x}_i}^{x_i} \big(\log \gamma_i(s) - \log \gamma_i(\overline{x}_i)\big)\, \mathrm{d}s \tag{2.12}$$

is a Lyapunov function of the system (2.5). Note, that (2.12) reduces to (2.4) in the mass action case.

Proposition 2.3.3. *Assume that the kinetic system* (2.5) *is quasi-thermodynamic. Then, each positive stoichiometric compatibility class contains precisely one positive equilibrium and that equilibrium is locally asymptotically stable, and there is no nontrivial periodic trajectory along which all species concentrations are positive.*

Proof. The fact that each positive stoichiometric compatibility class contains precisely one positive equilibrium follows from quasi-thermostaticity.

Let us consider any positive stoichiometric compatibility class $\mathcal{S}_p$ and denote its unique positive equilibrium by $\overline{x}$. Then, for any $x \in \mathcal{S}_p$ other than $\overline{x}$, we have that

$$\big(\rho(x) - \rho(\overline{x})\big) \cdot f(x) < 0. \tag{2.13}$$

It is easy to see that $V(x,\overline{x}) \geq 0$ and equality holds only if $x = \overline{x}$, and that $\nabla V(x,\overline{x}) = \rho(x) - \rho(\overline{x})$. This, combined with (2.13) show that

$$\nabla V(x,\overline{x}) \cdot f(x) < 0$$

holds for any $x \in \mathcal{S}_p$ other than $\overline{x}$. Standard arguments show that $V(x,\overline{x})$ is a strict Lyapunov function for $\overline{x}$ on its positive stoichiometric compatibility class $\mathcal{S}_p$, thus $\overline{x}$ is locally asymptotically stable relative to $\mathcal{S}_p$.

To show that no nontrivial periodic trajectories can exist along which all species concentrations are positive, assume by contradiction that $x : [0,T] \mapsto \mathbb{R}^N_+$ is such a solution with $x(T) = x(0)$ and denote the unique positive equilibrium of the corresponding positive stoichiometric compatibility class by $\overline{x}$. Then

$$V\big(x(T),\overline{x}\big) - V\big(x(0),\overline{x}\big) = \int_0^T \nabla V\big(x(t),\overline{x}\big) \cdot f\big(x(t)\big)\,\mathrm{d}t < 0,$$

and thus

$$V\big(x(T),\overline{x}\big) < V\big(x(0),\overline{x}\big),$$

contradicting $x(T) = x(0)$. □

In [62] the author considers systems of the form (2.5) or, equivalently, of the form (2.8), and assumes that the complex matrix Y is of full rank and none of its rows vanishes, and that $\tilde{K}$ is irreducible (implying that the reaction graph is strongly connected). Then, without using the above terminology, the author shows that such systems are quasi-thermodynamic. We note, that these assumptions imply that if $\overline{x}$ is an equilibrium of (2.8), then $\tilde{K}\Gamma(\overline{x}) = 0$; that is, the vector $\Gamma(\overline{x})$ is in the kernel of $\tilde{K}$. Thus, systems that satisfy the above assumptions are complex balanced, defined as follows.

Without any restrictions on Y or assuming that $\tilde{K}$ is irreducible, an equilibrium $\overline{x}$ is called *complex balanced* if $\tilde{K}\Gamma(\overline{x}) = 0$ or, equivalently, if for every complex $\eta \in \mathcal{K}$ we have that

$$\sum_{k:\eta=y_k} \kappa_k \gamma^{y_k}(\overline{x}) = \sum_{k:\eta=y_{k'}} \kappa_k \gamma^{y_k}(\overline{x}),$$

where the sum on the left-hand side is taken over the reactions where η is the source complex and the sum on the right-hand side is taken over the reactions where η is the product complex. Therefore, complex balanced equilibria are also called vertex-balanced in the literature [80]. We note that this setting is indeed more general than that of [62], as for mass action systems complex balancing can occur in weakly reversible systems, not just in strongly connected systems; that is, there can be more than one linkage classes.

First, we show that the existence of a positive complex balanced equilibrium affects every positive equilibrium.

Proposition 2.3.4. *Assume that the kinetic system* (2.5) *admits a positive complex balanced equilibrium. Then every positive equilibrium is complex balanced.*

Proof. Let us assume that $\overline{x} \in \mathbb{R}^N_+$ is a positive complex balanced equilibrium and $\tilde{x} \in \mathbb{R}^N_+$ is a positive equilibrium other than $\overline{x}$. Then $\tilde{x} \in \mathcal{E}$; that is, we have that $\rho(\tilde{x}) - \rho(\overline{x}) \in \mathcal{S}^{\perp}$. Let us define for $k = 1, 2, \ldots, M$ the function $q_k : \mathbb{R}^N_+ \mapsto \mathbb{R}$ by

$$q_k(x) = \big(\rho(x) - \rho(\overline{x})\big) \cdot y_k.$$

Then, for any complex $\eta \in \mathcal{K}$ we have that

$$\begin{aligned}\sum_{k:\eta=y_k} \kappa_k \gamma^{y_k}(\tilde{x}) - \sum_{k:\eta=y_{k'}} \kappa_k \gamma^{y_k}(\tilde{x}) &= \sum_{k:\eta=y_k} \kappa_k \gamma^{y_k}(\overline{x}) e^{q_k(\tilde{x})} - \sum_{k:\eta=y_{k'}} \kappa_k \gamma^{y_k}(\overline{x}) e^{q_k(\tilde{x})} \\ &= e^{q_\eta(\tilde{x})} \left(\sum_{k:\eta=y_k} \kappa_k \gamma^{y_k}(\overline{x}) - \sum_{k:\eta=y_{k'}} \kappa_k \gamma^{y_k}(\overline{x}) \right) = 0,\end{aligned}$$

thus $\tilde{x}$ is indeed complex balanced. □

The above Proposition shows that positive complex balancing is a system property. Thus, a system of the form (2.5) is called complex balanced if it admits a positive complex balanced equilibrium. Finally, the connection between complex balanced systems and quasi-thermodynamic systems are described in the following proposition.

Proposition 2.3.5. *Assume that the kinetic system* (2.5) *is complex balanced. Then it is quasi-thermodynamic.*

Proof. Let us consider the positive complex balanced equilibrium $\overline{x}$; that is, the equality

$$\sum_{k:\eta=y_k} \kappa_k \gamma^{y_k}(\overline{x}) = \sum_{k:\eta=y_{k'}} \kappa_k \gamma^{y_k}(\overline{x})$$

holds for any complex $\eta \in \mathcal{K}$. Observe that for any $x \in \mathbb{R}^N_+$ we have that

$$\big(\rho(x) - \rho(\overline{x})\big) \cdot f(x) = \sum_{k=1}^{M} \kappa_k \gamma^{y_k}(x) \big(q_{k'}(x) - q_k(x)\big) = \sum_{k=1}^{M} \kappa_k \gamma^{y_k}(\overline{x}) e^{q_k(x)} \big(q_{k'}(x) - q_k(x)\big).$$

Using the well-known inequality

$$e^a(b-a) \leq e^b - e^a \tag{2.14}$$

leads to

$$\begin{aligned}\big(\rho(x)-\rho(\overline{x})\big)\cdot f(x) &\leq \sum_{k=1}^{M}\kappa_k\gamma^{y_k}(\overline{x})\big(e^{q_{k'}(x)}-e^{q_k(x)}\big)\\ &=\sum_{\eta\in\mathcal{K}}e^{q_\eta(x)}\left(\sum_{k:\eta=y_{k'}}\kappa_k\gamma^{y_k}(\overline{x})-\sum_{k:\eta=y_k}\kappa_k\gamma^{y_k}(\overline{x})\right)=0,\end{aligned}\tag{2.15}$$

where equality holds if and only if $q_{k'}(x)=q_k(x)$ for each reaction $k=1,2,\dots,M$; that is, if and only if $\rho(x)-\rho(\overline{x})$ lies in $\mathcal{S}^\perp$. In particular, if $f(x)=0$, then $\rho(x)-\rho(\overline{x})$ lies in $\mathcal{S}^\perp$. It remains to be shown that if $\rho(x)-\rho(\overline{x})$ lies in $\mathcal{S}^\perp$, then $f(x)=0$, as a quasi-thermodynamic system needs to be quasi-thermostatic as well. Rewrite the species formation rate function as

$$\begin{aligned}f(x)&=\sum_{\eta\in\mathcal{K}}\eta\left(\sum_{k:\eta=y_{k'}}\kappa_k\gamma^{y_k}(x)-\sum_{k:\eta=y_k}\kappa_k\gamma^{y_k}(x)\right)\\ &=\sum_{\eta\in\mathcal{K}}\eta\left(\sum_{k:\eta=y_{k'}}\kappa_k\gamma^{y_k}(\overline{x})e^{q_k(x)}-\sum_{k:\eta=y_k}\kappa_k\gamma^{y_k}(\overline{x})e^{q_k(x)}\right).\end{aligned}$$

If x is such that $\rho(x)-\rho(\overline{x})\in\mathcal{S}^\perp$, then $\rho(x)-\rho(\overline{x})$ is orthogonal to every reaction vector, and thus

$$f(x)=\sum_{\eta\in\mathcal{K}}e^{q_\eta(x)}\eta\left(\sum_{k:\eta=y_{k'}}\kappa_k\gamma^{y_k}(\overline{x})-\sum_{k:\eta=y_k}\kappa_k\gamma^{y_k}(\overline{x})\right)=0;$$

that is, the vector x is an equilibrium. This shows that the set of positive equilibria coincides with the set $\mathcal{E}$, and thus the system is quasi-thermostatic. This, combined with (2.15) shows that the system is quasi-thermodynamic as well. □

2.4 Stability of delayed kinetic models

In this section, we consider kinetic systems with delayed reactions having the form (2.9). In order to do so, first, we have to extend the notion of positive stoichiometric compatibility classes to the delayed case. We note, that the following definition and invariance proof was already established in [71] for the case of mass action kinetics and in [73] for the general case. For each $v\in\mathbb{R}^N$ define the functional $c_v:\mathcal{C}_{+,\tau}\mapsto\mathbb{R}$ as

$$c_v(\psi)=v\cdot\left[\psi(0)+\sum_{k=1}^{M}\left(\kappa_k\int_{-\tau_k}^{0}\gamma^{y_k}\big(\psi(s)\big)\,\mathrm{d}s\right)y_k\right],\qquad\psi\in\mathcal{C}_{+,\tau}.$$

For each $\theta\in\mathcal{C}_{+,\tau}$ the positive stoichiometric compatibility class of (2.9) corresponding to θ is denoted by $\mathcal{D}_\theta$ and is defined by

$$\mathcal{D}_\theta=\big\{\psi\in\mathcal{C}_{+,\tau}\big|c_v(\psi)=c_v(\theta)\text{ for all }v\in\mathcal{S}^\perp\big\}.$$

Clearly, $\psi \in \mathcal{D}_\theta$ if and only if $\psi \in \mathcal{C}_{+,\tau}$ and

$$\psi(0) - \theta(0) + \sum_{k=1}^{M} \left(\kappa_k \int_{-\tau_k}^{0} \left(\gamma^{y_k}\big(\psi(r)\big) - \gamma^{y_k}\big(\theta(s)\big) \right) \mathrm{d}s \right) y_k \in \mathcal{S}. \tag{2.16}$$

This shows that if each delay τ_k is zero, then the delayed positive stoichiometric compatibility classes reduce to the positive compatibility classes of (2.5).

The following Proposition establishes the invariance property of $\mathcal{D}_\theta$.

Proposition 2.4.1. *For every $\theta \in \mathcal{C}_{+,\tau}$ the positive stoichiometric compatibility class $\mathcal{D}_\theta$ is a closed subset of $\mathcal{C}_{+,\tau}$. Moreover, $\mathcal{D}_\theta$ is positively invariant under* (2.9)*; that is, if $\psi \in \mathcal{D}_\theta$, then $x_t^\psi \in \mathcal{D}_\theta$ for all $t \geq 0$.*

Proof. The closedness follows from the continuity of c_v. We will show that for each $v \in \mathcal{S}^\perp$ the functional c_v is constant along the trajectories of (2.9). To see this, let us assume that x is a solution of (2.9). Then for $t \geq 0$ we have that

$$\begin{aligned} \frac{\mathrm{d}}{\mathrm{d}t} c_v(x_t) &= v \cdot \left(\dot{x}(t) + \sum_{k=1}^{M} \kappa_k \Big(\gamma^{y_k}\big(x(t)\big) - \gamma^{y_k}\big(x(t-\tau_k)\big) \Big) y_k \right) \\ &= v \cdot \left(\sum_{k=1}^{M} \kappa_k \gamma^{y_k}\big(x(t-\tau_k)\big)(y_{k'} - y_k) \right) = \sum_{k=1}^{M} \kappa_k \gamma^{y_k}\big(x(t-\tau_k)\big) v \cdot (y_{k'} - y_k) = 0, \end{aligned}$$

where the last equality follows from the fact that $v \in \mathcal{S}^\perp$. Thus, if $\psi \in \mathcal{D}_\theta$, then for every $v \in \mathcal{S}^\perp$ and $t \geq 0$ the equalities

$$c_v\big(x_t^\psi\big) = c_v\big(x_0^\psi\big) = c_v(\psi) = c_v(\theta)$$

hold, showing that $x_t^\psi \in \mathcal{D}_\theta$ as desired. □

The delayed kinetic system of form (2.9) is quasi-thermostatic if its nondelayed version, obtained by setting each $\tau_k = 0$, is quasi-thermostatic, since their equilibria coincide. The following proposition is the generalization of Proposition 2.3.1 for delayed systems.

Proposition 2.4.2. *Assume that the kinetic system* (2.9) *is quasi-thermostatic. Then, for every $\theta \in \mathcal{C}_{+,\tau}$ the corresponding delayed positive stoichiometric compatibility class $\mathcal{D}_\theta$ of the system* (2.9) *contains precisely one positive equilibrium.*

Proof. In the nondelayed case (see Proposition 2.3.1) existence is shown via [79, Proposition B.1] without modification. However, in the delayed case we need to adapt certain steps of the proof based on [76, Theorem 4.4], where the authors prove the statement for delayed mass action systems.

Let us for $\overline{x} \in \mathcal{E}$ define the positive vector $b \in \mathbb{R}^N_+$ by

$$b_i = \theta_i(0) + \sum_{k=1}^{M} \kappa_k \int_{-\tau_k}^{0} \gamma^{y_k}\big(\theta(s)\big)\,\mathrm{d}s$$

and the continuously differentiable function $g : \mathbb{R}^N \mapsto \mathbb{R}$ by

$$g(x) = \sum_{i=1}^{N} \left(\int_0^{x_i} \gamma_i^{-1}\big(\gamma_i(\overline{x}_i)e^s\big)\,\mathrm{d}s + \overline{x}_i - b_i x_i \right) + \sum_{k=1}^{M} \kappa_k \tau_k \big(\gamma(\overline{x})e^x\big)^{y_k}.$$

We note that adding $\overline{x}_i$ to the integral is not necessary for the following analysis, but adding it ensures that $g(x)$ reduces precisely to the analogous function in the known proof of this theorem for mass action systems.

The gradient of g is given by

$$\nabla g(x) = \gamma^{-1}\Big(\gamma(\overline{x})e^x\Big) - b + \sum_{k=1}^{M} \kappa_k \tau_k \big(\gamma(\overline{x})e^x\big)^{y_k} y_k$$

and that the Hessian of g is written as

$$H_g(x) = \operatorname{diag}\left(\frac{\gamma(\overline{x})e^x}{\gamma'\Big(\gamma^{-1}\big(\gamma(\overline{x})e^x\big)\Big)} \right) + \sum_{k=1}^{M} \kappa_k \tau_k \big(\gamma(\overline{x})e^x\big)^{y_k} y_k y_k^\top,$$

where the fraction in the diagonal matrix is defined element-wise. The corresponding quadratic form is positive-definite as the first term is a diagonal matrix with positive entries, and thus is positive-definite, and the second term consists of positive factors and the positive-semidefinite matrix $y_k y_k^\top$. Then the function g is strictly convex everywhere.

From the property (2.7) of the γ_i functions it follows that for any nonzero vector $x \in \mathbb{R}^N$ we have that

$$\lim_{a\to\infty} \left(\int_0^{x_i} \gamma_i^{-1}\big(\gamma_i(\overline{x}_i)e^{as}\big)\,\mathrm{d}s + \overline{x}_i - a b_i x_i \right) = \begin{cases} \infty, & x_i \neq 0, \\ \overline{x}_i & x_i = 0, \end{cases}$$

and thus

$$\lim_{a\to\infty} \sum_{i=1}^{N} \left(\int_0^{x_i} \gamma_i^{-1}\big(\gamma_i(\overline{x}_i)e^{as}\big)\,\mathrm{d}s + \overline{x}_i - a b_i x_i \right) \leq \lim_{a\to\infty} g(ax) = \infty. \tag{2.17}$$

Let $\overline{g} : \mathcal{S}^\perp \mapsto \mathbb{R}$ be the restriction of g to $\mathcal{S}^\perp$, which is also continuously differentiable and strictly convex. Define the subset

$$\mathcal{S}^\perp \supset G = \big\{ x \in \mathcal{S}^\perp \big| \overline{g}(x) \leq g(0) \big\}.$$

Clearly G is convex, closed in $\mathbb{R}^N$, contains the zero vector and contains no half line with endpoint 0 because of (2.17). Then G is bounded, and thus compact as well, since in

a finite-dimensional vector space every unbounded closed convex set containing 0 must contain a half line with endpoint 0 [81, Theorem 3.5.1]. The continuity of $\overline{g}$ and the compactness of G implies that there exists $\mu \in G$ such that

$$\overline{g}(\mu) \leq \overline{g}(x), \qquad \forall x \in G.$$

In fact, $\overline{g}(0) < \overline{g}(x)$ for $x \in \mathcal{S}^{\perp} \backslash G$, and thus

$$\overline{g}(\mu) \leq \overline{g}(x), \qquad \forall x \in \mathcal{S}^{\perp}.$$

Then for $\xi \in \mathcal{S}^{\perp}$, the equality

$$0 = \frac{\mathrm{d}}{\mathrm{d}t}\overline{g}(\mu + t\xi)\bigg|_{t=0} = \frac{\mathrm{d}}{\mathrm{d}t}g(\mu + t\xi)\bigg|_{t=0} = \nabla g(\mu) \cdot \xi$$

holds; that is, the vector $\nabla g(\mu)$ is in $\mathcal{S}$, and thus

$$\begin{aligned}
&\gamma^{-1}\big(\gamma(\overline{x})e^{\mu}\big) - b + \sum_{k=1}^{M} \kappa_k \tau_k \big(\gamma(\overline{x})e^{\mu}\big)^{y_k} y_k \\
&= \gamma^{-1}\big(\gamma(\overline{x})e^{\mu}\big) - \theta(0) + \sum_{k=1}^{M} \left(\kappa_k \int_{-\tau_k}^{0} \Big(\big(\gamma(\overline{x})e^{\mu}\big)^{y_k} - \gamma^{y_k}\big(\theta(s)\big) \Big)\, \mathrm{d}s \right) y_k \in \mathcal{S}.
\end{aligned}$$

Let $\tilde{x}$ be defined by

$$\tilde{x} = \gamma^{-1}\big(\gamma(\overline{x})e^{\mu}\big).$$

Then $\tilde{x} \in \mathcal{D}_{\theta}$ and taking logarithm shows that

$$\rho(\tilde{x}) - \rho(\overline{x}) = \mu \in \mathcal{S}^{\perp};$$

that is, we have that $\tilde{x} \in \mathcal{E}$ as well.

To show uniqueness, assume by contradiction that $\tilde{x}$ and $\overline{x}$ are distinct positive equilibria in $\mathcal{D}_{\theta}$. Then by (2.16) it follows that

$$\tilde{x} - \overline{x} + \sum_{k=1}^{M} \left(\kappa_k \int_{-\tau_k}^{0} \big(\gamma^{y_k}(\tilde{x}) - \gamma^{y_k}(\overline{x})\big)\, \mathrm{d}s \right) y_k \in \mathcal{S}.$$

This, combined with the characterization (2.11) shows that

$$\begin{aligned}
0 &= \big(\rho(\tilde{x}) - \rho(\overline{x})\big) \cdot \left[\tilde{x} - \overline{x} + \sum_{k=1}^{M} \left(\kappa_k \int_{-\tau_k}^{0} \big(\gamma^{y_k}(\tilde{x}) - \gamma^{y_k}(\overline{x})\big)\, \mathrm{d}s \right) y_k \right] \\
&= \sum_{i=1}^{N} \big(\log \gamma(\tilde{x}_i) - \log \gamma(\overline{x}_i)\big)(\tilde{x}_i - \overline{x}_i) \\
&\quad + \sum_{k=1}^{M} \left(\kappa_k \tau_k \big(\log \gamma^{y_k}(\tilde{x}) - \log \gamma^{y_k}(\overline{x})\big)\big(\gamma^{y_k}(\tilde{x}) - \gamma^{y_k}(\overline{x})\big) \right).
\end{aligned}$$

Since the functions γ_i and the logarithm are strictly increasing, the above expression is zero if and only if $\tilde{x} = \overline{x}$. □

As a clear consequence of our nondelayed analysis, a delayed complex balanced system is quasi-thermostatic. To discuss quasi-thermodynamicity we define the candidate Lyapunov-Krasovskii functional, a main contribution of the chapter, as

$$\begin{aligned} V(\psi) := V(\psi, \overline{x}) = &\sum_{i=1}^{N} \int_{\overline{x}_i}^{\psi_i(0)} \big(\log \gamma_i(s) - \log \gamma_i(\overline{x}_i)\big)\, \mathrm{d}s \\ &+ \sum_{k=1}^{M} \kappa_k \int_{-\tau_k}^{0} \left(\gamma^{y_k}\big(\psi(s)\big)\Big(\log \gamma^{y_k}\big(\psi(s)\big) - \log \gamma^{y_k}(\overline{x}) - 1\Big) + \gamma^{y_k}(\overline{x})\right) \mathrm{d}s\,. \end{aligned} \tag{2.18}$$

A delayed kinetic system of the form (2.9) is called quasi-thermodynamic if there exists $\overline{x} \in \mathbb{R}^N_+$ such that the system is quasi-thermostatic with respect to $\overline{x}$, and

$$\dot{V}(x_t, \overline{x}) \leq 0$$

holds along the trajectories x_t for $t \geq 0$, with equality holding only if $f(x) = 0$.

The following theorem is a generalization of Proposition 2.3.3 for delayed systems.

Theorem 2.4.3. *Assume that the kinetic system* (2.9) *is quasi-thermodynamic. Then, every positive equilibrium of the system is Lyapunov stable relative to its positive stoichiometric compatibility class.*

Proof. The fact that each positive stoichiometric compatibility class contains precisely one positive equilibrium follows from quasi-thermostaticity. Using (2.14) shows that the second term of (2.18) is nonnegative and zero if only if $x = \overline{x}$, while in [62] the author shows the same for the first term. Since the system is quasi-thermodynamic, the functional (2.18) is a Lyapunov-Krasovskii functional for the system and the proof is finished. □

Note, that in the nondelayed case Proposition 2.3.3 guaranteed local asymptotic stability and that there are no nontrivial periodic trajectories. In the delayed case the anologous definition only implies Lyapunov stability. However, in our final theorem that generalizes Proposition 2.3.5 to the delayed case, we can ensure these properties.

Theorem 2.4.4. *Assume that the delayed kinetic system* (2.9) *is complex balanced. Then it is quasi-thermodynamic. Moreover, each equilibrium is locally asymptotically stable relative to its positive stoichiometric compatibility class and there are no nontrivial periodic trajectory along which all species concentrations are positive.*

Proof. Let $\overline{x}$ be a complex balanced equilibrium. The gradient of the first term of (2.18) is $\rho(x) - \rho(\overline{x})$, and thus the Lyapunov-Krasovskii directional derivative along trajectories

of (2.9) is given by

$$\begin{aligned}\dot{V}(x_t) &= \sum_{k=1}^{M} \kappa_k \Big(\gamma^{y_k}\big(x(t-\tau_k)\big) q_{k'}\big(x(t)\big) - \gamma^{y_k}\big(x(t)\big) q_k\big(x(t)\big) \Big) \\ &+ \sum_{k=1}^{M} \kappa_k \Big(\gamma^{y_k}\big(x(t)\big) q_k\big(x(t)\big) - \gamma^{y_k}\big(x(t-\tau_k)\big) q_k\big(x(t-\tau_k)\big) \Big) \\ &+ \sum_{k=1}^{M} \kappa_k \Big(\gamma^{y_k}\big(x(t-\tau_k)\big) - \gamma^{y_k}\big(x(t)\big) \Big) \\ &= \sum_{k=1}^{M} \kappa_k \Big(\gamma^{y_k}\big(x(t-\tau_k)\big) \big(q_{k'}\big(x(t)\big) - q_k\big(x(t-\tau_k)\big) \big) + \gamma^{y_k}\big(x(t-\tau_k)\big) - \gamma^{y_k}\big(x(t)\big) \Big).\end{aligned}$$

Rewrite the above as

$$\dot{V}(x_t) = \sum_{k=1}^{M} \kappa_k \gamma^{y_k}(\overline{x}) \Big(e^{q_k(x(t-\tau_k))} \big(q_{k'}\big(x(t)\big) - q_k\big(x(t-\tau_k)\big) \big) + e^{q_k(x(t-\tau_k))} - e^{q_k(x(t))} \Big)$$

and use inequality (2.14) to find that

$$\begin{aligned}\dot{V}(x_t) &\le \sum_{k=1}^{M} \kappa_k \gamma^{y_k}(\overline{x}) \big(e^{q_{k'}(x(t))} - e^{q_k(x(t))} \big) \\ &= \sum_{\eta \in \mathcal{K}} e^{q_\eta(x(t))} \left(\sum_{k:\eta = y_{k'}} \kappa_k \gamma^{y_k}(\overline{x}) - \sum_{k:\eta = y_k} \kappa_k \gamma^{y_k}(\overline{x}) \right) = 0,\end{aligned}$$

as the system is complex balanced, and $\dot{V}(x_t) = 0$ if and only if the equality

$$q_{k'}\big(x(t)\big) = q_k\big(x(t-\tau_k)\big)$$

holds for each reaction $k = 1, 2, \ldots, M$. Standard arguments, see [71, Theorem 3], show that the largest invariant subset of the set

$$\mathcal{R} = \Big\{ \psi \in \mathcal{C}_{+,\tau} \Big| \dot{V}(\psi) = 0 \Big\} = \Big\{ \psi \in \mathcal{C}_{+,\tau} \Big| q_{k'}\big(x^\psi(t)\big) = q_k\big(x^\psi(t-\tau_k)\big),\ k = 1, 2, \ldots, M \Big\}$$

consists of constant functions that are positive complex balanced equilibria.

The fact that there are no nontrivial periodic trajectories along which all species concentrations are positive can be shown similarly as in 2.3.3, thus we omit the calculation. □

2.5 Discussion

In this section some further remarks are discussed about the results shown in Sections 3 and 4.

2.5.1 Interpretation of delayed entropy

In the nondelayed case, the Lyapunov function (2.12) depends only on the concentration configuration of the system and does not include any information about the reactions, such as the reactants, the products or the reaction rate coefficients. Such Lyapunov functions are called *universal*, a term used by [82]. In the delayed case, the Lyapunov-Krasovskii funtional (2.18) is not universal in this sense, since it explicitly contains the stoichiometric vectors and the rate coefficients. In the entropy (or free energy) interpretation of the Lyapunov function, the history of the trajectories temporarily increase the entropy. As we have shown, this residual entropy can be described by the second term of (2.18). While it might be possible to define the delayed entropy with less information about the reactions, our Lyapunov-Krasovskii functional is inherently tied to the delayed system. To see this, we can use the chain method to approximate the delayed reactions in (2.9) with cascades of first order mass action reactions [83, 84]. The Lyapunov function of the approximating system will then converge uniformly to (2.18) on compact subsets of $[0, \infty)$. For a more detailed explanation, we refer to [85], where the authors derive this in the mass action case.

2.5.2 Lyapunov-Krasovskii functional in a different notation

In the literature of CRNs, both system descriptions (2.5) and (2.8) are used frequently. In the former case, we sum the right-hand side w.r.t. the reactions, while in the latter case we sum w.r.t. the complexes. The delayed system (2.9) can be similarly rewritten as

$$\dot{x}(t) = \sum_{i=1}^{L}\sum_{j=1}^{L} \kappa_{ij}\big[\gamma^{y_i}\big(x(t-\tau_{ij})\big)y_j - \gamma^{y_i}\big(x(t)\big)y_i\big].$$

Then the Lyapunov-Krasovskii functional takes the form

$$\begin{aligned} V(\psi) := V(\psi, \overline{x}) = &\sum_{i=1}^{N} \int_{\overline{x}_i}^{\psi_i(0)} \big(\log \gamma_i(s) - \log \gamma_i(\overline{x}_i)\big)\,\mathrm{d}s \\ &+ \sum_{i=1}^{L}\sum_{j=1}^{L} \kappa_{ij} \int_{-\tau_{ij}}^{0} \Big(\gamma^{y_i}\big(\psi(s)\big)\Big(\log \gamma^{y_i}\big(\psi(s)\big) - \log \gamma^{y_i}(\overline{x}) - 1\Big) - \gamma^{y_i}(\overline{x})\Big)\,\mathrm{d}s\,. \end{aligned}$$

The computation on $\dot{V}(x_t)$ can be repeated with minor notational modifications to obtain

$$\dot{V}(x_t) \le \sum_{i=1}^{L}\sum_{j=1}^{L} \kappa_{ij}\gamma^{y_i}(\overline{x})\big(e^{q_j(x(t))} - e^{q_i(x(t))}\big).$$

The right-hand size is equal to

$$\sum_{j=1}^{L} e^{q_j(x(t))}\left(\sum_{i=1}^{L} \kappa_{ij}\gamma^{y_i}(\overline{x})\right) - \sum_{i=1}^{L} e^{q_i(x(t))}\left(\sum_{j=1}^{L} \kappa_{ij}\right)\gamma^{y_i}(\overline{x}) =: Q\big(x(t)\big)\tilde{K}\Gamma(\overline{x}).$$

Since $\overline{x}$ is a complex balanced equilibrium, the vector $\Gamma(\overline{x})$ is in the kernel of $\tilde{K}$; that is, we have that $\dot{V}(x_t) \leq 0$.

2.5.3 Connection with semistability

Our results also show that the positive equilibria of a delayed complex balanced CRN are semistable, defined as follows. An equilibrium $\overline{x}$ is called semistable, if it is Lyapunov stable and there exists $\delta > 0$ such that $\psi \in \mathcal{B}_\delta(\overline{x})$ implies that $x^\psi(t)$ converges to a Lyapunov stable equilibrium as $t \to \infty$. In [71] the authors showed semistability for delayed mass action complex balanced CRNs. We note that the existence of an equilibrium in each positive stoichiometric compatibility class was not known at that time, but it was since proved in [76] for delayed mass action systems and in Proposition 2.4.2 for the more general case.

2.6 Examples

In the following examples we illustrate our notations and results.

2.6.1 Example 1

First, let us consider the delayed kinetic system from [71] with mass action kinetics. The system consists of a reversible reaction

$$2X_1 \underset{\kappa_2=2,\tau_2=0.5}{\overset{\kappa_1=1}{\rightleftharpoons}} X_2.$$

The corresponding kinetic system takes the form

$$\dot{x}(t) = \kappa_1 \left(x_1^2(t) \begin{bmatrix} 0 \\ 1 \end{bmatrix} - x_1^2(t) \begin{bmatrix} 2 \\ 0 \end{bmatrix} \right) + \kappa_2 \left(x_2(t-\tau_2) \begin{bmatrix} 2 \\ 0 \end{bmatrix} - x_2(t) \begin{bmatrix} 0 \\ 1 \end{bmatrix} \right).$$

The stoichiometric subspace and its orthogonal complement is

$$\mathcal{S} = \operatorname{span}\left\{ \begin{bmatrix} 2 \\ -1 \end{bmatrix} \right\} \qquad \mathcal{S}^\perp = \operatorname{span}\left\{ \begin{bmatrix} 1 \\ 2 \end{bmatrix} \right\}.$$

It is easy to verify that $[2\ 2]^\top$ is a positive complex balanced equilibrium, and thus the positive equilibria are given by

$$\mathcal{E} = \left\{ x \in \mathbb{R}^2_+ \,\middle|\, \begin{bmatrix} \log x_1 - \log 2 \\ \log x_2 - \log 2 \end{bmatrix} \in \mathcal{S}^\perp \right\}.$$

For any $\overline{x} \in \mathcal{E}$ we consider the set of points

$$\mathcal{X}_{\overline{x}} = \left\{ x \in \mathbb{R}^2_+ \middle| \begin{bmatrix} x_1 - \overline{x}_1 \\ (1+\kappa_2\tau_2)(x_2 - \overline{x}_2) \end{bmatrix} \in \mathcal{S} \right\}.$$

If we construct constant functions in $\mathcal{C}_{+,\tau}$ from $\overline{x}$ and the elements of $\mathcal{X}_{\overline{x}}$ in the obvious way, then by (2.16) we have $\mathcal{X}_{\overline{x}} \in \mathcal{D}_{\overline{x}}$.

Let us consider the transformations $\gamma_1(s) = \frac{s^2}{1+s}$ and $\gamma_2(s) = \frac{s^3}{1+s}$; that is, the transformed system takes the form

$$\begin{aligned} \dot{x}(t) = \kappa_1 \left(\frac{x_1^4(t)}{\big(1+x_1(t)\big)^2} \begin{bmatrix} 0 \\ 1 \end{bmatrix} - \frac{x_1^4(t)}{\big(1+x_1(t)\big)^2} \begin{bmatrix} 2 \\ 0 \end{bmatrix} \right) \\ + \kappa_2 \left(\frac{x_2^3(t-\tau_2)}{1+x_2(t-\tau_2)} \begin{bmatrix} 2 \\ 0 \end{bmatrix} - \frac{x_2^3(t)}{1+x_2(t)} \begin{bmatrix} 0 \\ 1 \end{bmatrix} \right). \end{aligned}$$

Is it easy to verify that $\begin{bmatrix} \frac{\sqrt{5}}{2} + \frac{1}{2} & 1 \end{bmatrix}^\top$ is a positive complex balanced equilibrium, and thus the positive equilibria are given by

$$\mathcal{E} = \left\{ x \in \mathbb{R}^2_+ \middle| \begin{bmatrix} \log \frac{x_1^2}{1+x_1} - \log 1 \\ \log \frac{x_2^3}{1+x_2} - \log \frac{1}{2} \end{bmatrix} \in \mathcal{S}^\perp \right\},$$

and $\mathcal{X}_{\overline{x}}$ is given by

$$\mathcal{X}_{\overline{x}} = \left\{ x \in \mathbb{R}^2_+ \middle| \begin{bmatrix} x_1 - \overline{x}_1 \\ x_2 - \overline{x}_2 + \kappa_2\tau_2 \left(\frac{x_2^3}{1+x_2} - \frac{\overline{x}_2^3}{1+\overline{x}_2} \right) \end{bmatrix} \in \mathcal{S} \right\}.$$

In Figure 2.1, the positive equilibria, several positive stoichiometric compatibility classes and trajectories of the original mass action system are depicted with red dashed, green dashed and green continuous lines, respectively. The same objects for the transformed system are drawn with black dashed, blue dashed and blue continuous lines, respectively.

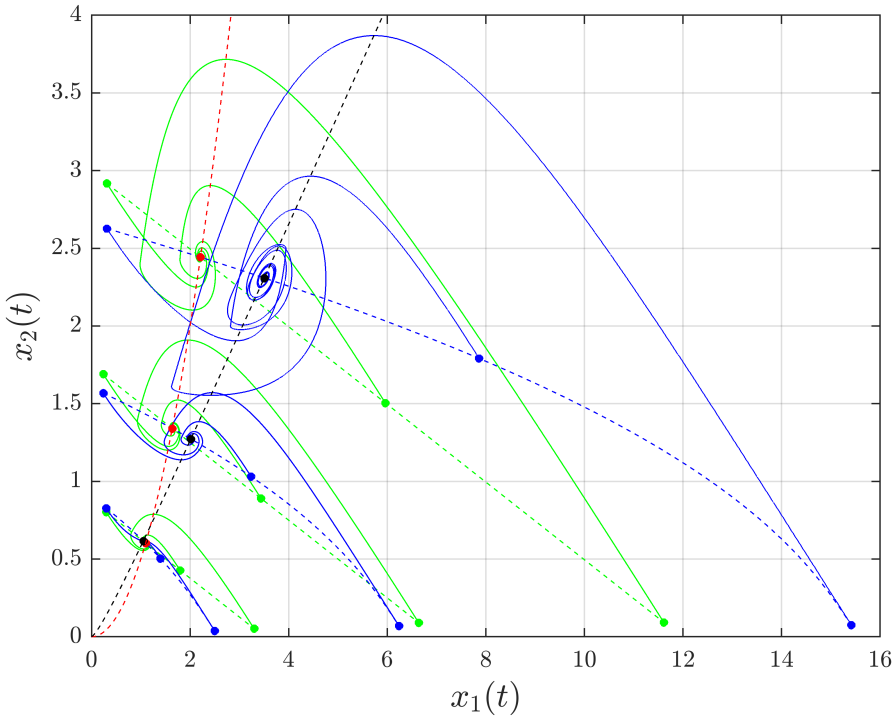

Figure 2.1: Phase plot of Example 1

Using the terminology of [73, 76] it is easy to see that the set $W = \{X_1, X_2\}$ is the only minimal semilocking set (called siphon in the theory of Petri nets). The L_W space consists of functions $w \in \overline{\mathcal{C}}_{+,\tau}$ such that

$$w_i(s) = 0, \qquad X_i \in W,$$
$$w_i(s) \neq 0, \qquad X_i \notin W$$

holds for $s \in [-\tau, 0]$. Then [76, Theorem 5.1] states that the boundary equilibria of the system is contained in

$$\bigcup_{\theta \in \mathcal{C}_{+,\tau}} \overline{\mathcal{D}}_\theta \cap L_W,$$

but the above set consists of only the constant zero function; that is, all nontrivial equilibria are positive and globally asymptotically stable w.r.t. their positive stoichiometric compatibility classes.

2.6.2 Example 2

Our next example is a delayed version of another complex balanced small reaction network, taken from [86]. We consider the set of reversible reactions

$$3X_1 \underset{\kappa_2=\frac{2.8}{3}}{\overset{\kappa_1=\frac{1.4}{3}}{\rightleftharpoons}} 3X_2 \qquad 3X_1 \underset{\kappa_4=0.126,\tau_4=0.4}{\overset{\kappa_3=0.1}{\rightleftharpoons}} 2X_1 + X_2 \qquad 3X_2 \underset{\kappa_6=0.063,\tau_6=0.6}{\overset{\kappa_5=0.1}{\rightleftharpoons}} 2X_1 + X_2$$

with the transformations $\gamma_1(s) = s$ and $\gamma_2(s) = \frac{s^2}{1+s}$. Then the system takes the form

$$\begin{aligned}\dot{x}(t) = \kappa_1 &\left(x_1^3(t) \begin{bmatrix} 0 \\ 3 \end{bmatrix} - x_1^3(t) \begin{bmatrix} 3 \\ 0 \end{bmatrix} \right) + \kappa_2 \left(\frac{x_2^6(t)}{\big(1+x_2(t)\big)^2} \begin{bmatrix} 3 \\ 0 \end{bmatrix} - \frac{x_2^6(t)}{\big(1+x_2(t)\big)^2} \begin{bmatrix} 0 \\ 3 \end{bmatrix} \right) \\ &+ \kappa_3 \left(x_1^3(t) \begin{bmatrix} 2 \\ 1 \end{bmatrix} - x_1^3(t) \begin{bmatrix} 3 \\ 0 \end{bmatrix} \right) \\ &+ \kappa_4 \left(x_1^2(t-\tau_4) \frac{x_2^2(t-\tau_4)}{1+x_2(t-\tau_4)} \begin{bmatrix} 3 \\ 0 \end{bmatrix} - x_1^2(t) \frac{x_2^2(t)}{1+x_2(t)} \begin{bmatrix} 2 \\ 1 \end{bmatrix} \right) \\ &+ \kappa_5 \left(\frac{x_2^6(t)}{\big(1+x_2(t)\big)^2} \begin{bmatrix} 2 \\ 1 \end{bmatrix} - \frac{x_2^6(t)}{\big(1+x_2(t)\big)^2} \begin{bmatrix} 0 \\ 3 \end{bmatrix} \right) \\ &+ \kappa_6 \left(x_1^2(t-\tau_6) \frac{x_2^2(t-\tau_6)}{1+x_2(t-\tau_6)} \begin{bmatrix} 0 \\ 3 \end{bmatrix} - x_1^2(t) \frac{x_2^2(t)}{1+x_2(t)} \begin{bmatrix} 2 \\ 1 \end{bmatrix} \right).\end{aligned}$$

The stoichiometric subspace and its orthogonal complement are

$$\mathcal{S} = \operatorname{span}\left\{ \begin{bmatrix} -3 \\ 3 \end{bmatrix} \right\} \qquad \mathcal{S}^\perp = \operatorname{span}\left\{ \begin{bmatrix} 3 \\ 3 \end{bmatrix} \right\}.$$

It is easy to verify via the Cardano formula that

$$\overline{x} = \begin{bmatrix} \sqrt[3]{2} \\ \sqrt[3]{\frac{1}{2} + \sqrt{\frac{23}{108}}} + \sqrt[3]{\frac{1}{2} - \sqrt{\frac{23}{108}}} \end{bmatrix}$$

is a positive complex balanced equilibrium, and thus the positive equilibria are given by

$$\mathcal{E} = \left\{ x \in \mathbb{R}^2_+ \,\middle|\, \begin{bmatrix} \log x_1 - \log \overline{x}_1 \\ \log \frac{x_2^2}{1+x_2} - \log \frac{\overline{x}_2^2}{1+\overline{x}_2} \end{bmatrix} \in \mathcal{S}^\perp \right\},$$

and $\mathcal{X}_{\overline{x}}$ is given by

$$\mathcal{X}_{\overline{x}} = \left\{ x \in \mathbb{R}^2_+ \,\middle|\, \begin{bmatrix} x_1 - \overline{x}_1 + 2(\kappa_4\tau_4 + \kappa_5\tau_5)\Big(x_1^2 \frac{x_2^2}{1+x_2} - \overline{x}_1^2 \frac{\overline{x}_2^2}{1+\overline{x}_2} \Big) \\ x_2 - \overline{x}_2 + (\kappa_4\tau_4 + \kappa_5\tau_5)\Big(x_1^2 \frac{x_2^2}{1+x_2} - \overline{x}_1^2 \frac{\overline{x}_2^2}{1+\overline{x}_2} \Big) \end{bmatrix} \in \mathcal{S} \right\}.$$

Similarly to the previous example, it can be shown via [76, Theorem 5.1] that all non-trivial equilibria of the system are positive and globally asymptotically stable w.r.t. their positive stoichiometric compatibility classes.

In Figure 2.2, the positive equilibria, several positive stoichiometric compatibility classes and trajectories of system are drawn with black dashed, blue dashed and blue continuous lines, respectively.

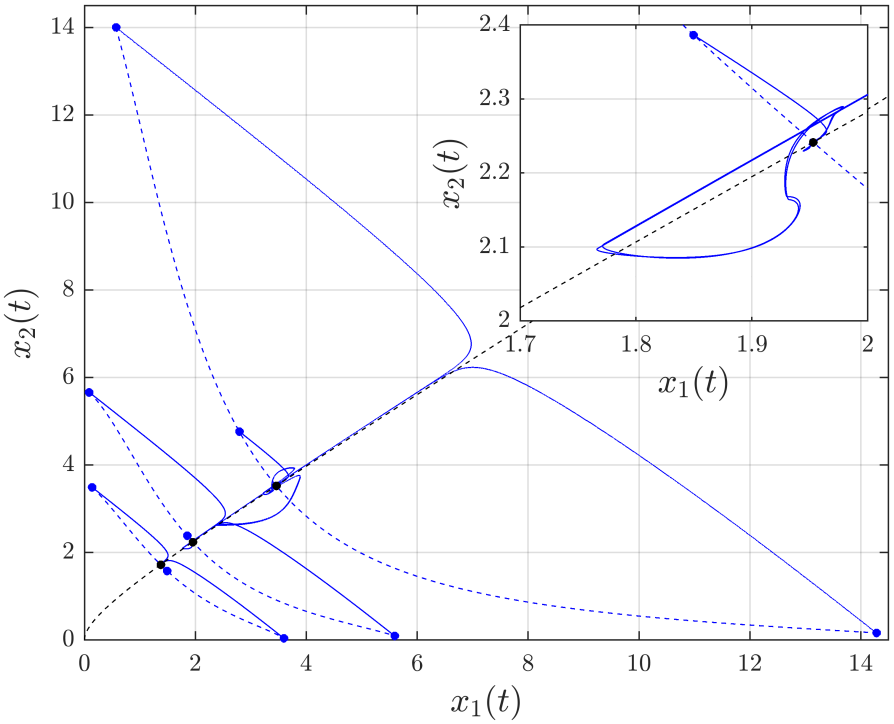

Figure 2.2: Phase plot of Example 2

2.6.3 Example 3

Our final example focuses on the Lyapunov-Krasovskii functional. Of course it cannot be visualized in general as it maps an infinite dimensional function space to nonnegative numbers. However, if we restrict the functional to constant history functions as in the previous examples, then we can compare it to the nondelayed Lyapunov function. In order to do so, we consider the following delayed reversible reactions

$$2X_1 \underset{\kappa_2=1}{\overset{\kappa_1=1,\tau_1=1}{\rightleftharpoons}} 2X_3 \qquad 2X_1 + X_2 \underset{\kappa_4=2,\tau_4=0.5}{\overset{\kappa_3=1}{\rightleftharpoons}} 3X_3,$$

with transformations $\gamma_1(s) = s$, $\gamma_2(s) = \frac{s^2}{1+s}$ and $\gamma_3(s) = \frac{s}{1+s}$. Omitting the vector notation, the corresponding delayed differential equation takes the form

$$\begin{aligned}
\dot{x}_1(t) &= -2\kappa_1 x_1^2(t) + 2\kappa_2 \left(\frac{x_3(t)}{1+x_3(t)}\right)^2 - 2\kappa_3 x_1^2(t)\frac{x_2^2(t)}{1+x_2(t)} + 2\kappa_4 \left(\frac{x_3(t-\tau_4)}{1+x_3(t-\tau_4)}\right)^3 \\
\dot{x}_2(t) &= \kappa_4 \left(\frac{x_3(t-\tau_4)}{1+x_3(t-\tau_4)}\right)^3 - \kappa_3 x_1^2(t)\frac{x_2^2(t)}{1+x_2(t)} \\
\dot{x}_3(t) &= 2\kappa_1 x_1^2(t-\tau_1) - 2\kappa_2 \left(\frac{x_3(t)}{1+x_3(t)}\right)^2 + 3\kappa_3 x_1^2(t)\frac{x_2^2(t)}{1+x_2(t)} - 3\kappa_4 \left(\frac{x_3(t)}{1+x_3(t)}\right)^3.
\end{aligned}$$

It is easy to see that the nondelayed system is conservative as $x_1+x_2+x_3$ is a first integral; that is, the nondelayed positive stoichiometric compatibility classes can be characterized

as

$$\mathcal{S}_p = \left\{x \in \mathbb{R}^3_+ \middle| x_1 + x_2 + x_3 = p_1 + p_2 + p_3\right\},$$

where $p \in \mathbb{R}^3_+$ is arbitrary. Then for any fixed $p \in \mathbb{R}^3_+$ we can visualize the Lyapunov function (2.12) as a two-dimensional function defined on the region

$$\mathcal{D}_p = \left\{x \in \mathbb{R}^2_+ \middle| x_1 + x_2 \leq p_1 + p_2 + p_3\right\}.$$

The delayed positive stoichiometric compatibility class of the delayed system is more complicated and, in particular, it is not a plane; that is, the delayed system is not conservative in this sense. However, it can be shown similarly to the previous examples that the system is persistent, and thus every delayed positive stoichiometric compatibility class contains precisely one positive equilibrium. Assuming a constant history function constructed from an element of $\mathcal{D}_p$, we can compute the value of the functional at the initial point of the corresponding trajectory. Figure 2.3 shows the contour plots of the Lyapunov function and the Lyapunov-Krasovskii functional on $\mathcal{D}_p$ with $p_1 + p_2 + p_3 = 1$.

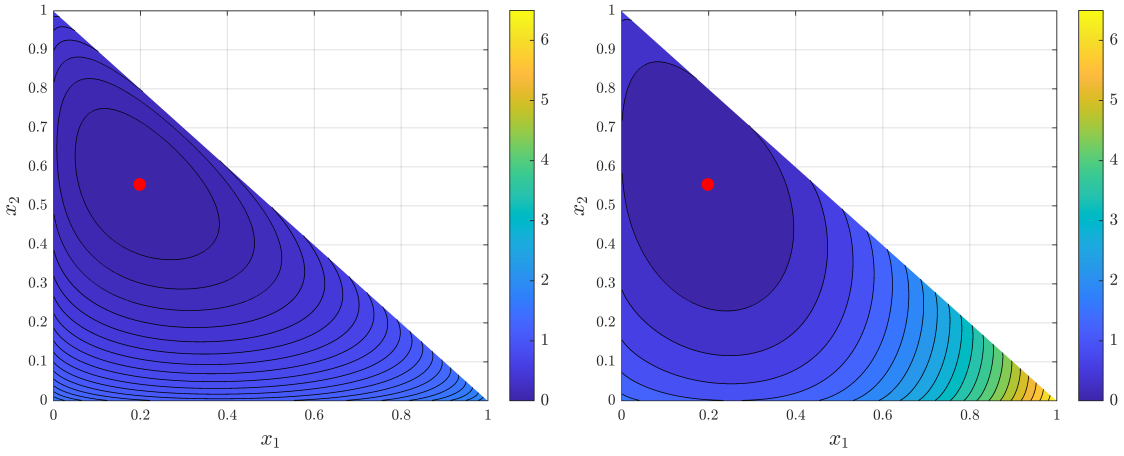

(a) Lyapunov function (b) Lyapunov-Krasovskii functional

Figure 2.3: Level curves of the Lyapunov function of the nondelayed system and the Lyapunov-Krasovskii functional of the delayed system for constant history functions

2.7 Conclusions

The stability of kinetic systems with time delays and general kinetics was studied in this chapter. In preparation for the subsequent analysis, certain stability results of [62] were slightly generalized using the notion of quasi-thermodynamicity introduced in [27]. Then it was shown for delayed complex balanced reaction networks that each positive stoichiometric compatibility class contains precisely one positive equilibrium that is locally asymptotically stable within their positive stoichiometric compatibility classes for

arbitrary finite time delays. A key result of the chapter allowing the stability proof is the construction of an appropriate Lyapunov-Krasovskii functional. Thus, the results proposed in [71] have been generalized for a wide class of delayed non-mass action reaction networks. It was also shown that the global stability of equilibria can be proved as well if the conditions in [73, 76] are fulfilled. Three illustrative examples were given to visualize the theoretical results.

The explicit description of time delays can increase our understanding of complex dynamical phenomena in nature and help to build reliable models. Another natural extension arises when considering interactions that are distributed in space or over structured populations. These effects lead to nonlocal models, often described by partial integro-differential equations, which we study in the next chapter.

Chapter 3

Nonlocal conservation laws

In this chapter we investigate a class of nonlocal conservation laws in several space dimensions, where the continuum average of weighted nonlocal interactions are considered over a finite horizon. We establish well-posedness for a broad class of flux functions and initial data via semigroup theory in Banach spaces and, in particular, via the celebrated Crandall-Liggett Theorem. We also show that the unique mild solution satisfies a Kružkov-type nonlocal entropy inequality. Similarly to the local case, we demonstrate an efficient way of proving various desirable qualitative properties of the unique solution.

3.1 Introduction

We study the semigroup theory of nonlocal conservation laws of the form

$$\begin{aligned} &\frac{\partial u}{\partial t} + \int_{\mathbb{R}^n} \sum_{i=1}^{k} \frac{\phi_i(u, \tau_{\beta_i(h)}u) - \phi_i(\tau_{-\beta_i(h)}u, u)}{\|\beta_i(h)\|_{\mathbb{R}^n}} \omega_i\big(\beta_i(h)\big)\,\mathrm{d}h = 0, \quad \text{in } \mathbb{R}^n \times \mathbb{R}_+; \\ &u(x,0) = u_0(x), \qquad\qquad x \in \mathbb{R}, \end{aligned} \tag{3.1}$$

where $\tau_{\pm h}u(x,t) = u(x \pm h, t)$ denote a spatial shift of the conserved quantity $u(x,t)$ and the flux functions $\phi_i : \mathbb{R} \times \mathbb{R} \mapsto \mathbb{R}$ are assumed to be increasing with respect to their first arguments and decreasing with respect to their second arguments, and to have the property $\phi_i(0,0) = 0$. The number $1 \le k \le n$ denotes the number of subinteractions and the functions $\beta_i : \mathbb{R}^n \mapsto \mathbb{R}^n$ are assumed to be of the form

$$\beta_i(h) = \sum_{j \in B_i} h_j e_j, \qquad h = (h_1, h_2, \ldots, h_n),$$

where the nonempty, pairwise disjoint sets $B_i \subset \{1, 2, \ldots, n\}$ are such that $\bigcup_{i=1}^{k} B_i = \{1, 2, \ldots, n\}$ and e_j denotes the jth unit vector in $\mathbb{R}^n$. The kernel functions $\omega_i \in \mathcal{L}^1(\mathbb{R}^n) \cap$

$\mathcal{L}^\infty(\mathbb{R}^n)$ are assumed to be nonnegative with $\big\|\omega_i\big(\beta_i(.)\big)\big\|_{\mathcal{L}^1(\mathbb{R}^n)} = 1$. We further assume that the support of the kernel functions are finite and are either

1. symmetric around the origin, in which case we further assume that the kernels are even, or

2. contained in $\mathbb{R}^n_+$ such that the closure contains the origin.

For example, in the context of nonlocal particle flows, the above cases allows us to differentiate between multidirectional and unidirectional flows.

Our main examples for the choice of k, β_i and ω_i are as follows.

1. If $k = 1$ and $\beta_1(h) = h$, then the conservation law (3.1) takes the form

$$\frac{\partial u}{\partial t} + \int_{\mathbb{R}^n} \frac{\phi_1(u, \tau_h u) - \phi_1(\tau_{-h} u, u)}{\|h\|_{\mathbb{R}^n}} \omega(h)\, \mathrm{d}h = 0. \tag{3.2}$$

   This case describes a natural multidirectional generalization of the one-dimensional unidirectional nonlocal pair-interaction model investigated in [60]. In fact, if $n = 1$ and $\mathrm{supp}(\omega) \subset \mathbb{R}_+$, the law (3.2) coincides with the latter.

2. If $k = n$ and $\beta_i(h) = h_i e_i$ and $\omega_i(h) = \prod_{j=1}^n \tilde{\omega}_j(h_j)$, where the kernel functions $\tilde{\omega}_j$ have analogous properties to that of ω_i in $\mathbb{R}$ with $\mathrm{supp}(\tilde{\omega}_j) = (-\delta_j, \delta_j)$ for $\delta_j > 0$, then the conservation law (3.1) takes the form

$$\frac{\partial u}{\partial t} + \sum_{i=1}^n \int_{-\delta_i}^{\delta_i} \frac{\phi_i(u, \tau_{h_i e_i} u) - \phi_i(\tau_{-h_i e_i} u, u)}{|h_i|} \tilde{\omega}_i(h_i)\, \mathrm{d}h_i = 0.$$

   Should the underlying model allow such considerations, this case corresponds to interactions that can be unfolded into subinteractions along the individual axes. A clear advantage of this example is the ease of numerical approximation of the integral as described in [60, Section 3.1]. If $n = 1$ and $\mathrm{supp}(\tilde{\omega}_1) = (0, \delta_1)$ instead, then again, we obtain the one-dimensional unidirectional nonlocal pair-interaction model of [60], as in the previous special case.

We say that the nonlocal flux functions ϕ_i are consistent with the local fluxes ψ_i if $\phi_i(a, a) = \psi_i(a)$ holds for all $a \in \mathbb{R}$. For consistent flux functions, if in addition, the weighting kernels are smooth with their support approaching zero, both special cases formally lead to the standard local conservation law

$$\frac{\partial u}{\partial t} + \sum_{i=1}^n \frac{\partial \psi_i(u)}{\partial x_i} = 0. \tag{3.3}$$

For the formal derivation of (3.1) we utilize the nonlocal vector calculus established in [87, 88]. Let $\boldsymbol{\nu}, \tilde{\boldsymbol{\nu}}, \boldsymbol{\alpha} : \mathbb{R}^n \times \mathbb{R}^n \mapsto \mathbb{R}^k$ be vector two-point functions defined by the coordinate functions

$$\begin{aligned}
\boldsymbol{\nu}_i(u)(x,y,t) &= \phi_i\Big(u(x,t), u\big(x+\beta_i(y-x),t\big)\Big),\\
\tilde{\boldsymbol{\nu}}_i(u)(x,y,t) &= \phi_i\Big(u\big(x+\beta_i(y-x),t\big), u(x,t)\Big),\\
\boldsymbol{\alpha}_i(x,y) &= \frac{\omega_i\big(\beta_i(y-x)\big)}{\|\beta_i(y-x)\|_{\mathbb{R}^n}}.
\end{aligned}$$

Then, the nonlocal point divergence is defined as

$$\mathcal{D}\big(\boldsymbol{\nu}(u), \tilde{\boldsymbol{\nu}}(u)\big)(x,t) = \int_{\mathbb{R}^n} \big(\boldsymbol{\nu}(u)(x,y,t) - \tilde{\boldsymbol{\nu}}(u)(x,y,t)\big) \cdot \boldsymbol{\alpha}(x,y)\,\mathrm{d}y$$

and repeated changes of variables in the integral gives

$$\begin{aligned}
\mathcal{D}\big(\boldsymbol{\nu}(u), \tilde{\boldsymbol{\nu}}(u)\big)(x,t) &= \int_{\mathbb{R}^n} \sum_{i=1}^{k} \frac{\phi_i(u, \tau_{\beta_i(h)}u) - \phi_i(\tau_{\beta_i(h)}u, u)}{\|\beta_i(h)\|_{\mathbb{R}^n}} \omega_i\big(\beta_i(h)\big)\,\mathrm{d}h\\
&= \int_{\mathbb{R}^n} \sum_{i=1}^{k} \frac{\phi_i(u, \tau_{\beta_i(h)}u) - \phi_i(\tau_{-\beta_i(h)}u, u)}{\|\beta_i(h)\|_{\mathbb{R}^n}} \omega_i\big(\beta_i(h)\big)\,\mathrm{d}h\,.
\end{aligned} \tag{3.4}$$

The theory of abstract balance laws thoroughly discussed in [87, Section 7] shows that in the absence of external sources a class of nonlocal balance laws are given by

$$\frac{\partial u}{\partial t}(x,t) + \mathcal{D}\big(\boldsymbol{\nu}(u), \tilde{\boldsymbol{\nu}}(u)\big)(x,t) = 0,$$

which, combined with (3.4), gives exactly the law (3.1).

It is well known that the solution of (3.1) (including the local case (3.3) as well) may develop spatial discontinuities (shock waves) over time, even if the initial data is smooth. Hence the Cauchy problem must be considered in a weak or generalized sense. However, there might be infinitely many weak solutions of (3.1) for given initial data. This fact lead to the development of additional constraints, such as the entropy condition, selecting the unique, physically relevant weak solution, which in this case is the so-called entropy solution.

The well-posedness of the local conservation law (3.3) is a thoroughly investigated problem, heavily influenced by the profound work of Kružkov [89]. Kružkov showed uniqueness via a priori estimates and existence using the vanishing viscosity method for bounded and measurable initial data and sufficiently smooth flux functions, thus achieving well-posedness. Existence of entropy solutions can often be proved by the convergence of an appropriate numerical scheme [90, 91] (the technique was first used to prove the existence of weak solutions [92, 93]). Another classical framework is nonlinear semigroup

theory and, in particular, the celebrated Crandall-Liggett Theorem [94], which was first used to prove well-posedness by Crandall [95]. Many combinations of these approaches were developed, a notable example being the approximation of semigroups of contractions [96].

The well-posedness of the one-dimensional nonlocal Cauchy problem with $\beta_1(h) = h$ was investigated in [60], where the existence of an entropy solution was proved through the convergence of an appropriate finite volume scheme, and the uniqueness of this solution was proved via Kružkov's method. While this approach could be extended for multidimensional non-homogeneous Cauchy problems in some special cases (see our second example above), the method is difficult to apply in the generality of (3.1) if $k < n$. Instead, we will also work with the semigroup framework, which provides an elegant way of handling further problems like inhomogeneous conservation laws [97] or error control of finite volume methods [98]. Another particular advantage of semigroup theory is the ability to handle $\mathcal{L}^1(\mathbb{R}^n)$ initial data, while with the methods of [60] one can only show existence and uniqueness for $\mathcal{L}^1(\mathbb{R}^n) \cap \mathcal{L}^\infty(\mathbb{R}^n)$ initial data. The semigroup framework considers generalized solutions of abstract Cauchy problems, often called mild solutions. In general, a mild solution can coincide with a weak solution or an entropy solution or, in some cases, with neither; after proving well-posedness an additional investigation is necessary to determine this.

The main results of the chapter are contained in Theorems 3.3.8 and 3.3.9 and Corollary 3.3.11. In Theorem 3.3.8, we give appropriate circumstances under which there exists an operator satisfying the assumptions of the Crandall-Liggett Theorem. In Theorem 3.3.9, we show that the unique mild solution of (3.1) satisfies a nonlocal Kružkov-type entropy inequality and has many other qualitative properties that are desirable from a physical point of view. In Corollary 3.3.11 we extend the well-posedness to conservation laws under Carathéodory forcing.

The outline of the chapter is as follows. In Section 3.2, we introduce notations and the abstract framework. In Section 3.3, we give the necessary definitions and state our main results. Section 3.4 contains the proof of the main results. The main steps of the proofs are based on [95], however, there are significant nontrivial differences in the details. The difficulty in carrying out this construction is the absence of flux derivatives rendering the method of integration by parts and thus many simplifying steps inapplicable. Most of these complications can be solved by a formally similar technique obtained via changes of variables in the integrals; the technique is often called integration by parts for difference

quotients, see, for example [99, page 295]. However, a significant step that cannot be resolved in such manner is the verification of the range condition. Crandall uses a perturbation results to establish this, namely [100, Theorem 3.2], but this approach does not seem to be applicable in the nonlocal setting. Instead, we use a fix-point based approach similar to that of [101, Chapter 4] and [102, Proposition IV.3]. Throughout the chapter the arguments of the functions β_i and ω_i are omitted unless necessary and C is used as a generic constant that may take on different values at different occurrences.

3.2 Preliminaries

We give a brief introduction of the abstract setting based on [95, 103, 104].

3.2.1 Mild solutions of the abstract Cauchy problem

Let X be a real Banach space and A be a possibly multivalued operator in X and $J = [0, T] \subset \mathbb{R}$ and $f \in \mathcal{L}^1(J, X)$. Consider the quasi-autonomous Cauchy problem

$$\begin{aligned} &u' + Au \ni f(t), \qquad t \in J; \\ &u(0) = u_0 \end{aligned} \tag{3.5}$$

for $u_0 \in \overline{D(A)}$. We call $u \in \mathcal{C}(J, X)$ a mild solution of (3.5) if for every $\epsilon > 0$ there exists a partition $0 = t_0 \le t_1 \le t_2 \le \cdots \le t_N$ of $[0, t_N]$ and sequences $\{z_1, z_2, \ldots, z_N\}$, $\{f_1, f_2, \ldots, f_N\}$ in X such that

$$\begin{aligned} &t_i - t_{i-1} < \epsilon, && i = 1, \ldots, N \\ &T - \epsilon < t_N \le T, \\ &\sum_{i=1}^{N} \int_{t_{i-1}}^{t_i} \|f(s) - f_i\| \, \mathrm{d}s < \epsilon, \\ &\frac{z_i - z_{i-1}}{t_i - t_{i-1}} + Az_i \ni f_i, && i = 1, \ldots, N \end{aligned}$$

and $\|z(t) - u(t)\| \le \epsilon$ on $[0, t_N]$, where $z : [0, t_N] \mapsto X$ is defined by

$$z(t) = z_i \qquad \text{for } t_{i-1} \le t < t_i, \ i = 1, 2, \ldots, N.$$

The piecewise constant function z is called an ϵ-approximate solution of (3.5).

Let $F : J \times \overline{D(A)} \mapsto 2^X \backslash \emptyset$. A mild solution of the Cauchy problem

$$\begin{aligned} &u' \in -Au + F(t, u), \qquad t \in J; \\ &u(0) = u_0 \end{aligned}$$

is a function that is a mild solution of the quasi-autonomous problem

$$\begin{aligned} &u' + Au \ni f(t), \qquad t \in J; \\ &u(0) = u_0 \end{aligned}$$

with some $f \in \mathcal{L}^1(J, X)$ such that $f(t) \in F\big(t, u(t)\big)$ a.e.

3.2.2 Crandall-Liggett Theorem

Let X be a Banach space and A be a possibly multivalued operator in X. The operator A is called accretive if, for any $\lambda > 0$ and $x, y \in D(A)$, the inequality

$$\|(x + \lambda u) - (y + \lambda v)\| \geq \|x - y\|$$

holds, where $u \in Ax$ and $v \in Ay$. The operator A is called m-accretive if it is accretive and the operator $I + \lambda A$ is surjective for $\lambda > 0$; that is, we have

$$R(I + \lambda A) = \bigcup_{x \in D(A)} \bigcup_{v \in Ax} \{x + \lambda v\} = X. \tag{3.6}$$

Theorem 3.2.1 (Crandall-Liggett Theorem)**.** *Let X be a Banach space and A be a possibly multivalued m-accretive operator in X. Then for $\epsilon > 0$ and $u_0 \in X$ the problem*

$$\begin{aligned} &\frac{1}{\epsilon}\big(u_\epsilon(t) - u_\epsilon(t - \epsilon)\big) + Au_\epsilon(t) \ni 0, \qquad && t \geq 0; \\ &u_\epsilon(0) = u_0, && t < 0 \end{aligned} \tag{3.7}$$

has a unique solution $u_\epsilon(t)$ on $[0, \infty)$. If $u_0 \in \overline{D(A)}$, then $\lim_{\epsilon \to 0} u_\epsilon(t)$ converges uniformly to the unique mild solution of (3.5) in bounded sets and $\big(S(t)\big)_{t \geq 0}$ defined by $S(t)u_0 = \lim_{\epsilon \to 0} u_\epsilon(t)$ is a semigroup of contractions on $\overline{D(A)}$; that is, we have

(i) *$S(t) : \overline{D(A)} \mapsto \overline{D(A)}$ for $t \geq 0$,*

(ii) *$S(t)S(\tau) = S(t + \tau)$ for $t, \tau \geq 0$,*

(iii) *$\|S(t)v - S(t)w\| \leq \|v - w\|$ for $t \geq 0$ and $v, w \in D(A)$,*

(iv) *$S(0) = I$,*

(v) *$S(t)v$ is continuous in the pair (t, v).*

3.3 Statement of new results

The abstract framework of operator semigroups and, in particular, the fundamental Crandall-Liggett Theorem utilizes the notion of mild solutions. Later we will show that

the unique mild solution of the conservation law (3.1) also satisfies a Kružkov-type entropy inequality. For the exact formulation of this inequality let us define the function $\eta : \mathbb{R}^n \mapsto \mathbb{R}$ to be an entropy of (3.1) with entropy fluxes $q_i : \mathbb{R}^n \times \mathbb{R}^n \mapsto \mathbb{R}$ given that it is continuously differentiable and the equality

$$\eta'(u) \int_{\mathbb{R}^n} \frac{\phi_i(u, \tau_{\beta_i} u) - \phi_i(\tau_{-\beta_i} u, u)}{\|\beta_i\|_{\mathbb{R}^n}} \omega_i \, \mathrm{d}h = \int_{\mathbb{R}^n} \frac{q_i(u, \tau_{\beta_i} u) - q_i(\tau_{-\beta_i} u, u)}{\|\beta_i\|_{\mathbb{R}^n}} \omega_i \, \mathrm{d}h \tag{3.8}$$

holds for all $i = 1, 2, \ldots, k$. Then if $u(t, x)$ is a $\mathcal{C}^1$ solution of (3.1) then it also satisfies

$$\frac{\partial \eta(u)}{\partial t} + \int_{\mathbb{R}^n} \sum_{i=1}^{k} \frac{q_i(u, \tau_{\beta_i} u) - q_i(\tau_{-\beta_i} u, u)}{\|\beta_i\|_{\mathbb{R}^n}} \omega_i \, \mathrm{d}h = 0.$$

In the case of an $\eta \in \mathcal{C}^2$ convex entropy standard vanishing viscosity arguments (using integration by parts for difference quotients) show that the inequality

$$\int_0^T \int_{\mathbb{R}^n} \eta(u) \frac{\partial f}{\partial t} \, \mathrm{d}x \, \mathrm{d}t + \int_0^T \int_{\mathbb{R}^n} \int_{\mathbb{R}^n} \sum_{i=1}^{k} \frac{\tau_{\beta_i} f - f}{\|\beta_i\|_{\mathbb{R}^n}} q_i(u, \tau_{\beta_i}) \omega_i \, \mathrm{d}h \, \mathrm{d}x \, \mathrm{d}t \geq 0$$

holds for any $T > 0$, nonnegative $f \in \mathcal{C}_0^\infty\big(\mathbb{R}^n \times (0, T)\big)$. Our goal is to utilize classical Kružkov-entropies of the form $\eta(u) := \eta(u, c) = |u - c|$, however, in this case, an explicit formula for q_i does not seem to reveal itself. Instead, during the vanishing viscosity derivation we rely on (3.8) to arrive at the following definition:

Definition 3.3.1. *A function $u \in \mathcal{L}^1(\mathbb{R}^n \times (0, T)) \cap \mathcal{L}^\infty(\mathbb{R}^n \times (0, T))$ is an entropy solution of* (3.1) *if the inequality*

$$0 \leq \int_0^T \int_{\mathbb{R}^n} \Bigg(|u - c| \frac{\partial f}{\partial t} + \int_{\mathbb{R}^n} \sum_{i=1}^{k} \frac{\tau_{\beta_i} f \operatorname{sign}_0(\tau_{\beta_i} u - c) - f \operatorname{sign}_0(u - c)}{\|\beta_i\|_{\mathbb{R}^n}} \big(\phi_i(u, \tau_{\beta_i} u) - \phi_i(c, c)\big) \omega_i \, \mathrm{d}h \Bigg) \mathrm{d}x \, \mathrm{d}t$$

holds for any $T > 0$, nonnegative $f \in \mathcal{C}_0^\infty\big(\mathbb{R}^n \times (0, T)\big)$ and $c \in \mathbb{R}$.

Remark 3.3.2. *Let the functions $\tilde{q}_i$ be given by*[1]

$$\begin{aligned} \tilde{q}_i(a, b, c) &= \phi_i(a \vee c, b \vee c) - \phi_i(a \wedge c, b \wedge c) \\ &= \phi_i\big(\max\{a, c\}, \max\{b, c\}\big) - \phi_i\big(\min\{a, c\}, \min\{b, c\}\big) \\ &= \frac{\operatorname{sign}_0(a - c) + \operatorname{sign}_0(b - c)}{2} \big(\phi_i(a, b) - \phi_i(c, c)\big) \\ &+ \frac{\operatorname{sign}_0(a - c) - \operatorname{sign}_0(b - c)}{2} \big(\phi_i(a, c) - \phi_i(c, b)\big), \end{aligned}$$

[1] As already noted by [105, Definition 2.2], the second line is not identical to the corresponding equation in [60, p. 2470], which is assumed to be a misprint. Here we gave a more straightforward formula.

where

$$\operatorname{sign}_0(x) = \begin{cases} 1 & x > 0, \\ 0 & x = 0, \\ -1 & x < 0. \end{cases}$$

For the sake of notational simplicity, let us omit the sum in this remark. The properties of ϕ_i after adding and subtracting $\phi_i(c,c)$ imply that

$$\operatorname{sign}_0(u-c)\int_{\mathbb{R}^n}\frac{\phi_i(u,\tau_{\beta_i}u)-\phi_i(\tau_{-\beta_i}u,u)}{\|\beta_i\|_{\mathbb{R}^n}}\omega_i\,\mathrm{d}h \geq \int_{\mathbb{R}^n}\frac{\tilde{q}_i(u,\tau_{\beta_i}u,c)-\tilde{q}_i(\tau_{-\beta_i}u,u,c)}{\|\beta_i\|_{\mathbb{R}^n}}\omega_i\,\mathrm{d}h\,,$$

and thus it seems reasonable to define entropy solutions using $\tilde{q}_i$ as entropy fluxes corresponding to the entropy $|u-c|$. But, in fact, using the product rule for difference quotients shows that

$$\begin{aligned}
&\int_0^T\int_{\mathbb{R}^n}\int_{\mathbb{R}^n}\frac{\tau_{\beta_i}f\operatorname{sign}_0(\tau_{\beta_i}u-c)-f\operatorname{sign}_0(u-c)}{\|\beta_i\|_{\mathbb{R}^n}}\big(\phi_i(u,\tau_{\beta_i}u)-\phi_i(c,c)\big)\omega_i\,\mathrm{d}h\,\mathrm{d}x\,\mathrm{d}t\\
&=\int_0^T\int_{\mathbb{R}^n}\int_{\mathbb{R}^n}\frac{\tau_{\beta_i}f-f}{\|\beta_i\|_{\mathbb{R}^n}}\operatorname{sign}_0(\tau_{\beta_i}u-c)\big(\phi_i(u,\tau_{\beta_i}u)-\phi_i(c,c)\big)\omega_i\,\mathrm{d}h\,\mathrm{d}x\,\mathrm{d}t+\\
&\int_0^T\int_{\mathbb{R}^n}\int_{\mathbb{R}^n}f\frac{\operatorname{sign}_0(\tau_{\beta_i}u-c)-\operatorname{sign}_0(u-c)}{\|\beta_i\|_{\mathbb{R}^n}}\big(\phi_i(u,\tau_{\beta_i}u)-\phi_i(c,c)\big)\omega_i\,\mathrm{d}h\,\mathrm{d}x\,\mathrm{d}t\,.
\end{aligned}$$

Clearly

$$\begin{aligned}
&\operatorname{sign}_0(\tau_{\beta_i}v-c)\big[\phi_i(v,\tau_{\beta_i}v)-\phi_i(c,c)\big]\\
&\leq \phi_i(v\vee c,\tau_{\beta_i}v\vee c)-\phi_i(v\wedge c,\tau_{\beta_i}v\wedge c)=\tilde{q}_i(v,\tau_{\beta_i}v,c)
\end{aligned}$$

and similarly

$$-\operatorname{sign}_0(v-c)\big[\phi_i(v,\tau_{\beta_i}v)-\phi_i(c,c)\big]\leq -\tilde{q}_i(v,\tau_{\beta_i}v,c)$$

holds, thus

$$\big[\operatorname{sign}_0(\tau_{\beta_i}v-c)-\operatorname{sign}_0(v-c)\big]\big[\phi_i(v,\tau_{\beta_i}v)-\phi_i(c,c)\big]\leq 0 \tag{3.9}$$

and finally

$$\begin{aligned}
&\int_0^T\int_{\mathbb{R}^n}\int_{\mathbb{R}^n}\frac{\tau_{\beta_i}f\operatorname{sign}_0(\tau_{\beta_i}u-c)-f\operatorname{sign}_0(u-c)}{\|\beta_i\|_{\mathbb{R}^n}}\big(\phi_i(u,\tau_{\beta_i}u)-\phi_i(c,c)\big)\omega_i\,\mathrm{d}h\,\mathrm{d}x\,\mathrm{d}t\\
&\leq\int_0^T\int_{\mathbb{R}^n}\int_{\mathbb{R}^n}\frac{\tau_{\beta_i}f-f}{\|\beta_i\|_{\mathbb{R}^n}}\tilde{q}_i(u,\tau_{\beta_i}u,c)\omega_i\,\mathrm{d}h\,\mathrm{d}x\,\mathrm{d}t\,;
\end{aligned}$$

that is, in some sense, the inequality in Definition 3.3.1 is more precise *in selecting the physically relevant weak solution than the right-hand side of the above inequality. This precision turns out to be crucial in later steps; the operator defined in Definition 3.3.6 does not seem to be accretive with the functions $\tilde{q}_i$ which is an essential property to derive uniqueness of solutions via the Crandall-Liggett theorem.*

Throughout the chapter difference quotients will be denoted by

$$D^y f = \frac{\tau_y f - f}{\|y\|_{\mathbb{R}^n}},$$

where $y \in \mathbb{R}^n$ and the partial derivative of the ϕ_i functions with respect to their first and second argument will be denoted by $\phi'_{i,1}$ and $\phi'_{i,2}$, respectively. For open subsets Ω of $\mathbb{R}^n$ let $\mathcal{W}^{k,p}(\Omega)$ denote the Sobolev space of functions whose distributional derivatives of order at most k are in $\mathcal{L}^p(\Omega)$. The space $\mathcal{W}_0^{k,p}(\Omega) \subset \mathcal{W}^{k,p}(\Omega)$ denotes the set of functions vanishing at the boundary of Ω and $\mathcal{W}_{loc}^{k,p}(\Omega)$ denotes the set of locally integrable functions whose restriction to any pre-compact $Q \Subset \Omega$ lies in $\mathcal{W}^{k,p}(Q)$. We will use the standard notation $\mathcal{H}^k(\Omega) := \mathcal{W}^{k,2}(\Omega)$.

We rewrite the nonlocal conservation law (3.1) using the operator

$$Bu = \int_{\mathbb{R}^n} \sum_{i=1}^{k} \frac{\phi_i(u, \tau_{\beta_i} u) - \phi_i(\tau_{-\beta_i} u, u)}{\|\beta_i\|_{\mathbb{R}^n}} \omega_i \, \mathrm{d}h$$

as

$$\frac{\partial u}{\partial t} + Bu = 0. \tag{3.10}$$

The following lemma shows that for continuously differentiable fluxes the operator B maps $\mathcal{W}^{1,p}(\mathbb{R}^n)$ to $\mathcal{L}^p(\mathbb{R}^n)$.

Lemma 3.3.3. *Let $\phi_i \in \mathcal{C}^1(\mathbb{R} \times \mathbb{R})$ have bounded partial derivatives. Then $v \in \mathcal{W}^{1,p}(\mathbb{R}^n)$ implies $Bv \in \mathcal{L}^p(\mathbb{R}^n)$ for all $1 \le p < \infty$. In particular, there is a constant $C = C(p) > 0$ such that $\|Bv\|_{\mathcal{L}^p(\mathbb{R}^n)} \le C \|\nabla v\|_{\mathcal{L}^p(\mathbb{R}^n)}$ for all $v \in \mathcal{W}^{1,p}(\mathbb{R}^n)$.*

Proof. Let $|\phi'_{i,1}| \le K_{i,1}$ and $|\phi'_{i,2}| \le K_{i,2}$ and $\frac{1}{p} + \frac{1}{q} = 1$. Setting $K_i = \max\{K_{i,1}, K_{i,2}\}$ we find that

$$\begin{aligned}
\|Bv\|^p_{\mathcal{L}^p(\mathbb{R}^n)} &= \int_{\mathbb{R}^n} \left| \int_{\mathbb{R}^n} \sum_{i=1}^{k} \frac{\phi_i(v, \tau_{\beta_i} v) - \phi_i(\tau_{-\beta_i} v, v)}{\|\beta_i\|_{\mathbb{R}^n}} \omega_i \, \mathrm{d}h \right|^p \mathrm{d}x \\
&\le \int_{\mathbb{R}^n} \left(\int_{\mathbb{R}^n} \sum_{i=1}^{k} K_i \frac{|v - \tau_{-\beta_i} v| + |\tau_{\beta_i} v - v|}{\|\beta_i\|_{\mathbb{R}^n}} \omega_i \, \mathrm{d}h \right)^p \mathrm{d}x \\
&\le k^{p-1} \sum_{i=1}^{k} K_i^p \int_{\mathbb{R}^n} \left(\int_{\mathbb{R}^n} \left(\left| D^{\beta_i} \tau_{-\beta_i} v \right| + \left| D^{\beta_i} v \right| \right) \omega_i \, \mathrm{d}h \right)^p \mathrm{d}x \qquad (3.11) \\
&\le k^{p-1} \sum_{i=1}^{k} K_i^p \|\omega_i\|^p_{\mathcal{L}^q(\mathbb{R}^n)} \int_{\mathbb{R}^n} \int_{\mathrm{supp}(\omega_i)} \left(\left| D^{\beta_i} \tau_{-\beta_i} v \right| + \left| D^{\beta_i} v \right| \right)^p \mathrm{d}h \, \mathrm{d}x \\
&\le 2^{p-1} k^{p-1} \sum_{i=1}^{k} K_i^p \|\omega_i\|^p_{\mathcal{L}^q(\mathbb{R}^n)} \int_{\mathrm{supp}(\omega_i)} \|\nabla v\|^p_{\mathcal{L}^p(\mathbb{R}^n)} \, \mathrm{d}h = C \|\nabla v\|^p_{\mathcal{L}^p(\mathbb{R}^n)},
\end{aligned}$$

where we used the Lipschitz continuity of ϕ in the first inequality, Hölder's inequality in the third inequality and finally Fubini's theorem and [106, Proposition 9.3(iii)] in the fourth inequality. □

The continuity of B is established by our next lemma.

Lemma 3.3.4. *Let the assumptions of Lemma 3.3.3 hold. Then B is continuous from $\mathcal{H}^1(\mathbb{R}^n)$ to $\mathcal{L}^2(\mathbb{R}^n)$.*

Proof. Let $u, v \in \mathcal{H}^1(\mathbb{R}^n)$. Similar estimates as in the proof of Lemma 3.3.3 lead to

$$\begin{aligned}
&\|Bu - Bv\|^2_{\mathcal{L}^2(\mathbb{R}^n)} \\
&= \int_{\mathbb{R}^n} \left(\int_{\mathbb{R}^n} \sum_{i=1}^{k} D^{\beta_i} \big[\phi_i(\tau_{-\beta_i} u, u) - \phi_i(\tau_{-\beta_i} v, v)\big] \omega_i \, \mathrm{d}h \right)^2 \mathrm{d}x \\
&\leq C \sum_{i=1}^{k} \int_{\mathrm{supp}(\omega_i)} \Big\| D^{\beta_i} \big[\phi_i(\tau_{-\beta_i} u, u) - \phi_i(\tau_{-\beta_i} v, v)\big] \Big\|^2_{\mathcal{L}^2(\mathbb{R}^n)} \mathrm{d}h \\
&\leq C \sum_{i=1}^{k} \int_{\mathrm{supp}(\omega_i)} \big\| \nabla \big[\phi_i(\tau_{-\beta_i} u, u) - \phi_i(\tau_{-\beta_i} v, v)\big] \big\|^2_{\mathcal{L}^2(\mathbb{R}^n)} \mathrm{d}h \\
&= C \sum_{i=1}^{k} \int_{\mathrm{supp}(\omega_i)} \Big\| \phi'_{i,1}(\tau_{-\beta_i} u, u) \nabla \tau_{-\beta_i} u + \phi'_{i,2}(\tau_{-\beta_i} u, u) \nabla u \\
&\quad - \phi'_{i,1}(\tau_{-\beta_i} v, v) \nabla \tau_{-\beta_i} v - \phi'_{i,2}(\tau_{-\beta_i} v, v) \nabla v \Big\|^2_{\mathcal{L}^2(\mathbb{R}^n)} \mathrm{d}h \,.
\end{aligned}$$

By introducing mixed terms we find that

$$\begin{aligned}
&\|Bu - Bv\|^2_{\mathcal{L}^2(\mathbb{R}^n)} \\
&\leq C \sum_{i=1}^{k} \int_{\mathrm{supp}(\omega_i)} \Big(\big\| \big[\phi'_{i,1}(\tau_{-\beta_i} u, u) - \phi'_{i,1}(\tau_{-\beta_i} v, v)\big] \nabla \tau_{-\beta_i} u \big\|_{\mathcal{L}^2(\mathbb{R}^n)} \\
&+ \big\| \big[\phi'_{i,2}(\tau_{-\beta_i} u, u) - \phi'_{i,2}(\tau_{-\beta_i} v, v)\big] \nabla u \big\|_{\mathcal{L}^2(\mathbb{R}^n)} \\
&+ \big\| \phi'_{i,1}(\tau_{-\beta_i} v, v) \big\|^2_{\mathcal{L}^\infty(\mathbb{R}^n)} \|\nabla \tau_{-\beta_i} (u - v)\|^2_{\mathcal{L}^2(\mathbb{R}^n)} \\
&+ \big\| \phi'_{i,2}(\tau_{-\beta_i} v, v) \big\|^2_{\mathcal{L}^\infty(\mathbb{R}^n)} \|\nabla (u - v)\|^2_{\mathcal{L}^2(\mathbb{R}^n)} \Big) \, \mathrm{d}h \,.
\end{aligned} \tag{3.12}$$

Let v converge to u in $\mathcal{H}^1(\mathbb{R}^n)$ through a sequence $\{u_n\} \subset \mathcal{H}^1(\mathbb{R}^n)$ and let $\{u_{n_k}\}$ be a subsequence of $\{u_n\}$. Since u_{n_k} also converges to u as $n_k \to \infty$, there exists a subsequence $\{u_{n_{k_l}}\}$ of $\{u_{n_k}\}$ such that $u_{n_{k_l}} \to u$ a.e. as $n_{k_l} \to \infty$. Let $|\phi'_{i,1}| \leq K_{i,1}$ and $|\phi'_{i,2}| \leq K_{i,2}$ and observe that

$$\begin{aligned}
\Big| \big[\phi'_{i,1}(\tau_{-\beta_i} u, u) - \phi'_{i,1}(\tau_{-\beta_i} u_{n_{k_l}}, u_{n_{k_l}})\big] \nabla \tau_{-\beta_i} u \Big| &\leq 2K_{i,1} \big| \nabla \tau_{-\beta_i} u \big|, \\
\Big| \big[\phi'_{i,2}(\tau_{-\beta_i} u, u) - \phi'_{i,2}(\tau_{-\beta_i} u_{n_{k_l}}, u_{n_{k_l}})\big] \nabla \tau_{-\beta_i} u \Big| &\leq 2K_{i,2} \big| \nabla u \big|.
\end{aligned}$$

Using the dominated convergence theorem and the continuity of ϕ_i we find that the first two terms in (3.12) converge to zero as $n_{k_l} \to \infty$. Similarly, since $\phi'_{i,1}$ and $\phi'_{i,2}$ are bounded and $u_{n_{k_l}} \to u$ in $\mathcal{H}^1(\mathbb{R}^n)$, the second two terms also converge to zero as $n_{k_l} \to \infty$. Since $\{u_{n_k}\}$ was arbitrary we conclude that each subsequence of the sequence $\|Bu - Bu_n\|^2_{\mathcal{L}^2(\mathbb{R})}$

has a convergent subsequence with limit zero; that is, the sequence itself converges to zero and the proof is complete. □

Remark 3.3.5. *In [105] the authors consider the case (in one dimension) when* $\int_{\mathbb{R}^n} \frac{\omega_i(\beta_i)}{\|\beta_i\|_{\mathbb{R}^n}} < \infty$. *In this case the above calculations can be modified to show that* $B : \mathcal{L}^1(\mathbb{R}^n) \mapsto \mathcal{L}^1(\mathbb{R}^n)$ *is Lipschitz continuous. Hence, standard contraction mapping principle shows existence and uniqueness without entropy conditions. However, in this special case the kernels* ω_i *assign small weight to close interactions and more weight as the interaction distance increases. As such, the model's applicability to physically relevant problems is reduced.*

We will consider $X = \mathcal{L}^1(\mathbb{R}^n)$ and proceed by verifying the hypotheses of the Crandall-Liggett Theorem for an appropriate operator A in $\mathcal{L}^1(\mathbb{R}^n)$ that is, in some sense, the generalization of the B of (3.10). The operator A will be the closure of the operator A_0 defined as follows.

Definition 3.3.6. *Let* A_0 *be the operator in* $\mathcal{L}^1(\mathbb{R}^n)$ *defined by:* $v \in D(A_0)$ *and* $w \in A_0 v$ *if*

(i) $v, w \in \mathcal{L}^1(\mathbb{R}^n)$,

(ii) $\phi_i(v, \tau_{\beta_i(h)} v) \in \mathcal{L}^1(\mathbb{R}^n)$ *for* $h \in \operatorname{supp}(\omega_i)$ *and* $i = 1, 2, \ldots, k$,

(iii) *the inequality*

$$\begin{aligned} &\int_{\mathbb{R}^n} \operatorname{sign}_0(v - c) w f \, \mathrm{d}x \\ &+ \int_{\mathbb{R}^n} \int_{\mathbb{R}^n} \sum_{i=1}^{k} D^{\beta_i} \big[f \operatorname{sign}_0(v - c) \big] \big(\phi_i(v, \tau_{\beta_i} v) - \phi_i(c, c) \big) \omega_i \, \mathrm{d}h \, \mathrm{d}x \geq 0 \end{aligned} \tag{3.13}$$

holds for any nonnegative $f \in \mathcal{C}_0^\infty(\mathbb{R}^n)$ *and* $c \in \mathbb{R}$.

As we will see later, inequality in Definition 3.3.6(iii) ensures that if $u \in D(A_0)$ is a solution of the abstract Cauchy problem, then it satisfies the entropy inequality in Definition 3.3.1. Lemmata 3.4.1 and 3.4.2 show that under appropriate circumstances A_0 is single-valued and coincides with B, further substantiating our definition.

While the accretivity of A_0, and thus the accretivity of its closure A, can be established in a straightforward manner using a tool described in [95, Proposition 2.1] (see Proposition 3.4.6), the verification of the range condition (3.6) is more intricate. In fact, it requires the treatment of the stationary equation

$$u + Bu = g. \tag{3.14}$$

We define the generalized solutions of (3.14) in terms of A.

Definition 3.3.7. *Let $g \in \mathcal{L}^1(\mathbb{R}^n)$. Then $u \in \mathcal{L}^1(\mathbb{R}^n)$ is a generalized solution of* (3.14) *if $u \in D(A)$ and $g \in (I + A)u$.*

Our first main result is the following theorem.

Theorem 3.3.8. *Let $\phi_i \in \mathcal{W}^{1,\infty}_{loc}(\mathbb{R} \times \mathbb{R})$ and $g \in \mathcal{L}^1(\mathbb{R}^n)$. Then A satisfies the assumptions of the Crandall-Liggett Theorem on $\mathcal{L}^1(\mathbb{R}^n)$ and the unique generalized solution of* (3.14) *is given by $u = (I + A)^{-1}g$.*

Theorem 3.3.8 and the Crandall-Liggett Theorem show that a semigroup of contractions is determined by the operator A, whose various properties are listed in the next theorem.

Theorem 3.3.9. *Let the assumptions of Theorem 3.3.8 hold and S be the semigroup of contractions on $\overline{D(A)}$ obtained from A via the Crandall-Liggett Theorem on $\mathcal{L}^1(\mathbb{R}^n)$. Let $u, v \in \overline{D(A)} \cap \mathcal{L}^\infty(\mathbb{R}^n)$ and $t \geq 0$. Then*

(i) (integrability) *$S(t)v \in \mathcal{L}^p(\mathbb{R}^n)$ for $p \geq 1$, furthermore the estimate $\|S(t)v\|_{\mathcal{L}^p(\mathbb{R}^n)} \leq \|v\|^{\frac{1}{p}}_{\mathcal{L}^1(\mathbb{R}^n)}\|v\|^{1-\frac{1}{p}}_{\mathcal{L}^\infty(\mathbb{R}^n)}$ holds,*

(ii) (maximum principle) *$-\|v^-\|_{\mathcal{L}^\infty(\mathbb{R}^n)} \leq S(t)v \leq \|v^+\|_{\mathcal{L}^\infty(\mathbb{R}^n)}$, where $v^- = \max\{0, -v\}$ and $v^+ = \max\{0, v\}$.*

(iii) (monotonicity) *$\|(S(t)u - S(t)v)^+\|_{\mathcal{L}^1(\mathbb{R}^n)} \leq \|(u - v)^+\|_{\mathcal{L}^1(\mathbb{R}^n)}$,*

(iv) (equicontinuity) *if $y \in \mathbb{R}^n$, then*

$$\int_{\mathbb{R}^n} \big|S(t)v(x + y) - S(t)v(x)\big| \,\mathrm{d}x \leq \int_{\mathbb{R}^n} \big|v(x + y) - v(x)\big| \,\mathrm{d}x\,,$$

(v) (conservation of mass) *$\int_{\mathbb{R}^n} S(t)v(x) \,\mathrm{d}x = \int_{\mathbb{R}^n} v(x) \,\mathrm{d}x$,*

(vi) *$S(t)v$ satisfies the nonlocal entropy inequality in Definition 3.3.1.*

Remark 3.3.10. *Note that the properties (iii)-(v) still hold if we only assume $u, v \in \overline{D(A)}$.*

Corollary 3.3.11. *Let $g : [0, T] \times \overline{D(A)} \mapsto \mathcal{L}^1(\mathbb{R}^n)$ be strongly measurable with respect to t and locally Lipschitz with respect to u such that*

$$\|g(t, u)\|_{\mathcal{L}^1(\mathbb{R}^n)} \leq c(t)\big(1 + \|u\|_{\mathcal{L}^1(\mathbb{R}^n)}\big)$$

holds for some $c \in \mathcal{L}^1([0, T])$. Then the Cauchy problem

$$\frac{\partial u}{\partial t} + \int_{\mathbb{R}^n} \sum_{i=1}^{k} \frac{\phi_i(u, \tau_{\beta_i} u) - \phi_i(\tau_{-\beta_i} u, u)}{\|\beta_i\|_{\mathbb{R}^n}} \omega_i \,\mathrm{d}h = g(t, u), \quad \text{in } \mathbb{R}^n \times (0, T];$$

$$u(x, 0) = u_0(x), \qquad x \in \mathbb{R}$$

has a unique mild solution for each $u_0 \in \overline{D(A)}$ *that depends continuously on* u_0*; that is, the map* $u_0(.) \to u(.,t)$ *is continuous in the Banach space* $X = \mathcal{L}^1(\mathbb{R}^n)$.

Proof. The statement follows directly from [97, Theorem 5.2]. □

3.4 Proofs of the main results

The following lemma shows that A_0 is single-valued for bounded functions.

Lemma 3.4.1. *Let* A_0 *be given by Definition 3.3.6 and* $v \in D(A_0) \cap \mathcal{L}^\infty(\mathbb{R}^n)$. *Then* A_0 *is single-valued and the equality*

$$\int_{\mathbb{R}^n} A_0 v f \,\mathrm{d}x = -\int_{\mathbb{R}^n}\int_{\mathbb{R}^n} \sum_{i=1}^{k} D^{\beta_i} f \phi_i(v, \tau_{\beta_i} v)\omega_i \,\mathrm{d}h \,\mathrm{d}x$$

holds for any nonnegative $f \in \mathcal{C}_0^\infty(\mathbb{R}^n)$.

Proof. Let $w \in A_0 v$. Then by (3.13) for any nonnegative $f \in \mathcal{C}_0^\infty(\mathbb{R}^n)$ and $c \in \mathbb{R}$ we have

$$\int_{\mathbb{R}^n} wf \,\mathrm{d}x + \int_{\mathbb{R}^n}\int_{\mathbb{R}^n} \sum_{i=1}^{k} D^{\beta_i}\big[f \operatorname{sign}_0(v-c)\big]\big(\phi_i(v, \tau_{\beta_i} v) - \phi_i(c,c)\big)\omega_i \,\mathrm{d}h \,\mathrm{d}x \geq 0,$$

thus for $c = \|v\|_{\mathcal{L}^\infty(\mathbb{R}^n)} + 1$, we have that

$$\int_{\mathbb{R}^n} wf \,\mathrm{d}x \leq -\int_{\mathbb{R}^n}\int_{\mathbb{R}^n} \sum_{i=1}^{k} D^{\beta_i} f \phi_i(v, \tau_{\beta_i} v)\omega_i \,\mathrm{d}h \,\mathrm{d}x\,.$$

Similarly, letting $c = -(\|v\|_{\mathcal{L}^\infty(\mathbb{R}^n)} + 1)$ yields

$$\int_{\mathbb{R}^n} wf \,\mathrm{d}x \geq -\int_{\mathbb{R}^n}\int_{\mathbb{R}^n} \sum_{i=1}^{k} D^{\beta_i} f \phi_i(v, \tau_{\beta_i} v)\omega_i \,\mathrm{d}h \,\mathrm{d}x\,,$$

showing that for any $w \in A_0 v$, the following equality holds

$$\int_{\mathbb{R}^n} wf \,\mathrm{d}x = -\int_{\mathbb{R}^n}\int_{\mathbb{R}^n} \sum_{i=1}^{k} D^{\beta_i} f \phi_i(v, \tau_{\beta_i} v)\omega_i \,\mathrm{d}h \,\mathrm{d}x\,.$$

To show that $A_0 v$ is single-valued, suppose that $w_1, w_2 \in A_0 v$. Then the equality $\int_{\mathbb{R}^n} w_1 f \,\mathrm{d}x = \int_{\mathbb{R}^n} w_2 f \,\mathrm{d}x$ holds for all nonnegative $f \in \mathcal{C}_0^\infty(\mathbb{R}^n)$, thus $w_1 = w_2$ a.e. □

The following lemma shows that A_0 extends B on $\mathcal{C}_0^1(\mathbb{R}^n)$.

Lemma 3.4.2. *Let* $\phi_i \in \mathcal{C}^1(\mathbb{R}\times\mathbb{R})$ *and* A_0 *be given by Definition 3.3.6. Then* $\mathcal{C}_0^1(\mathbb{R}^n) \subset D(A_0)$ *and for any* $v \in \mathcal{C}_0^1(\mathbb{R}^n)$, *the equality* $A_0 v = Bv$ *holds.*

Proof. The fact $v \in \mathcal{C}_0^1(\mathbb{R}^n)$ implies that $\phi_i(v, \tau_{\beta_i(h)}v) \in \mathcal{L}^1(\mathbb{R}^n)$ holds for all $h \in \operatorname{supp}(\omega_i)$ and $i = 1, 2, \ldots, k$. Let $f \in \mathcal{C}_0^\infty(\mathbb{R}^n)$ be nonnegative and $c \in \mathbb{R}$. Multiply Bv by $\operatorname{sign}_0(v-c)f$ and integrate over $\mathbb{R}^n$ to find that

$$\begin{aligned} &\int_{\mathbb{R}^n} \operatorname{sign}_0(v-c) f Bv \,\mathrm{d}x \\ &= -\int_{\mathbb{R}^n}\int_{\mathbb{R}^n} \sum_{i=1}^{k} D^{\beta_i}[f \operatorname{sign}_0(v-c)]\big(\phi_i(v, \tau_{\beta_i}v) - \phi_i(c,c)\big)\omega_i \,\mathrm{d}h \,\mathrm{d}x\,; \end{aligned} \tag{3.15}$$

that is, we have $v \in D(A_0)$ and $Bv \in A_0 v$. This, combined with Lemma 3.4.1 implies that $A_0 v = Bv$ a.e. □

We will use an efficient tool of Crandall to prove accretivity, characterized by the following definition and the two subsequent lemmata.

Definition 3.4.3. *[95, Definition 2.1] For $u : \mathbb{R}^n \mapsto \mathbb{R}$ measurable, let*

$$\operatorname{sign}(u) := \big\{ v : \mathbb{R}^n \mapsto \mathbb{R} \big| |v| \le 1 \text{ a.e. and } vu = |u| \text{ a.e.} \big\}.$$

Note that $\operatorname{sign}_0(u) \in \operatorname{sign}(u)$, thus $\operatorname{sign}(u)$ is always nonempty.

Lemma 3.4.4. *[95, Lemma 2.1] Let $u, v \in \mathcal{L}^1(\mathbb{R}^n)$ and $\alpha \in \operatorname{sign}(u)$. If $\int_{\mathbb{R}^n} \alpha v \,\mathrm{d}x \ge 0$, then $\|u + \lambda v\|_{\mathcal{L}^1(\mathbb{R}^n)} \ge \|u\|_{\mathcal{L}^1(\mathbb{R}^n)}$ holds for $\lambda > 0$.*

Lemma 3.4.5. *[95, Lemma 2.2] Let $\{\beta_k\}$ be a sequence in $\mathcal{L}^1(\mathbb{R}^n)$ with $\lim \beta_k = \beta$ in $\mathcal{L}^1(\mathbb{R}^n)$. If $\alpha_k \in \operatorname{sign}(\beta_k)$, then there exists a subsequence $\{\alpha_{k_l}\}$ and function $\alpha \in \operatorname{sign}(\beta)$ such that $\{\alpha_{k_l}\}$ converges to α in the weak-star topology on $\mathcal{L}^\infty(\mathbb{R}^n)$.*

Proposition 3.4.6. *Let A_0 be given by Definition 3.3.6. Then A_0 is accretive in $\mathcal{L}^1(\mathbb{R}^n)$.*

Proof. Let $v \in D(A_0)$ and $w \in A_0 v$ and choose $u \in \mathcal{L}^1(\mathbb{R}^n)$ such that Definition 3.3.6 (ii) holds. Set $c = u(y)$ and $f(x) = g(x,y)$ in (3.13), where $g \in \mathcal{C}_0^\infty(\mathbb{R}^n \times \mathbb{R}^n)$ is nonnegative. We introduce the notations $\Pi = \big(\mathbb{R}^n\big)^2$ and

$$\begin{aligned} D_1^{\beta_i} g(x,y) &= \frac{g(x+\beta_i, y) - g(x,y)}{\|\beta_i\|_{\mathbb{R}^n}}, \\ D_2^{\beta_i} g(x,y) &= \frac{g(x, y+\beta_i) - g(x,y)}{\|\beta_i\|_{\mathbb{R}^n}}. \end{aligned}$$

For the sake of readability we omit most arguments in this proof. Integrating over y yields

$$\begin{aligned} &\int_{\Pi} \operatorname{sign}_0(v-u) w g \,\mathrm{d}x \,\mathrm{d}y \\ &+ \int_{\Pi}\int_{\mathbb{R}^n} \sum_{i=1}^{k} D_1^{\beta_i}\big[g \operatorname{sign}_0(v-u)\big]\Big(\phi_i(v, \tau_{\beta_i}v) - \phi_i(u,u)\Big)\omega_i \,\mathrm{d}h \,\mathrm{d}x \,\mathrm{d}y \ge 0. \end{aligned} \tag{3.16}$$

Suppose that $u \in D(A_0)$ as well and let $z \in A_0 u$. Set $c = v(x)$ and $f(y) = g(x,y)$ in (3.13) and integrate over x to find that

$$\begin{aligned}&\int_\Pi \operatorname{sign}_0(u-v) z g \,\mathrm{d}y \,\mathrm{d}x \\ &+ \int_\Pi \int_{\mathbb{R}^n} \sum_{i=1}^k D_2^{\beta_i}\big[g \operatorname{sign}_0(u-v)\big]\Big(\phi_i(u,\tau_{\beta_i}u) - \phi_i(v,v)\Big)\omega_i \,\mathrm{d}h \,\mathrm{d}y \,\mathrm{d}x \geq 0.\end{aligned} \tag{3.17}$$

and adding the inequalities (3.16) and (3.17) yields

$$\begin{aligned}&\int_\Pi \operatorname{sign}_0(v-u)(w-z) g \,\mathrm{d}x \,\mathrm{d}y \\ &+ \int_\Pi \int_{\mathbb{R}^n} \sum_{i=1}^k \Big(D_1^{\beta_i}\big[g \operatorname{sign}_0(v-u)\big]\Big(\phi_i(v,\tau_{\beta_i}v) - \phi_i(u,u)\Big) \\ &+ D_2^{\beta_i}\big[g \operatorname{sign}_0(u-v)\big]\Big(\phi_i(u,\tau_{\beta_i}u) - \phi_i(v,v)\Big)\Big)\omega_i \,\mathrm{d}h \,\mathrm{d}x \,\mathrm{d}y \geq 0.\end{aligned} \tag{3.18}$$

Let $\delta \in \mathcal{C}_0^\infty(\mathbb{R})$ be nonnegative and even such that $\|\delta\|_{\mathcal{L}^1(\mathbb{R}^n)} = 1$ and

$$\begin{aligned}\lambda(x) &= \prod_{i=1}^n \delta(x_i), \\ \lambda_\epsilon(x) &= \frac{1}{\epsilon^n}\lambda\left(\frac{x}{\epsilon}\right)\end{aligned}$$

for $\epsilon > 0$. Let $f \in \mathcal{C}_0^\infty(\mathbb{R}^n)$ nonnegative and set

$$g(x,y) = f\left(\frac{x+y}{2}\right)\lambda_\epsilon\left(\frac{x-y}{2}\right).$$

Setting $2\xi = x + y$, $2\eta = x - y$ in (3.18) yields

$$\int_{\mathbb{R}^n}\left(\int_{\mathbb{R}^n} \operatorname{sign}_0(v-u)(w-z) f \,\mathrm{d}\xi\right)\lambda_\epsilon(\eta)\,\mathrm{d}\eta + \int_\Pi J_f^\epsilon(\xi,\eta)\,\mathrm{d}\xi\,\mathrm{d}\eta \geq 0. \tag{3.19}$$

where

$$\begin{aligned}J_f^\epsilon(\xi,\eta) &= \int_{\mathbb{R}^n} \sum_{i=1}^k \frac{\omega_i}{\|\beta_i\|_{\mathbb{R}^n}} \\ &\times \Big[\Big(\tau_{\frac{\beta_i}{2}} f \tau_{\frac{\beta_i}{2}} \lambda_\epsilon \operatorname{sign}_0(\tau_{\beta_i}v - u) - f\lambda_\epsilon \operatorname{sign}_0(v-u)\Big)\Big(\phi_i(v,\tau_{\beta_i}v) - \phi_i(u,u)\Big) \\ &+ \Big(\tau_{\frac{\beta_i}{2}} f \tau_{-\frac{\beta_i}{2}} \lambda_\epsilon \operatorname{sign}_0(\tau_{\beta_i}u - v) - f\lambda_\epsilon \operatorname{sign}_0(u-v)\Big)\Big(\phi_i(u,\tau_{\beta_i}u) - \phi_i(v,v)\Big)\Big]\,\mathrm{d}h\,.\end{aligned}$$

Denote the integral in parenthesis in the first term of (3.19) with $I_f(\eta)$. We want to let $\epsilon \to 0$. Since I_f is bounded and $\|\lambda_\epsilon\|_{\mathcal{L}^1(\mathbb{R}^n)} = 1$ we have that

$$\liminf_{\epsilon\to 0} \int_{\mathbb{R}^n} I_f(\eta)\lambda_\epsilon(\eta)\,\mathrm{d}\eta \leq \limsup_{\|\eta\|_{\mathbb{R}^n}\to 0} I_f(\eta).$$

A similar argument after a change of variables shows that

$$\liminf_{\epsilon\to 0} \int_\Pi J_f^\epsilon(\xi,\eta)\,\mathrm{d}\xi\,\mathrm{d}\eta$$

$$\leq \limsup_{\|\eta\|_{\mathbb{R}^n}\to 0} \int_{\mathbb{R}^n}\int_{\mathbb{R}^n} \sum_{i=1}^{k} \frac{\omega_i}{\|\beta_i\|_{\mathbb{R}^n}} \Big(\tau_{\beta_i} f q_i^{(1)}(v, \tau_{\beta_i} v, \tau_{\beta_i} u) - f q_i^{(2)}(v, \tau_{\beta_i} v, u)$$
$$+ \tau_{\beta_i} f q_i^{(1)}(u, \tau_{\beta_i} u, \tau_{\beta_i} v) - f q_i^{(2)}(u, \tau_{\beta_i} u, v) \Big) \,\mathrm{d}h \,\mathrm{d}\xi \,,$$

where

$$q_i^{(1)}(a,b,c) = \operatorname{sign}_0(a-c)\big(\phi_i(a,b) - \phi_i(c,c)\big),$$
$$q_i^{(2)}(a,b,c) = \operatorname{sign}_0(b-c)\big(\phi_i(a,b) - \phi_i(c,c)\big).$$

Introducing mixed terms yields

$$\liminf_{\epsilon\to 0} \int_\Pi J_f^\epsilon(\xi,\eta)\,\mathrm{d}\xi\,\mathrm{d}\eta$$
$$\leq \limsup_{\|\eta\|_{\mathbb{R}^n}\to 0} \int_{\mathbb{R}^n}\int_{\mathbb{R}^n} \sum_{i=1}^{k} \Big(f\Big(\big(q_i^{(1)} - q_i^{(2)}\big)(v, \tau_{\beta_i} v, u) + \big(q_i^{(1)} - q_i^{(2)}\big)(u, \tau_{\beta_i} u, v) \Big)$$
$$+ (\tau_{\beta_i} f - f) q_i^{(1)}(v, \tau_{\beta_i} v, \tau_{\beta_i} u) + (\tau_{\beta_i} f - f) q_i^{(1)}(u, \tau_{\beta_i} u, \tau_{\beta_i} v) \Big) \frac{\omega_i}{\|\beta_i\|_{\mathbb{R}^n}} \,\mathrm{d}h \,\mathrm{d}\xi \,.$$

But then (3.9) shows that the first two terms are nonpositive, thus we conclude that

$$\liminf_{\epsilon\to 0} \int_\Pi J_f^\epsilon(\xi,\eta)\,\mathrm{d}\xi\,\mathrm{d}\eta \leq \limsup_{\|\eta\|_{\mathbb{R}^n}\to 0} \int_{\mathbb{R}^n}\int_{\mathbb{R}^n} \sum_{i=1}^{k} \frac{\omega_i}{\|\beta_i\|_{\mathbb{R}^n}}$$
$$\times \Big((\tau_{\beta_i} f - f) q_i^{(1)}(v, \tau_{\beta_i} v, \tau_{\beta_i} u) + (\tau_{\beta_i} f - f) q_i^{(1)}(u, \tau_{\beta_i} u, \tau_{\beta_i} v) \Big) \,\mathrm{d}h \,\mathrm{d}\xi$$
$$=: \limsup_{\|\eta\|_{\mathbb{R}^n}\to 0} \tilde{J}_f(\eta).$$

Choose a sequence $\{\eta_k\} \subset \mathbb{R}^n$ such that $\|\eta_k\|_{\mathbb{R}^n} \to 0$ and $\lim_{k\to\infty} I_f(\eta_k) = \limsup_{\|\eta\|_{\mathbb{R}^n}} \tilde{I}_f(\eta)$ and $\lim_{k\to\infty} \tilde{J}_f(\eta_k)) = \limsup_{\|\eta\|_{\mathbb{R}^n}\to 0} \tilde{J}_f(\eta)$ (note that it might be necessary to choose two different sequences for I_f and $\tilde{J}_f$). Using Lemma 3.4.5 we assume (passing to subsequences if necessary) that the sequence

$$\alpha_k(\xi) = \operatorname{sign}_0\big(v(\xi+\eta_k) - u(\xi-\eta_k)\big)$$

converges weakly-star in $\mathcal{L}^\infty(\mathbb{R}^n)$ to $\alpha \in \operatorname{sign}\big(v(\xi) - u(\xi)\big)$. We similarly assume that the sign_0 sequences appearing in $\tilde{J}_f(\eta_k)$ converge weakly-star in $\mathcal{L}^\infty(\mathbb{R}^n)$ and we denote the limit as

$$\lim_{k\to\infty} \tilde{J}_f(\eta_k) = \int_{\mathbb{R}^n}\int_{\mathbb{R}^n} \sum_{i=1}^{k} D^{\beta_i} f\big(\gamma_i(v, \tau_{\beta_i} v, \tau_{\beta_i} u) + \gamma_i(u, \tau_{\beta_i} u, \tau_{\beta_i} v)\big)\omega_i \,\mathrm{d}h \,\mathrm{d}\xi \,.$$

Then

$$\lim_{k\to\infty} \big(I_f(\eta_k) + \tilde{J}_f(\eta_k)\big) = \int_{\mathbb{R}^n} \alpha(w-z) f \,\mathrm{d}\xi$$
$$+ \int_{\mathbb{R}^n}\int_{\mathbb{R}^n} \sum_{i=1}^{k} D^{\beta_i} f\big(\gamma_i(v, \tau_{\beta_i} v, \tau_{\beta_i} u) + \gamma_i(u, \tau_{\beta_i} u, \tau_{\beta_i} v)\big)\omega_i \,\mathrm{d}h \,\mathrm{d}\xi \geq 0. \tag{3.20}$$

Let $\kappa \in \mathcal{C}_0^\infty(\mathbb{R})$ be nonnegative such that $\kappa(s) = 1$ for $|s| \leq 1$. Set $f_l(\xi) = \kappa\Big(\frac{\|\xi\|_{\mathbb{R}^n}}{l}\Big)$ and let $l \to \infty$. Since the difference quotient

$$D^{\beta_i} f_l(x) = \int_0^1 \nabla f_l(x + \beta_i s) \cdot \frac{\beta_i}{\|\beta_i\|_{\mathbb{R}^n}} \, \mathrm{d}s \tag{3.21}$$

is bounded and is zero for $x \in \mathbb{R}^n$ such that $\|x \pm \beta_i\|_{\mathbb{R}^n} \leq l$, the second integral in (3.20) converges to zero; that is, we conclude that

$$\int_{\mathbb{R}^n} \alpha(w - z) \, \mathrm{d}\xi \geq 0.$$

Lemma 3.4.4 shows that the inequality

$$\|v - u + \lambda(w - z)\|_{\mathcal{L}^1(\mathbb{R}^n)} \geq \|v - u\|_{\mathcal{L}^1(\mathbb{R}^n)}$$

holds for $\lambda > 0$. Since $u, v \in D(A_0)$ were arbitrary we conclude that A_0 is indeed accretive. □

Remark 3.4.7. *One can observe that in the above proof we did not use the fact that the kernels ω_i have finite support.*

The stationary equation (3.14) will be investigated through the regularized equation

$$u + \lambda B u - \epsilon \Delta u = g, \tag{3.22}$$

where $\lambda, \epsilon > 0$. In [95, Proposition 2.2] the author shows existence of solutions using a special version of the perturbation result [100, Theorem 3.2] without further preparations. A key step of the proof is the fact that for $u \in \mathcal{L}^2(\mathbb{R}^n)$, the $\tilde{B}$ local version of the operator B (see (3.3)) has the property $\langle \tilde{B}u, u \rangle = 0$. However, this is no longer true in the nonlocal case, and thus we instead use a fix-point approach based on [101, Chapter 4] and [102, Proposition IV.3]. In order to do so, we first establish some a priori estimates on the solutions.

Lemma 3.4.8. *Let $\phi_i \in \mathcal{C}^1(\mathbb{R} \times \mathbb{R})$ have bounded partial derivatives and let $u \in \mathcal{H}^1(\mathbb{R}^n) \cap \mathcal{H}^2_{loc}(\mathbb{R}^n)$ satisfy (3.22) for $g \in \mathcal{L}^1(\mathbb{R}^n) \cap \mathcal{L}^\infty(\mathbb{R}^n)$. Then we have $u \in \mathcal{L}^1(\mathbb{R}^n) \cap \mathcal{L}^\infty(\mathbb{R}^n)$ and*

$$\|u\|_{\mathcal{L}^1(\mathbb{R}^n)} \leq \|g\|_{\mathcal{L}^1(\mathbb{R}^n)},$$
$$\|u\|_{\mathcal{L}^\infty(\mathbb{R}^n)} \leq \|g\|_{\mathcal{L}^\infty(\mathbb{R}^n)}.$$

Proof. We treat the case of $\mathcal{L}^1(\mathbb{R}^n)$ first. Define

$$\Phi_l(s) = \begin{cases} -s & \text{if } s \leq -\frac{1}{l}, \\ \frac{l}{2} s^2 + \frac{1}{2l} & \text{if } |s| \leq \frac{1}{l}, \\ s & \text{if } s \geq \frac{1}{l} \end{cases} \tag{3.23}$$

and let $f \in \mathcal{C}_0^\infty(\mathbb{R}^n)$ be such that $0 \le f \le 1$. Multiplying (3.22) by $\Phi_l'(u)f$ and integrating over $\mathbb{R}^n$ gives

$$\int_{\mathbb{R}^n} \left(u\Phi_l'(u)f + \lambda Bu\Phi_l'(u)f - \epsilon\Delta u\Phi_l'(u)f\right) \mathrm{d}x = \int_{\mathbb{R}^n} g\Phi_l'(u)f \,\mathrm{d}x \le \|g\|_{\mathcal{L}^1(\mathbb{R}^n)}. \tag{3.24}$$

Since the sequence $\left\{u\Phi_l'(u)f\right\}$ is a nonnegative and pointwise non-decreasing sequence with $u\Phi_l'(u)f \to |u|f$ as $l \to \infty$, the monotone convergence theorem and the fact that $0 \le \Phi_l' f \le 1$ implies

$$\lim_{l\to\infty} \int_{\mathbb{R}^n} u\Phi_l'(u)f \,\mathrm{d}x = \int_{\mathbb{R}^n} uf \,\mathrm{d}x\,. \tag{3.25}$$

Since Φ_l' is monotone, and f is nonnegative we have that

$$\begin{aligned} \int_{\mathbb{R}^n} \Delta u\Phi_l'(u)f \,\mathrm{d}x &= -\int_{\mathbb{R}^n} \Phi_l''(u)|\nabla u|^2 f \,\mathrm{d}x - \int_{\mathbb{R}^n} \Phi_l'(u)\nabla u\nabla f \,\mathrm{d}x \\ &= -\int_{\mathbb{R}^n} \Phi_l''(u)|\nabla u|^2 f \,\mathrm{d}x + \int_{\mathbb{R}^n} \Phi_l(u)\Delta f \,\mathrm{d}x \le \int_{\mathbb{R}^n} \Phi_l(u)\Delta f \,\mathrm{d}x\,. \end{aligned} \tag{3.26}$$

By letting $l \to \infty$ we conclude that

$$-\limsup_{l\to\infty} \int_{\mathbb{R}^n} \Delta u\Phi_l'(u)f \,\mathrm{d}x \ge -\int_{\mathbb{R}^n} u\Delta f \,\mathrm{d}x\,.$$

Finally, the sequence $\left\{Bu\Phi_l'(u)f\right\}$ converges pointwise to $Bu\,\mathrm{sign}_0(u)f$ as $l \to \infty$ and is dominated by $|Bu|f$. The fact that $|Bu|f$ is integrable follows from Sobolev's embedding of $\mathcal{H}^2$ into $\mathcal{W}^{1,1}$ on the support of f and Lemma 3.3.3. Thus, using the dominated convergence theorem yields

$$\lim_{l\to\infty} \int_{\mathbb{R}^n} Bu\Phi_l'(u)f \,\mathrm{d}x = \int_{\mathbb{R}^n} Bu\,\mathrm{sign}_0(u)f \,\mathrm{d}x\,.$$

Use the integration by parts formula for difference quotients to find that

$$\begin{aligned} \lim_{l\to\infty} \int_{\mathbb{R}^n} Bu\Phi_l'(u)f \,\mathrm{d}x = &-\int_{\mathbb{R}^n}\int_{\mathbb{R}^n} \sum_{i=1}^k D^{\beta_i}\,\mathrm{sign}_0(u)\tau_{\beta_i} f\phi_i(u,\tau_{\beta_i}u)\omega_i \,\mathrm{d}h\,\mathrm{d}x \\ &-\int_{\mathbb{R}^n}\int_{\mathbb{R}^n} \Phi_l'(u)D^{\beta_i} f\phi_i(u,\tau_{\beta_i}u)\omega_i \,\mathrm{d}h\,\mathrm{d}x\,, \end{aligned}$$

and apply inequality (3.9) with $c = 0$ to conclude that

$$\lim_{l\to\infty} \int_{\mathbb{R}^n} Bu\Phi_l'(u)f \,\mathrm{d}x \ge -\int_{\mathbb{R}^n}\int_{\mathbb{R}^n} \sum_{i=1}^k \mathrm{sign}_0(u)D^{\beta_i} f\phi_i(u,\tau_{\beta_i}u)\omega_i \,\mathrm{d}h\,\mathrm{d}x\,. \tag{3.27}$$

Substituting (3.25), (3.26) and (3.27) into (3.24) yields

$$\int_{\mathbb{R}^n} (uf - \epsilon u\Delta f) \,\mathrm{d}x - \int_{\mathbb{R}^n}\int_{\mathbb{R}^n} \sum_{i=1}^k \mathrm{sign}_0(u)D^{\beta_i} f\phi_i(u,\tau_{\beta_i}u)\omega_i \,\mathrm{d}h\,\mathrm{d}x \le \|g\|_{\mathcal{L}^1(\mathbb{R}^n)}.$$

Let $\kappa \in \mathcal{C}_0^\infty(\mathbb{R})$ nonnegative such that $\kappa(s) = 1$ for $|s| \le 1$. Set $f_l(\xi) = \kappa\Big(\frac{\|\xi\|_{\mathbb{R}^n}}{l}\Big)$. Since the difference quotient $D^{\beta_i} f_l$ is bounded and is zero for $x \in \mathbb{R}^n$ such that $\|x \pm \beta_i\|_{\mathbb{R}^n} \le l$ (see (3.21)), letting $l \to \infty$ yields

$$\|u\|_{\mathcal{L}^1(\mathbb{R}^n)} \le \|g\|_{\mathcal{L}^1(\mathbb{R}^n)}.$$

For the case of $\mathcal{L}^\infty(\mathbb{R}^n)$, let $M \in \mathbb{R}$ be such that $M \geq g^+$ a.e. Subtract M from (3.22), multiply by $\Phi_l'^+(u-M)$ and integrate over $\mathbb{R}^n$ to find that

$$\int_{\mathbb{R}^n} (u - M + \lambda Bu - \epsilon\Delta u)\Phi_l'^+(u-M)\,\mathrm{d}x = \int_{\mathbb{R}^n} (g-M)\Phi_l'^+(u-M)\,\mathrm{d}x \leq 0. \tag{3.28}$$

A similar argument as in (3.26) gives

$$\lim_{l\to\infty} \int_{\mathbb{R}^n} \Delta u \Phi_l'^+(u-M)\,\mathrm{d}x \leq 0, \tag{3.29}$$

as before. Again, integration by parts for difference quotients and the inequality (3.9) with $c = M$ (the reader may want to check that sign_0 and $\operatorname{sign}_0^\pm$ are interchangeable in (3.9)) imply that

$$\begin{aligned} &\lim_{l\to\infty} \int_{\mathbb{R}^n} Bu\Phi_l'^+(u-M)\,\mathrm{d}x \\ &= -\int_{\mathbb{R}^n}\int_{\mathbb{R}^n} \sum_{i=1}^k D^{\beta_i} \operatorname{sign}_0^+(u-M)\big[\phi_i(u,\tau_{\beta_i}u) - \phi_i(M,M)\big]\omega_i\,\mathrm{d}h\,\mathrm{d}x \geq 0. \end{aligned} \tag{3.30}$$

Substituting (3.29) and (3.30) into (3.28) yields

$$\int_{\mathbb{R}^n} (u-M)\Phi_l'^+(u-M)\,\mathrm{d}x \leq 0,$$

which implies that $u \leq M$ a.e.

To establish an analogous lower bound, let M be such that $M \leq g^-$ a.e. Add M to (3.22), multiply by $\Phi_l'^-(u+M)$ and integrate over $\mathbb{R}^n$ to conclude that

$$\int_{\mathbb{R}^n} (u + M + \lambda Bu - \epsilon\Delta u)\Phi_l'^-(u+M)\,\mathrm{d}x = \int_{\mathbb{R}^n} (g+M)\Phi_l'(u+M)^-\,\mathrm{d}x \leq 0.$$

Similar estimates as before show that

$$\int_{\mathbb{R}^n} (u+M)\Phi_l'^-(u+M)\,\mathrm{d}x \leq 0,$$

which implies that $-M \leq u$ a.e. Setting $M = \|g\|_{\mathcal{L}^\infty(\mathbb{R}^n)}$ concludes the proof. □

Remark 3.4.9. *The proof also shows that the maximum principle holds for equation* (3.22)*; that is, any solution* $u \in \mathcal{H}^1(\mathbb{R}^n) \cap \mathcal{H}^2_{loc}(\mathbb{R}^n)$ *of* (3.22) *satisfies the inequalities* $-\|g^-\|_{\mathcal{L}^\infty(\mathbb{R}^n)} \leq u \leq \|g^+\|_{\mathcal{L}^\infty(\mathbb{R}^n)}$ *a.e.*

Hölder's inequality immediately yields the following result.

Corollary 3.4.10. *Let the assumptions of Lemma 3.4.8 hold and let* $g \in \mathcal{L}^1(\mathbb{R}^n) \cap \mathcal{L}^\infty(\mathbb{R}^n)$*. Then* $u \in \mathcal{L}^p(\mathbb{R}^n)$ *for* $p \geq 1$ *with* $\|u\|_{\mathcal{L}^p(\mathbb{R}^n)} \leq \|g\|^{\frac{1}{p}}_{\mathcal{L}^1(\mathbb{R}^n)} \|g\|^{1-\frac{1}{p}}_{\mathcal{L}^\infty(\mathbb{R}^n)}$.

The next result shows the uniqueness of solutions of (3.22) for $g \in \mathcal{L}^1(\mathbb{R}^n)$.

Lemma 3.4.11. *Let the assumptions of Lemma 3.4.8 hold and let* $u, v \in \mathcal{H}^1(\mathbb{R}^n) \cap \mathcal{H}^2_{loc}(\mathbb{R}^n)$ *satisfy*

$$u + \lambda Bu - \epsilon \Delta u = g_1,$$
$$v + \lambda Bv - \epsilon \Delta v = g_2.$$

If $g_1, g_2 \in \mathcal{L}^1(\mathbb{R}^n)$, *then*

$$\big\|(u-v)^+\big\|_{\mathcal{L}^1(\mathbb{R}^n)} \leq \big\|(g_1-g_2)^+\big\|_{\mathcal{L}^1(\mathbb{R}^n)}.$$

Proof. The proof follows the proof of Lemma 3.4.8. Let $w = u - v$. Then w satisfies

$$w + \lambda(Bu - Bv) - \epsilon \Delta w = g_1 - g_2. \tag{3.31}$$

Let $f \in \mathcal{C}_0^\infty(\mathbb{R}^n)$ be such that $0 \leq f \leq 1$. Define Ψ_l by setting $\Psi_l' = \Phi_l'^+$ and $\Psi_l(0) = 0$. Multiply (3.31) by $\Psi_l'(w)f$ and integrate over $\mathbb{R}^n$ to find that

$$\begin{aligned} &\int_{\mathbb{R}^n} \big(w + \lambda(Bu - Bv) - \epsilon\Delta w\big)\Psi_l'(w) f \,\mathrm{d}x \\ &= \int_{\mathbb{R}^n} (g_1 - g_2)\Psi_l'(w) f \,\mathrm{d}x \leq \big\|(g_1-g_2)^+\big\|_{\mathcal{L}^1(\mathbb{R}^n)} \end{aligned} \tag{3.32}$$

holds, since $0 \leq \Psi_l' f \leq 1$. The facts that $\Psi_l(w) \in \mathcal{H}^1_{loc}(\mathbb{R}^n)$ and that both $\Psi_l'', f \geq 0$ imply that

$$\int_{\mathbb{R}^n} \Delta w \Psi_l'(w) f \,\mathrm{d}x \leq \int_{\mathbb{R}^n} \Psi_l(w) \Delta f \,\mathrm{d}x\,,$$

and thus

$$-\limsup_{l\to\infty} \int_{\mathbb{R}^n} \Delta w \Psi_l'(w) f \,\mathrm{d}x \geq -\int_{\mathbb{R}^n} w^+ \Delta f \,\mathrm{d}x\,. \tag{3.33}$$

as before. Integration by parts for difference quotients yields

$$\begin{aligned} &\int_{\mathbb{R}^n} (Bu - Bv)\Psi_l'(w) f \,\mathrm{d}x \\ &= -\int_{\mathbb{R}^n}\int_{\mathbb{R}^n} \sum_{i=1}^k D^{\beta_i}\Psi_l'(w)\tau_{\beta_i} f \big[\phi_i(u, \tau_{\beta_i}u) - \phi_i(v, \tau_{\beta_i}v)\big]\omega_i \,\mathrm{d}h \,\mathrm{d}x \\ &- \int_{\mathbb{R}^n}\int_{\mathbb{R}^n} \sum_{i=1}^k \Psi_l'(w) D^{\beta_i} f \big[\phi_i(u, \tau_{\beta_i}u) - \phi_i(v, \tau_{\beta_i}v)\big]\omega_i \,\mathrm{d}h \,\mathrm{d}x\,. \end{aligned}$$

Letting $l \to \infty$ in the first integral and using a similar argument as in (3.9) we find that

$$-\lim_{l\to\infty} \int_{\mathbb{R}^n}\int_{\mathbb{R}^n} \sum_{i=1}^k D^{\beta_i}\Psi_l'(w)\tau_{\beta_i} f \big[\phi_i(u, \tau_{\beta_i}u) - \phi_i(v, \tau_{\beta_i}v)\big]\omega_i \,\mathrm{d}h \,\mathrm{d}x \geq 0,$$

and thus, by the dominated convergence theorem,

$$\begin{aligned} &\lim_{l\to\infty} \int_{\mathbb{R}^n} (Bu - Bv)\Psi_l'(w) f \,\mathrm{d}x \\ &\geq -\int_{\mathbb{R}^n}\int_{\mathbb{R}^n} \sum_{i=1}^k \operatorname{sign}_0^+(w) D^{\beta_i} f \big[\phi_i(u, \tau_{\beta_i}u) - \phi_i(v, \tau_{\beta_i}v)\big]\omega_i \,\mathrm{d}h \,\mathrm{d}x\,. \end{aligned} \tag{3.34}$$

Using (3.33) and (3.34) in (3.32) and letting $l \to \infty$ gives

$$\int_{\mathbb{R}^n} w^+ f \,\mathrm{d}x - \lambda \int_{\mathbb{R}^n} \int_{\mathbb{R}^n} \sum_{i=1}^{k} \operatorname{sign}_0^+(w) D^{\beta_i} f \big[\phi_i(u, \tau_{\beta_i} u) - \phi_i(v, \tau_{\beta_i} v)\big] \omega_i \,\mathrm{d}h \,\mathrm{d}x$$
$$- \epsilon \int_{\mathbb{R}^n} w^+ \Delta f \,\mathrm{d}x \leq \big\|(g_1 - g_2)^+\big\|_{\mathcal{L}^1(\mathbb{R}^n)}.$$

By the same argument as before, let $\kappa \in \mathcal{C}_0^\infty(\mathbb{R})$ nonnegative such that $\kappa(s) = 1$ for $|s| \leq 1$. Set $f_l(\xi) = \kappa\Big(\frac{\|\xi\|_{\mathbb{R}^n}}{l}\Big)$. Since the difference quotient $D^{\beta_i} f_l$ is bounded and is zero for $x \in \mathbb{R}^n$ such that $\|x \pm \beta_i\|_{\mathbb{R}^n} \leq l$ (see (3.21)), letting $l \to \infty$ yields

$$\int_{\mathbb{R}^n} w^+ \,\mathrm{d}x = \big\|(u - v)^+\big\|_{\mathcal{L}^1(\mathbb{R}^n)} \leq \big\|(g_1 - g_2)^+\big\|_{\mathcal{L}^1(\mathbb{R}^n)}.$$

□

Corollary 3.4.12. *Let the assumptions of Lemma 3.4.8 hold and let* $u, v \in \mathcal{H}^1(\mathbb{R}^n) \cap \mathcal{H}^2_{loc}(\mathbb{R}^n)$ *satisfy*

$$u + Bu - \epsilon \Delta u = g_1$$
$$v + Bv - \epsilon \Delta v = g_2.$$

If $g_1, g_2 \in \mathcal{L}^1(\mathbb{R}^n)$, *then*

$$\|u - v\|_{\mathcal{L}^1(\mathbb{R}^n)} \leq \|g_1 - g_2\|_{\mathcal{L}^1(\mathbb{R}^n)}.$$

Proof. Notice that the equality

$$\|a - b\|_{\mathcal{L}^1(\mathbb{R}^n)} = \big\|(a - b)^+\big\|_{\mathcal{L}^1(\mathbb{R}^n)} + \big\|(b - a)^+\big\|_{\mathcal{L}^1(\mathbb{R}^n)}$$

holds for any $a, b \in \mathcal{L}^1(\mathbb{R}^n)$. Lemma 3.4.11 shows that

$$\big\|(u - v)^+\big\|_{\mathcal{L}^1(\mathbb{R}^n)} \leq \big\|(g_1 - g_2)^+\big\|_{\mathcal{L}^1(\mathbb{R}^n)},$$
$$\big\|(v - u)^+\big\|_{\mathcal{L}^1(\mathbb{R}^n)} \leq \big\|(g_2 - g_1)^+\big\|_{\mathcal{L}^1(\mathbb{R}^n)}.$$

Hence, the inequality $\|u - v\|_{\mathcal{L}^1(\mathbb{R}^n)} \leq \|g_1 - g_2\|_{\mathcal{L}^1(\mathbb{R}^n)}$ holds as claimed. □

The next result shows the existence of a unique generalized solution of (3.22) for $g \in \mathcal{L}^1(\mathbb{R}^n) \cap \mathcal{L}^\infty(\mathbb{R}^n)$ and plays an essential role in our developments. In order to do so we consider the problem on the ball $B_r \subset \mathbb{R}^n$ for $r > 0$ with zero Dirichlet boundary condition. Let $u^r \in \mathcal{H}^1_0(B_r) \cap \mathcal{H}^2(B_r) =: \mathcal{H}^2_0(B_r)$ satisfy

$$\begin{aligned} u^r(x) + \lambda B u^r(x) - \epsilon \Delta u^r(x) &= g(x), && x \in B_r; \\ u^r(x) &= 0, && x \in \partial B_r, \end{aligned} \tag{3.35}$$

where Δ denotes the Dirichlet-Laplacian Δ_D on $\mathcal{L}^2(B_r)$ with $D(\Delta_D) = \mathcal{H}_0^2(B_r)$. For the operator B to remain meaningful we use the $E : \mathcal{H}_0^1(B_r) \mapsto \mathcal{H}^1(\mathbb{R}^n)$ extension operator [99, Chapter 5.4] on u^r supplemented with the fact that $\text{supp}(Eu^r) = \text{supp}(u^r)$ and $\|Eu^r\|_{\mathcal{H}^1(\mathbb{R}^n)} = \|u^r\|_{\mathcal{H}_0^1(B_r)}$ [107]. Then we use the restriction operator $R : \mathcal{L}^2(\mathbb{R}^n) \mapsto \mathcal{L}^2(B_r)$ on BEu^r to obtain the operator $RBE : \mathcal{H}_0^1(B_r) \mapsto \mathcal{L}^2(B_r)$. As in (3.35), we will denote Δ_D by Δ and RBE by B for brevity.

Remark 3.4.13. *One can verify from the proof of Lemmata 3.3.3, 3.3.4, 3.4.8 and 3.4.11 and Corollaries 3.4.10 and 3.4.12 that they all hold for the Dirichlet problem too. Minor steps of the proofs have to be modified, for example, in the proof of Lemma 3.4.8, instead of multiplying by $\Phi_l'(u)$ and integrating over $\mathbb{R}^n$ we multiply by $\Phi_l'(Eu^r)$ and integrate over B_r. Then we can repeat the same estimates as before. Similar arguments should be used in the rest of the proofs as well.*

Proposition 3.4.14. *Let the assumptions of Lemma 3.4.8 hold. Then for each $g \in \mathcal{L}^1(\mathbb{R}^n) \cap \mathcal{L}^\infty(\mathbb{R}^n)$ there is a unique solution $u \in \mathcal{H}^1(\mathbb{R}^n) \cap \mathcal{H}_{loc}^2(\mathbb{R}^n)$ of (3.22).*

Proof. We consider the Dirichlet problem (3.35) first. Define the operator $T : \mathcal{H}_0^1(B_r) \mapsto \mathcal{H}_0^2(B_r)$ by $T = -(I - \epsilon\Delta)^{-1}\lambda Bu + (I - \epsilon\Delta)^{-1}g$ and let

$$\mathcal{S} := \big\{u \in \mathcal{H}_0^1(B_r) : u = \eta Tu,\ \eta \in [0,1]\big\}.$$

Note that $\mathcal{H}_0^2(B_r)$ can be compactly embedded into $\mathcal{H}_0^1(B_r)$, which implies that T is continuous (see also Lemma 3.3.4) and compact and maps the Banach space $\mathcal{H}_0^1(B_r)$ into itself. Observe that $u \in \mathcal{S}$ implies in fact $u \in \mathcal{H}_0^2(B_r)$, and thus $u = \eta Tu$ is equivalent to

$$u + \eta\lambda Bu - \epsilon\Delta u = \eta g \tag{3.36}$$

on B_r a.e. Multiply by u and integrate over B_r to find that

$$\begin{aligned}
&\|u\|_{\mathcal{L}^2(B_r)}^2 + \epsilon\|\nabla u\|_{\mathcal{L}^2(B_r)}^2 = \eta\int_{B_r} gu\,\mathrm{d}x - \eta\lambda\int_{B_r} Buu\,\mathrm{d}x\\
&\le \eta\|g\|_{\mathcal{L}^2(B_r)}\|u\|_{\mathcal{L}^2(B_r)} + \eta\lambda\|Bu\|_{\mathcal{L}^2(B_r)}\|u\|_{\mathcal{L}^2(B_r)}\\
&\le \frac{\eta}{2}\|g\|_{\mathcal{L}^2(B_r)}^2 + \frac{\eta}{2}\|u\|_{\mathcal{L}^2(B_r)}^2 + \eta\lambda\delta^2\|Bu\|_{\mathcal{L}^2(B_r)}^2 + \frac{\eta\lambda}{\delta^2}\|u\|_{\mathcal{L}^2(B_r)}^2\\
&\le \frac{1}{2}\|g\|_{\mathcal{L}^2(B_r)}^2 + \frac{1}{2}\|u\|_{\mathcal{L}^2(B_r)}^2 + \lambda\delta^2\|Bu\|_{\mathcal{L}^2(B_r)}^2 + \frac{\lambda}{\delta^2}\|u\|_{\mathcal{L}^2(B_r)}^2
\end{aligned}$$

for any $\delta > 0$. Using (3.11) and Corollary 3.4.10 (note that the right-hand side is ηg in (3.36) and g in (3.22)) we find that

$$\|u\|_{\mathcal{L}^2(B_r)}^2 \le \eta\|g\|_{\mathcal{L}^1(B_r)}\|g\|_{\mathcal{L}^\infty(B_r)} \le \|g\|_{\mathcal{L}^1(B_r)}\|g\|_{\mathcal{L}^\infty(B_r)} \tag{3.37}$$

and that

$$\begin{aligned}(\epsilon - C\lambda\delta^2)\|\nabla u\|^2_{\mathcal{L}^2(B_r)} &\leq \frac{1}{2}\|g\|^2_{\mathcal{L}^2(B_r)} + \left(\frac{1}{2} + \frac{\lambda}{\delta^2}\right)\|u\|^2_{\mathcal{L}^2(B_r)} \\ &\leq \left(1 + \frac{\lambda}{\delta^2}\right)\|g\|_{\mathcal{L}^1(B_r)}\|g\|_{\mathcal{L}^\infty(B_r)}.\end{aligned} \tag{3.38}$$

The inequalities (3.37) and (3.38) show that by choosing δ small enough $\mathcal{S}$ is bounded in $\mathcal{H}^1_0(B_r)$. Then Schaefer's fixed point theorem shows that T has a fixed point [108, Corollary 8.1] and, in fact, Lemma 3.4.11 ensures that the fixed point is unique on B_r.

Choose a sequence $\{r_m\} \subset \mathbb{R}$ such that $r_m \to \infty$ in an increasing fashion as $m \to \infty$ and let $u^{r_m} \in \mathcal{H}^2_0(B_{r_m})$ be the corresponding sequence of solutions. Then clearly $\{Eu^{r_m}\} \subset \mathcal{H}^2(\mathbb{R}^n)$ and by Lemma 3.4.8 we also have $\|Eu^{r_m}\|_{\mathcal{L}^\infty(B_{r_m})} \leq \|g\|_{\mathcal{L}^\infty(B_{r_m})} \leq \|g\|_{\mathcal{L}^\infty(\mathbb{R}^n)}$. For any $r < r'$ we have by Corollary 3.4.12 that

$$\left\|Eu^r - Eu^{r'}\right\|_{\mathcal{L}^1(\mathbb{R}^n)} \leq \|g\|_{\mathcal{L}^1\left(B_{r'}\setminus B_r\right)},$$

and thus the sequence is Cauchy and converges in $\mathcal{L}^1(\mathbb{R}^n)$ to some $u \in \mathcal{L}^1(\mathbb{R}^n) \cap \mathcal{L}^\infty(\mathbb{R}^n)$. Futhermore, elliptic regularity [99, Section 6.3.1] combined with inequalities (3.37) and (3.38) imply that $\{Eu^{r_m}\}$ is uniformly bounded with

$$\begin{aligned}&\|Eu^{r_m}\|_{\mathcal{H}^2(\mathbb{R}^n)} = \|u^{r_m}\|_{\mathcal{H}^2_0(B_{r_m})} \leq C\big(\|g\|_{\mathcal{L}^2(B_{r_m})} + \|Bu^{r_m}\|_{\mathcal{L}^2(B_{r_m})}\big) \\ &\leq C\big(\|g\|_{\mathcal{L}^2(B_{r_m})} + \|u^{r_m}\|_{\mathcal{H}^1_0(B_{r_m})}\big) \leq C\Big(\|g\|_{\mathcal{L}^2(\mathbb{R}^n)} + \|g\|^{\frac{1}{2}}_{\mathcal{L}^1(\mathbb{R}^n)}\|g\|^{\frac{1}{2}}_{\mathcal{L}^\infty(\mathbb{R}^n)}\Big).\end{aligned} \tag{3.39}$$

Let us consider B_{r_0} for some $r_0 > 0$ and let $\{Eu^{r_{m_k}}\}$ be any subsequence, which is then bounded in $\mathcal{H}^2(B_{r_0})$ and thus by the compact embedding of $\mathcal{H}^2(B_{r_0})$ into $\mathcal{H}^1(B_{r_0})$ it has a subsequence $\left\{Eu^{r_{m_{k_l}}}\right\}$ that converges in $\mathcal{H}^1(B_{r_0})$ to u. Since any subsequence has a convergent sequence with the same limit the original sequence converges in $\mathcal{H}^1(B_{r_0})$ to u. By (3.39) $\|u\|_{\mathcal{H}^1(B_{r_0})} \leq C$ independently of r_0 showing that u is in fact in $\mathcal{H}^1(\mathbb{R}^n)$ and is a weak solution. Thus, by elliptic regularity $u \in \mathcal{H}^2_{loc}(B_{r_0})$ as well and since $r_0 > 0$ was arbitrary we conclude that $u \in \mathcal{H}^1(\mathbb{R}^n) \cap \mathcal{H}^2_{loc}(\mathbb{R}^n)$ is a strong solution solution and by Corollary 3.4.12 it is unique. □

In our next result we take the limit $\epsilon \to 0$. This will not only allow us to consider flux functions in $\mathcal{W}^{1,\infty}_{loc}(\mathbb{R}\times\mathbb{R})$ but will show that the various properties established for the solutions of (3.22) hold for the generalized solutions of (3.14), which in turn will imply that they hold for the semigroup as well.

Proposition 3.4.15. *Let $\phi_i \in \mathcal{W}^{1,\infty}_{loc}(\mathbb{R}\times\mathbb{R})$ and A_0 be given by Definition 3.3.6. Then $\mathcal{L}^1(\mathbb{R}^n) \cap \mathcal{L}^\infty(\mathbb{R}^n) \subseteq R(I + \lambda A_0)$ for $\lambda > 0$. Accordingly, let $T_\lambda : \mathcal{L}^1(\mathbb{R}^n) \cap \mathcal{L}^\infty(\mathbb{R}^n) \mapsto \mathcal{L}^1(\mathbb{R}^n)$ be the restriction of $(I+\lambda A_0)^{-1}$ to $\mathcal{L}^1(\mathbb{R}^n)\cap\mathcal{L}^\infty(\mathbb{R}^n)$. If $g_1, g_2 \in \mathcal{L}^1(\mathbb{R}^n)\cap\mathcal{L}^\infty(\mathbb{R}^n)$, then*

(i) $T_\lambda g_1 \in \mathcal{L}^p(\mathbb{R}^n)$ *for* $p \geq 1$ *with* $\|T_\lambda g_1\|_{\mathcal{L}^p(\mathbb{R}^n)} \leq \|g_1\|^{\frac{1}{p}}_{\mathcal{L}^1(\mathbb{R}^n)} \leq \|g_1\|^{1-\frac{1}{p}}_{\mathcal{L}^\infty(\mathbb{R}^n)}$,

(ii) $-\|g_1^-\|_{\mathcal{L}^\infty(\mathbb{R}^n)} \leq T_\lambda g_1 \leq \|g_1^+\|_{\mathcal{L}^\infty(\mathbb{R}^n)}$,

(iii) $\|(T_\lambda g_1 - T_\lambda g_2)^+\|_{\mathcal{L}^1(\mathbb{R}^n)} \leq \|(g_1 - g_2)^+\|_{\mathcal{L}^1(\mathbb{R}^n)}$,

(iv) T_λ *commutes with translations,*

(v) $\int_{\mathbb{R}^n} T_\lambda g_1 \,\mathrm{d}x = \int_{\mathbb{R}^n} g_1 \,\mathrm{d}x$.

Proof. Let $\{\phi_i^m\} \subset \mathcal{C}^1(\mathbb{R}\times\mathbb{R})$ be a sequence such that each ϕ_i^m is bounded and have the property $\phi_i^m(0,0) = 0$ and $\{\phi_i^m\}$ converges to ϕ_i uniformly on compact sets. Define

$$B_m u = \int_{\mathbb{R}^n} \sum_{i=1}^{k} \frac{\phi_i^m(u, \tau_{\beta_i} u) - \phi_i^m(\tau_{-\beta_i} u, u)}{\|\beta_i\|_{\mathbb{R}^n}} \omega_i \,\mathrm{d}h$$

and the operator $T_{\lambda,m} : \mathcal{L}^1(\mathbb{R}^n) \cap \mathcal{L}^\infty(\mathbb{R}^n) \mapsto \mathcal{L}^1(\mathbb{R}^n) \cap \mathcal{L}^\infty(\mathbb{R}^n)$ by $T_{\lambda,m} g = u$ if $u \in \mathcal{H}^1(\mathbb{R}^n) \cap \mathcal{H}^2_{loc}(\mathbb{R}^n)$ and

$$u + \lambda B_m u - \frac{1}{m}\Delta u = g. \tag{3.40}$$

Proposition 3.4.14, Lemmata 3.4.8 and 3.4.11, Remark 3.4.9, Corollaries 3.4.10 and 3.4.12 and the fact that $T_{\lambda,m}$ commutes with translations imply that $T_{\lambda,m}$ is well-defined and has the properties (i)-(iv). Let $g \in \mathcal{L}^1(\mathbb{R}^n) \cap \mathcal{L}^\infty(\mathbb{R}^n)$ and $u_m = T_{\lambda,m} g$. By Lemma 3.4.11 and the translation invariance of $T_{\lambda,m}$ we conclude that

$$\int_{\mathbb{R}^n} \big|u_m(x+y) - u_m(x)\big| \,\mathrm{d}x \leq \int_{\mathbb{R}^n} \big|g(x+y) - g(x)\big| \,\mathrm{d}x$$

for $y \in \mathbb{R}^n$. The above estimate and $\|u_m\|_{\mathcal{L}^1(\mathbb{R}^n)} \leq \|g\|_{\mathcal{L}^1(\mathbb{R}^n)}$, by the means of the Fréchet-Kolmogorov compactness theorem, imply that $\{u_m\}$ is precompact in $\mathcal{L}^1_{loc}(\mathbb{R}^n)$. Thus, there is a subsequence $\{u_{m_j}\}$ which converges a.e. in $\mathcal{L}^1_{loc}(\mathbb{R}^n)$ to a limit $u \in \mathcal{L}^1(\mathbb{R}^n)$. This convergence will be denoted as $u_{m_j} \twoheadrightarrow u$. Let $f \in \mathcal{C}_0^\infty(\mathbb{R}^n)$ be nonnegative and Φ_l be given by (3.23). Multiply (3.40) by $\Phi_l'(u_m - c)f$ and integrate over $\mathbb{R}^n$ to find that

$$\int_{\mathbb{R}^n} \left(u_m + \lambda B_m u_m - \frac{1}{m}\Delta u_m\right) \Phi_l'(u_m - c) f \,\mathrm{d}x = \int_{\mathbb{R}^n} g \Phi_l'(u_m - c) f \,\mathrm{d}x\,.$$

Integration by parts gives

$$\begin{aligned}\int_{\mathbb{R}^n} \Big(&(u_m - g)\Phi_l'(u_m - c)f + \lambda B_m u_m \Phi_l'(u_m - c) f \\ &+ \frac{1}{m}\big(\Phi_l''(u_m - c)|\nabla u_m|^2 f - \Phi_l(u_m - c)\Delta f\big)\Big) \,\mathrm{d}x = 0.\end{aligned}$$

Note that both $\Phi_l'', f \geq 0$ implies that

$$\frac{1}{m}\int_{\mathbb{R}^n} \Phi_l''(u_m - c)|\nabla u_m|^2 f \,\mathrm{d}x \geq 0$$

and $\|u_m\|_{\mathcal{L}^\infty(\mathbb{R}^n)} \le \|g\|_{\mathcal{L}^\infty(\mathbb{R}^n)}$ implies that the integral

$$\int_{\mathbb{R}^n} \Phi_l(u_m - c)\Delta f \,\mathrm{d}x$$

is bounded. Letting $m \to \infty$ through the subsequence $\{m_j\}$ and using the convergences $u_{m_j} \twoheadrightarrow u$ and $\phi_i^m \to \phi_i$ uniformly on compact sets yields

$$\int_{\mathbb{R}^n} \big((u-g)\Phi_l'(u-c)f + \lambda B u \Phi_l(u-c)f\big)\,\mathrm{d}x \le 0.$$

Letting $l \to \infty$ and using (3.15) gives

$$\begin{aligned}&\int_{\mathbb{R}^n} \Bigg(\operatorname{sign}_0(u-c)(u-g)f \\ &- \lambda \int_{\mathbb{R}^n} \sum_{i=1}^k D^{\beta_i}\big[f \operatorname{sign}_0(u-c)\big]\big(\phi_i(u,\tau_{\beta_i}u) - \phi_i(c,c)\big)\omega_i \,\mathrm{d}h \Bigg)\,\mathrm{d}x \le 0.\end{aligned}$$

Since $\|u\|_{\mathcal{L}^\infty(\mathbb{R}^n)} \le \|g\|_{\mathcal{L}^\infty(\mathbb{R}^n)}$ and $\phi_i \in \mathcal{W}^{1,\infty}_{loc}(\mathbb{R}\times\mathbb{R})$ we have $\phi_i(u,\tau_{\beta_i}u) \in \mathcal{L}^1(\mathbb{R}^n)$. Thus, we have $g \in (I + \lambda A_0)u$ by Definition 3.3.6 and, in fact, by Lemma 3.4.1 the equality

$$u + \lambda A_0 u = g \tag{3.41}$$

holds. The accretivity of A_0 shows that u is unique, hence $\lim_{m\to\infty} T_{\lambda,m}g = T_\lambda g$ holds with convergence in $\mathcal{L}^1_{loc}(\mathbb{R}^n)$. Properties (i)-(iv) are preserved under $\mathcal{L}^1_{loc}(\mathbb{R}^n)$ convergence. Choose $f \in \mathcal{C}_0^\infty(\mathbb{R}^n)$ nonnegative, multiply (3.41) with f and integrate over $\mathbb{R}^n$ to find that

$$\begin{aligned}&\int_{\mathbb{R}^n} uf \,\mathrm{d}x + \lambda \int_{\mathbb{R}^n} A_0 uf \,\mathrm{d}x \\ &= \int_{\mathbb{R}^n} uf \,\mathrm{d}x - \lambda \int_{\mathbb{R}^n}\int_{\mathbb{R}^n} \sum_{i=1}^k D^{\beta_i} f \phi_i(u,\tau_{\beta_i}u)\omega_i \,\mathrm{d}h\,\mathrm{d}x = \int_{\mathbb{R}^n} gf \,\mathrm{d}x\end{aligned}$$

also holds by Lemma 3.4.1. Let $\kappa \in \mathcal{C}_0^\infty(\mathbb{R})$ be nonnegative such that $\kappa(s) = 1$ for $|s| \le 1$. Set $f_l(\xi) = \kappa\Big(\frac{\|\xi\|_{\mathbb{R}^n}}{l}\Big)$ and let $l \to \infty$. Using (3.21) we find that the integral

$$\int_{\mathbb{R}^n}\int_{\mathbb{R}^n} \sum_{i=1}^k D^{\beta_i} f_l \phi_i(u,\tau_{\beta_i}u)\omega_i \,\mathrm{d}h\,\mathrm{d}x$$

converges to zero as $l \to \infty$ and thus property (v) holds as well. □

Remark 3.4.16. *By Definition 3.3.6 it is clear that $\overline{D(A)} \subset \mathcal{L}^1(\mathbb{R}^n)$ and in some cases, in fact, the equality $\overline{D(A)} = \mathcal{L}^1(\mathbb{R}^n)$ holds, see Lemma 3.4.2. However, this remains to be shown under our general assumption that $\phi_i \in \mathcal{W}^{1,\infty}_{loc}(\mathbb{R}\times\mathbb{R})$.*

Proof of Theorem 3.3.8. Since A_0 is accretive it follows that the closure A is also accretive. Let $g \in \mathcal{L}^1(\mathbb{R}^n)$ and $\{g_m\} \subset \mathcal{L}^1(\mathbb{R}^n) \cap \mathcal{L}^\infty(\mathbb{R}^n)$ be such that $g_m \to g$ in $\mathcal{L}^1(\mathbb{R}^n)$. Since T_λ is a contraction, the sequence $\{T_\lambda g_m\}$ is Cauchy. Let $\lambda w_m = (I - T_\lambda)g_m$, so $w_m \in A_0 T_\lambda g_m$ and the sequence $\{w_m\}$ is also Cauchy. If $T_\lambda g_m \to v$ and $w_m \to w$, then $w \in Av$ and $g = v + \lambda w \in (I + \lambda A)v$. This shows that A is m-accretive and the proof is complete. □

Proof of Theorem 3.3.9. The solution $u_\epsilon(t)$ of (3.7) is given by

$$u_\epsilon(t) = (I + \epsilon A)^{-\left\lfloor \frac{t}{\epsilon} \right\rfloor - 1} u_0.$$

The uniform convergence $\lim_{\epsilon \to 0} u_\epsilon(t) = S(t)u_0$ for t in $\mathcal{L}^1(\mathbb{R}^n)$ shows that properties (i)-(v) hold for $S(t)$, since by Proposition 3.4.15 they hold for $T_\lambda = (I + \lambda A)^{-1}$.

For property (vi) let $u_0 \in \mathcal{L}^1(\mathbb{R}^n) \cap \mathcal{L}^\infty(\mathbb{R}^n)$ (note that by Lemma 3.4.1 the operator A_0 is single-valued in this case) and $u_\epsilon(x,t)$ satisfy

$$\begin{aligned} &\frac{1}{\epsilon}\big(u_\epsilon(x,t) - u_\epsilon(x,t-\epsilon)\big) + A_0 u_\epsilon(x,t) = 0, && (x,t) \in \mathbb{R}^n \times (0,T); \\ &u_\epsilon(x,0) = u_0(x), && x \in \mathbb{R}^n. \end{aligned}$$

The definition of A_0 implies that

$$\begin{aligned} &\int_{\mathbb{R}^n} \operatorname{sign}_0\big(u_\epsilon(x,t) - c\big) A_0 u_\epsilon(x,t) f \,\mathrm{d}x \\ &+ \int_{\mathbb{R}^n} \int_{\mathbb{R}^n} \sum_{i=1}^{k} D^{\beta_i}\big[f \operatorname{sign}_0(u-c)\big]\big(\phi_i(u_\epsilon, \tau_{\beta_i} u_\epsilon) - \phi_i(c,c)\big)\omega_i \,\mathrm{d}h \,\mathrm{d}x \geq 0 \end{aligned}$$

holds for any nonnegative $f \in \mathcal{C}_0^\infty\big(\mathbb{R}^n \times (0,T)\big)$ and any $c \in \mathbb{R}$. Notice that

$$A_0 u_\epsilon(x,t) = \frac{1}{\epsilon}\big(u_\epsilon(x,t-\epsilon) - u_\epsilon(x,t)\big)$$

and that

$$\begin{aligned} &\operatorname{sign}_0\big(u_\epsilon(x,t) - c\big)\big(u_\epsilon(x,t-\epsilon) - u_\epsilon(x,t)\big) = \operatorname{sign}_0\big(u_\epsilon(x,t) - c\big)\big(u_\epsilon(x,t-\epsilon) - c\big) \\ &+ \operatorname{sign}_0\big(u_\epsilon(x,t) - c\big)\big(u_\epsilon(x,t) - c\big) \leq \big|u_\epsilon(x,t-\epsilon) - c\big| - \big|u_\epsilon(x,t) - c\big|. \end{aligned}$$

Using the above and integrating over $(0,T)$ yields

$$\begin{aligned} &\int_0^T \int_{\mathbb{R}^n} \frac{1}{\epsilon}\Big(\big|u_\epsilon(x,t-\epsilon) - c\big| - \big|u_\epsilon(x,t) - c\big|\Big) f(x,t) \,\mathrm{d}x \,\mathrm{d}t \\ &+ \int_0^T \int_{\mathbb{R}^n} \int_{\mathbb{R}^n} \sum_{i=1}^{k} D^{\beta_i}\big[f \operatorname{sign}_0(u-c)\big]\big(\phi_i(u_\epsilon, \tau_{\beta_i} u_\epsilon) - \phi_i(c,c)\big)\omega_i \,\mathrm{d}h \,\mathrm{d}x \,\mathrm{d}t \geq 0. \end{aligned} \tag{3.42}$$

Observe that

$$\begin{aligned}
&\frac{1}{\epsilon}\int_0^T\int_{\mathbb{R}^n}\Big(\big|u_\epsilon(x,t-\epsilon)-c\big|-\big|u_\epsilon(x,t)-c\big|\Big)f(x,t)\,\mathrm{d}x\,\mathrm{d}t\\
&=\frac{1}{\epsilon}\left(\int_0^\epsilon\int_{\mathbb{R}^n}\big|u_\epsilon(x,t-\epsilon)-c\big|f(x,t)\,\mathrm{d}x\,\mathrm{d}t-\int_{T-\epsilon}^T\int_{\mathbb{R}^n}\big|u_\epsilon(x,t)-c\big|f(x,t)\,\mathrm{d}x\,\mathrm{d}t\right)\\
&+\int_\epsilon^{T-\epsilon}\int_{\mathbb{R}^n}\big|u_\epsilon(x,t)-c\big|\frac{1}{\epsilon}\big(f(x,t+\epsilon)-f(x,t)\big)\,\mathrm{d}x\,\mathrm{d}t\,.
\end{aligned}$$

Since $f\in\mathcal{C}_0^\infty\big(\mathbb{R}^n\times(0,T)\big)$ the first two integrals after the equal sign vanish for ϵ small enough. The uniform convergence $\lim_{\epsilon\to 0}u_\epsilon(x,t)=S(t)u_0(x)$ in $\mathcal{L}^1(\mathbb{R}^n)$ implies that the third integral tends to

$$\int_0^T\int_{\mathbb{R}^n}\big|S(t)u_0(x)-c\big|\frac{\partial f}{\partial t}\,\mathrm{d}x\,\mathrm{d}t\,;$$

that is, by taking the limit $\epsilon\to 0$ in (3.42) the proof is complete. □

3.5 Conclusions

In this chapter we inverstigated a class of nonlocal conservation laws and established well-posedness results via nonlinear semigroup theory. This ensures that the mathematical model reliably models the underlying physical phenomena. To connect these models back to the spatially discrete framework of CRNs, the next chapter considers the discretization of the nonlocal equations developed here. We will show that, under suitable assumptions, these discretizations give rise to finite-dimensional reaction networks whose dynamics approximate those of the original nonlocal system.

Chapter 4

Dynamical analysis of generalized ribosome flows

In this chapter we consider compartmental systems and their representation as a chemical reaction network. We show that one-dimensional nonlocal flow models in PDE form with Lighthill-Whitham-Richards flux can be spatially discretized with a finite volume scheme to formally obtain a special case of generalized ribosome flows. The CRN representation, called generalized ribosome flows, have physically meaningful reaction graphs structure, allowing the utilization of the vast theory of CRNs. We demonstrate this via the stability analysis of a flow model with circular topology. We then consider generalized ribosome flow models. The existence and stability of equilibria are investigated for strongly connected systems. Finally, we consider general time-varying rate functions corresponding to the transitions. Persistence of the dynamics is shown using the CRN representation of the system. The L^1 contractivity of solutions is also proved in the case of periodic reaction rates having the same period. Further we prove the stability of different compartmental structures including strongly connected ones with entropy-like logarithmic Lyapunov functions through embedding the model into a weakly reversible CRN with time-varying reaction rates in a reduced state space. Moreover, it is shown that different Lyapunov functions may be assigned to the same model depending on the non-unique factorization of the reaction rates. The results are illustrated through several examples with biological meaning including the classical ribosome flow model on a ring.

4.1 Introduction

The dynamical modeling of the mRNA translation process has been in the focus of research since the second half of the 20th century (see, e.g. [109, 110, 111]). The first large scale analysis of gene translation through the so-called ribosome flow model (RFM) was presented in [112], where the applied second order nonnegative and nonlinear model based on the principle of Totally Asymmetric Exclusion [113] was able to capture the most important dynamical features of the translation process. Also in [112], the RFM model was validated through biological data obtained from three different organisms, and it was clearly shown that its predictive power is superior to several other popular techniques. In [114] the RFM was equipped with an appropriate input-output pair, and it was shown that after applying an affine positive output feedback, the system had a unique equilibrium point which is globally stable in the bounded operating domain. A circular RFM structure was analyzed in [35], where the authors proved using the theory of cooperative systems that the system has a continuum of equilibria, but each equilibrium is globally asymptotically stable within the equivalence class of trajectories determined by the initial conditions. The stability of periodic solutions was also shown. In [115] a bounded pool of free ribosomes was added to the RFM generating a competition among the arbitrary number of mRNA molecules for ribosomes. This generates a special network structure for RFM subsystems, for which the uniqueness and stability of equilibria together with the properties of periodic solutions were proved, too. Different compartment sizes of the RFM were assumed in [116], and it was shown that this modification does not change the favorable dynamical properties of the system. In [117], the ribosome flow model with Langmuir kinetics (RFMLK) is introduced, and a network structure is constructed with RFMLK subsystems connected through a pool. Among other results, it is shown that the trajectories of such a network always converge to a unique equilibrium. We also mention that ODE models with essentially the same structure can be obtained by an appropriate finite volume discretization of local conservation laws governed by hyperbolic partial differential equations describing the flow of material or vehicles [118].

It is well-known that the (nonlocal) conservation laws described by hyperbolic partial differential equations (PDEs) may develop irregularities even with smooth initial functions [119]. This implies that solution concepts of these equations have to allow for discontinuous functions. Another consequence of the loss of regularity is that one is confined to a restricted class of applicable numerical schemes, such as, for example, finite volume methods [120]. Two of the most commonly used schemes in the field of traffic

flows are the modified Lax-Friedrichs scheme and the Godunov scheme [121]. While these schemes possess numerous desired properties, the obtained form of ordinary differential equations (ODEs) computed via spatial discretization (also called semi-discretization) is often not optimal for dynamical analysis.

The aim of the chapter is to apply a finite volume method to nonlocal conservation laws and to show that the semi-discretized system inherits several advantageous properties from the PDE. Then we generalize the interconnection structure and the reaction rate functions and finally, we investigate the persistence and stability for strongly connected systems.

The structure of the chapter is as follows. In Section 4.2 we give a brief overview of nonlocal flow models, kinetic systems and compartmental systems. In Section 4.3 we introduce the kinetic representation of general compartmental models. Section 4.4 contains the spatial discretization of the nonlocal flow, including the derivation of the kinetic property with the exact topology and interpretation of compartments and reactions. Section 4.5 contains stability results for strongly connected systems. Finally, Section 4.6 contains presistence and stability results for strongly connected systems with time-varying transition rates.

4.2 Notations and background

4.2.1 Nonlocal flows

In this subsection we introduce the unidirectional nonlocal flow model based on the nonlocal pair-interaction model of Chapter 3, supplemented with terms representing in- and out-flows.

Let $\overline{\mathbb{R}}_+$ denote the set of nonnegative real numbers. Nonlocality is formally introduced as a continuum average of the finite difference approximation weighted with a bounded and nonnegative nonlocal interaction kernel $\omega \in \mathcal{L}^1(\mathbb{R})$ supported on $(0, \delta)$ with $\delta > 0$ and $\|\omega\|_{\mathcal{L}^1(\mathbb{R})} = 1$, as follows:

$$\begin{aligned} &\frac{\partial \rho}{\partial t} + \int_0^\delta \frac{F(\rho, \tau_h \rho) - F(\tau_{-h}\rho, \rho)}{h} \omega(h)\, \mathrm{d}h = r - s; \\ &\rho(x, 0) = \rho_0(x), \end{aligned} \tag{4.1}$$

where $\rho : \mathbb{R} \times (0, T) \mapsto \overline{\mathbb{R}}_+$ is the conserved quantity at a given point and at a given time, $F : \mathbb{R} \times \mathbb{R} \mapsto \mathbb{R}$ is the flux function, $\tau_{\pm h}\rho(x, t) = \rho(x \pm h, t)$ denotes a spatial shift and $r, s : \mathbb{R} \times (0, t) \times \overline{\mathbb{R}}_+ \mapsto \overline{\mathbb{R}}_+$ are the source and sink terms, respectively. Throughout

the chapter, we call (4.1) closed if the functions r and s are identically zero; that is, the system does not have in- and out-flows. In any other case, the system is called open.

4.2.2 Compartmental models

Throughout the chapter we consider systems containing a set of interconnected compartments and objects (such as ribosomes, particles, molecules, vehicles etc.) moving between them. We assume that the rate of transfer between compartments depends on the amount of objects in the source compartment as well as on the amount of free space in the target compartment. This naturally implies that each compartment has a well-defined finite capacity that limits the amount of modeled quantities that can be contained in the given compartment. We also allow explicit time dependence and in some cases dependence on the amount of objects and free space in other compartments.

For the formal definition, let us consider the set $Q = \{q_1, q_2, \ldots, q_m\}$ of compartments and the set $A \subset Q \times Q$ of transitions, where $(q_i, q_j) \in A$ represents the transition from compartment q_i into q_j. Then, the directed graph $D = (Q, A)$ is called the compartmental graph and it describes the structure of the compartmental model. The transitions are assumed to be immediate, thus loop edges are not allowed in the model since they do not introduce additional dynamical terms. Similarly, we do not allow parallel edges between two compartments in the same direction since they can be replaced by a single transition. In general, any compartment can be connected to to the environment in both directions. We denote with F_{ij} the flow from the compartment q_j to the compartment q_i, with I_i the material inflow from the environment to compartment q_i and with F_{0i} the material outflow from compartment q_i to the environment. Loop flows are not allowed, i.e. $i \neq j$ in F_{ij}. Then the time-evolution of the system is given by the following system of differential equations:

$$\dot{q}_i = \sum_{j \neq i} (-F_{ji} + F_{ij}) + I_i - F_{0i}. \tag{4.2}$$

We impose the following physical assumptions to the system:

1. for any $i, j, t \geq 0$, $i \neq j$ we have that $F_{ij} \geq 0$, $I_i \geq 0$ and $F_{0i} \geq 0$,

2. for any $i, t \geq 0$ if $q_i(t) = 0$, then $F_{0i} = F_{ji} = 0$ for each j.

These properties ensure the invariance of the nonnegative orthant; that is, assuming a nonnegative initial condition, our solution is guaranteed to be nonnegative. In general, the above functions can depend on the mass of any compartment and possibly on t as

well. Then it can be shown that if each F_{ij} and F_{0i} is at least $\mathcal{C}^k$, then we can rewrite (4.2) as

$$\dot{q}_i = -\left(f_{0i} + \sum_{j \neq i} f_{ji}\right) q_i + \sum_{j \neq i} f_{ij} q_j + I_i, \tag{4.3}$$

where $F_{ij} = f_{ij} q_i$ and the so-called fractional transfer coefficients f_{ij} are at least $\mathcal{C}^{k-1}$. We can then naturally rewrite (4.3) in matrix form as

$$q = fq + I.$$

If each fractional transfer coefficient f_{ij} only depends on q_j, then the system is called a donor controlled system. If each coefficient is constant, then the system is called a linear donor controlled system.

Linear donor controlled systems can naturally be represented as chemical reaction networks, or kinetic systems. For a brief introduction, we refer to [23]. For each compartment with index i, q_i represents the mass (or alternatively, the concentration) of the one-specie complex Q_i, and for each transition from compartment i to j, we assign the reaction $Q_i \to Q_j$. Using this construction, we can not only rely on the comprehensive theory of compartmental models but on that of kinetic systems as well.

We say that a (compartmental) graph is strongly connected if there exists a directed path between any two vertices in both directions, and we say that a graph is weakly reversible if it is a collection of isolated strongly connected subgraphs.

For each compartment q_i we introduce the sets of donors and receptors, respectively, as

$$\mathcal{D}_i = \big\{ j \in \{1, 2, \ldots, m\} \big| (q_j, q_i) \in A \big\},$$
$$\mathcal{R}_i = \big\{ j \in \{1, 2, \ldots, m\} \big| (q_i, q_j) \in A \big\};$$

that is, the set of donors of a given compartment are the compartments where an incoming transition originates from and the set of receptors are the compartments where an outgoing transition terminates in.

4.3 Kinetic representation of compartmental models

In this section we construct a kinetic representation of the above compartmental system class. To do so, we assign a CRN that incorporates the compartmental structure. This allows the introduction of a system of ODEs of the form (2.2) describing the time evolution of the compartmental model.

Let us consider a compartmental model $D = (Q, A)$. Let the set of species be $\Sigma = \{N_1, N_2, \ldots, N_m\} \cup \{S_1, S_2, \ldots, S_m\}$ where N_i and S_i represent the number of particles

and available spaces in compartment q_i, respectively. To each transition $(q_i, q_j) \in A$ we assign a reaction of the form (see, also [30])

$$N_i + S_j \xrightarrow{\mathcal{K}_{ij}} N_j + S_i,$$

where $\mathcal{K}_{ij}$ is the rate function of the transition. Such a reaction represents that during the transition from compartment q_i to compartment q_j the number of items decreases in q_i and increases in q_j, while the number of available spaces increases in q_i and decreases in q_j. Let n_i and s_i denote the continuous amount of particles and free space in q_i, respectively.

Based on (2.2) the dynamics of the system is given by

$$\begin{aligned} \dot{n}_i &= \sum_{j \in \mathcal{D}_i} \mathcal{K}_{ji}(n_j, s_i) - \sum_{j \in \mathcal{R}_i} \mathcal{K}_{ij}(n_i, s_j), \\ \dot{s}_i &= -\sum_{j \in \mathcal{D}_i} \mathcal{K}_{ji}(n_j, s_i) + \sum_{j \in \mathcal{R}_i} \mathcal{K}_{ij}(n_i, s_j), \end{aligned} \tag{4.4}$$

where n and s denote the vectorized form of the variables n_i and s_i, respectively. It is easy to check that the model class in Eq. (4.4) contains ribosome flow models described in [29] or [116], and extends them in two ways: firstly, the reaction rate function $\mathcal{K}$ is not necessarily mass-action type and moreover, is time-varying, and secondly, the compartmental graph of the system can be arbitrary (i.e., there can be transitions between any two compartments). Therefore, we call (4.4) a generalized time-varying ribosome flow model. Thus, our novel results not only extend the theory of ribosome flow models, but can be applied to other TASEP based transport models [122, 123, 124, 125, 126] and other flow models, such as the Traffic Reaction Model of [118]. Finally, we note, that while more complicated network structures may not be biologically relevant in the case of ribosome flows, but can serve as a great tool for the analysis of other flow based physical models, e.g. traffic flows.

System (4.4) exhibits conservation in several senses. First of all, we have that

$$\sum_{i=1}^{m} \left(\dot{n}_i + \dot{s}_i \right) = 0,$$

thus the sum of modeled quantities and free spaces in the system is constant along the trajectories of (4.4); that is, the function $\tilde{H} : \mathbb{R}^{2m} \mapsto \mathbb{R}$ defined for $x \in \mathbb{R}^{2m}$ as

$$\tilde{H}(x) = \sum_{i=1}^{2m} x_i, \tag{4.5}$$

is a first integral, where $x_1, x_2, \ldots, x_m$ and $x_{m+1}, x_{m+2}, \ldots, x_{2m}$ correspond to the variables $n_1, n_2, \ldots, n_m$ and $s_1, s_2, \ldots, s_m$, respectively. Our next observation is that $\dot{n}_i + \dot{s}_i =$

0 holds for each compartment, thus $c_i := n_i + s_i$ is the constant capacity of compartment q_i. Substituting $s_i = c_i - n_i$ we can rewrite (4.4) in a reduced state space as

$$\dot{n}_i = \sum_{j \in \mathcal{D}_i} \mathcal{K}_{ji}\big(n_j, c_i - n_i\big) - \sum_{j \in \mathcal{R}_i} \mathcal{K}_{ij}\big(n_i, c_j - n_j\big) \tag{4.6}$$

or after an analogous substitution, as

$$\dot{s}_i = -\sum_{j \in \mathcal{D}_i} \mathcal{K}_{ji}\big(c_j - s_j, s_i\big) + \sum_{j \in \mathcal{R}_i} \mathcal{K}_{ij}\big(c_i - s_i, s_j\big). \tag{4.7}$$

As a consequence of the preceding observations, the function $H : \mathbb{R}^m \mapsto \mathbb{R}$, defined for $x \in \mathbb{R}^m$ as

$$H(x) = \sum_{i=1}^{m} x_i \tag{4.8}$$

is a first integral for (4.6), in which case each $x_i = n_i$ (and similarly for (4.7) if each $x_i = s_i$). This shows that while the state space of the decomposed systems is $C := [0, c_1] \times [0, c_2] \times \cdots \times [0, c_m]$, for a given initial condition $x(0) \in C$ the trajectories are contained in the $(m-1)$-dimensional manifold (hyperplane) defined by

$$\big\{x \in C \big| H(x) - H\big(x(0)\big) = 0\big\}.$$

For a generalized ribosome flow define $c = \sum_{i=1}^{n} c_i$ and for $r \in [0, c]$ let $L_r \subset C$ be the level set of H corresponding to r; that is,

$$L_r = \big\{a \in C : H(a) = r\big\}. \tag{4.9}$$

Using the terminology of CRN theory [15], the level sets defined in Eq. (4.9) are also called stoichiometric compatibility classes.

Clearly the reaction graph of the assigned CRN of a compartmental model is generally not strongly connected nor weakly reversible even if the compartmental graph is strongly connected. In fact, the reaction graph is weakly reversible if and only if each transition in the compartmental system is reversible. Even though the reaction graph, in some sense, loses the regularities of the compartmental graph, we can explicitly determine its deficiency from the compartmental topology.

For a compartmental system $D = (Q, A)$ let $|D| = \big(Q, \tilde{A}\big)$ denote the undirected graph where the parallel edges are merged.

Theorem 4.3.1. *The deficiency of a CRN assigned to a compartmental model $D = (Q, A)$ is equal to the number of chordless cycles in the undirected graph $|D| = \big(Q, \tilde{A}\big)$.*

Proof. For each transition between q_i and q_j we assign two complexes, namely $N_i + S_j$ and $S_i + N_j$, regardless of the transitions' direction, so reversible reactions do not introduce

additional complexes, and thus the number of stoichiometrically distinct complexes is $m = 2|\tilde{A}|$. A complex of the form $N_i + S_j$ is only connected with the complex $S_i + N_j$, and thus we have $\ell = |\tilde{A}|$ linkage classes each consisting of exactly two complexes. To find the dimension of the stoichiometric subspace, denoted by $s = \dim \mathcal{S}$, observe that the reaction vector of a reaction of the form $N_i + S_j \to N_j + S_i$ is

$$y_{i\to j} = -e_i + e_j + e_{m+i} - e_{m_j}, \tag{4.10}$$

where $e_k \in \mathbb{R}^{2m}$ denotes the kth unit vector. Again, since $y_{i\to j} = -y_{j\to i}$ it suffices to consider the undirected graph $|D|$. Assume that $y_{i\to j}$ is such that

$$y_{i\to j} = \sum c_{l\to l'} y_{l\to l'}.$$

Then by (4.10) we have that for each non-zero term of the form $c_{\cdot\to l'} y_{\cdot\to l'}$ the right-hand side also contains at least one non-zero term $c_{l'\to\cdot} y_{l'\to\cdot}$, including the terms $c_{i\to\cdot} y_{i\to\cdot}$ and $c_{\cdot\to j} y_{\cdot\to j}$. This shows that the edges corresponding to the reaction vectors of the right-hand side form possibly multiple cycles in $|D|$. Without the loss of generality we may assume that this subgraph does not contain cycles isolated from (q_i, q_j). We have to consider the following cases:

1. First, we assume that the right-hand side is a single chordless cycle and contains the transitions

   $$q_i \to q_{l_1} \to q_{l_2} \to \cdots \to q_{l_r} \to q_j \to q_i.$$

   Taking the inner product of unit vectors $e_i, e_{l_1}, e_{l_2}, \ldots, e_{l_r}, e_j$ and

   $$y_{i\to j} = c_{i\to l_1} y_{i\to l_1} + \sum_{k=1}^{r-1} c_{l_k\to l_{k+1}} y_{l_k\to l_{k+1}} + c_{l_r\to j} y_{l_r\to j}$$

   yields the system of linear equations:

   $$\begin{aligned} -1 &= -c_{i\to l_1} \\ 0 &= c_{i\to l_1} - c_{l_1\to l_2} \\ 0 &= c_{l_1\to l_2} - c_{l_2\to l_3} \\ &\vdots \\ 0 &= c_{l_{r-1}\to l_r} - c_{l_r\to j} \\ 1 &= c_{l_r\to j} \end{aligned}$$

   which clearly has one solution where each weight is equal to one.

2. If the right-hand side consists of multiple cycles, then repeatedly using the previous argument we can replace the arcs not containing (q_i, q_j) with chords. Note, that if the reaction vector corresponding to the chord is already on the right-hand side, then we just have to modify its coefficient. This method decomposes the right-hand side and will leave us with one chordless cycle containing (q_i, q_j), leading back to the previous case with exactly one solution. Repeating the arc substitutions we can see that each arc becomes a chordless cycle with the reintroduced edges and the arising systems of linear equations have exactly one solution.

The first case above shows that the dimension of the stiochiometric subspace reduces by one for each set of reaction vectors that correspond to edges forming a chordless cycle in $|D|$ and the second case shows that is reduced by that exact amount. If σ denotes the number of chordless cycles in $\tilde{Q}$, then the deficiency of the reaction network can be computed as $\delta = m - \ell - s = 2|\tilde{A}| - |\tilde{A}| - \big(|\tilde{A}| - \sigma\big) = \sigma$. □

4.4 Discretization of one-dimensional nonlocal flows

In this section we consider nonlocal flows and carry out the spatial segmentation of the flow model (4.1), with clear compartmental interpretation.

Our main motivation comes from the theory of particle flows, thus ρ will denote particle density; that is, the number of particles per unit length. There are multiple flux functions appropriate for modeling such flows. One of the most widely used flux functions is the so-called Lighthill-Whitham-Richards (LWR) flux, which assumes that the speed of the flow is proportional to the particle density and available free spaces [127, 128]. Note that this assumption is applicable in many areas, including ribosome flows [112]. The local flux is given by

$$f(u) = \frac{v_{max}}{\rho_{max}} u(\rho_{max} - u) = wu(\rho_{max} - u),$$

where v_{max} and ρ_{max} are the maximal particle speed and density, respectively. The nonlocal flux is given by

$$F(u, v) = wu(\rho_{max} - v).$$

We assume that the in- and out-flows (source and sink terms) of an open system are of the form

$$r(x, t, \rho) = 1_{in}(x) w(x) \rho_{in}(t) \big(\rho_{max} - \rho(x, t)\big)$$
$$s(x, t, \rho) = 1_{out}(x) w(x) \rho_{out}(t) \rho(x, t),$$

where $\rho_{in}, \rho_{out} : \mathbb{R}_+ \mapsto \overline{\mathbb{R}}_+$ are the rates of the in- and out-flows, respectively. The spatial positions are described by the indicator functions $1_{in}, 1_{out}$ defined by

$$1_{in}(x) = \sum_{i=1}^{\mathcal{I}} \chi_{\left[x_i^{in}, x_{i'}^{in}\right]}(x), \quad 1_{out}(x) = \sum_{j=1}^{\mathcal{J}} \chi_{\left[x_j^{out}, x_{j'}^{out}\right]}(x),$$

where the space coordinates defining the above intervals are strictly ordered as follows:

$$x_1^{in} < x_{1'}^{in} < \cdots < x_{\mathcal{I}}^{in} < x_{\mathcal{I}'}^{in},$$
$$x_1^{out} < x_{1'}^{out} < \cdots < x_{\mathcal{J}}^{out} < x_{\mathcal{J}'}^{out}.$$

We will use the finite volume approach to spatially discretize (also called semi-discretize) the flow model (4.1) by introducing a grid defined by an increasing sequence of real values $\left(x_{i+\frac{1}{2}}\right)_{i\in\mathbb{Z}}$ such that $\mathbb{R} = \bigcup_{i\in\mathbb{Z}} \left[x_{i-\frac{1}{2}}, x_{i+\frac{1}{2}}\right]$. Then the grid is the set as the set $\left\{K_i = \left(x_{i-\frac{1}{2}}, x_{i+\frac{1}{2}}\right) \middle| i \in \mathbb{Z}\right\}$ where the length of the cell K_i is $h_i = x_{i+\frac{1}{2}} - x_{i-\frac{1}{2}}$. The derivation of the discretized model is analogous to the local case in [118] with the additional approximation of the integral in (4.1).

We introduce the variables $\rho_i(t)$ approximating the average particle density in the ith cell at time t as

$$\rho_i(t) \approx \frac{1}{h_i} \int_{K_i} \rho(x,t)\,\mathrm{d}x$$

and the variables $1_{in,i}$ and $1_{out,i}$ as

$$1_{in,i} = \frac{1}{h_i} \int_{K_i} 1_{in}(x)\,\mathrm{d}x\,, \quad 1_{out,i} = \frac{1}{h_i} \int_{K_i} 1_{out}(x)\,\mathrm{d}x\,.$$

Let f_i be such that $\sum_{j=1}^{f_i} h_{i+j} \geq \delta$ and $\sum_{j=1}^{f_i-1} h_{i+j} < \delta$ and b_i be such that $\sum_{j=1}^{b_i} h_{i-j} \geq \delta$ and $\sum_{j=1}^{b_i-1} h_{i-j} < \delta$; that is, f_i and b_i denote the number of cells affected by the ith cell and the number of cells affecting the ith cell, respectively. Finally, define

$$W_{i,j} = \frac{1}{jh_{i+j}} \int_0^{h_{i+j}} \omega\left(\sum_{k=1}^{j-1} h_{i+k} + h\right) \mathrm{d}h\,,$$
$$W_{i,-j} = \frac{1}{jh_{i-j}} \int_0^{h_{i-j}} \omega\left(\sum_{k=1}^{j-1} h_{i-k} + h\right) \mathrm{d}h\,.$$

The approximation for the ith cell at time t is

$$\int_0^{\delta} \frac{F(\rho, \tau_h\rho) - F(\tau_{-h}\rho, \rho)}{h} \omega(h)\,\mathrm{d}h \approx \sum_{j=1}^{f_i} G(\rho_i, \rho_{i+j}) W_{i,j} - \sum_{j=1}^{b_i} G(\rho_{i-j}, \rho_i) W_{i,-j},$$

where G is the so-called numerical flux. Since ω is of unit norm, we have

$$\sum_{j=1}^{f_i} jh_{i+j} W_{i,j} = 1, \quad \sum_{j=1}^{b_i} jh_{i-j} W_{i,-j} = 1.$$

The choice of the numerical flux G determines many important qualitative properties of the numerical scheme. The two most commonly used schemes especially in the field of traffic flows are the modified Lax-Friedrichs scheme and the Godunov scheme [119]. The former uses

$$G(u,v) = \frac{f(u)+f(v)}{2} + D(u-v)$$

where $2D \geq v_{max}$ is the coefficient of the numerical diffusion term, and the latter utilizes

$$G(u,v) = \begin{cases} \min_{s\in[u,v]} f(s) & \text{if } u \leq v, \\ \max_{s\in[v,u]} f(s) & \text{otherwise.} \end{cases}$$

When used in time-space discretization of local conservation laws, both schemes are monotone flux schemes implying advantageous properties like the maximum principle, also called ℓ^∞-stability [120], but the physical interpretation is not straightforward. Furthermore, these fluxes are complicated to handle from a control point of view. Note that while the theory of monotone flux schemes have been widely studied for local equations the theory is rather incomplete for nonlocal models. Recent advancements include the characterization of equidistant monotone flux schemes for closed nonlocal conservation laws and an appropriate Courant-Friedrichs-Lewy (CFL) condition under which the scheme is conservative, consistent, enjoys the maximum principle and is total variation diminishing (TVD) [60].

Our main result is that using the naturally defined nonlocal flux as the numerical flux $G(u,v) = F(u,v) = wu(\rho_{max} - v)$ in the case of open conservation laws, the (not necessarily equidistant) discretization scheme will still have many desired qualitative properties mentioned above and the obtained system of ODEs is of a quite special form, namely, it is kinetic.

Definition 4.4.1. *The spatial numerical segmentation of* (4.1) *is given by*

$$\begin{aligned} \dot\rho_i &= \sum_{j=1}^{b_i} w\rho_{i-j}(\rho_{max}-\rho_i)W_{i,-j} - \sum_{j=1}^{f_i} w\rho_i(\rho_{max}-\rho_{i+j})W_{i,j} + \\ &+ 1_{in,i} w\rho_{in}(\rho_{max}-\rho_i) - 1_{out,i} w\rho_{out}\rho_i, \quad (i,t) \in \mathbb{Z}\times\mathbb{R}_+; \\ \rho_i(0) &= \frac{1}{h_i}\int_{K_i} \rho_0(x)\,\mathrm{d}x\,, \quad i \in \mathbb{Z}. \end{aligned}$$

For the sake of generality we may also consider variable maximal density and particle speed at different spatial points. These will be given by the functions $\rho_{max} : \mathbb{R} \mapsto \mathbb{R}_+$ and $v_{max} : \mathbb{R} \mapsto \mathbb{R}_+$, respectively. The local flux in this case is

$$\tilde f(u,x) = \frac{v_{max}(x)}{\rho_{max}(x)} u\big(\rho_{max}(x) - u\big) = w(x)u\big(\rho_{max}(x)-u\big)$$

and the nonlocal flux is

$$\tilde{F}(u,v,x,y) = w(x)u\big(\rho_{max}(y) - v\big).$$

We further introduce the variables $\rho_{max,i}$ and $v_{max,i}$ denoting the average maximal particle density and speed in cell K_i as

$$\rho_{max,i} = \frac{1}{h_i}\int_{K_i} \rho_{max}(x)\,\mathrm{d}x\,, \quad v_{max,i} = \frac{1}{h_i}\int_{K_i} v_{max}(x)\,\mathrm{d}x$$

and the variables $w_i = \frac{v_{max,i}}{\rho_{max,i}}$. Using the numerical flux

$$\tilde{G}(u,v,i,j) = w_i u(\rho_{max,j} - v)$$

we obtain the following generalization.

$$\begin{aligned}
\dot{\rho}_i(t) &= \sum_{j=1}^{b_i} w_{i-j}\rho_{i-j}(t)\big(\rho_{max,i} - \rho_i(t)\big)W_{i,-j} - \sum_{j=1}^{f_i} w_i\rho_i(t)\big(\rho_{max,i+j} - \rho_{i+j}(t)\big)W_{i,j} \\
&\quad + R_i(t,\rho_i) - S_i(t,\rho_i), \quad (i,t) \in \mathbb{Z}\times\mathbb{R}_+; \\
\rho_i(0) &= \frac{1}{h_i}\int_{K_i} \rho_0(x)\,\mathrm{d}x\,, \quad i \in \mathbb{Z},
\end{aligned} \tag{4.11}$$

where

$$\begin{aligned}
R_i(t,\rho_i) &= 1_{in,i} w_i \rho_{in}(t)\big(\rho_{max,i} - \rho_i(t)\big), \\
S_i(t,\rho_i) &= 1_{out,i} w_i \rho_{out}(t)\rho_i(t).
\end{aligned}$$

Equation (4.11) is formally kinetic, which ensures some advantageous properties of the model and most importantly, allows us to use the well-developed theory of chemical reaction networks [20, 15]. Furthermore, the underlying CRN has physically meaningful compartments and topology. In fact, let N_i and S_i denote particles and available space slots for particles in the ith cell, respectively. Then the particle flow can be represented as transformations of complexes (that is, as reactions) as follows:

$$N_{i-j} + S_i \xrightarrow{k_{i-j,i}} N_i + S_{i-j} \qquad j = 1,2,\ldots,b_i \tag{4.12}$$

$$N_i + S_{i+j} \xrightarrow{k_{i,i+j}} N_{i+j} + S_i \qquad j = 1,2,\ldots,f_i \tag{4.13}$$

$$S_i \xrightarrow{k_{in,i}} N_i \tag{4.14}$$

$$N_i \xrightarrow{k_{out,i}} S_i. \tag{4.15}$$

Reaction (4.12) shows that during the particles' transition from the $(i-j)$th cell to the ith cell the available spaces increase in the $(i-j)$th cell and decrease in the ith cell, while the number of particles decrease in the $(i-j)$th cell and increase in the ith cell. Reaction (4.13) expresses the same transition from the ith cell to the $(i+j)$th cell. Finally, reactions

(4.14) and (4.15) show the behaviour of in- and out-flows. Note that (4.12) and (4.13) are redundant when enumerating all reactions. Figure 4.1 shows the exact structure of the compartments and the topology of the intra- and intercell reactions.

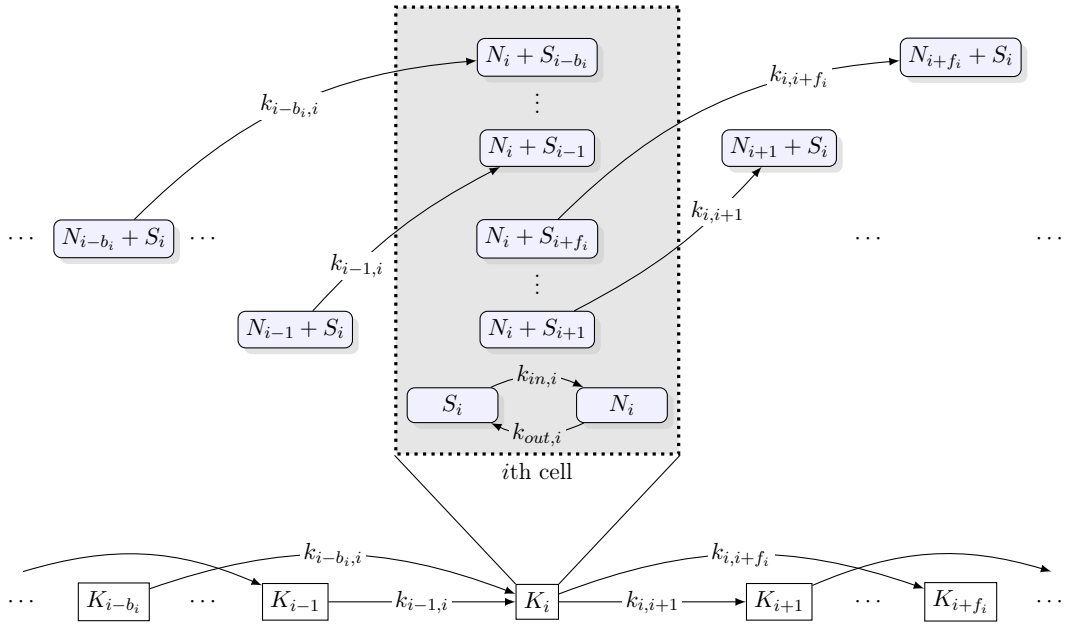

Figure 4.1: Compartmental model of the generalized (4.11)

Let n_i and s_i denote the continuous number of particles and available spaces in the ith cell per unit length, respectively. Using Eq. (2.2), the system of ODEs derived from the reactions are:

$$\begin{aligned}\dot{n}_i &= \sum_{j=1}^{b_i} k_{i-j,i} n_{i-j} s_i - \sum_{j=1}^{f_i} k_{i,i+j} n_i s_{i+j} + k_{in,i} s_i - k_{out,i} n_i, \\ \dot{s}_i &= -\sum_{j=1}^{b_i} k_{i-j,i} n_{i-j} s_i + \sum_{j=1}^{f_i} k_{i,i+j} n_i s_{i+j} - k_{in,i} s_i + k_{out,i} n_i.\end{aligned} \tag{4.16}$$

We can see that $\dot{n}_i + \dot{s}_i = 0$; that is, the sum of particles and available spaces is conserved in each cell. Let $n_i + s_i = c_i$, and substitute $s_i = c_i - n_i$ into (4.16) to obtain

$$\begin{aligned}\dot{n}_i = &\sum_{j=1}^{b_i} \left(k_{i-j,i} n_{i-j} c_i - k_{i-j,i} n_{i-j} n_i \right) + k_{in,i}(c_i - n_i) \\ &- \sum_{j=1}^{f_i} \left(k_{i,i+j} n_i c_{i+j} - k_{i,i+j} n_i n_{i+j} \right) - k_{out,i} n_i,\end{aligned}$$

which is equivalent to (4.11) with $n_i = \rho_i$, $c_i = \rho_{max,i}$, $k_{i-j,i} = w_{i-j} W_{i,-j}$, $k_{i,i+j} = w_{i+j} W_{i,j}$, $k_{in,i} = 1_{in,i} w_{in} \rho_{in}$ and $k_{out,i} = 1_{out,i} w_i \rho_{out}$.

Theorem 4.4.2. *The following statements hold for the proposed numerical scheme* (4.11)*:*

(i) *It is nonnegative and capacitated; that is, we have* $0 \leq \rho_i(t) \leq \rho_{max,i}$ *for all* $i \in \mathbb{Z}$ *and* $t \geq 0$.

(ii) *It is conservative in the sense that*

$$\sum_{i\in\mathbb{Z}} \rho_i(t) = \sum_{i\in\mathbb{Z}} \rho_i(0) + \int_0^t \big(R_i(\tau,\rho_i) - S_i(\tau,\rho_i)\big)\,\mathrm{d}\tau$$

holds for any $t \geq 0$.

Proof. (i) These are immediate consequences of the kinetic property [15].

(ii) Since

$$\sum_{i\in\mathbb{Z}} \dot{\rho}_i(t) = \sum_{i\in\mathbb{Z}} \big(R_i(t,\rho_i) - S_i(t,\rho_i)\big)$$

the scheme is conservative. □

Let us consider a closed system with constant maximal particle density and speed and with circular or ring-like topology obtained via equidistant spatial discretization. Let the number of compartments be N. In an equidistant setting $b_i = f_i =: r$ for $i = 1, 2, \ldots, N$ and $W_{i,-j} = W_{i,j} =: W_j$ for $i = 1, 2, \ldots, N$ and $j = 1, 2, \ldots, r$. For simplicity of notations we assume that $N > 2r$; that is, the nonlocality does not loop. Under such assumptions ring topology means that $\rho_{N+j} = \rho_j$ and $\rho_{1-j} = \rho_{N-j}$ for $j = 1, 2, \ldots, r$. An equilibrium point with densities ρ_i^* satisfies the following constraints

$$\sum_{j=1}^{r} w\rho_{i-j}^*(\rho_{max} - \rho_i^*)W_j = \sum_{j=1}^{r} w\rho_i^*(\rho_{max} - \rho_{i+j}^*)W_j$$

for $i = 1, 2, \ldots, N$. This shows that we obtain an equilibrium if each cell has equal density and since the number of particles is constant in the closed system we have

$$\rho_i^* = \overline{\rho} = \frac{1}{N}\sum_{i=1}^{N} \rho_i(0).$$

We will use the entropy-like Lyapunov function candidate well-known from the theory of chemical reaction networks [15, Section 7.7]

$$V(\rho) = \sum_{i=1}^{N} \rho_i \left[\log\left(\frac{\rho_i}{\overline{\rho}}\right) - 1\right] + N\overline{\rho} = \sum_{i=1}^{N} \rho_i \log\left(\frac{\rho_i}{\overline{\rho}}\right).$$

Note that $\overline{\rho} = 0$ is only possible when there are no particles in the system which is clearly not relevant.

It is easy to see that $V(\rho^*) = 0$ and $\rho \neq \rho^*$ implies $V(\rho) > 0$. Furthermore, partial summation yields

$$\dot{V}(\rho) = \sum_{i=1}^{N} \log\left(\frac{\rho_i}{\overline{\rho}}\right)\dot{\rho}_i = \sum_{i=1}^{N} \log\left(\frac{\rho_i}{\overline{\rho}}\right) \sum_{j=1}^{r} w\big[\rho_{i-j}(\rho_{max} - \rho_i) - \rho_i(\rho_{max} - \rho_{i+j})\big]W_j$$
$$= w\overline{\rho} \sum_{i=1}^{N}\sum_{j=1}^{r} \frac{\rho_i(\rho_{max} - \rho_{i+j})}{\overline{\rho}} \left[\log\left(\frac{\rho_{i+j}}{\overline{\rho}}\right) - \log\left(\frac{\rho_i}{\overline{\rho}}\right)\right] W_j.$$

Using the inequality $e^a(b-a) \leq e^b - e^a$ with $a = \log\left(\frac{\rho_i}{\overline{\rho}}\right)$ and $b = \log\left(\frac{\rho_{i+j}}{\overline{\rho}}\right)$ and noting that equality holds if and only if $a = b$, we find that

$$\dot{V}(\rho) \leq w \sum_{i=1}^{N}\sum_{j=1}^{r} (\rho_{max} - \rho_{i+j})(\rho_{i+j} - \rho_i)W_j = w \sum_{i=1}^{N}\sum_{j=1}^{r} \big(-\rho_{i+j}^2 + \rho_i\rho_{i+j}\big)W_j$$
$$= -\frac{w}{2} \sum_{i=1}^{N}\sum_{j=1}^{r} \big(\rho_i^2 - 2\rho_i\rho_{i+j} + \rho_{i+j}^2\big)W_j = -\frac{w}{2} \sum_{i=1}^{N}\sum_{j=1}^{r} (\rho_i - \rho_{i+j})^2 W_j \leq 0.$$

This shows that $\dot{V}(\rho^*) = 0$ and $\rho \neq \rho^*$ implies $\dot{V}(\rho) < 0$ and we conclude that this equilibrium point is asymptotically stable.

4.5 Stability of generalized ribosome flows

Consider a generalized ribosome flow with strongly connected compartmental structure, in reduced state space. The Jacobian of (4.6) is given by

$$\big[J(n)\big]_{ik} = \begin{cases} -\sum_{j\in\mathcal{D}_i} \frac{\partial \mathcal{K}_{ji}(n_j, c_i - n_i)}{\partial n_i} - \sum_{j\in\mathcal{R}_i} \frac{\partial \mathcal{K}_{ij}(n_i, c_j - n_j)}{\partial n_i} & \text{if } i = k, \\ \frac{\partial \mathcal{K}_{ki}(n_k, c_i - n_i)}{\partial n_k} & \text{if } k \in \mathcal{D}_i \text{ and } k \notin \mathcal{R}_i, \\ \frac{\partial \mathcal{K}_{ik}(n_i, c_k - n_k)}{\partial n_k} & \text{if } k \notin \mathcal{D}_i \text{ and } k \in \mathcal{R}_i, \\ \frac{\partial \mathcal{K}_{ki}(n_k, c_i - n_i)}{\partial n_k} + \frac{\partial \mathcal{K}_{ik}(n_i, c_k - n_k)}{\partial n_k} & \text{if } k \in \mathcal{D}_i \text{ and } k \in \mathcal{R}_i, \\ 0 & \text{otherwise.} \end{cases}$$

The (A2) property of the rate functions imply that each diagonal entry is nonpositive and each off-diagonal entry is nonnegative. Since the sum of each column is zero, we conclude that the system is compartmental in the sense of [9]. Systems satisfying the latter property are also called cooperative.

The following lemmata and proofs will adapt the ideas of [29] and [35] for the studied more general system class. Moreover, we will also use the persistence result of [129, Corollary 4.9].

Lemma 4.5.1. *Consider a compartmental system of the form* (4.6) *with a strongly connected compartmental structure. Then, for any* $n(0)$ *in the interior of* C*, denoted by* $\mathrm{int}(C)$*, the solution satisfies* $n(t) \in \mathrm{int}(C)$ *for any* $t \geq 0$*.*

In other words, $\mathrm{int}(C)$ is an invariant set of such a system.

Proof. To obtain a contradiction, suppose that there exists a (minimal) time $\tau > 0$ such that $n(\tau) \in \partial C$. We need to consider the following two cases.

1. There exists an empty compartment. In this case, due to the strongly connected structure, there must exist an empty compartment with at least one non-empty donor compartment as well. To see this, consider a directed path from any non-empty compartment to any empty compartment. Stepping backwards from the empty compartment along this path until we reach a non-empty compartment establishes our assertion.

   Let i be an index such that $n_i(\tau) = 0$ and $n_k(\tau) > 0$ holds for some $k \in \mathcal{D}_i$. Then (4.6) takes the form

   $$\dot{n}_i(\tau) = \sum_{j \in \mathcal{D}_i} \mathcal{K}_{ji}(n_j, c_i) \geq \mathcal{K}_{ki}(n_k, c_i) > 0$$

   which means that $\dot{n}_i(t) > 0$ on the interval $[\tau - \sigma, \tau]$ for some $\sigma > 0$. This leads to a contradiction with $n_i(\tau) = 0$, further implying that there are no empty compartments altogether.

2. There exists a full compartment. In this case, by a similar argument, there must exist a full compartment with at least one non-full recipient compartment as well; that is, there exists an index i such that $n_i(\tau) = c_i$ and $n_k(\tau) < c_k$ holds for some $k \in \mathcal{R}_i$. Then (4.6) takes the form

   $$\dot{n}_i(\tau) = -\sum_{j \in \mathcal{R}_i} \mathcal{K}_{ij}(c_i, c_j - n_j) \leq -\mathcal{K}_{ik}(c_i, c_k - n_k) < 0$$

   which means that $\dot{n}_i(t) < 0$ on the interval $[\tau - \sigma, \tau]$ for some $\sigma > 0$. This leads to a contradiction with $n_i(\tau) = c_i$, further implying that there are no full compartments altogether.

□

Let $0^{(m)}, c^{(m)} \in \mathbb{R}^m$ be defined by

$$0^{(m)} = \begin{bmatrix} 0 & 0 & \cdots & 0 \end{bmatrix}^\top \qquad c^{(m)} = \begin{bmatrix} c_1 & c_2 & \cdots & c_m \end{bmatrix}^\top.$$

Lemma 4.5.2. *Consider a compartmental system of the form* (4.6) *with a strongly connected compartmental structure. Then, for any* $n(0) \in \partial C$, $n(0) \neq 0^{(m)}$, $n(0) \neq c^{(m)}$ *the solution satisfies* $n(\tau) \in \operatorname{int}(C)$ *for some* $\tau > 0$.

Proof. First we define the following boundary-repelling property.

(**BR**) For each $\delta > 0$ and sufficiently small $\Delta > 0$, there exists $K = K(\delta, \Delta) > 0$ such that for each $t \geq 0$

1. the conditions

   (a) $n_i(t) \leq \Delta$,

   (b) there exists $k \in \mathcal{D}_i$ such that $n_k(t) \geq \delta$

   imply $\dot{n}_i(t) \geq K$, and

2. the conditions

   (a) $n_i(t) \geq c_i - \Delta$

   (b) there exists $k \in \mathcal{R}_i$ such that $n_k(t) \leq c_k - \delta$

   imply $\dot{n}_i(t) \leq -K$.

Eq. (4.6) satisfies the above property. To see this, consider any compartment q_i. Without the loss of generality we can assume that $\mathcal{D}_i$ contains at least one index, let this be k. In this case

$$\dot{n}_i(t) \geq \mathcal{K}_{ki}(\delta, c_i - \Delta) - \sum_{j \in \mathcal{R}_i} \mathcal{K}_{ij}(\Delta, c_j) := K_1.$$

Similarly, we can assume that $\mathcal{R}_i$ contains at least one index, let this be l. In this case

$$\dot{n}_i(t) \leq \sum_{j \in \mathcal{D}_i} \mathcal{K}_{ji}(c_j, \Delta) - \mathcal{K}_{il}(c_i - \Delta, c_l - \delta) := -K_2.$$

The properties of the rate functions imply that for a sufficiently small Δ we have $K_1 > 0$ and $-K_2 < 0$, thus taking $K = \min\{K_1, K_2\}$ concludes our assertion.

Next, we will show that for each compartment $n_i(\tau) > 0$ holds for some $\tau > 0$.

Without the loss of generality we can assume that there exists an index i such that $n_i(t) \geq \epsilon_0$ on the interval $[0, \tau]$ for some $\epsilon_0 > 0$ and $\tau > 0$. Define $\tau_m = \frac{\tau}{m}$ and proceed by induction. For $k = 1, 2, \ldots, m$ we will define an appropriate $\epsilon_k > 0$ and show that the

kth generation recipients of the compartment q_i have particle concentration of at least ϵ_k on the interval $[k\tau_m, \tau]$.

Pick any $j \in \mathcal{R}_i$ (first generation recipient) and sufficiently small $\Delta > 0$, define $K = K(\epsilon_0, \Delta)$ and $\epsilon_1 = \min\{\Delta, K\tau_m\}$ and let $t_0 \in [0, \tau_m]$ such that $n_j(t_0) \geq \epsilon_1$. Such a t_0 must exist, since assuming $n_j(t) < \epsilon_1 \leq \Delta$ for each $t \in [0, \tau_m]$ would imply via (**BR**) that $\dot{n}_j(t) \geq K$ for each $t \in [0, \tau_m]$. This further implies that $n_j(\tau_m) \geq n_j(0) + K\tau_m \geq \epsilon_1$. This leads to a contradiction with $n_j(\tau_m) < \epsilon_1$.

Our next claim is that $n_j(t) \geq \epsilon_1$ for each $t \in [t_0, \tau]$ and in particular $[\tau_m, \tau]$. Conversely, suppose that there exists some $t_1 \in (t_0, \tau]$ such that $\xi := n_j(t_1) < \epsilon_1$ and define $\sigma = \min\{t \in (t_0, \tau) : n_j(t) \leq \xi\}$. Since $n_j(\sigma) \leq \xi < \epsilon_1 \leq \Delta$, (**BR**) shows that $\dot{n}_j(\sigma) \geq K$; that is, $\dot{n}_j(t) > 0$ on the interval $[\sigma - \nu, \sigma]$ for some $\nu > 0$. But this would imply that $n_j(\sigma - \nu) < n_j(\sigma)$, contradicting the minimality of σ.

Define $K = K(\epsilon_1, \Delta)$ and $\epsilon_2 = \min\{\Delta, K\tau_m\}$ and repeat the above steps for the set $\mathcal{R}_j$ for $j \in \mathcal{R}_i$ (second generation recipients). In subsequent induction steps define $K = K(\epsilon_k, \Delta)$ and $\epsilon_{k+1} = \min\{\Delta, K\tau_m\}$ and repeat the above for the kth generation recipients of the compartment q_i. Since the compartments are strongly connected after at most m induction steps we conclude that $n_i(\tau) > 0$ for each $i = 1, 2, \ldots, m$.

To show that $n_i(\tau) < c_i$ holds as well, consider the complementary system given in (4.7). Repeating the above steps for (4.7) shows that $s_i(\tau) > 0$, further implying that $n_i(\tau) < c_i$; that is, indeed $n(\tau) \in \text{int}(C)$. □

Remark 4.5.3. *The proof also shows that for each $\tau > 0$ there exists $\epsilon(\tau) > 0$ with $\epsilon(\tau) \to 0$ as $\tau \to 0$, such that $n(\tau) \in [\epsilon, c_1 - \epsilon] \times [\epsilon, c_2 - \epsilon] \times \cdots \times [\epsilon, c_m - \epsilon]$; that is, even if the initial value is on ∂C the orbit enters* $\text{int}(C)$ *after an arbitrarily short time.*

Remark 4.5.4. *A similar argument shows that ∂C only contains the two trivial equilibria corresponding to an empty and a full network.*

To see this, let us first assume that n^* is an equilibrium and for a compartment q_i we have $n_i^* = 0$. Then, by (4.6)

$$\dot{n}_i^* = \sum_{j \in \mathcal{D}_i} \mathcal{K}_{ji}(n_j^*, c_i) = 0$$

which is only possible if $n_j^* = 0$ for each $j \in \mathcal{D}_i$. Induction shows that $n^* = 0^{(m)}$.

Next, let us assume that for a compartment q_i we have $n_i^* = c_i$. Then, by (4.6)

$$\dot{n}_i^* = -\sum_{j \in \mathcal{R}_i} \mathcal{K}_{ij}(c_i, c_j - n_j^*) = 0$$

which is only possible if $n_j^* = c_j$ for each $j \in \mathcal{R}_i$. Induction shows that $n^* = c^{(m)}$.

For a given initial condition $a \in C$, let $\varrho(t,a)$ denote the solution at time t with $\varrho(0,a) = a$; that is $\varrho(t,a) = n(t)$ with $n(0) = a$.

Proposition 4.5.5. *Consider a compartmental system of the form* (4.6) *with a strongly connected compartmental structure. Then, for any* $s \in \left[0, H(c^{(m)})\right]$, *where* H *is given in* (4.8), *the set* L_s *contains a unique steady state* e_s *satisfying* $\lim_{t\to\infty} \varrho(t,a) = e_s$ *for any* $a \in L_s$.

Proof. Since $L_0 = \left\{0^{(m)}\right\}$ and $\varrho(t, 0^{(m)}) = 0^{(m)}$, the statement holds for an empty network with $e_0 = 0^{(m)}$. Similarly, since $L_{H(c^{(m)})} = \left\{c^{(m)}\right\}$ and $\varrho(t, c^{(m)}) = c^{(m)}$, the statement holds for a full network with $e_{H(c^{(m)})} = c^{(m)}$.

Choose $s \in \left(0, H(c^{(m)})\right)$ and $a \in L_s$. By the strongly connected compartmental structure the Jacobian $J(n)$ is irreducible on $\mathrm{int}(C)$ but may become reducible on ∂C. However, Lemmata 4.5.1 and 4.5.2 along with Remak 4.5.3 show that (4.6) has repelling boundary; that is, $\varrho(t,a) \in \mathrm{int}(C)$ after an arbitrarily short time even if $a \in L_s \cap \partial C$. As a consequence, (4.6) is a cooperative irreducible system evolving in $\mathrm{int}(C)$ admitting a first integral with positive gradient. The result [130, Theorem 10.] shows that L_s either has precisely one equilibrium that attracts the whole level set or has zero equilibria and each ω-limit set of the level set is empty. However, by the boundedness of the sequence $\{\varrho(k,a) : k = 1, 2, \dots\} \subset \mathrm{int}(C)$ the Bolzano-Weierstrass theorem implies that there is a convergent subsequence; that is, the ω-limit set of a cannot be empty. Furthermore, [129, Corollary 4.9] implies that $\omega(a) \cap \partial C = \emptyset$ and the proof is complete. □

In the proofs above we used the notion of cooperative systems directly, however, the underlying theory involves so-called (strongly) monotone systems, which in our case, is a direct consequence of cooperativity, as shown by our next result.

For two points $x, y \in \mathbb{R}^m$, let

$$\begin{aligned} x \le y \quad & \text{if } x_i \le y_i \text{ for } i = 1, 2, \dots, m, \\ x < y \quad & \text{if } x \le y \text{ and } x \ne y, \\ x \ll y \quad & \text{if } x_i < y_i \text{ for } i = 1, 2, \dots, m. \end{aligned}$$

Proposition 4.5.6. *Consider a compartmental system of the form* (4.6) *with a strongly connected compartmental structure. Then, for any* $s \in \left[0, H(c^{(m)})\right]$ *and* $a, b \in L_s$, *the relation* $a \le b$ *implies* $\varrho(t,a) \le \varrho(t,b)$ *and* $a < b$ *implies* $\varrho(t,a) \ll \varrho(t,b)$ *for any* $t > 0$.

Proof. If x or y is equal to $0^{(m)}$ or $c^{(m)}$, then the statement trivially holds. In any other case, use the proof of Proposition 4.5.5 to conclude that (4.6) is a cooperative irreducible

system evolving in a convex and open set, namely, $\mathrm{int}(C)$. The statement is a direct consequence of [130, Theorem 1., Theorem 3.]. □

Our final result in this topic gives further insight into the qualitative behaviour of (4.6).

Proposition 4.5.7. *Consider a compartmental system of the form* (4.6) *with a strongly connected compartmental structure. Then, for any $a, b \in C$ initial values and $t \geq 0$*

$$\|\varrho(t,a) - \varrho(t,b)\|_{\ell^1(\mathbb{R}^m)} \leq \|a-b\|_{\ell^1(\mathbb{R}^m)}.$$

In other words, using the usual $\ell^1(\mathbb{R}^m)$ norm, the distance of two trajectories at any given time cannot be larger than the distance of the initial values. In particular, if $b = e_{H(a)}$, then we find that the convergence to $e_{H(a)}$ is monotone.

Proof. By [131, Chapter 2.2] the induced matrix measure by the ℓ^1 vector norm is

$$\mu(A) = \max_i \left\{ [A]_{ii} + \sum_{j \neq i} \big|[A]_{ji}\big| \right\}.$$

Since $\mu\big(J(n)\big) = 0$, the result [132, Theorem 1.] implies the assertion of the proposition. □

Remark 4.5.8. *It is straightforward to extend our persistence and stability results to systems with a weakly reversible compartmental graph, when the dynamics unfold into isolated subsystems having strongly connected compartmental graphs. Furthermore, some of the above results on the qualitative behaviour, for example the monotonicity in Proposition 4.5.6 and Proposition 4.5.7 can be extended to systems with arbitrary compartmental topology.*

Propositions 4.5.5, 4.5.6 and 4.5.7 imply that the steady states form a linearly ordered set. For $i = 1, 2, \ldots, m$ let $e_i : [0, c] \mapsto [0, c_i]$ denote the ith coordinate function of the steady state; that is, let

$$e_i(r) := \lim_{t \to \infty} \rho\big(t, n(0)\big)_i$$

where $n(0) \in L_r$ is arbitrary and $\rho\big(t, n(0)\big)$ denotes the solution at time t with $\rho\big(0, n(0)\big) = n(0)$. Clearly each e_i is continuous and the monotonicity of the system also shows that each e_i function is strictly increasing; that is, they are differentiable almost everywhere and their derivative are positive.

Example 1: (generalized) RFMR

As a small example let us consider a Ribosome Flow Model on a Ring (RFMR) [35] with three sites. The underlying compartmental model is given by $D = (Q, A)$, where

$$Q = \{q_1, q_2, q_2\},$$
$$A = \big\{(q_1, q_2), (q_2, q_3), (q_3, q_1)\big\}.$$

The topology is shown in Fig 4.2.

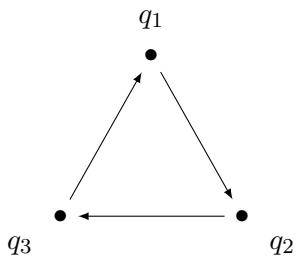

Figure 4.2: Compartmental graph of a three-dimensional RFMR

The corresponding CRN has the following species and reactions:

$$\Sigma = \{N_1, N_2, N_3, S_1, S_2, S_3\}$$
$$R_1 : N_1 + S_2 \xrightarrow{\mathcal{K}_{12}} S_1 + N_2$$
$$R_2 : N_2 + S_3 \xrightarrow{\mathcal{K}_{23}} S_2 + N_3$$
$$R_3 : N_3 + S_1 \xrightarrow{\mathcal{K}_{31}} S_3 + N_1.$$

It is easy to see that, indeed, the reaction graph is not weakly reversible and its deficiency is one. The dynamics of the model in the full state space is given by (4.4) as

$$\dot{n}_1 = \mathcal{K}_{31}(n_3, s_1) - \mathcal{K}_{12}(n_1, s_2)$$
$$\dot{s}_1 = -\mathcal{K}_{31}(n_3, s_1) + \mathcal{K}_{12}(n_1, s_2)$$
$$\dot{n}_2 = \mathcal{K}_{12}(n_1, s_2) - \mathcal{K}_{23}(n_2, s)_3$$
$$\dot{s}_2 = -\mathcal{K}_{12}(n_1, s_2) + \mathcal{K}_{23}(n_2, s_3)$$
$$\dot{n}_3 = \mathcal{K}_{23}(n_2, s)_3 - \mathcal{K}_{31}(n_{,3}\, s_1)$$
$$\dot{s}_3 = -\mathcal{K}_{23}(n_2, s)_3 + \mathcal{K}_{31}(n_{,3}\, s_1)$$

which can be rewritten in the reduced state space based on (4.6) as

$$\dot{n}_1 = \mathcal{K}_{31}(n_3, c_1 - n_1) - \mathcal{K}_{12}(n_1, c_2 - n_2)$$
$$\dot{n}_2 = \mathcal{K}_{12}(n_1, c_2 - n_2) - \mathcal{K}_{23}(n_2, c_3 - n_3)$$
$$\dot{n}_3 = \mathcal{K}_{23}(n_2, c_3 - n_3) - \mathcal{K}_{31}(n_3, c_1 - n_1).$$

In a classical RFMR each $c_i = 1$ and each transition-rate $\mathcal{K}_{ij}$ follows the mass-action law. In an RFMR with different site sizes [116] we allow arbitrary site sizes, in which case the above equation can be written as

$$\dot{n}_1 = k_{31}n_3(c_1 - n_1) - k_{12}n_1(c_2 - n_2)$$
$$\dot{n}_2 = k_{12}n_1(c_2 - n_2) - k_{23}n_2(c_3 - n_3)$$
$$\dot{n}_3 = k_{23}n_2(c_3 - n_3) - k_{31}n_3(c_1 - n_1).$$

Fig 4.3 shows the equilibrium curves of the system with capacities $c_1 = 5$, $c_2 = 25$, $c_3 = 50$ and $k_{12} = 100$, $k_{23} = 40$, $k_{31} = 60$. We consider the above mass action case along with

$$\mathcal{K}_{ij}(n_i, c_j - n_j) = k_{ij}\frac{n_i^3}{(l + n_i)^3} \cdot \frac{(c_j - n_j)^3}{(l + c_j - n_j)^3}$$

for various $l > 0$.

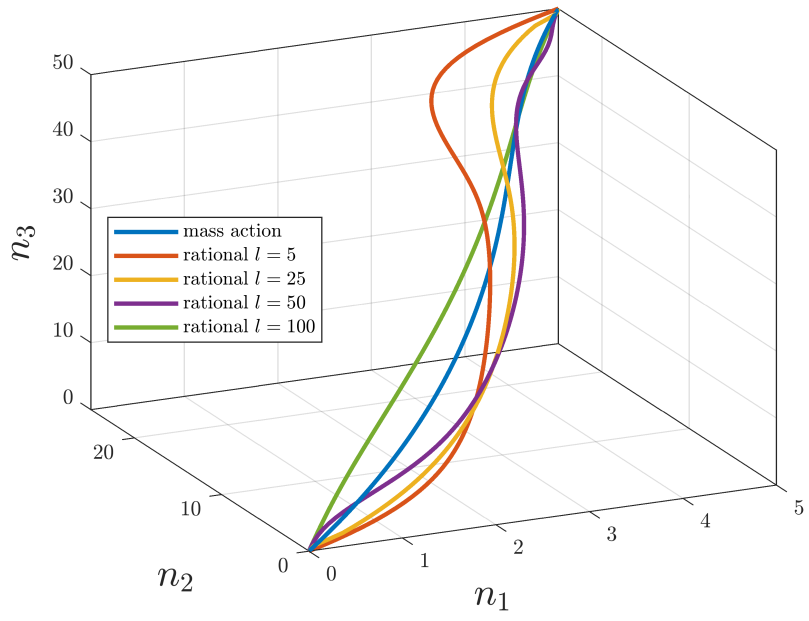

Figure 4.3: Loci of equilibria of a generalized RFMR as a function of the total number of ribosomes for different l saturation parameters

Example 2: not strongly connected model

Let us consider consider a not strongly connected compartmental model given by $D = (Q, A)$, where

$$Q = \{q_1, q_2, q_2\},$$
$$A = \big\{(q_2, q_3), (q_3, q_2), (q_3, q_1)\big\}.$$

The topology is shown in Fig 4.4.

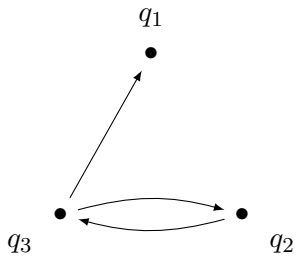

Figure 4.4: Compartmental graph of a not strongly connected model

The corresponding CRN has the following species and reactions:

$$\Sigma = \{N_1, N_2, N_3, S_1, S_2, S_3\}$$
$$R_1 : N_2 + S_3 \xrightarrow{\mathcal{K}_{23}} S_2 + N_3$$
$$R_2 : N_3 + S_2 \xrightarrow{\mathcal{K}_{32}} S_3 + N_2$$
$$R_3 : N_3 + S_1 \xrightarrow{\mathcal{K}_{31}} S_3 + N_1.$$

The dynamics of the system in the reduced state space is given by

$$\dot{n}_1 = \mathcal{K}_{31}\big(n_3, c_1 - n_1\big)$$
$$\dot{n}_2 = \mathcal{K}_{32}\big(n_3, c_2 - n_2\big) - \mathcal{K}_{23}\big(n_2, c_3 - n_3\big)$$
$$\dot{n}_3 = \mathcal{K}_{23}\big(n_2, c_3 - n_3\big) - \mathcal{K}_{32}\big(n_3, c_2 - n_2\big) - \mathcal{K}_{31}\big(n_3, c_1 - n_1\big).$$

Since the compartmental graph is not strongly connected the persistence and stability results of [129] are not applicable. However, empirical results show that the long-time behaviour of the system still exhibits some regularity, which can be divided into two cases base on the initial values of the system:

1. If $r := H\big(n(0)\big) \leq c_1$, then

$$\lim_{t\to\infty} n_2(t) = \lim_{t\to\infty} n_3(t) = 0 \quad \text{and} \quad \lim_{t\to\infty} n_1(t) = r.$$

2. If $r := H\big(n(0)\big) > c_1$, then

$$\lim_{t\to\infty} n_1(t) = c_1$$

and $n_1(t)$ and $n_2(t)$ will converge to the unique equilibrium on the level set

$$\big\{(n_2, n_3) \in [0, c_2] \times [0, c_3] \big| n_2 + n_3 = r - c_1\big\}$$

of the reduced compartmental model $D' = (Q', A')$ given by $Q' = \{q_2, q_3\}$, $A' = \big\{(q_2, q_3), (q_3, q_2)\big\}$. Note that since D' is strongly connected, the results of [129] and the above investigation can be applied.

For the simulations we set $c_1 = c_2 = c_3 = 100$. The rate functions in the different cases are assumed to have form $\mathcal{K}_{ij}(n_i, c_j - n_j) = k_{ij} n_i (c_j - n_j)$ (corresponding to mass-action kinetics) or to be rational functions of the form

$$\mathcal{K}_{ij}(n_i, c_j - n_j) = k_{ij} \frac{n_i}{l + n_i} \cdot \frac{c_j - n_j}{l + c_j - n_j}$$

for some $l > 0$ with $k_{23} = 15$, $k_{32} = 25$, $k_{31} = 35$. Fig 4.5 shows the equilibrium curves for these rate functions with various l values. As described by the above cases we see that until the sum of the initial value exceed the capacity of the q_1 compartment the equilibrium lies on the n_1 axis. After that the equilibrium lies on the plane $\{n_1 = c_1\} \subset \mathbb{R}^3$ and since D' is strongly connected we have that the coordinate functions of the equilibria $e_2(r)$ and $e_3(r)$, restricted to the set $[c_1, c]$, are continuous and strictly increasing.

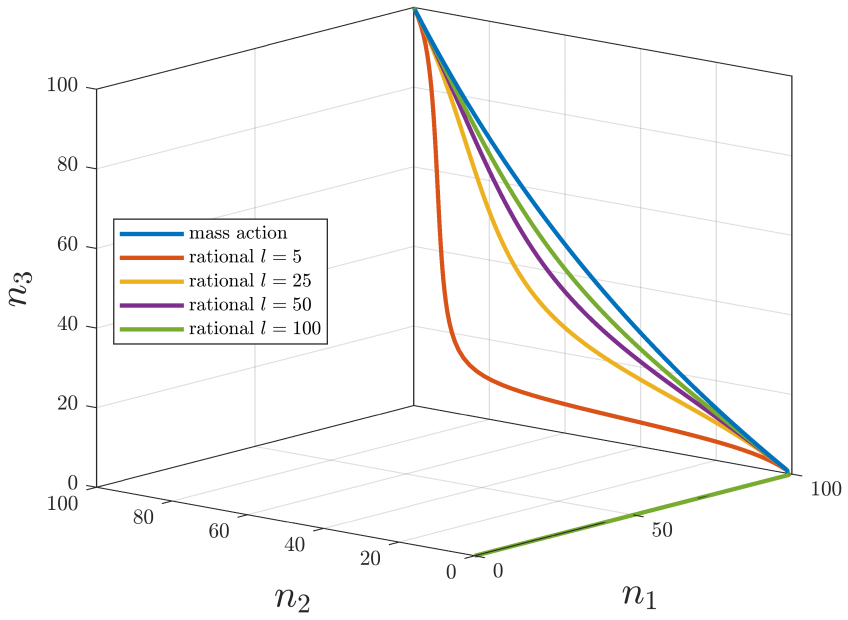

Figure 4.5: Loci of equilibria of a not strongly connected model as a function of the amount of modeled quantities for different l saturation parameters

Remark 4.5.9. *The authors hypothesize that the long-time behaviour of a compartmental model with* ***arbitrary*** *compartmental structure can be similarly described. Recall that a (compartmental) graph $D = (Q, A)$ can be written as a directed acyclic hypergraph of strongly connected components. The hypergraph will then contain three types of components:*

1. *we call a component trap if it does not have any outgoing edges,*

2. *we call a component source if it does not have any incoming edges,*

3. *we call a component intermediate if it is not a trap and not a source.*

Based on the initial value and the exact compartmental structure the following phenomena can be observed:

- *Traps (and only traps) can become full, thus possibly creating new traps.*
- *Sources (and only sources) can become empty, thus possibly creating new sources.*
- *After a sufficient number of traps are filled and sources are emptied, the compartmental graph D is decomposed into isolated strongly connected components; that is, the resulting graph is weakly reversible, in which case the results of [129] can be applied.*

While these observations are elementary and show that the system is stable, the equilibria are clearly non-unique with respect to the total mass of the network and in general it is not straightforward to predict from the initial value which components will fill and empty.

4.6 Persistence and stability of generalized ribosome flow models with time-varying transition rates

In this section we consider time-varying systems, where the transition rates can depend on all compartments, not just the donor and the recipient. That is, based on (4.4), we consider systems of the general form

$$\begin{aligned} \dot{n}_i &= \sum_{j\in\mathcal{D}_i} \mathcal{K}_{ji}(n,s,t) - \sum_{j\in\mathcal{R}_i} \mathcal{K}_{ij}(n,s,t), \\ \dot{s}_i &= -\sum_{j\in\mathcal{D}_i} \mathcal{K}_{ji}(n,s,t) + \sum_{j\in\mathcal{R}_i} \mathcal{K}_{ij}(n,s,t). \end{aligned} \tag{4.17}$$

The exact assumptions on the reaction rates will be specified later.

4.6.1 Persistence

First, we will investigate the persistence of time-varying generalized ribosome flows of the form (4.17) only under mild regularity assumptions described by the following theorem, which is based on the results of [75] but the statements are rephrased to be more aligned with our framework. For the definition of notions related to Petri nets (e.g. siphons) and their exact connection with CRNs we refer to [75, 129].

Theorem 4.6.1. *[75] The dynamics of a CRN of the form* (2.2) *is persistent if*

(i) *Each siphon of the CRN contains a subset of species which define a positive linear conserved quantity for the dynamics.*

(ii) *There exists a positive linear conserved quantity $c^\top x$ for the dynamics.*

(iii) *There are nonnegative, continuous functions $\underline{\mathcal{K}}_j(x)$, $\overline{\mathcal{K}}_j(x)$ such that*

(a) if $x_k > \tilde{x}_k$ for each $k \in \operatorname{supp}(y_j)$, then $\underline{\mathcal{K}}_j(x) > \underline{\mathcal{K}}_j(\tilde{x})$ (and similarly for $\overline{\mathcal{K}}_j$) holds for each $j = 1, 2, \ldots, R$, and

(b) for each $j = 1, 2, \ldots, R$, for all $x \in \mathbb{R}^N_+$ and for all $t \geq 0$ we have $\underline{\mathcal{K}}_j(x) \leq \mathcal{K}_j(x,t) \leq \overline{\mathcal{K}}_j(x)$.

To verify condition (i) we would, in general, need to enumerate all siphons of the CRN, which is well-known to be an NP-hard problem. However, in our recent paper [129] we explicitly characterized the siphons of a CRN assigned to a strongly connected compartmental models in the time-invariant case. However, one can observe that conditions (i) and (ii) of 4.6.1 are independent of the choice of transition rates and even independent from whether the system is time-invariant or not; that is, our results, formulated in the following theorem, hold for time-varying compartmental systems as well.

Theorem 4.6.2. *[129, Corollary 4.6] A siphon in the Petri net of a strongly connected compartmental graph either contains the vertices N_i and S_i corresponding to the same compartment q_i, or it contains all the vertices $N_1, N_2, \ldots, N_m$ or $S_1, S_2, \ldots, S_m$.*

Then the conclusions of Section 4.3 show that conditions (i) and (ii) are satisfied by virtue of the first integrals (4.8) and (4.5), respectively.

It is not straightforward to determine exactly what types of reaction rates satisfy condition (iii). For the sake of specificity, we characterize a class of reaction rates of special interest which can be written in the following form

$$\mathcal{K}_{ij}(n,s,t) = k_{ij}(t)\frac{\theta_i(n_i)\nu_j(s_j)}{1+\Psi_{ij}(n,s)} \tag{4.18}$$

where we assume that the transformations $\theta_i, \nu_j \in \mathcal{C}^1(\mathbb{R})$ are nondecreasing, have $\theta_i(0) = \nu_j(0) = 0$ and satisfy $\int_0^1 |\log \theta_i(r)|\,\mathrm{d}r < \infty$ and $\int_0^1 |\log \nu_j(r)|\,\mathrm{d}r < \infty$ for each $i, j = 1, 2, \ldots, m$. We also assume that the functions Ψ_{ij} take the form

$$\Psi_{ij}(n,s) = \sum \alpha_{r^{(1)},r^{(2)}} \prod_{l=1}^{m} \theta_l^{r_l^{(1)}}(n_l)\nu_l^{r_l^{(2)}}(s_l)$$

where $r^{(1)}, r^{(2)} \in \mathbb{N}^m$ and $\alpha_{r^{(1)},r^{(2)}} \in \overline{\mathbb{R}}_+$. We further assume that for $k_{ij}(t)$ there exist $\underline{k}_{ij}, \overline{k}_{ij} > 0$ such that $\underline{k}_{ij} \leq k_{ij}(t) \leq \overline{k}_{ij}$ for all $t \geq 0$. In this case we have

$$\underline{\mathcal{K}}_{ij}(n_i,s_j) := \frac{\underline{k}_{ij}\theta_i(n_i)\nu_j(s_j)}{1+\Psi_{ij}(c^{(m)},c^{(m)})} \leq \mathcal{K}_{ij}(n,s,t) \leq \overline{k}_{ij}\theta_i(n_i)\nu_j(s_j) =: \overline{\mathcal{K}}_{ij}(n_i,s_j),$$

which are clearly monotonous in the sense of Theorem 4.6.1, and thus condition (i) is satisfied and the system is persistent.

Remark 4.6.3. *The above investigation and, in particular, condition (iii) of Theorem 4.6.1 shows that Lemmata 5.1, 5.2 and Remark 5.3 of [129] can be modified to the time-varying case; that is, for a system of the form* (4.17) *with strongly connected compartmental graph and reaction rates of the form* (4.18)*, for each* $\tau > 0$ *there exists* $\epsilon(\tau) > 0$ *with* $\epsilon(\tau) \to 0$ *as* $\tau \to 0$ *such that* $n_i(t), s_i(t) \in [\epsilon, c_i - \epsilon]$ *holds for each* $i = 1, 2, \ldots, m$ *and* $t \geq \tau$*.*

The denominator of (4.18) contains positive terms which can be interpreted as the inhibitory effect of other species, and the time-varying coefficient $k_{ij}(t)$ introduces the dependence of the system parameters on various factors such as temperature or the dynamical behaviour of other species that are not explicitly modeled as state variables. This class of rate functions contains many well-known examples, demonstrating the range and flexibility of reaction rates of the above form:

1. Setting each $\theta_i(n_i) = n_i$ and $\nu_j(s_j) = s_j$ and $\Psi_{ij}(n, s) = 0$ we obtain the case of classical mass-action kinetics with time-varying rate coefficients: $\mathcal{K}_{ij}(n, s, t) = k_{ij}(t) n_i s_j$.

2. Setting each $\theta_i(n_i) = n_i$ and $\nu_j(s_j) = s_j$ and $\Psi_{ij}(n, s) = l^2 - 1 + l n_i + l s_j + n_i s_j$ for some $l > 0$ yields

$$\mathcal{K}_{ij}(n, s, t) = k_{ij}(t) \frac{n_i s_j}{(l + n_i)(l + s_j)}$$

   corresponding to simple saturating kinetics described by the Monod equation.

3. The previous example can also be obtained by setting $\theta_i(n_i) = \frac{n_i}{l+n_i}$ and $\nu_j(s_j) = \frac{s_j}{l+s_j}$ and $\Psi_{ij}(n, s) = 0$, showing that (4.18) is not unique. Notice however, that for fixed θ_i, ν_j transformations the function Ψ_{ij}, and thus the fraction itself, is unique.

4. Setting each $\theta_i(n_i) = \frac{n_i^L}{l+n_i^L}$ and $\nu_j(s_j) = \frac{s_j^L}{l+s_j^L}$ for some $l > 0$ yields the classical Hill kinetics.

4.6.2 Stability of the solutions for periodic transition rates

In this section we investigate the periodic behaviour of the generalized ribosome flows based on the ideas of [133]. Let us consider a generalized ribosome flow in the reduced state space of the form (4.6) with transition rates of the form (4.18) and assume that

the transition functions are $\mathcal{C}^1$ and periodic with the same period (but having possibly different phases). Write (4.6) as $\dot{n} = F(t, n)$ and assume that the right-hand side satisfies the following monotonicity condition: $F_i(t, x) \leq F_i(t, y)$ for any two distinct points $x, y \in C$ such that $x_i = y_i$ and $x_j \leq y_j$ for $j \neq i$. This condition is satisfied if, for example, the transition rates are such that $\Psi_{ij} \equiv 0$; that is, if there are no inhibitory phenomena. Then the system phase locks (or entrains) with the periodic excitations.

Theorem 4.6.4. *Consider a system of the form* (4.6) *satisfying the above monotonicity assumption, where each $\mathcal{K}_{ij}(t)$ is periodic with a common period T. Then for each $r \in [0, c]$ there exists a unique periodic function $\phi_r : \overline{\mathbb{R}}_+ :\mapsto C$ with period T such that for all $a \in L_r$ we have that*

$$\lim_{t\to\infty} \|\rho(t, a) - \phi_r(t)\|_{L^1} = 0.$$

Proof. The properties of the rate functions and the fact that ∇H is positive implies the result via [134, 135]. □

Remark 4.6.5. *Since, in some sense, time-invariant systems can be seen as periodic, the stability result [129, Proposition 5.5] is a special case of the above theorem, where ϕ_r is reduced to a single point of the manifold L_r.*

Example 3: entrainment of generalized RFMR

Let us again consider a generalized version of the RFMR from Fig 4.2. For this example we set $c_1 = c_2 = c_3 = 100$ and

$$\begin{aligned}
\mathcal{K}_{12}(n_1, c_2 - n_2, t) &= 100\big(3 + 2\cos(t + 0.5)\big)\frac{n_1(c_2 - n_2)}{(l + n_1)(l + c_2 - n_2)},\\
\mathcal{K}_{23}(n_2, c_3 - n_3, t) &= 100\big(7 + 5\sin(3t - 2.5)\big)\frac{n_2(c_3 - n_3)}{(l + n_2)(l + c_3 - n_3)},\\
\mathcal{K}_{31}(n_3, c_1 - n_1, t) &= 100\big(2 + \cos(2t - 1)\big)\frac{n_3(c_1 - n_1)}{(l + n_3)(l + c_1 - n_1)},
\end{aligned}$$

which clearly have the same period $T = 2\pi$. Figs 4.6a and 4.6b show the phase portrait of the system starting from various initial conditions with $l = 100$, $H\big(n(0)\big) = 150$ and the time evolution of the state variables with $n(0) = [5\ 45\ 100]^\top$, respectively.

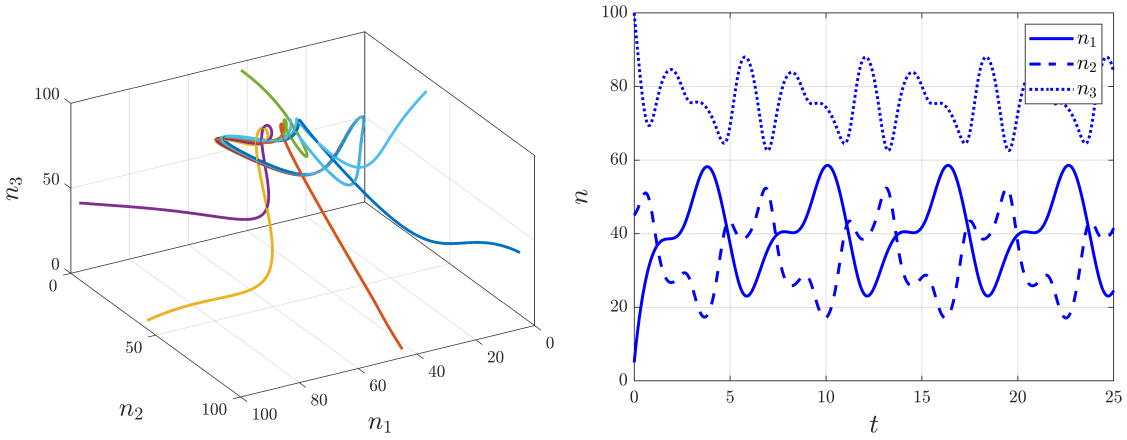

(a) Phase portrait of the system

(b) Time evolution of state variables

Figure 4.6: Entrainment of a generalized RFMR with periodic transition rates

4.6.3 Lyapunov stability analysis

In this section we show that generalized ribosome flows with reaction rate functions of the form (4.18) with piecewise locally Lipschitz $k_{ij}(t)$ coefficients satisfy a certain notion of robustness to the changes in the time-varying rate functions that can be traced back to the input-to-state stability of rate-controlled biochemical networks thoroughly investigated in [28]. The main difficulty in applying these results lies in the aforementioned fact that the CRN assigned to a compartmental model is generally not weakly reversible and its deficiency is generally not zero (see, Theorem 4.3.1) even if the compartmental topology is strongly connected. In order to circumvent this, we will perform a model reduction and rewrite (4.6) by factoring out appropriate terms. Let us first recall the most important notions and results of [28].

Consider the system corresponding to a CRN with R reactions

$$\dot{x} = f(x,u) = \sum_{i=1}^{R}\sum_{j=1}^{R} u_{ij}(t)\prod_{l=1}^{n}\theta_i^{y_{ij}}(x_i)[y_i - y_j], \tag{4.19}$$

where the nonnegative functions u_{ij} are piecewise locally Lipschitz with a finite number of discontinuities and the stoichiometric coefficient vectors y_i, y_j are as described in 2.2. Motivated by control designs for ribosome flow models [136] we introduce such time dependence not only to handle some uncertainty originating from fluctuating external factors but to measure the robustness of the system to certain control inputs.

In this section, however, we restrict the conditions on the transformation functions $\theta_i : \overline{\mathbb{R}}_+ \mapsto [0,\infty)$. Namely, we assume that

1. θ_i is real analytic,
2. $\theta_i(0) = 0$,
3. $\int_0^1 |\log \theta_i(r)| \, \mathrm{d}r < \infty$
4. θ_i is strictly increasing and onto the set $[0, \sigma_i)$ for some $\sigma_i \in [0, \infty)$,
5. $\lim_{t \to \log \sigma_i} \int_a^t \rho_i^{-1}(r) \, \mathrm{d}r - pt = \infty$ for any $a < \log \sigma_i$ and any constant $p > 0$, where $\rho_i = \log \theta_i$.

Before continuing with the definitions, we consider the case when $u(t)$ is a constant matrix A. We assume that A has nonnegative entries and is irreducible; that is, the underlying reaction graph is strongly connected. We denote the set of such A matrices as $\mathcal{A}$. Then the equilibria of $\dot{x} = f(x, A)$ can be divided into the sets of boundary equilibria and positive equilibria:

$$E_0 = \big\{ x \in \partial \overline{\mathbb{R}}_+^n \big| f(x, A) = 0 \big\},$$
$$E_{A,+} = \big\{ x \in \mathbb{R}_+^n \big| f(x, A) = 0 \big\}.$$

Then, the result [28, Theorem 2.1] (and also [62, Theorem 2]) shows that if there are no boundary equilibria in any positive class, then each positive class contains a unique globally (relative to the positive class) asymptotically stable positive equilibrium. Denote the unique positive equilibrium in the same class as x_0 as $\overline{x}(x_0, A)$ and notice that $E_{A,+} = \big\{ \overline{x}(x_0, A) \big| x_0 \in \mathbb{R}_+^n \big\}$. Finally, denote

$$\mathcal{E} = \bigcup_{A \in \mathcal{A}} E_{A,+}.$$

Definition 4.6.6. *We define the following function classes:*

1. *A function $\alpha : \overline{\mathbb{R}}_+ \mapsto \overline{\mathbb{R}}_+$ is said to be of class $\mathcal{K}$ if it is continuous, strictly increasing and has $\alpha(0) = 0$.*
2. *The subset of unbounded functions of class $\mathcal{K}$ are denoted by $\mathcal{K}_\infty$.*
3. *A function $\beta : \overline{\mathbb{R}}_+ \times \overline{\mathbb{R}}_+$ is said to be of class $\mathcal{KL}$ if $\beta(., t)$ is of class $\mathcal{K}$ for all $t \geq 0$ and $\beta(r, .)$ is strictly decreasing to zero for all $r > 0$.*

We consider nonnegative time-varying inputs such that at any time instant the reaction graph is strongly connected; that is, the input-value set $\mathbb{U}$ is a subset of $\mathcal{A}$. Furthermore, let $\|.\|_2$ denote the spectral norm induced by the Euclidian norm and for $u : \overline{\mathbb{R}}_+ \mapsto \mathbb{U}$ define

$$\|u\|_{\mathbb{U}} = \operatorname*{ess\,sup}_{t \in [0, \infty)} \|u(t)\|_2.$$

Definition 4.6.7. *A system $\dot{x} = f(x,u)$ is uniformly input-to-state stable (ISS) with input-value set $\mathbb{U}$ if for every compact set $P \subset \mathcal{E}$ and every compact set $F \subset \overline{\mathbb{R}}^n_+$ containing P, there exist functions $\beta = \beta_P$ of class $\mathcal{KL}$ and $\phi = \phi_P$ of class $\mathcal{K}_\infty$ such that, for every $\overline{x}_o \in P \cap E_{u_0,+}$ for some $u_0 \in \mathbb{U}$ we have that*

$$\|x(t) - \overline{x}_0\| \leq \beta\big(\|x_0 - \overline{x}_0\|, t\big) + \phi\big(\|u - u_0\|_{\mathbb{U}}\big)$$

holds for each $u : \overline{\mathbb{R}}_+ \mapsto \mathbb{U}$ input and every initial condition $x_0 \in F \cap \mathcal{S}_{\overline{x}_0}$ and for all $t \geq 0$ such that $x(s) \in F$ for $s \in [0,t]$.

According to the above definition we say that a system is ISS if it is globally asymptotically stable in the absence of external inputs and if its trajectories are bounded by an appropriate function of the input. In some sense this definition is intended to capture the idea of "bounded input bounded output" stability, since for bounded u input ($u - u_0$ to be more precise) the trajectories will remain in a ball and, in fact, approach the ball $\phi(\|u - u_0\|_{\mathbb{U}})$ as t increases [137].

We assume that there exists a uniform lower bound on the parameters; that is, we consider input-value sets of the form

$$\mathcal{A} \supset \mathbb{U}_\epsilon = \big\{u \in \mathcal{A} \big| u_{ij}(t) \geq \epsilon \ \forall t \geq 0, \text{ or } u_{ij}(t) = 0 \ \forall t \geq 0\big\}.$$

We also recall that the input functions are piecewise locally Lipschitz in time with a finite number of discontinuities, thus we introduce

$$\mathcal{W} = \big\{w : \overline{\mathbb{R}}_+ \mapsto \mathbb{U}_\epsilon \big| w \text{ is piecewise locally Lipschitz}\big\}.$$

Then the main Theorem of [28] states:

Theorem 4.6.8. *Consider the system* (4.19) *and suppose that is is mass-conservative; that is, there exists $v \in \mathbb{R}^n_+$ such that $v^\top f(x,u) = 0$ for all $x \in \overline{\mathbb{R}}^n_+$ and $u \in \mathcal{A}$. Then the system with input maps $u \in \mathcal{W}$ is uniformly ISS with input-value set $\mathbb{U}_\epsilon$.*

The proof relies on the candidate ISS-Lyapunov function (for the definition of which and for the exact connection with ISS stability we refer to [28])

$$V(x,\overline{x}) = \sum_{i=1}^{n} \int_{\overline{x}_i}^{x_i} \big(\log \theta_i(r) - \log \theta_i(\overline{x}_i)\big)\, \mathrm{d}r \tag{4.20}$$

which, for mass-action systems, yields the classical entropy-like Lyapunov function well-known from the theory of chemical reaction networks, see (4.27). We note that $V(x,\overline{x})$

is uniquely determined by the θ_i functions and does not depend explicitly on the reaction/compartmental structure or the time-varying $u_{ij}(t)$ functions; that is, it is universal in the sense of [138].

Remark 4.6.9. *We note that the assumption that the compartmental graph (and thus the reaction graph of the factored model) is strongly connected is purely technical. For time-invariant systems it simply ensures that the unique equilibrium on each level set of the first integral is positive (except for the trivial case of an empty network of course). In fact, in some cases the initial values of the network can ensure the positivity of the equilibrium even for not strongly connected systems (see Example 2), in which case the above Lyapunov function can be applied.*

Factorization of the transition rates

Let us consider a generalized ribosome flow (4.17) in the reduced state space, in this case given by

$$\begin{aligned}\dot{n}_i &= \sum_{j\in\mathcal{D}_i} \mathcal{K}_{ji}(n, c-n, t) - \sum_{j\in\mathcal{R}_i} \mathcal{K}_{ij}(n, c-n, t) \\ &= \sum_{j\in\mathcal{D}_i} k_{ji}(t)\frac{\theta_j(n_j)\nu_i(c_i-n_i)}{1+\Psi_{ji}(n, c^{(m)}-n)} - \sum_{j\in\mathcal{R}_i} k_{ij}(t)\frac{\theta_i(n_i)\nu_j(c_j-n_j)}{1+\Psi_{ij}(n, c^{(m)}-n)}.\end{aligned} \tag{4.21}$$

Notice that we can naturally factor some terms of the transition rates into the time-varying coefficient as

$$k_{ij}(t)\frac{\theta_i(n_i)\nu_j(c_j-n_j)}{1+\Psi_{ij}(n, c^{(m)}-n)} = \frac{k_{ij}(t)\nu_j(c_j-n_j)}{1+\Psi_{ij}(n, c^{(m)}-c)}\theta_i(n_i) =: \tilde{k}_{ij}(t)\theta_i(n_i).$$

Then (4.21) can be rewritten as

$$\dot{n}_i = \sum_{j\in\mathcal{D}_i} \tilde{k}_{ji}(t)\theta_j(n_j) - \sum_{j\in\mathcal{R}_i} \tilde{k}_{ij}(t)\theta_i(n_i). \tag{4.22}$$

This equation can be clearly embedded into the class of strongly connected systems of the form (4.19), since the reaction graph of (4.22) consists of species $\Sigma = \{N_1, N_2, \ldots, N_m\}$, has the $m \times m$ identity matrix as its stoichiometric matrix and for each transition $(q_i, q_j) \in A$ we assign a reaction of the form

$$N_i \xrightarrow{\tilde{\mathcal{K}}_{ij}(t)} N_j,$$

and thus the system of differential equations can be written as

$$\dot{n} = I\tilde{A}_k(t)\theta(n) \tag{4.23}$$

where the elements of $\tilde{A}_k$ are given by

$$\left[\tilde{A}_k(t)\right]_{ij} = \begin{cases} -\sum_{l\in\mathcal{R}_i} \tilde{k}_{il}(t) & \text{if } i = j, \\ \tilde{k}_{ji}(t) & \text{if } j \in \mathcal{D}_i, \\ 0 & \text{otherwise.} \end{cases}$$

Note that the fractions $\frac{\nu_j(c_j-n_j)}{1+\Psi_{ij}(n,c^{(m)}-n)}$ are differentiable (and thus Lipschitz) and each $k_{ij}(t)$ is piecewise locally Lipschitz, hence each $\tilde{k}_{ij}(t)$ is piecewise locally Lipschitz. This shows that generalized ribosome flows can be embedded into the class of rate-controlled biochemical networks described in [28] in a way that preserves the compartmental structure; that is, the reaction graph of (4.23) is topologically isomorph to the compartmental graph. In particular if the compartmental model is strongly connected, then the reaction graph of the reduced system (4.23) is strongly connected as well. Furthermore, combining the persistence of the system with Remark 4.6.3 we find that $\tilde{A}_k \in \mathcal{W}$, and thus Theorem 4.6.8 ensures input-to-state stability.

Quasi-LTV factorization

A classical argument shows that the model reduction above can result in a Linear Time-Varying (LTV) system [9]. Consider an $F(x) \in \mathcal{C}^k(\mathbb{R})$ nonnegative function such that $F(0) = 0$, where $k \geq 1$. Then for the function $F(rx)$ we have

$$\frac{\mathrm{d}F(rx)}{\mathrm{d}r} = xF'(rx)$$

and thus

$$F(x) - F(0) = x\int_0^1 F'(rx)\,\mathrm{d}r = xf(x)$$

and since $F(0) = 0$, we find that $F(x) = xf(x)$. Note, that the calculation also shows that $f \in \mathcal{C}^{k-1}(\mathbb{R})$. Since θ_i is real analytic we have that $\theta_i(n_i) = \hat{\theta}_i(n_i)n_i$ for some $\hat{\theta}_i$ real analytic function. Then (4.22) can be rewritten as

$$\dot{n}_i = \sum_{j\in\mathcal{D}_i} \hat{k}_{ji}(t)n_j - \sum_{j\in\mathcal{R}_i} \hat{k}_{ij}(t)n_i \tag{4.24}$$

where

$$\hat{k}_{ij}(t) = \frac{k_{ij}(t)\hat{\theta}_i(n_i)\nu_j(c_j - n_j)}{1 + \Psi_{ij}(n, c^{(m)} - n)}.$$

Similarly as before, the reaction graph of (4.24) consists of species $\Sigma = \{N_1, N_2, \ldots, N_m\}$, has the $m\times m$ identity matrix as its stoichiometric matrix and for each transition $(q_i, q_j) \in A$ we assign a reaction of the form

$$N_i \xrightarrow{\hat{K}_{ij}(t)} N_j,$$

and thus the system of differential equations can be written as

$$\dot{n} = I\hat{A}_k(t)n$$

where the elements of $\hat{A}_k$ are given by

$$\left[\hat{A}_k(t)\right]_{ij} = \begin{cases} -\sum_{l\in\mathcal{R}_i}\hat{k}_{il}(t) & \text{if } i=j, \\ \hat{k}_{ji}(t) & \text{if } j\in\mathcal{D}_i, \\ 0 & \text{otherwise.} \end{cases}$$

Again, each $\hat{k}_{ij}(t)$ is piecewise locally Lipschitz, thus for strongly connected compartmental models Theorem 4.6.8 ensures input-to-state stability via Remark 4.6.3.

Factorization of Monod kinetics

Let us consider a generalized version of the RFMR in Fig 4.2 with rational rate functions corresponding to Monod kinetics of the form

$$\begin{aligned} \dot{n}_1 &= k_{31}(t)\frac{n_3}{l+n_3}\frac{c_1-n_1}{l+c_1-n_1} - k_{12}(t)\frac{n_1}{l+n_1}\frac{c_2-n_2}{l+c_2-n_2} \\ \dot{n}_2 &= k_{12}(t)\frac{n_1}{l+n_1}\frac{c_2-n_2}{l+c_2-n_2} - k_{23}(t)\frac{n_2}{l+n_2}\frac{c_3-n_3}{l+c_3-n_3} \\ \dot{n}_3 &= k_{23}(t)\frac{n_2}{l+n_2}\frac{c_3-n_3}{l+c_3-n_3} - k_{31}(t)\frac{n_3}{l+n_3}\frac{c_1-n_1}{l+c_1-n_1} \end{aligned} \tag{4.25}$$

for some $l>0$. As discussed before, the corresponding CRN is not strongly connected. However, using the functions

$$\tilde{k}_{31}(t) = k_{31}(t)\frac{c_1-n_1}{l+c_1-n_1} \qquad \tilde{k}_{12}(t) = k_{12}(t)\frac{c_2-n_2}{l+c_2-n_2} \qquad \tilde{k}_{23}(t) = k_{23}(t)\frac{c_3-n_3}{l+c_3-n_3}$$

we can to rewrite (4.25) as

$$\begin{aligned} \dot{n}_1 &= \tilde{k}_{31}(t)\frac{n_3}{l+n_3} - \tilde{k}_{12}(t)\frac{n_1}{l+n_1} \\ \dot{n}_2 &= \tilde{k}_{12}(t)\frac{n_1}{l+n_1} - \tilde{k}_{23}(t)\frac{n_2}{l+n_2} \\ \dot{n}_3 &= \tilde{k}_{23}(t)\frac{n_2}{l+n_2} - \tilde{k}_{31}(t)\frac{n_3}{l+n_3}. \end{aligned} \tag{4.26}$$

Then the CRN corresponding to (4.26) has the following species and reactions:

$$\Sigma = \{N_1, N_2, N_3\}$$

$$R_1 : N_1 \xrightarrow{\tilde{k}_{12}} N_2$$

$$R_2 : N_2 \xrightarrow{\tilde{k}_{23}} N_3$$

$$R_3 : N_3 \xrightarrow{\tilde{k}_{31}} N_1.$$

which is strongly connected and isomorph to the compartmental model in Fig 4.2. We arrive at the same conclusion if we instead use the functions

$$\hat{k}_{31}(t) = k_{31}(t)\frac{1}{l+n_3}\frac{c_1-n_1}{l+c_1-n_1}$$
$$\hat{k}_{12}(t) = k_{12}(t)\frac{1}{l+n_1}\frac{c_2-n_2}{l+c_2-n_2}$$
$$\hat{k}_{23}(t) = k_{23}(t)\frac{1}{l+n_2}\frac{c_3-n_3}{l+c_3-n_3}$$

to rewrite (4.25) as

$$\dot{n}_1 = \hat{k}_{31}(t)n_3 - \hat{k}_{12}(t)n_1$$
$$\dot{n}_2 = \hat{k}_{12}(t)n_1 - \hat{k}_{23}(t)n_2$$
$$\dot{n}_3 = \hat{k}_{23}(t)n_2 - \hat{k}_{31}(t)n_3.$$

Note that the quasi-LTV factorization might be more complicated in some cases, but the construction described in Section 4.6.3 guarantees its existence.

Induced family of Lyapunov functions

The above investigation demonstrates that generalized ribosome flows can be embedded into rate-controlled biochemical networks in at least two different ways, where each embedding induces a different Lyapunov function of the form (4.20). Thus, in general, we may use at least two different Lyapunov functions governing the same dynamics. To characterize their exact relation, consider a factored system of the form (4.23) with its ISS-Lyapunov function $V(n,\overline{n})$. The quasi-LTV representation of the system admits an ISS-Lyapunov function of the form

$$\begin{aligned} V^{LTV}(n,\overline{n}) &= \sum_{i=1}^{m}\int_{\overline{n}_i}^{n_i}\left(\log r - \log \overline{n}_i\right)\mathrm{d}r \\ &= \sum_{i=1}^{m}\left(n_i\log\frac{n_i}{\overline{n}_i} + \overline{n}_i - n_i\right) =: \sum_{i=1}^{m} V_i^{LTV}(n_i,\overline{n}_i) \end{aligned} \tag{4.27}$$

so that we can write

$$\begin{aligned} V(n,\overline{n}) &= \sum_{i=1}^{m}\int_{\overline{n}_i}^{n_i}\left(\log\left(\hat{\theta}_i(r)r\right) - \log\left(\hat{\theta}(\overline{n}_i)\overline{n}_i\right)\right)\mathrm{d}r = \sum_{i=1}^{m}\int_{\overline{n}_i}^{n_i}\left(\log\hat{\theta}_i(r) - \log\hat{\theta}_i(\overline{n}_i)\right)\mathrm{d}r \\ &+ \sum_{i=1}^{m}\int_{\overline{n}_i}^{n_i}\left(\log r - \log\overline{n}_i\right)\mathrm{d}r = \sum_{i=1}^{m}\int_{\overline{n}_i}^{n_i}\left(\log\hat{\theta}_i(r) - \log\hat{\theta}_i(\overline{n}_i)\right)\mathrm{d}r + V^{LTV}(n,\overline{n}). \end{aligned}$$

Remark 4.6.10. *Since* $\sum_{i=1}^{m}\overline{n}_i = \sum_{i=1}^{m} n_i$ *we have that*

$$V^{LTV}(n,\overline{n}) = \sum_{i=1}^{m} n_i\log\frac{n_i}{\overline{n}_i},$$

which is exactly the Kullback-Leibler divergence $D_{KL}(n||\overline{n})$. It is important to note that the Kullback-Leibler divergence is not a metric, since $D_{KL}(n||\overline{n}) \neq D_{KL}(\overline{n}||n)$ and it does not satisfy the triangle inequality. However, it is a nonnegative measure, meaning that it is nonnegative and zero if and only if $n = \overline{n}$ and it is often used to measure the "distance" of probability distributions for example in information theory and machine learning [139].

While in general we are restricted to the above factorizations, in some special cases we may use a whole family of factorizations and corresponding Lyapunov functions. To illustrate this, consider an example when each $\theta_i(r) = \frac{r^{a_i}}{(l+r)^{b_i}}$ for some $l > 0$ and $a_i \in \mathbb{N}$, $b_i \in \mathbb{N}_0$, $a_i \geq b_i$ (these properties ensure that the functions θ_i are nondecreasing). Then, after the factorization described in Section 4.6.3, the Lyapunov function (4.20) becomes

$$V^{(l,a,b)}(n,\overline{n}) = \sum_{i=1}^{m} \left((a_i - b_i)(\overline{n}_i - n_i) + a_i n_i \log \frac{n_i}{\overline{n}_i} + b_i(l+n_i) \log \frac{l+\overline{n}_i}{l+n_i} \right). \tag{4.28}$$

We emphasize that (4.20) only depends on the θ_i functions, in this case parametrized with the l, a_i, b_i values; that is, it is independent of the network structure and transition rate coefficients. We can also perform the factorization $\theta_i(r) = \tilde{\theta}_i(r)\frac{r^{\hat{a}_i}}{(l+r)^{\hat{b}_i}}$ with $\hat{a}_i \in \mathbb{N}$, $\hat{a}_i < a_i$, $\hat{b}_i \in \mathbb{N}_0$, $\hat{a}_i \geq \hat{b}_i$ yielding the Lyapunov function $V^{(l,\hat{a},\hat{b})}$ of the same form as in (4.28). This shows that the parameters a and b can be freely (apart from the constraints above) chosen in (4.28). We may also observe some interesting behaviour at the extrema of the parameters $\hat{b}$ and l, namely, that if we choose each $\hat{b}_i = 0$ then the Lyapunov function in (4.28) is independent of l; that is, we have that

$$V^{(l,\hat{a},0)}(n,\overline{n}) = \sum_{i=1}^{m} \hat{a}_i V_i^{LTV}(n_i,\overline{n}_i).$$

Moreover, letting $l \to \infty$ yields the convergence

$$\lim_{l\to\infty} V^{(l,\hat{a},\hat{b})}(n,\overline{n}) = \sum_{i=1}^{m} \hat{a}_i V_i^{LTV}(n_i,\overline{n}_i) \tag{4.29}$$

where V_i^{LTV} is defined in (4.27).

Example 4: family of Lyapunov functions of a generalized RFMR

Let us again consider a generalized version of the RFMR in the reduced state space from Fig 4.2. For a given initial condition n_0 we can substitute $n_3 = H(n_0) - n_1 - n_2$, and thus the Lyapunov function restricted to the manifold $\{H(n) = H(n_0)\}$ can be seen as a two dimensional function with local coordinates n_1 and n_2.

We set the capacities as $c_1 = c_2 = c_3 = 100$ and $k_{12} = 100$, $k_{23} = 60$, $k_{31} = 20$. The system has transition rates as described above with each $a_i = b_i = 3$; that is, we have

that

$$\mathcal{K}_{12}(n_1, c_2 - n_2) = 100 \cdot \frac{n_1^3}{(l + n_1)^3} \cdot \frac{(c_2 - n_2)^3}{(l + c_2 - n_2)^3}$$
$$\mathcal{K}_{23}(n_2, c_3 - n_3) = 60 \cdot \frac{n_2^3}{(l + n_2)^3} \cdot \frac{(c_3 - n_3)^3}{(l + c_3 - n_3)^3}$$
$$\mathcal{K}_{31}(n_3, c_1 - n_1) = 20 \cdot \frac{n_3^3}{(l + n_3)^3} \cdot \frac{(c_1 - n_1)^3}{(l + c_1 - n_1)^3}.$$

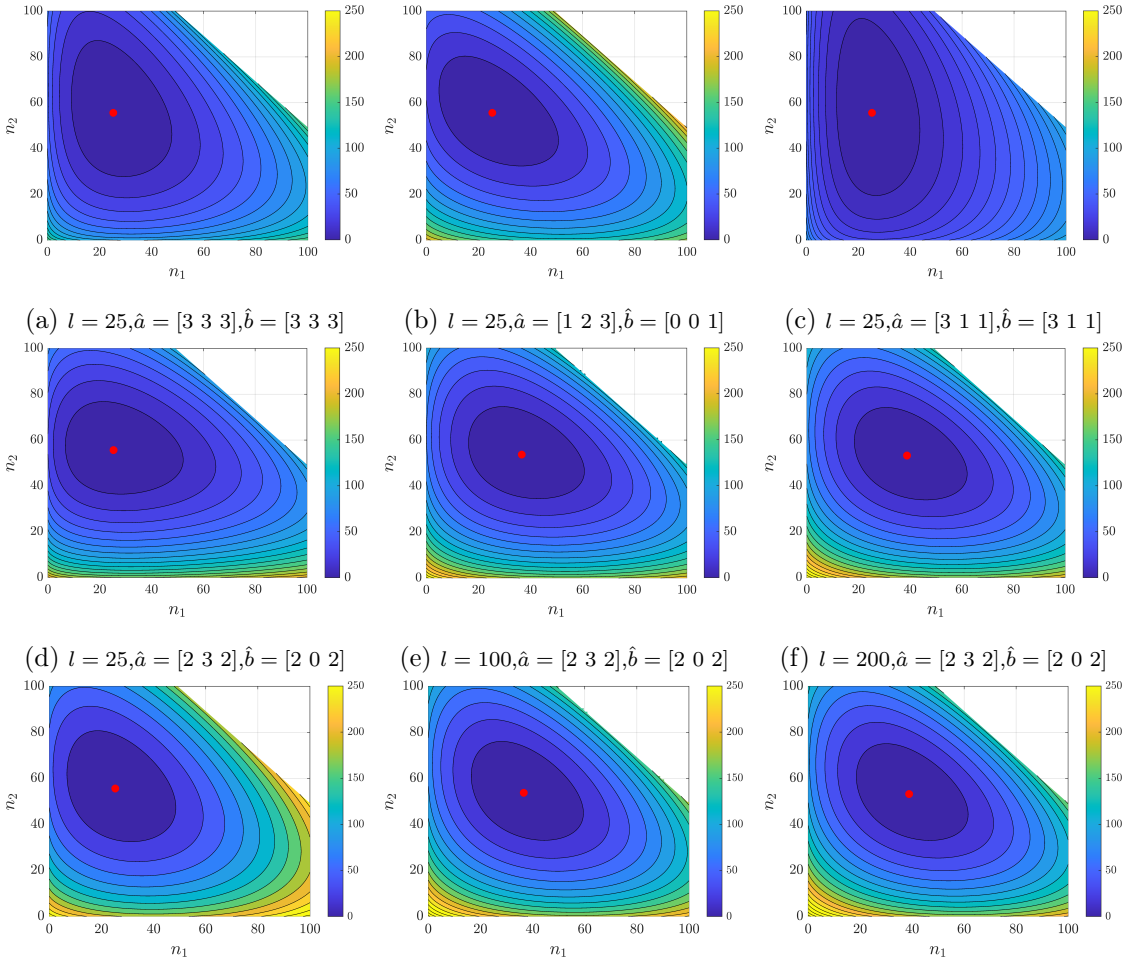

(a) $l = 25, \hat{a} = [3\ 3\ 3], \hat{b} = [3\ 3\ 3]$ (b) $l = 25, \hat{a} = [1\ 2\ 3], \hat{b} = [0\ 0\ 1]$ (c) $l = 25, \hat{a} = [3\ 1\ 1], \hat{b} = [3\ 1\ 1]$

(d) $l = 25, \hat{a} = [2\ 3\ 2], \hat{b} = [2\ 0\ 2]$ (e) $l = 100, \hat{a} = [2\ 3\ 2], \hat{b} = [2\ 0\ 2]$ (f) $l = 200, \hat{a} = [2\ 3\ 2], \hat{b} = [2\ 0\ 2]$

(g) $l = 25, \hat{a} = [2\ 3\ 2], \hat{b} = [2\ 0\ 2]$ (h) $l = 100, \hat{a} = [2\ 3\ 2], \hat{b} = [2\ 0\ 2]$ (i) $l = 200, \hat{a} = [2, 3, 2], \hat{b} = [2, 0, 2]$

Figure 4.7: Comparison of Lyapunov functions for a generalized RFMR

The simulations were performed with $H(n_0) = 150$. Figs 4.7a-4.7c show the Lyapunov function $V^{(l,\hat{a},\hat{b})}$ for various choices of $\hat{a}$ and $\hat{b}$ with $l = 25$ fixed. The second and third rows demonstrate the convergence characterized in (4.29); figs 4.7d-4.7f show $V^{(l,\hat{a},\hat{b})}$ for increasing l values and 4.7g-4.7i show $\sum_{i=1}^{m} \hat{a}_i V_i^{LTV}$ for the same increasing l values. While the level sets of these Lyapunov functions are similar, their anisotropy and range is quite different, suggesting, for example, that they might lead to different convergence speed estimates.

Example 5: family of Lyapunov functions for a larger network

Let us consider a compartmental system with $m = 100$ compartments in the reduced state space. We assume that the transition rate functions are corresponding to Hill kinetics (modified intentionally to have different powers in the numerator and the denominator) and are of the form

$$\mathcal{K}_{ij}(n_i, c_j - n_j) = k_{ij} \frac{n_i^3 (c_j - n_j)^3}{\big(l + n_i^2\big)\big(l + (c_j - n_j)^2\big)} \tag{4.30}$$

with $l = 350$. We assume that the only nonzero coefficients are

$$k_{i(i+1)} = 20 \quad k_{i(i+2)} = 18 \quad k_{i(i+3)} = 16 \quad k_{i(i+4)} = 14$$
$$k_{i(i+5)} = 12 \quad k_{i(i+6)} = 10 \quad k_{i(i+7)} = 8 \quad k_{i(i+8)} = 6$$

for $i = 1, 2, \ldots, m$, where indices are understood as modulo m. Clearly this compartmental graph is strongly connected. Finally, we set capacities

$$c_1 = c_2 = \cdots = c_{50} = 50 \quad c_{51} = c_{52} = \cdots = c_{100} = 100$$

Then the Lyapunov function (4.20) takes the form

$$V_{Hill}^{(l,3,2)}(n, \overline{n}) = \sum_{i=1}^{m} \Bigg((\overline{n}_i - n_i) + 3n_i \log \frac{n_i}{\overline{n}_i} + n_i \log \frac{\overline{n}_i^2 + l}{n_i^2 + l} + 2\sqrt{l} \bigg(\operatorname{atan} \frac{\overline{n}_i}{\sqrt{l}} - \operatorname{atan} \frac{n_i}{\sqrt{l}} \bigg) \Bigg).$$

We can also factorize as $\theta_i(r) = \hat{\theta}_i(r) \frac{r^2}{l + r^2}$, when (4.20) becomes

$$V_{Hill}^{(l,2,2)}(n, \overline{n}) = \sum_{i=1}^{m} \Bigg(2n_i \log \frac{n_i}{\overline{n}_i} + n_i \log \frac{\overline{n}_i^2 + l}{n_i^2 + l} + 2\sqrt{l} \bigg(\operatorname{atan} \frac{\overline{n}_i}{\sqrt{l}} - \operatorname{atan} \frac{n_i}{\sqrt{l}} \bigg) \Bigg).$$

Fig 4.8 shows the time evolution of Lyapunov functions $V_{Hill}^{(l,3,2)}$, $V_{Hill}^{(l,2,2)}$ and V^{LTV} and their time derivatives.

Remark 4.6.11. *In the above examples we restricted the factorizations to integer exponents so that we have real analytic transformations. However, the underlying dynamics is not changed through the factorizations and real analyticity is not directly used in the investigation of the ISS-Lyapunov function* (4.20)*. Thus, as long as the factored $\hat{k}_{ij}(t)$ is piecewise locally Lipschitz (which holds after an arbitrarily short time in virtue of Remark 4.6.3), we can generalize* (4.28) *for other values as well; to be precise, we can use any $0 < \hat{a}_i \leq a_i$ and $0 \leq \hat{b}_i \leq \hat{a}_i$ real numbers.*

Next, focusing on the Hill kinetics in (4.30)*, we note that while the denominator of the transformation* $\theta_i(r) = \frac{r^3}{l+r^2}$ *in* (4.30) *cannot be factorized we can rearrange the transformation as*

$$\theta_i(r) = \frac{r^3}{l+r^2} = \underbrace{\frac{r^{3-a_i}(l+r^{b_i})}{l+r^2}}_{\hat{\theta}_i(r)} \frac{r^{a_i}}{l+r^{b_i}} = \hat{\theta}_i(r)\frac{r^{a_i}}{l+r^{b_i}}$$

where choosing $0 < a_i \leq 3$ *and* $0 \leq b_i \leq a_i$ *ensures that the time-varying coefficient functions are piecewise locally Lipschitz. In this case the exact value of the integral in* (4.20) *involves the generalized hypergeometric function and generally cannot be expressed in a closed form. However, in some special cases (such as* $b_i = 2$ *above) we can calculate the integral explicitly; for example setting* $a_i = 1.5$ *and* $b_i = 0.5$ *yields*

$$V_{Hill}^{(l,1.5,0.5)}(n,\overline{n}) = \sum_{i=1}^{m}\left((\overline{n}_i - n_i) + \frac{3}{2}n_i \log\frac{n_i}{\overline{n}_i} + \left(n_i - l^2\right)\log\frac{\sqrt{\overline{n}_i}+l}{\sqrt{n_i}+l} + l\left(\sqrt{\overline{n}_i} - \sqrt{n_i}\right)\right).$$

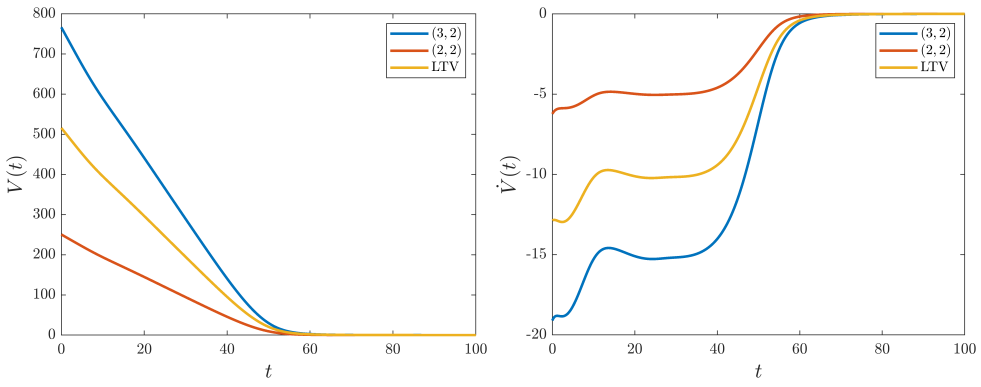

(a) Time evolution of Lyapunov functions (b) Derivative of Lyapunov functions

Figure 4.8: Time evolution and time derivative of Lyapunov functions obtained from various factorizations of the transition rates

Example 6: competition for ribosomes in the cell

In this example we introduce a set of generalized ribosome flows connected by a finite pool of ribosomes to model competition in the cell. We follow [115], where the authors introduced a model for simultaneous translation and [117], where the authors generalized the model to include premature drop-off and attachment effects modeled with Langmuir kinetics. We will focus on the latter case and show that with a slight modification it can be formalized as a generalized ribosome flow model with a clear and natural compartmental interpretation. This demonstrates the usefulness and modeling power of generalized ribosome flows as one can prove various properties of many existing models of

different conceptual levels. Moreover, our results show that many qualitative properties of the system carry over to more general settings, e.g. when the translation, drop-off and attachment rates are modeled with more sophisticated functions or when some (or all) rates are time-dependent.

For the sake of simplicity we will present this example in the reduced state space. Let us consider N mRNAs consisting of $m_1, m_2, \dots, m_N$ number of sites. Let n_i^j denote the continuous amount of ribosomes in the ith site of the j mRNA stand and let c_i^j denote its capacity. Let c_z denote the capacity of the pool and n_z denote the amount of ribosomes in the pool. For the sake of notational simplicity let n_0^j and $n_{m_j+1}^j$ also denote n_z and similarly for the capacities. Let the translation rate functions from the ith site the to $(i+1)$th site on the jth mRNA be denoted as $\mathcal{K}_{i(i+1)}^j$. Finally, let the detachment and attachment rates at the ith site of the jth mRNA be denoted respectively as $\mathcal{K}_{iz}^j$ and $\mathcal{K}_{zi}^j$. The attachment rate to the first site and the detachment rate from the last site will be called initiation rate and production rate, respectively. Then the dynamics of the model is given by:

$$\begin{aligned}
\dot{n}_i^j &= \mathcal{K}_{(i-1)i}^j\big(n_{i-1}^j, c_i^j - n_i^j, t\big) - \mathcal{K}_{i(i+1)}^j\big(n_i^j, c_{i+1}^j - n_{i+1}^j, t\big) \\
&\quad + \mathcal{K}_{zi}^j\big(n_z, c_i^j - n_i^j, t\big) - \mathcal{K}_{iz}^j\big(n_i^j, c_z - n_z, t\big), \\
\dot{n}_z &= \sum_{j=1}^{N} \big(\mathcal{K}_{m_j z}^j(n_{m_j}^j, c_z - n_z, t) - \mathcal{K}_{z1}^j(n_z, c_1^j - n_1^j, t)\big) \\
&\quad + \sum_{j=1}^{N}\sum_{i=1}^{m_j} \Big(\mathcal{K}_{iz}^j(n_i^j, c_z - n_z, t) - \mathcal{K}_{zi}^j(n_z, c_i^j - n_i^j, t)\Big).
\end{aligned}$$

Thus, indeed, simultaneous translation with a finite pool can be described by a generalized ribosome flow. Clearly the following function defines a linear first integral

$$H(n) = n_z + \sum_{j=1}^{N}\sum_{i=1}^{m_j} n_i^j$$

and is a crucial factor in the dynamical analysis of the system.

Remark 4.6.12. *In [117] the authors consider the following special case:*

- *the capacity of each site is one; that is, each* $c_i^j = 1$,
- *the translation rate are time-invariant and obey the mass-action law; that is, each* $\mathcal{K}_{i(i+1)}^j(n_i^j, 1 - n_{i+1}^j, t) = \lambda_i^j n_i^j (1 - n_{i+1}^j)$ *for some* $\lambda_i^j > 0$,
- *the initiation and attachment rates are time-invariant and are given by* $\mathcal{K}_{zi}^j(n_z, 1 - n_i^j, t) = \beta_i^j G_j(z)(1 - n_i^j)$ *for some* $\beta_i^j \geq 0$ *and* $G_j(z)$ *continuously differentiable strictly increasing function with* $G_j(0) = 0$,

- *the drop-off rates are time-invariant and are given by* $\mathcal{K}_{iz}^j(n_i^j, c_z - n_z, t) = \alpha_i^j n_i^j$ *for some* $\alpha_i^j \geq 0$.

Since the drop-off rates are donor controlled the pool does not have a predefined capacity and the amount of ribosomes in the pool are only bounded by $H\big(n(0)\big)$. *Therefore, this special case does not fit in our compartmental framework, although, as most of our results are a consequence of the linear first integral combined with the cooperativity of the system they can be generalized to include donor controlled terms as well. It is assumed that the authors consider this case to capture the fact that the capacity of the pool might be several orders higher than the actual number of ribosomes, and thus the dependence on the available space in the pool may be negligible. However, some physical meaning is lost with this assumption and it might in fact lead to less precise simulations.*

To see this, let us consider a network with $N = 10$ *mRNAs with* $m = 5$ *sites. For the sake of simplicity let* $\lambda_i^j = \beta_1^j = \alpha_5^j = 1$ *for each* i *and* j, *and assume that there are no premature drop-offs and attachments. We consider initation rates* $G_j(z) = z$, $G_j(z) = \tanh(z)$ *and* $G_j(z) = z^2$ *and set* $c_z = 10^4$. *Since the equilibrium is unique on the level sets of the first integral we set each* $n_i^j = 0$ *and we only change* $n_z(0)$. *Fig. 4.9 shows the ratio of the steady state of the pool in the case of donor controlled and mass-action production rates as we increase the ratio* $\frac{n_z(0)}{c_z}$ *from* $5 \cdot 10^{-2}$ *to* 1.

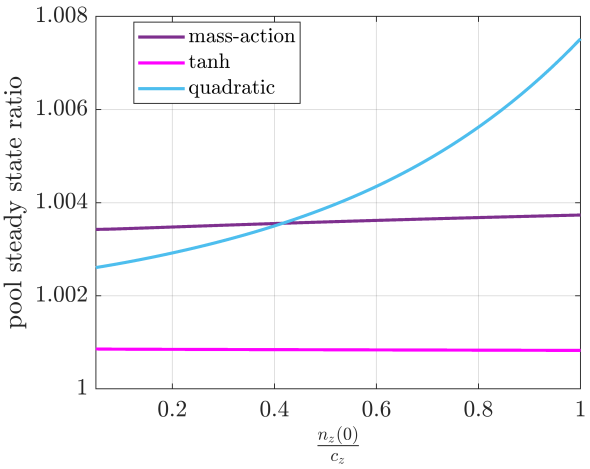

Figure 4.9: Steady state ratio of the donor controlled and the mass-action production rate for various initiation rates as a function of the ratio of the total number of ribosomes and the capacity of the pool

As expected, the steady state ratio is close to one for saturating rate functions and for $n_z(0) \ll c_z$. However, the ratio can get higher when the total number of ribosomes

have the same magnitude as the capacity; that is, the inaccuracy of the donor controlled kinetics increases. While this assumption might be valid for realistic parameters of ribosome flows in other TASEP based flow models (especially with non-saturating kinetics) it might be crucial to model these transitions accurately.

Effect of the total number of ribosomes. In the next simulation we follow [117, Example 3.2] and we consider a single mRNA strand with $m_1 = 3$ sites. The initiation rate is set to $\beta_1^1 = 1$ while the attachment rates are $\beta_2^1 = 0.1$ and $\beta_3^1 = 0$. The drop-off rates and production rate are set as $\alpha_1^1 = 0$, $\alpha_2^1 = 0.01$, $\alpha_3^1 = 1$. We assume that the translation rates obey the mass-action law with each $\lambda_i^1 = 1$. We set the initial values to $n_j^1 = 0$ and $n_0(z) = c_z$ as before. Fig. 4.10 shows the steady state of the system as we increase c_z from 0 to 5 for various rate functions. One can see that in each case the mRNA saturates as we increase the number of ribosomes and the rest of the ribosomes are accumulated in the pool. Finally, the same effect as in Fig. 4.9 can be observed; that is, the donor controlled detachment rates shift the steady state of the pool to higher values.

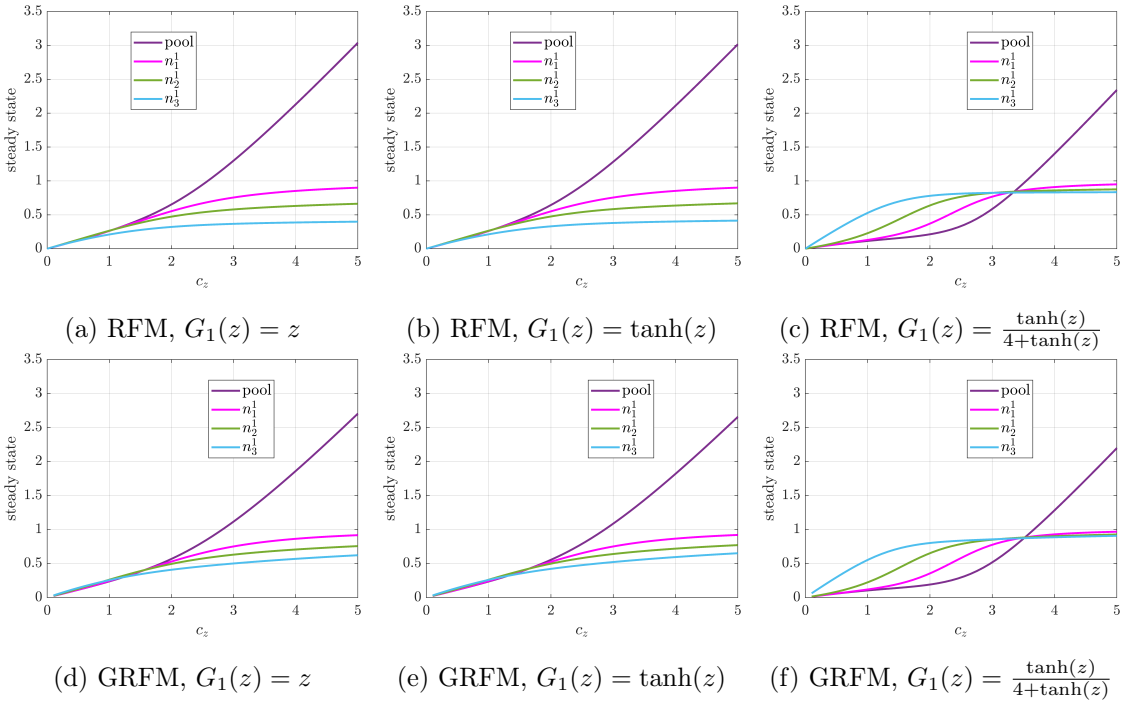

(a) RFM, $G_1(z) = z$ (b) RFM, $G_1(z) = \tanh(z)$ (c) RFM, $G_1(z) = \frac{\tanh(z)}{4+\tanh(z)}$

(d) GRFM, $G_1(z) = z$ (e) GRFM, $G_1(z) = \tanh(z)$ (f) GRFM, $G_1(z) = \frac{\tanh(z)}{4+\tanh(z)}$

Figure 4.10: Steady state of a single mRNA strand in a pool modeled with an RFM and a GRFM with mass-action translation rate and drop-off rates, and attachment rate corresponding to different $G_1(z)$ functions

We again emphasize the versatility of generalized ribosome flows as the initiation, translation, production, attachment and detachment rate function can be different on

each site. For example let us consider a particular mRNA strand with saturating initation and attachment rates given by $\mathcal{K}^1_{zi}(n_z, n^1_i) = \beta^1_i \tanh(n_z)(c^1_i - n^1_i)$, with mass-action translation rates and with production and drop-off rates given by $\mathcal{K}^1_{iz}(n^1_i, n_z) = \alpha^1_i \cdot \frac{n^1_i}{1+n^1_i} \cdot n^3_z$. Fig. 4.11 shows evolution of the steady states as we increase $n_z(0) = c_z$ as before. As expected the steady states of the mRNA sites are moved to lower values.

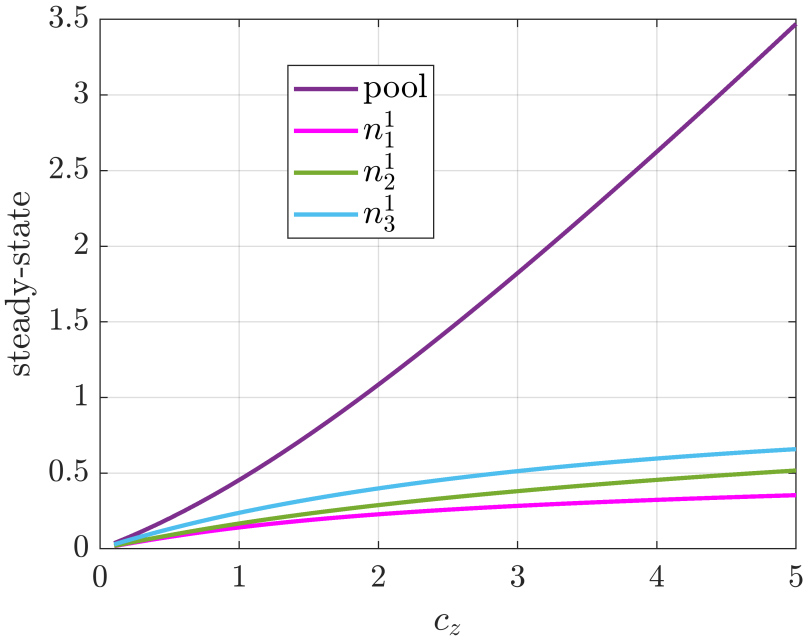

Figure 4.11: Steady state of a single mRNA strand in a pool modeled with a GRFM with mass-action translation rate, rational fraction drop-off rates, and saturating attachment rates

4.7 Conclusions

We considered compartmental models and their kinetic representations, called generalized ribosome flows, with physically meaningful reaction graph structure. We showed that one-dimensional nonlocal particle flows with Lighthill-Whitham-Richards flux supplemented with appropriate in- and out-flow terms can be spatially discretized with a finite volume scheme to obtain special cases of generalized ribosome flows. Then it was shown that for strongly connected compartmental models, a unique equilibrium point exists within each stoichiometric compatibility class, and this equilibrium is asymptotically stable within each compatibility class even if the initial conditions are on the boundary of the nonnegative orthant (except for the two trivial boundary equlibria).

Finally, we considered time-varying transition rates. We showed that time-varying

generalized ribosome flows are persistent under mild regularity assumptions on the transition rates, and a wide set of reaction rates satisfying this assumption was characterized, containing well-known examples such as mass-action type rates. It was shown that the studied models can be embedded in at least two ways into the class of rate-controlled biochemical networks originally described in [28]. This embedding allows us to prove stability with entropy-like logarithmic Lyapunov functions known from the theory of CRNs. It was illustrated that the non-unique factorization of the rate functions gives rise to a whole family of various possible Lyapunov functions. Finally, periodic model behaviour was also studied, where we showed that trajectories with the same overall initial mass and periodic transition rates having the same period (but possibly different phase) converge to a unique periodic solution.

While the nonlocal equations considered here are based on a particular pair-interaction coupling, alternative forms of nonlocality can lead to qualitatively different discretizations and network structures. In the next chapter, we investigate a distinct class of nonlocal models and show how their discretization likewise produces CRNs, though with different topologies and interaction patterns. This further illustrates the breadth of CRN dynamics that can arise from spatially or structurally extended systems.

Chapter 5

A kinetic finite volume discretization of the multidimensional PIDE model for gene regulatory networks

5.1 Introduction

Gene expression is a fundamental biological process of actually realizing DNA information in the form of proteins in living organisms. Therefore, the (quantitative) modeling of gene expression has been in the focus of research during the last decades [140, 141]. Gene regulatory networks (GRNs) are complex mechanisms through which cells are able to react to internal and external signals in a controlled way [142]. The set of techniques successfully applied for the modeling of GRNs is really wide [143, 144, 145]. It was pointed out already in the 1970s that the stochastic nature of gene expression has to be taken into consideration during modeling [146]. Experimental results and model analysis clearly show that both translational and transcriptional bursting contribute to stochasticity in prokaryote and eukaryote gene expression [147, 148]. It is also known that in many cases, stochasticity in gene expression is functionally advantageous, and it can even result in robust phenotypes [149].

The dynamical model studied in this chapter is originated in [150], where an analytical approach is proposed for describing the stationary distribution of protein concentration in living cells in the form of partial integro-differential equations (PIDEs). The model is based on the master equation, and considers protein production in random bursts (see, also [151, 152]) extended by transcription autoregulation. Feasible stationary distributions for this PIDE model with a slightly modified transcription rate were derived and

classified in [153]. The so-called generalized Friedman (or multidimensional PIDE) model was later introduced in [154] which describes the operation of a genetic circuit of n genes expressed into n different protein types. Since finding analytical solutions for the stationary distributions of the generalized Friedman model is not straightforward due to its generality, [154] proposed a numerical procedure for the computation. The approach is based on a semilagrangian method for the discretization of the PIDE, and the computational results show that it is suitable to describe the behaviour of a wide class of GRNs with several different regulatory interactions and protein degradation rates. The generalized Friedman model and the subsequently developed simulation framework SELANSI [155] has since been widely used for design [156], identification [157] and control [158, 159] of GRNs. In [160] a truncated version of the master equation corresponding to a special version of the one-dimensional Friedman model was proposed. As we will show later, this can be formally seen as a semi-discretization of the PIDE and can be generalized to both variable degradation rates and multidimensional GRNs.

Many hyperbolic conservation laws are derived in a so-called integral form, which, in the case of sufficiently smooth solutions and fluxes, can be rewritten in their usual differential form [119]. However, many practical problems involve discontinuous solutions, where shocks can develop quickly even from smooth initial data. Thus, numerical methods derived from the differential form, such as finite differences, are expected to lose accuracy near discontinuities. This problem can for example be mitigated by an appropriate Finite Volume Method (FVM) based on the integral form of the PDE. Instead of computing possibly unreliable pointwise approximations we define grid cells and approximate the cell averages of the solution. This approach introduces a clear compartmental interpretation of semi-discretized PDEs and can naturally capture the underlying conservation law, too. [120].

Motivated by the above results, the aim of this chapter is to propose an efficient novel computational approach based on compartmental discretization for the numerical solution of the multidimensional PIDE model introduced in [154], and to use to for solving control problems. Section 5.2 gives a brief overview of the PIDE model. In Section 5.3 we introduce the kinetic discretization. Section 5.4 contains the qualitative analysis of the kinetic discreziation. In Section 5.5 we perform numerical experiments. Finally, Section 5.6 contains the control of a genetic toggle switch.

5.2 Multidimensional gene regulatory networks

In this section we give a brief introduction of multidimensional GRNs based on [150, 154]. We consider a gene regulatory network consisting of n different genes, denoted by $G = \{DNA_1, DNA_2, \dots, DNA_n\}$, that express n proteins $X = \{X_1, X_2, \dots, X_n\}$ via the corresponding messenger RNAs $M = \{mRNA_1, mRNA_2, \dots, mRNA_n\}$. We follow the central dogma of molecular biology, which asserts that the gene instructions are transcribed into messenger RNAs, that are translated into proteins. The continuous number of mRNA molecules and proteins are denoted by $\boldsymbol{m}, \boldsymbol{x} \in \mathbb{R}^n$, respectively.

The promoters corresponding to each gene are assumed to switch between active and inactive states, denoted by $DNA_{i,\text{on}}$ and $DNA_{i,\text{off}}$, respectively. The transition is controlled by the binding of proteins. Note that in general, the feedback mechanism may require the binding of multiple types of proteins besides the one expressed by the given gene. For the sake of generality, we assume that any protein can repress or activate any gene in the network. This mechanism is typically modelled by multivariate Hill functions. We define the matrix $H \in \mathbb{Z}^{n\times n}$, where H_{ij} represents the Hill coefficient of the cross-regulation. If H_{ij} is positive (respectively, negative), then X_j inhibits (respectively, promotes) the expression of X_i.

The transcription of DNA_i into $mRNA_i$ is assumed to be a first order processes occurring with rate k_m^i per unit time and with transcriptional leakage $\epsilon_i \in (0, 1)$. Then the transcription can be written as

$$R_T^i(\boldsymbol{x}) = k_m^i c_i(\boldsymbol{x}),$$

where $c_i : \mathbb{R}_+^n \to [\epsilon_i, 1]$ depend on the feedback regulation mechanism. See, section 5.5 for some examples off c_i Hill functions. Finally, the translation rate of protein X_i is defined as

$$R_X^i(m_i) = k_x^i m_i.$$

The messenger RNA and protein degradation is assumed to take the form

$$G_m^i(m_i) = -\gamma_m^i m_i \qquad G_X^i(\boldsymbol{x}) = -\gamma_x^i(\boldsymbol{x}) x_i,$$

where $\gamma_m^i > 0$ and $\gamma_x^i : \mathbb{R}_+^n \mapsto \mathbb{R}_+$. Following [154] it is assumed that $\frac{\gamma_m^i}{\gamma_x^i(\boldsymbol{x})} \gg 1$ in order to ensure the validity of the subsequent model.

We use the standard exponential distribution to model protein bursting; that is, the conditional probability of the protein level jumping from $y_i > 0$ to $x_i > y_i$ is

$$\omega_i(x_i - y_i) = \frac{1}{b_i} \exp\left[-\frac{x_i - y_i}{b_i}\right],$$

where $b_i = \frac{k_x^i}{\gamma_m^i}$.

With the above assumptions the probability density function (PDF) of the protein level, $p(t, \boldsymbol{x})$, can be modelled with the following PIDE:

$$\frac{\partial p(t,\boldsymbol{x})}{\partial t} = \sum_{i=1}^{n} \frac{\partial}{\partial x_i}\big[\gamma_x^i(\boldsymbol{x}) x_i p(t,\boldsymbol{x})\big] + \sum_{i=1}^{n} k_m^i \int_0^{x_i} \beta_i(x_i - y_i) c_i(\boldsymbol{y_i}) p(t, \boldsymbol{y_i})\, \mathrm{d}y_i\,, \qquad (5.1)$$

where $\boldsymbol{y_i} = \boldsymbol{x} + (y_i - x_i)e_i$ and the β_i functions have the following form:

$$\beta_i(x) = \omega_i(x) - \delta(x).$$

In [161] the authors show the well-posedness of (5.1), under assumptions satisfied by our setup, in the generalized (mild) sense; that is, for $p_0 \in \mathcal{L}^1(\mathbb{R}^n)$ there exists a unique mild solution $p \in \mathcal{C}\big(\mathbb{R}_+; \mathcal{L}^1(\mathbb{R}^n)\big)$ with the following properties:

(i) nonnegativity: if p_0 is nonnegative, then so is the solution $p(t, .)$ for all $t \geq 0$,

(ii) mass conservation:

$$\int_{\mathbb{R}_+^n} p(t,\boldsymbol{x})\, \mathrm{d}\boldsymbol{x} = \int_{\mathbb{R}_+^n} p_0(\boldsymbol{x})\, \mathrm{d}\boldsymbol{x}\,.$$

In fact, if $p_0 \in \mathcal{C}^{1,b}(\mathbb{R}_+^n)$ for some appropriate $b > 0$ (e.g., in one dimension $b = b_1$), then there exists a unique classical solution $p \in \mathcal{C}^1\big(\mathbb{R}_+; \mathcal{L}^1(\mathbb{R}_+^n)\big)$. Note, that in the probabilistic setting in applications we usually assume that p_0 is nonnegative and its integral is one.

5.3 Kinetic finite volume discretization

In this section we formulate a finite volume discretization of (5.1), the result of which is a mass conservative kinetic system. We also note that since (5.1) is linear (that is, if p and q are solutions, then so is $p + q$), the result of the semi-discretization is anticipated to also be linear.

5.3.1 One-dimensional case

Let us first consider the one-dimensional Friedman model describing the temporal evolution of protein distribution given by

$$\frac{\partial p(t,x)}{\partial t} = \frac{\partial}{\partial x}\big[\gamma_x^1(x) x p(t,x)\big] + k_m^1 \int_0^x \beta_1(x-y) c_1(y) p(t,y)\, \mathrm{d}y\,, \qquad (5.2)$$

with initial condition $p(0, x) = p_0(x)$ that has integral one. The mass conservation of (5.2) is well-known but the subsequent informal investigation provides further insight

that can be transferred to the design of the numerical scheme. Integrating over $\mathbb{R}_+$ shows that

$$\begin{aligned}
&\int_0^\infty \frac{\partial p(t,x)}{\partial t}\,\mathrm{d}x = \frac{\partial}{\partial t}\int_0^\infty p(t,x)\,\mathrm{d}x = \int_0^\infty \frac{\partial}{\partial x}\left[\gamma_x^1(x)xp(t,x)\right]\mathrm{d}x \\
&+ k_m^1 \int_0^\infty \int_0^x \beta_1(x-y)c_1(y)p(t,y)\,\mathrm{d}y\,\mathrm{d}x = \underbrace{\lim_{x\to\infty}\gamma_x^1(x)xp(t,x)}_{=0} - \gamma_x^1 \cdot 0 \cdot p(t,0) \\
&+ k_m^1 \int_0^\infty \int_y^\infty \beta_1(x-y)c_1(y)p(t,y)\,\mathrm{d}x\,\mathrm{d}y \\
&= k_m^1 \int_0^\infty c_1(y)p(t,y)\underbrace{\int_y^\infty \beta_1(x-y)\,\mathrm{d}x}_{=0}\,\mathrm{d}y = 0,
\end{aligned} \tag{5.3}$$

so that the equality

$$\int_0^\infty p(t,x)\,\mathrm{d}x = \int_0^\infty p_0(x)\,\mathrm{d}x = 1$$

holds for any $t \geq 0$.

In a finite volume setting the coefficients are calculated as averages (that is, integrals) over appropriate subdomains. Hence, as an intuition we should note that the mass conservation property of the novel scheme should be the result of a calculation very similar to (5.3).

Our main goal is to perform a spatial discretization (with resolution h) to obtain an infinite dimensional dynamical system describing the temporal evolution of the functions $\left\{p_i(t)\right\}_{i\in\mathbb{Z}}$ with the usual properties of a PDF; that is, we should have that:

1. $0 \leq p_i(t)$ for all $i \in \mathbb{Z}$ and $t \geq 0$,
2. $\sum_{i=1}^\infty h p_i(t) = 1$ for all $t \geq 0$.

In order to do so, consider the set of intervals

$$K_i = \left[x_{i-\frac{1}{2}}, x_{i+\frac{1}{2}}\right] = \left[(i-1)h, ih\right],\ i = 1, 2, \ldots$$

for some $h > 0$ and introduce the set of variables $p_i(t)$, where

$$p_i(t) \approx \frac{1}{|K_i|}\int_{K_i} p(t,y)\,\mathrm{d}y = \frac{1}{h}\int_{K_i} p(t,y)\,\mathrm{d}y\,;$$

that is, the value $p_i(t)$ is assumed to approximate the average in the cell K_i and we set the initial values accordingly. Further introduce the cell averages of the functions γ_x^1 and c_1 given as

$$\gamma_i^1 = \frac{1}{|K_i|}\int_{K_i} \gamma_x^1(y)\,\mathrm{d}y\,, \qquad c_i^1 = \frac{1}{|K_i|}\int_{K_i} c_1(y)\,\mathrm{d}y\,.$$

Let x_i be the midpoint of K_i for $i = 1, 2, \dots$ and define

$$b^1_{i,i} = \frac{1}{h/2}\int_{[(i-1)h,(i-1/2)h]} \beta_1(x_i - y)\,\mathrm{d}y = \frac{1}{h/2}\int_{[x_i - h/2, x_i]} \beta_1(x_i - y)\,\mathrm{d}y\,,$$
$$b^1_{i,j} = \frac{1}{|K_j|}\int_{K_j} \beta_1(x_i - y)\,\mathrm{d}y\,, \quad j = 1, 2, \dots, i-1.$$

As the derivative on the right-hand side of (5.2) describes protein degradation (that is, a vector field pointing towards the origin) we will approximate it with a difference quotient of the form

$$\frac{\partial}{\partial x}\big[\gamma^1_x(x)xp(t,x)\big]\bigg|_{K_i} \approx \frac{1}{h}\big(\gamma^1_{i+1}x_{i+\frac{1}{2}}p_{i+1}(t) - \gamma^1_i x_{i-\frac{1}{2}}p_i(t)\big).$$

Then approximating the integral in (5.2) with a sum yields the system

$$\begin{aligned} \dot{p}_i(t) &= \frac{1}{h}\big(\gamma^1_{i+1}x_{i+\frac{1}{2}}p_{i+1}(t) - \gamma^1_i x_{i-\frac{1}{2}}p_i(t)\big) + k^1_m \sum_{j=1}^{i} h^1_{i,j}b^1_{i,j}c^1_j p_j(t); \\ p_i(0) &= \frac{1}{|K_i|}\int_{K_i} p_0(y)\,\mathrm{d}y\,, \end{aligned} \tag{5.4}$$

where

$$h^1_{i,j} = \begin{cases} h/2, & i = j, \\ h, & i \neq j. \end{cases}$$

Observe, that the resulting infinite dimensional system (5.4) is clearly a linear donor controlled compartmental system of the form

$$\dot{p}(t) = \Gamma p(t),$$

where the infinite matrix defined element-wise as

$$\Gamma_{ij} = \begin{cases} k^1_m h^1_{i,j}b^1_{i,j}c^1_j, & j < i, \\ -\frac{1}{h}\gamma^1_i x_{i-\frac{1}{2}} + k^1_m h^1_{i,i}b^1_{i,i}c^1_i, & j = i, \\ \frac{1}{h}\gamma^1_{i+1}x_{i+\frac{1}{2}}, & j = i+1, \\ 0, & j > i+1 \end{cases}$$

is an infinite Kirchhoff matrix; that is, it has nonnegative off-diagonal elements (i.e. it is a Metzler matrix) with zero column-sums.

Remark 5.3.1. *In the following calculation we assume that* $\lim_{l\to\infty}\gamma^1_{l+1}x_{l+\frac{1}{2}}p_{l+1}(t) = 0$*, and we will do so in the multidimensional case as well. This is a natural assumption based on the well-posedness results of [161] and it is satisfied if for example* γ^1_x *is bounded and* p *has finite expectation. This, however, is not trivial in the infinite case, since* Γ *is*

unbounded with respect to (w.r.t.) the usual matrix norms. The authors are investigating the behaviour of the infinite system, however, the derivation can be transferred to the truncated system (described in the forthcoming section 5.3.3), which is of more practical interest.

Formally, we have that

$$\begin{aligned}
&\sum_{i=1}^{\infty} \dot{p}_i(t) = \sum_{i=1}^{\infty} \frac{1}{h}\big(\gamma_{i+1}^1 x_{i+\frac{1}{2}} p_{i+1}(t) - \gamma_i^1 x_{i-\frac{1}{2}} p_i(t)\big) + k_m^1 \sum_{i=1}^{\infty}\sum_{j=1}^{i} h_{i,j}^1 b_{i,j}^1 c_j^1 p_j(t) \\
&= \lim_{l\to\infty} \frac{1}{h}\gamma_{l+1}^1 x_{l+\frac{1}{2}} p_{l+1}(t) - \frac{1}{h}\gamma_1^1 \cdot 0 \cdot p_1(t) + k_m^1 \sum_{j=1}^{\infty}\sum_{i=j}^{\infty} h_{i,j}^1 b_{i,j}^1 c_j^1 p_j(t) \\
&= k_m^1 \sum_{j=1}^{\infty} c_j^1 p_j(t) \sum_{i=j}^{\infty} h_{i,j}^1 b_{i,j}^1 \\
&= k_m^1 \sum_{j=1}^{\infty} c_j^1 p_j(t) \left(\int_{[x_j - h/2, x_j]} \beta_1(x_j - y)\,\mathrm{d}y + \sum_{i=j+1}^{\infty} \int_{K_j} \beta_1(x_i - y)\,\mathrm{d}y \right) \\
&= k_m^1 \sum_{j=1}^{\infty} c_j^1 p_j(t) \left(\int_0^{h/2} \beta_1(y)\,\mathrm{d}y + \sum_{i=j+1}^{\infty} \int_{[(i-j-1/2)h,(i-j+1/2)h]} \beta_1(y)\,\mathrm{d}y \right) \\
&= k_m^1 \sum_{j=1}^{\infty} c_j^1 p_j(t) \underbrace{\int_0^{\infty} \beta_1(y)\,\mathrm{d}y}_{=0} = 0,
\end{aligned}$$

so that the equality

$$\sum_{i=1}^{\infty} h p_i(t) = \sum_{i=1}^{\infty} h p_i(0) = 1$$

holds for any $t \geq 0$. The above facts combined also show that $p_i(t) \leq \frac{1}{h}$ for any $t \geq 0$.

5.3.2 Multidimensional case

Let us consider the multidimensional model (5.1) with $n > 1$. Define the positive step sizes $h_1, h_2, \ldots, h_n$ and sets

$$K_\alpha = \bigtimes_{i=1}^{n} \big[(\alpha_i - 1)h_i, \alpha_i h_i\big],$$

where $\alpha \in \mathbb{N}^n$ is a multi-index. Let us note that each cell has the same size and define $h = |K_\alpha| = \prod_{i=1}^n h_i$. Similarly to the one-dimensional case, for each cell K_α we introduce the function $p_\alpha(t)$ assumed to approximate the cell average as

$$p_\alpha(t) \approx \frac{1}{h} \int_{K_\alpha} p(t, \boldsymbol{y})\,\mathrm{d}\boldsymbol{y}\,.$$

For $i = 1, 2, \ldots, n$ we also compute the variables

$$\begin{aligned}
\gamma_\alpha^i &= \frac{1}{h} \int_{K_\alpha} \gamma_x^i(\boldsymbol{y})\,\mathrm{d}\boldsymbol{y}\,, \\
c_\alpha^i &= \frac{1}{h} \int_{K_\alpha} c_i(\boldsymbol{y})\,\mathrm{d}\boldsymbol{y}\,.
\end{aligned}$$

Let $x_\alpha = [x_\alpha^1\ x_\alpha^2\ \dots\ x_\alpha^n]^{\mathrm{T}}$ be the midpoint (w.r.t. each dimension) of K_α and $x_\alpha^{i\pm\frac{1}{2}} = x_\alpha^i \pm \frac{h_i}{2}$; that is, the variables $x_\alpha^{i\pm\frac{1}{2}}$ correspond to the coordinates of the boundaries of K_α. For $i = 1, 2, \dots, n$ define

$$b^i_{\alpha,\alpha_i} = \frac{1}{h_i/2}\int_{[(i-1)h_i,(i-1/2)h_i]} \beta_i(x^i_\alpha - y)\,\mathrm{d}y = \frac{1}{h_i/2}\int_{[x^i_\alpha - h_i/2, x^i_\alpha]} \beta_i(x^i_\alpha - y)\,\mathrm{d}y\,,$$
$$b^i_{\alpha,j} = \frac{1}{h_i}\int_{[(j-1)h_i,jh_i]} \beta_i(x^i_\alpha - y)\,\mathrm{d}y\,, \qquad j = 1, 2, \dots, \alpha_i - 1.$$

Similarly to the one-dimensional case the derivatives are approximated with difference quotients of the form

$$\frac{\partial}{\partial x_i}\big[\gamma^i_x(\boldsymbol{x})x_i p(t,\boldsymbol{x})\big]\bigg|_{K_\alpha} \approx \frac{1}{h_i}\big(\gamma^i_{\alpha+e_i} x_\alpha^{i+\frac{1}{2}} p_{\alpha+e_i}(t) - \gamma^i_\alpha x_\alpha^{i-\frac{1}{2}} p_\alpha(t)\big).$$

Approximating the integrals in (5.1) with sums as before, yields the system

$$\begin{aligned}\dot{p}_\alpha(t) &= \sum_{i=1}^n \frac{1}{h_i}\big(\gamma^i_{\alpha+e_i} x_\alpha^{i+\frac{1}{2}} p_{\alpha+e_i}(t) - \gamma^i_\alpha x_\alpha^{i-\frac{1}{2}} p_\alpha(t)\big)\\ &\quad + \sum_{i=1}^n k^i_m \sum_{j=1}^{\alpha_i} h^i_{\alpha,j} b^i_{\alpha,j} c^i_{\boldsymbol{\alpha_{i,j}}} p_{\boldsymbol{\alpha_{i,j}}}(t); \qquad (5.5)\\ p_\alpha(0) &= \frac{1}{h}\int_{K_\alpha} p_0(\boldsymbol{y})\,\mathrm{d}\boldsymbol{y}\,,\end{aligned}$$

where $\boldsymbol{\alpha_{i,j}} = \alpha + (j - \alpha_i)e_i$ and

$$h^i_{\alpha,j} = \begin{cases} h_i/2, & j = \alpha_i,\\ h_i, & j \neq \alpha_i.\end{cases}$$

Again, the system is clearly kinetic and the mass conservation follows from a calculation very similar to the one-dimensional case:

$$\begin{aligned}&\sum_\alpha \dot{p}_\alpha(t) = \sum_\alpha \sum_{i=1}^n \frac{1}{h_i}\big(\gamma^i_{\alpha+e_i} x_\alpha^{i+\frac{1}{2}} p_{\alpha+e_i}(t) - \gamma^i_\alpha x_\alpha^{i-\frac{1}{2}} p_\alpha(t)\big)\\ &+ \sum_\alpha \sum_{i=1}^n k^i_m \sum_{j=1}^{\alpha_i} h^i_{\alpha,j} b^i_{\alpha,j} c^i_{\boldsymbol{\alpha_{i,j}}} p_{\boldsymbol{\alpha_{i,j}}}(t)\\ &= \sum_\alpha \sum_{i=1}^n k^i_m \sum_{j=\alpha_i}^{\infty} h^i_{\boldsymbol{\alpha_{i,j}},j} b^i_{\boldsymbol{\alpha_{i,j}},j} c^i_\alpha p_\alpha(t) = \sum_{i=1}^n k^i_m \sum_\alpha c^i_\alpha p_\alpha(t) \underbrace{\sum_{j=\alpha_i}^{\infty} h^i_{\boldsymbol{\alpha_{i,j}},j} b^i_{\boldsymbol{\alpha_{i,j}},j}}_{=0} = 0.\end{aligned}$$

This shows for any $t \geq 0$ that

$$\sum_\alpha h p_\alpha(t) = \sum_\alpha h p_\alpha(0) = 1,$$

further implying that $p_\alpha(t) \leq \frac{1}{h}$ for each α.

5.3.3 Discretization on a truncated domain

In practical applications we may assume that there can only be a finite number of proteins of each kind. This consideration is naturally backed by the fact that the solution of (5.1) is integrable so that $\lim_{\|\boldsymbol{x}\|_{\mathbb{R}^n}\to\infty} p(t,\boldsymbol{x}) = 0$ for any $t \geq 0$. Thus, we discretize over the finite domain $\Omega = \bigtimes_{i=1}^{n}(0, L_i)$ for appropriately large $L_i > 0$ values. According to these considerations we also assume that $\int_\Omega p_0(\boldsymbol{x})\,\mathrm{d}\boldsymbol{x} = 1$.

We divide the $(0, L_i)$ intervals into N_i equal subintervals and proceed to calculate the variables $p_\alpha(0)$ and the coefficients γ^i_α and c^i_j as before. We similarly compute $b^i_{\alpha,j}$ for $j = 1, 2, \ldots, \alpha_i - 1$, but modify b^i_{α,α_i} to capture the fact that the number of ith kind of protein is maximalized in L_i.

Note, that the resulting system can still be given by (5.5) with the difference that the set of variables $\{p_\alpha\}$ is finite. While the bursts and degradations inherently define some "spatial" structure between the p_α variables (discussed in detail later), it might be more useful to think of the truncated semi-discretized model as a flattened N-dimensional system of the form

$$\dot{p}(t) = \tilde{\Gamma}^{(N)} p(t) \quad \text{with } N := \prod_{i=1}^{n} N_i. \tag{5.6}$$

5.4 Qualitative analysis

In this section we show that the result of the truncated kinetic finite volume discretization is not only a mass conservative nonnegative system but it has several advantageous qualitative properties.

5.4.1 Structural descriptions

While we could rely on the linearity of (5.6) to investigate its dynamical behaviour, the large number of variables and the complexity of the coefficient matrix $\tilde{\Gamma}^{(N)}$ renders this approach futile. Instead, let us focus on the inner structure of the system through its compartmental and CRN representations. These observations will immediately imply most qualitative properties of interest.

Compartmental representation

Consider the N-dimensional truncated system of the form (5.5). Based on the burst and degradation structure the system has a compartmental topology as follows:

- Each compartment K_α has an incoming edge from $K_{\alpha+e_i}$ due to protein degradation

if $\alpha_i < N_i$ for $i = 1, 2, \ldots, n$.

- Each compartment K_α has an incoming edge from $K_{\boldsymbol{\alpha_{i,j}}}$ for $i = 1, 2, \ldots, n$ and $j = 1, 2, \ldots, \alpha_i - 1$ due to protein production in bursts.

Clearly, the compartmental topology is strongly connected, which property is essential for our further analysis. Based on this structure (and the flattening method) one can easily determine the elements of the matrix $\tilde{\Gamma}^{(N)} \in \mathbb{R}^{N \times N}$ of (5.6).

To gain further insight into the compartmental topology, let us focus on some low-dimensional (in terms of the PIDE) examples. Figure 5.1 shows the structure of compartments for a two-dimensional PIDE. Degradations and bursts are denoted with red and blue arrows, respectively. Let $G^{(N_1,N_2)}$ denote the graph in Figure 5.1; that is, a compartmental graph of appropriate size corresponding to (5.6). Notice, that the graph $G^{(N_1,N_2)}$ can be decomposed to the interconnected $G_1^{(N_1)}, G_2^{(N_1)}, \ldots, G_{N_2}^{(N_1)}$ graphs that are isomorphic to the compartmental graph of a one-dimensional model of size N_1. This shows that $G^{(N_1,N_2)}$ is isomorphic to the Cartesian product $G^{(N_1)} \times G^{(N_2)}$. In fact, the $G^{(N_1,N_2,\ldots,N_n)}$ compartmental graph of an n-dimensional model (5.6) is isomorphic to $\bigtimes_{i=1}^{n} G^{(N_i)}$.

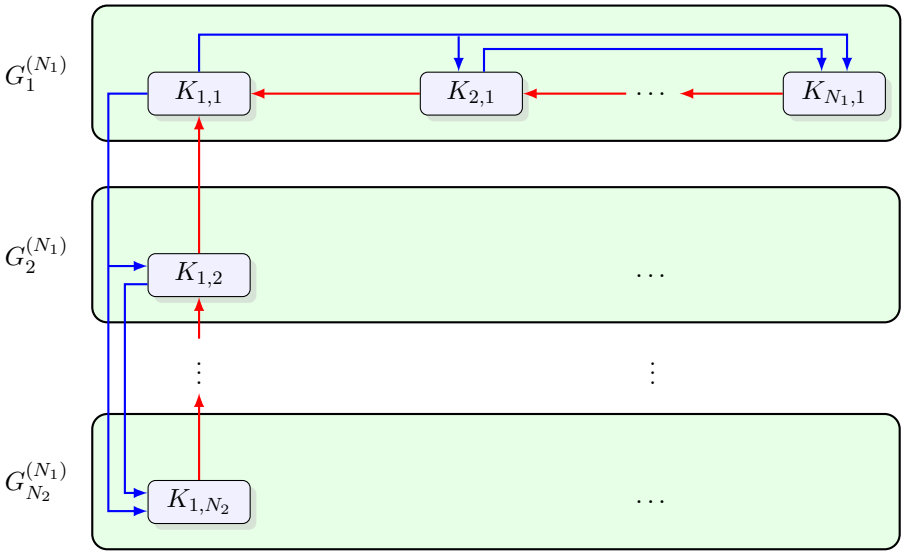

Figure 5.1: Compartmental topology of a two-dimensional model. Each subsystem is isomorphic to that of a one-dimensional model.

CRN representation

For each continuous variable p_α we introduce the specie P_α and assign the complex P_α to the compartment K_α. Then the complex composition matrix containing the stoichiometric coefficients of the complexes as its columns is the identity matrix $I \in \mathbb{R}^{N \times N}$,

and the reaction structure is identical to the above compartmental topology; that is, the reaction graph is identical (isomorphic) to the compartmental graph and, in particular, is strongly connected. This readily shows that the deficiency of the reaction graph, as defined in CRN theory [162], is zero as there are N distinct complexes, one linkage class and a spanning tree in the reaction graph of size $N-1$. Since the system is linear, the reaction vectors corresponding to the edges of the spanning tree spans the stoichiometric subspace. Hence the deficiency is indeed $\delta = N - 1 - (N-1) = 0$.

5.4.2 Long time behaviour

Asymptotic stability

By standard results on compartmental systems, since the truncated system (5.6) is strongly connected, there is a unique positive equilibrium (that is, a stationary PDF) $\overline{p} \in \mathbb{R}^N_+$ that attracts every admissible initial value [163, Theorem 6].

Remark 5.4.1. *As a conclusion of the above assertions a mass-action CRN can be assigned to the truncated conservative system* (5.6) *whose reaction graph is strongly connected and has deficiency zero. thus, the same assertion follows from CRN theory and, in particular, from the deficiency zero theorem [162, 164].*

Furthermore, we also know that the system is Lyapunov stable with the standard entropy-like logarithmic Lyapunov function

$$V(p, \overline{p}) = \sum_{\alpha} \left(p_\alpha \log \frac{p_\alpha}{\overline{p}_\alpha} + \overline{p}_\alpha - p_\alpha \right). \tag{5.7}$$

Finally, a well-known result [165] shows that for two solutions $p(t)$ and $q(t)$ of (5.6), the following inequality holds:

$$\|p(t_1) - q(t_1)\|_{L^1} \leq \|p(t_2) - q(t_2)\|_{L^1} \qquad t_1 \geq t_2 \geq 0.$$

In particular, if we set $q = \overline{p}$ this shows that the convergence to the unique equilibrium is monotone in the L^1 norm.

5.4.3 Computing the equilibrium

We can easily approximate $\overline{p}$ by simulating the system on an appropriately large time interval. However, such a simulation can be computationally expensive and it is not trivial to determine the necessary time interval. Furthermore, in many applications we may not be interested in the time evolution of the system, only in the equilibrium $\overline{p}$.

Instead, relying on the linear nature of the system (5.6) we may explicitly compute the equilibrium with the following approach.

We can incorporate the conservation into the equilibrium condition as

$$\hat{\Gamma}^{(N)}\overline{p} = \begin{bmatrix} 1 & 0 & 0 & \cdots & 0 \end{bmatrix}^\top =: e_1 \tag{5.8}$$

where $\hat{\Gamma}^{(N)}$ is obtained from $\tilde{\Gamma}^{(N)}$ by replacing the first row with $h\mathbf{1}_N^{\mathrm{T}} \in \mathbb{R}^N$. Since $\tilde{\Gamma}^{(N)}$ has a one-dimensional left kernel (by virtue of the rank-nullity theorem and the fact that zero is a simple eigenvalue, see [166]) spanned by $\mathbf{1}_N$, any $N-1$ rows are independent. To see this, assume by contradiction that not any $N-1$ rows are independent. Then there exists a nonzero vector in the left kernel of $\tilde{\Gamma}^{(N)}$ that has a zero coordinate, but then the left kernel cannot be spanned by $\mathbf{1}_N$. Clearly $\mathbf{1}_N$ is not in the left kernel of $\hat{\Gamma}^{(N)}$ and $\mathrm{Im}\tilde{\Gamma}^{(N)} \subsetneq \mathrm{Im}\hat{\Gamma}^{(n)}$, and thus $\operatorname{rank}\hat{\Gamma}^{(N)} = N$, hence we can find the equilibrium $\overline{p}$ by simply solving the linear system of equations (5.8).

5.5 Numerical experiments

In this section, we present biologically relevant examples from the literature and compare the performance of our method to that of SELANSI [155]. For more information about the examples the reader is referred to [154]. The numerical simulations have been performed on a computer with Intel(R) Core(TM) i7-8565U CPU @ 1.80GHz and 16 GB of RAM in MATLAB R2022b. The solution (5.8) is solved with built-in iterative solvers. The final time and time step of the SELANSI simulations are noted for each example.

Example 1: single gene self-regulation with positive feedback

The first example is a GRN consisting of a single gene. The regulation is described by the Hill function

$$c_1(x_1) = \frac{K_1^{H_{11}} + \epsilon_1 x_1^{H_{11}}}{K_1^{H_{11}} + x_1^{H_{11}}}.$$

We consider a negative Hill coefficient, corresponding to a positive self-regulation. In this case, as described in [153] (see also [150]) the stationary solution of (5.2) can be explicitly calculated as follows:

$$\overline{p}(x) = C\rho^{\frac{k_m^1(1-\epsilon_1)}{H_{11}}}(x)x^{-(1-k_m^1\epsilon_1)}e^{-\frac{x}{b_1}},$$

where $\rho(x) = \frac{x^{H_{11}}}{K_1^{H_{11}}+x_1^{H_{11}}}$ and $C > 0$ is a constant ensuring that $\overline{p}(x)$ integrates to one.

The computational times of both methods are depicted in Table 5.1, from where we can observe that the FVM has also better computational efficiency compared to that of SELANSI.

Mesh	FVM	SELANSI
$2.5 \times 10^4 \times 800$	0.0335 s	1.8208 s
$2.5 \times 10^4 \times 1200$	0.0899 s	2.1993 s
$2.5 \times 10^4 \times 1600$	0.1460 s	2.5510 s
$2.5 \times 10^4 \times 2000$	0.3561 s	2.8866 s
$2.5 \times 10^4 \times 5000$	3.8066 s	7.9131 s

Table 5.1: Average runtime of 100 simulations of a one-dimensional GRN with various mesh sizes.

Table 5.2 shows the relative error (in the L^2 norm) of the different methods compared to the analytical solution, computed as follows:

$$E(p, p_{ref}) = \frac{\|p - p_{ref}\|_{L^2}}{\|p_{ref}\|_{L^2}} = \frac{\sqrt{\sum_{i=1}^{N} \left(p(x_i) - p_{ref}(x_i)\right)^2}}{\sqrt{\sum_{i=1}^{N} p_{ref}^2(x_i)}}.$$

Mesh	FVM ($\times 10^{-3}$)			SELANSI ($\times 10^{-3}$)		
	$L_1 = 300$	$L_1 = 350$	$L_1 = 400$	$L_1 = 300$	$L_1 = 350$	$L_1 = 400$
$2.5 \times 10^4 \times 800$	7.4358	8.6799	9.9106	29.6010	5.4881	9.2314
$2.5 \times 10^4 \times 1200$	4.9886	5.8169	6.6366	28.6252	4.3113	8.3388
$2.5 \times 10^4 \times 1600$	3.7665	4.3870	5.0013	29.5308	3.4255	8.0746
$2.5 \times 10^4 \times 2000$	3.0335	3.5298	4.0209	29.9408	2.8899	7.2511
$2.5 \times 10^4 \times 5000$	1.4271	1.4761	1.6675	31.0859	2.5960	6.0042

Table 5.2: Relative error of the simulation of a one-dimensional GRN on various domains.

Figure 5.2 shows the simulation results for different L_1 values.

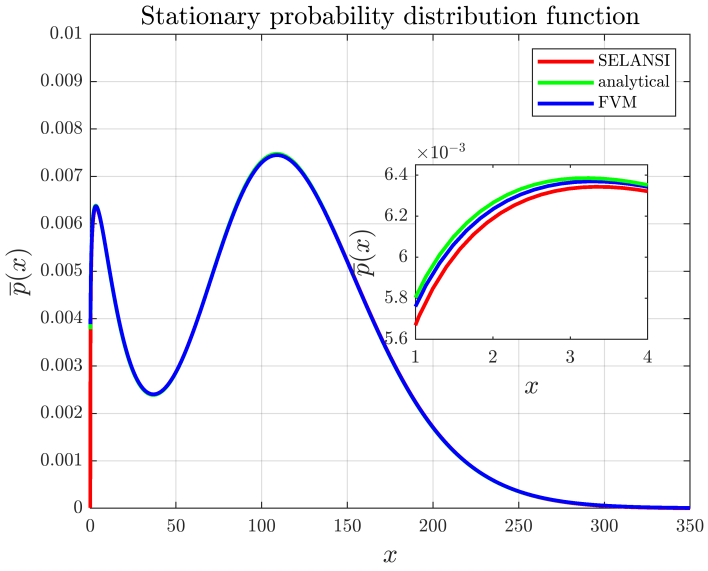

(a) $L_1 = 350$

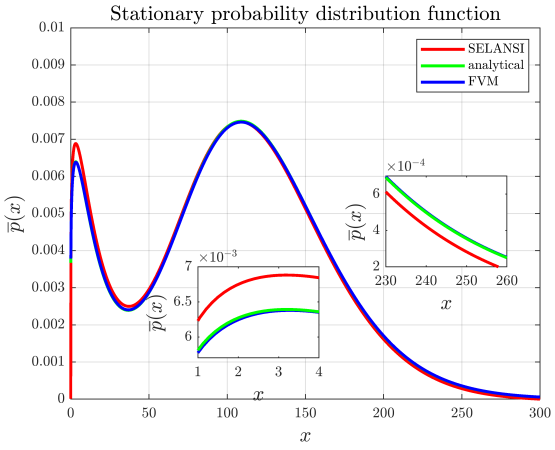

(b) $L_1 = 300$

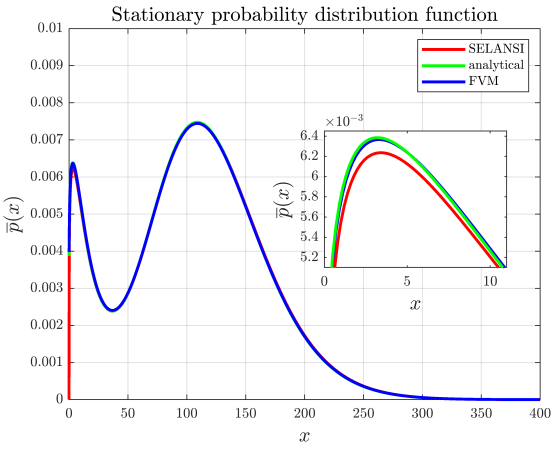

(c) $L_1 = 400$

Figure 5.2: Self-regulated single gene network with parameters $H_{11} = -4$, $K_1 = 45$, $\epsilon_1 = 0.15$, $k_m^1 = 3.2 \times 10^{-3}$, $b_1 = 16$ and $\gamma_x^1(x) = 4 \times 10^{-4}$. The simulations are performed with $N_1 = 2000$, $\tau = t\gamma_x^1 = 50$ and $\Delta t = 0.002$.

We can see that on an appropriately large domain both methods perform well, however, SELANSI seems to be more sensitive to the choice of the domain. This is assumed to be because SELANSI renormalizes the solution in each iteration and it imposes zero boundary condition at both boundaries, since the solution is expected to decay as x increases. However, this method perturbs the solution if the domain is not set properly, which might be the case for unknown gene regulatory network structures or parameter sets. Compared to this, the kinetic discretization does not impose such boundary conditions, does not require renormalizations and, in fact, as noted in section 5.4, the equilibrium is strictly positive, and thus adapts better to different domains.

Example 2: mutual activation of two genes

In this example we consider Hill functions in the form of

$$c_1(\boldsymbol{x}) = \frac{K_{12}^{H_{12}} + \epsilon_1 x_2^{H_{12}}}{K_{12}^{H_{12}} + x_2^{H_{12}}},$$
$$c_2(\boldsymbol{x}) = \frac{K_{21}^{H_{21}} + \epsilon_2 x_1^{H_{21}}}{K_{21}^{H_{21}} + x_1^{H_{21}}},$$

where $H_{12} < 0$ and $H_{21} < 0$, corresponding to positive cross-regulation or activation. Figure 5.3 shows the stationary joint PDE.

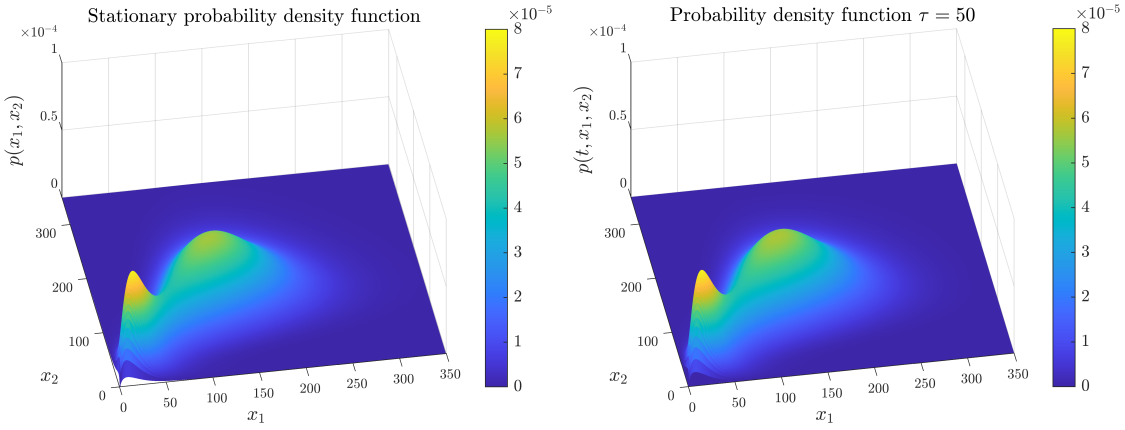

(a) Kinetic FVM with $L_1 = L_2 = 400$.

(b) SELANSI with $L_1 = L_2 = 400$.

Figure 5.3: Mutual activation with parameters $H_{12} = H_{21} = -4$, $K_{12} = K_{21} = 70$, $\epsilon_1 = \epsilon_2 = 0.2$, $k_m^1 = k_m^2 = 3.4 \times 10^{-3}$, $b_1 = b_2 = 18$, $\gamma_x^1(x) = \gamma_x^2(x) = 4 \times 10^{-4}$, $N_1 = N_2 = 400$, $\tau = t\gamma_x^1$=50 and $\Delta t = 0.005$.

Note, that the GRN is symmetric w.r.t. the proteins, thus we only plot one set of marginal PDFs. We can observe the sensitivity of SELANSI to the domain, while the finite volume discretization is quite robust to it. In this example we can see that the solution computed by SELANSI deteriorates not just for too small, but even for too large domains. Since for multidimensional GRNs the analytic solution of (5.1) cannot be computed in a straightforward manner, we cannot compute the empirical error as in the case of the one-dimensional example. Instead, we only compare the running times of the two methods, the results of which are collected in Table 5.3. Figure 5.4 shows the stationary marginal stationary PDF on multiple domains.

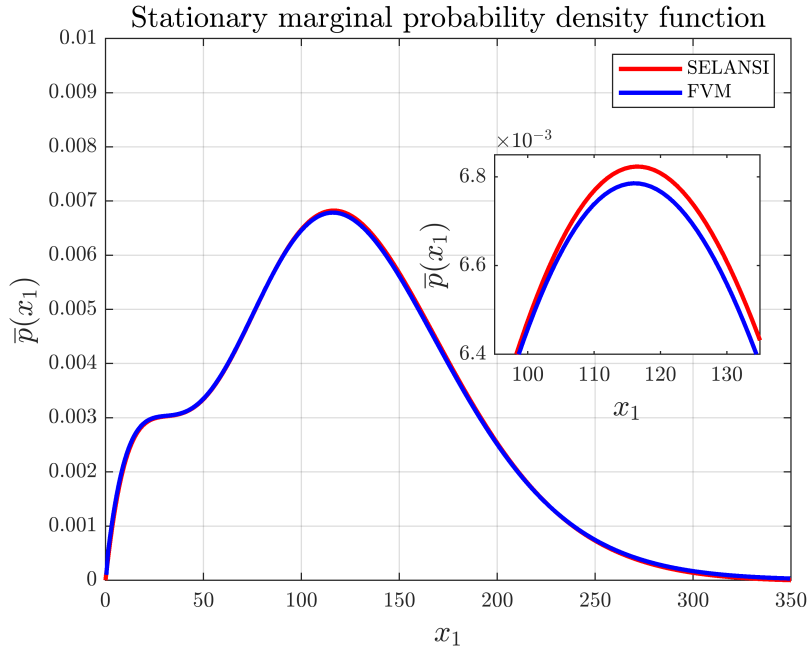

(a) Marginal PDF with $L_1 = L_2 = 350$.

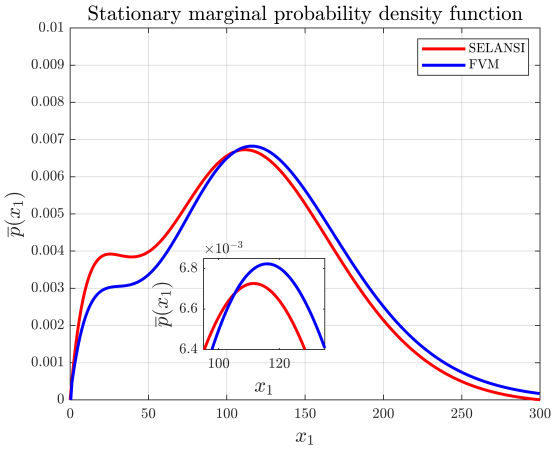

(b) Marginal PDF with $L_1 = L_2 = 300$.

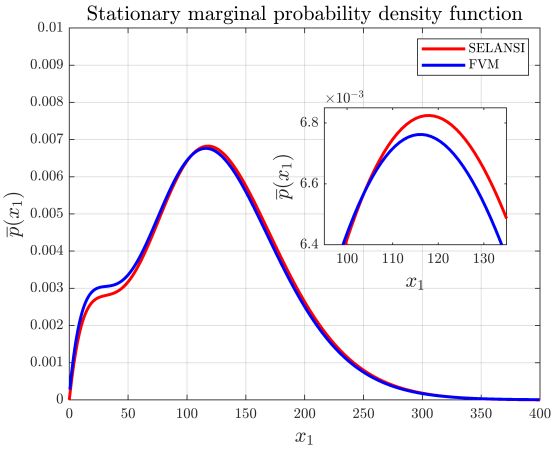

(c) Marginal PDF with $L_1 = L_2 = 400$.

Figure 5.4: Mutual activation with parameters $H_{12} = H_{21} = -4$, $K_{12} = K_{21} = 70$, $\epsilon_1 = \epsilon_2 = 0.2$, $k_m^1 = k_m^2 = 3.4 \times 10^{-3}$, $b_1 = b_2 = 18$, $\gamma_x^1(x) = \gamma_x^2(x) = 4 \times 10^{-4}$, $N_1 = N_2 = 400$, $\tau = t\gamma_x^1$=50 and $\Delta t = 0.005$.

Example 3: mutual repression of two genes

In this example we consider Hill functions in the form of

$$c_1(\boldsymbol{x}) = \frac{K_{12}^{H_{12}} + \epsilon_1 x_2^{H_{12}}}{K_{12}^{H_{12}} + x_2^{H_{12}}}, \qquad c_2(\boldsymbol{x}) = \frac{K_{21}^{H_{21}} + \epsilon_2 x_1^{H_{21}}}{K_{21}^{H_{21}} + x_1^{H_{21}}},$$

where $H_{12} > 0$ and $H_{21} > 0$, corresponding to negative cross-regulation or repression. Figure 5.5 shows the stationary joint PDF and the marginal stationary PDF on multiple domains. Again, the GRN is symmetric w.r.t. the proteins and the same dependence on

the domain can be observed in the case of SELANSI. The running time of both methods with various mesh sizes are presented in Table 5.3.

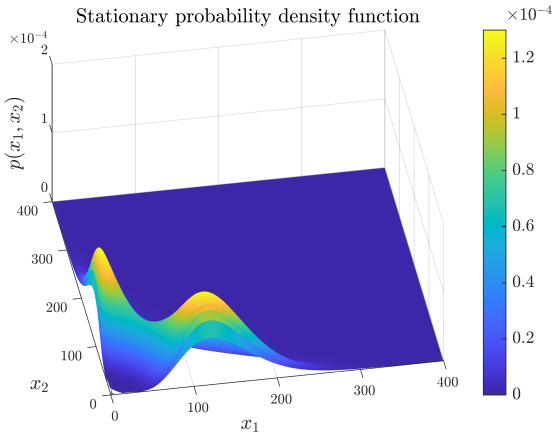

(a) Kinetic FVM with $L_1 = L_2 = 400$.

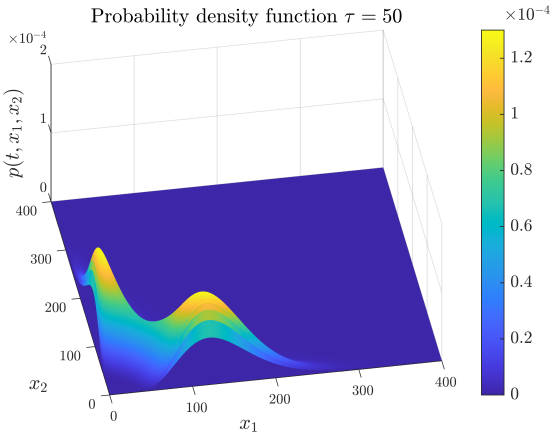

(b) SELANSI with $L_1 = L_2 = 400$.

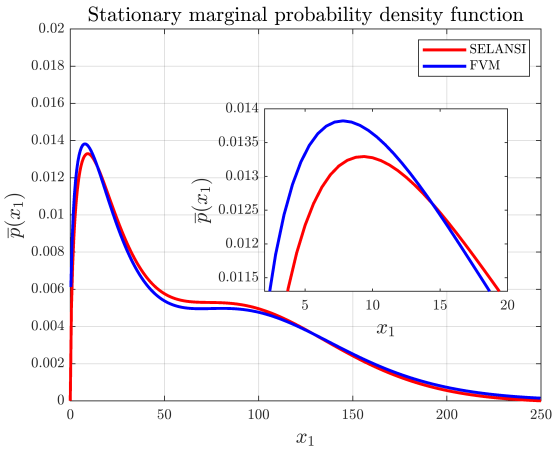

(c) Marginal PDF $L_1 = L_2 = 250$.

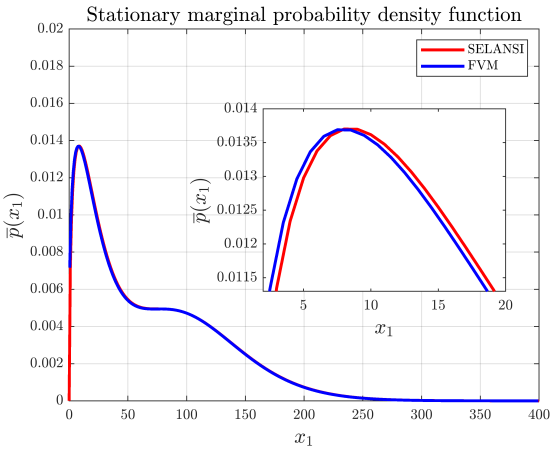

(d) Marginal PDF with $L_1 = L_2 = 400$.

Figure 5.5: Mutual repression with parameters $H_{12} = H_{21} = 4$, $K_{12} = K_{21} = 45$, $\epsilon_1 = \epsilon_2 = 0.15$, $k_m^1 = k_m^2 = 3.2 \times 10^{-3}$, $b_1 = b_2 = 16$, $\gamma_x^1(x) = \gamma_x^2(x) = 4 \times 10^{-4}$, $N_1 = N_2 = 400$, $\tau = t\gamma_x^1 = 50$ and $\Delta t = 0.005$.

Example 4: self and mutual regulation

In this example we consider two genes, one of which is activated by both, the other is repressed by both. The corresponding Hill functions can be given as follows:

$$c_1(\boldsymbol{x}) = \frac{\epsilon_{11} x_1^{H_{11}} x_2^{H_{12}} + \epsilon_{12} K_{11}^{H_{11}} x_2^{H_{12}} + \epsilon_{13} x_1^{H_{11}} K_{12}^{H_{12}} + K_{11}^{H_{11}} K_{12}^{H_{12}}}{x_1^{H_{11}} x_2^{H_{12}} + K_{11}^{H_{11}} x_2^{H_{12}} + x_1^{H_{11}} K_{12}^{H_{12}} + K_{11}^{H_{11}} K_{12}^{H_{12}}},$$

$$c_2(\boldsymbol{x}) = \frac{\epsilon_{21} x_1^{H_{21}} x_2^{H_{22}} + \epsilon_{23} K_{21}^{H_{21}} x_2^{H_{22}} + \epsilon_{12} x_2^{H_{21}} K_{22}^{H_{22}} + K_{21}^{H_{21}} K_{22}^{H_{22}}}{x_1^{H_{21}} x_2^{H_{22}} + K_{21}^{H_{21}} x_2^{H_{22}} + x_2^{H_{21}} K_{22}^{H_{22}} + K_{21}^{H_{21}} K_{22}^{H_{22}}},$$

where $H_{11} < 0$, $H_{21} < 0$, $H_{12} > 0$ and $H_{22} > 0$. We note that the above functions are generalized Hill functions, and thus have to be defined in a separate file for the SELANSI simulation. Figure 5.6 shows the stationary joint PDF.

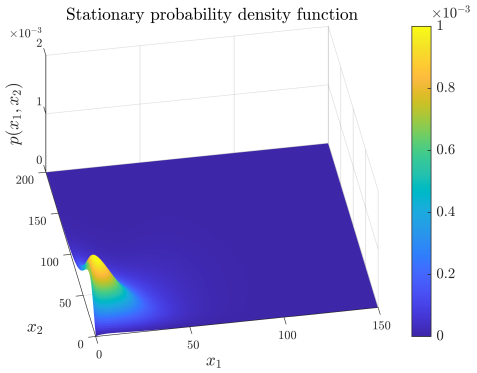

(a) Kinetic FVM with $L_1 = 150$, $L_2 = 200$.

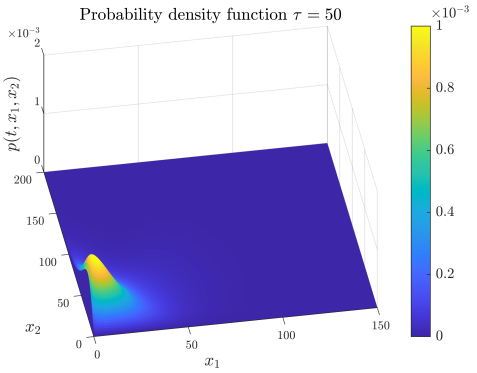

(b) SELANSI with $L_1 = 150$, $L_2 = 200$.

Figure 5.6: Self and mutual regulation with parameters $H_{11} = -4$, $H_{21} = -6$, $H_{12} = H_{22} = 2$, $K_{11} = K_{12} = 45$, $K_{21} = K_{22} = 70$, $\epsilon_{11} = \epsilon_{21} = 0.002$, $\epsilon_{12} = 0.02$, $\epsilon_{22} = 0.1$, $\epsilon_{13} = \epsilon_{23} = 0.2$, $k_m^1 = 4{\times}10^{-3}$, $k_m^2 = 8{\times}10^{-3}$, $b_1 = 10$, $b_2 = 20$, $\gamma_x^1(x) = \gamma_x^2(x) = 4{\times}10^{-4}$, $N_1 = N_2 = 400$, $\tau = t\gamma_x^1 = 50$.

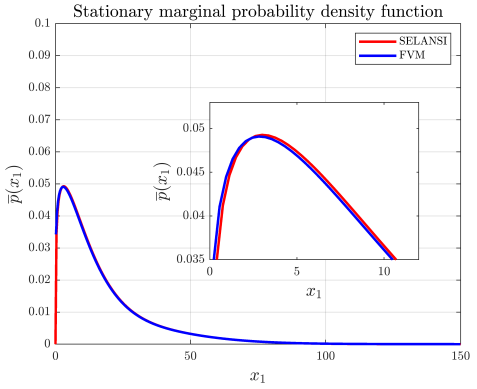

(a) Marginal PDF with $L_1 = 150$, $L_2 = 200$.

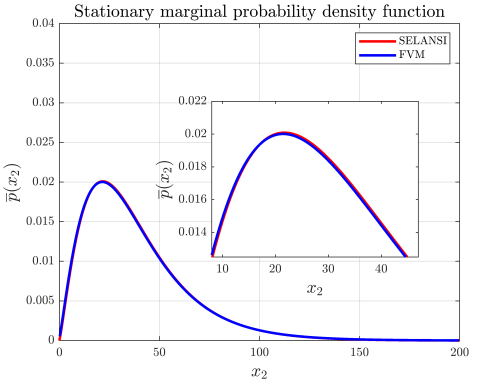

(b) Marginal PDF with $L_1 = 150$, $L_2 = 200$.

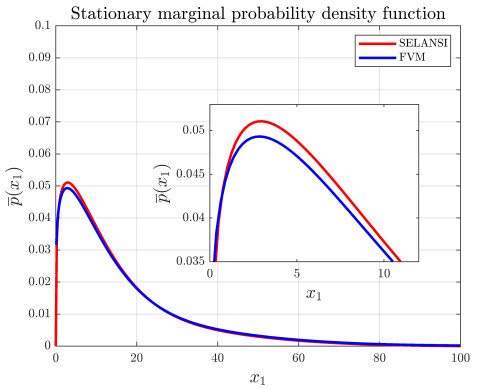

(c) Marginal PDF with $L_1 = 100$, $L_2 = 150$.

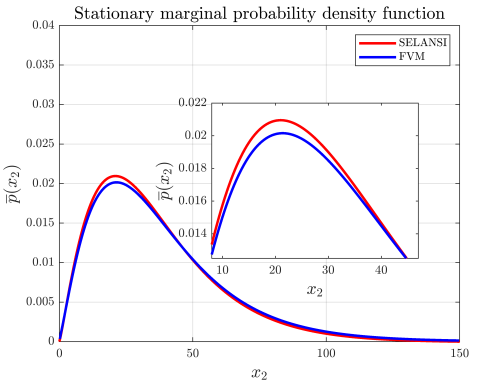

(d) Marginal PDF with $L_1 = 100$, $L_2 = 150$.

Figure 5.7: Self and mutual regulation with parameters $H_{11} = -4$, $H_{21} = -6$, $H_{12} = H_{22} = 2$, $K_{11} = K_{12} = 45$, $K_{21} = K_{22} = 70$, $\epsilon_{11} = \epsilon_{21} = 0.002$, $\epsilon_{12} = 0.02$, $\epsilon_{22} = 0.1$, $\epsilon_{13} = \epsilon_{23} = 0.2$, $k_m^1 = 4{\times}10^{-3}$, $k_m^2 = 8{\times}10^{-3}$, $b_1 = 10$, $b_2 = 20$, $\gamma_x^1(x) = \gamma_x^2(x) = 4{\times}10^{-4}$, $N_1 = N_2 = 400$, $\tau = t\gamma_x^1 = 50$.

Figure 5.7 shows the marginal stationary PDF on multiple domains. This example is not symmetric w.r.t. the different kind of proteins, thus we plot both marginal density functions. The running time of both methods with various mesh sizes are presented in Table 5.3.

Example 5: bacterial competence

In *Bacillus subtilis*, competence is a probabilistic and transiently differentiated state. In this physiological state bacteria has the capability of DNA uptake from their environment. The phenomena is modelled with a two-dimensional gene regulatory network, consisting of the master regulator self-activated ComK which represses the transcription factor ComS [167]. Protein degradation is mediated by the MecA complex. After ComK (ComS) binds to the complex an intermediate complex MecA-ComK (MecA-ComS) complex is formed, in which the ComK (ComS) protein is degraded by the ClpP-ClpC proteases [168]. Instead of explicitly modelling the effects of the MecA complex, the authors consider a variable degradation rate. Using this reduced order stochastic differential equation developed in [168] a discrete stochastic CME model is presented in [169], simulated using a Monte-Carlo based Stochastic Simulation Algorithm. A corresponding PIDE is presented in [154] with parameters adapted from the CME model of [169] as follows: $\alpha_k = 0.0028$, $\beta_k = 0.049$, $\beta_s = 0.057$, $K_k = 100$, $K_s = 110$, $\delta_k = \delta_s = 0.0014$, $\Gamma_k = 500$, $\Gamma_s = 50$, $b_1 = 2$, $b_2 = 5$, $k_m^1 = \frac{\alpha_k+\beta_k}{b_1}$, $k_m^2 = \frac{\beta_s}{b_2}$, $\epsilon_1 = \frac{\alpha_k}{\alpha_k+\beta_k}$, $\epsilon_2 = 0$, $H_{11} = -2$, $H_{21} = 5$. The coefficient functions are set as:

$$c_1(\boldsymbol{x}) = \frac{K_k^{H_{11}} + \epsilon_1 x_1^{H_{11}}}{K_k^{H_{11}} + x_1^{H_{11}}}, \qquad \gamma_x^1(\boldsymbol{x}) = \frac{\delta_k \Gamma_k \Gamma_s}{\Gamma_k \Gamma_s + \Gamma_s x_1 + \Gamma_k x_2},$$
$$c_2(\boldsymbol{x}) = \frac{K_s^{H_{21}} + \epsilon_2 x_1^{H_{21}}}{K_s^{H_{21}} + x_1^{H_{21}}}, \qquad \gamma_x^2(\boldsymbol{x}) = \frac{\delta_s \Gamma_k \Gamma_s}{\Gamma_k \Gamma_s + \Gamma_s x_1 + \Gamma_k x_2}.$$

We note that the currently publicly available SELANSI version cannot handle variable degradation rates, thus we could not reproduce the plots of [154]. Figure 5.8 shows the stationary PDFs and its contour plot, both of which are in accordance with the plots of [154]. The running times of the finite volume method for various mesh sizes are shown in Table 5.3.

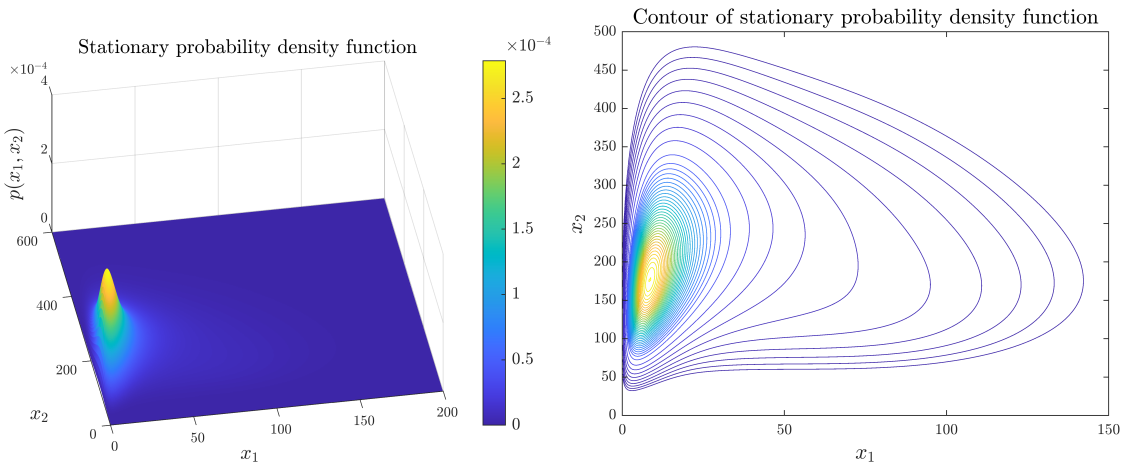

Figure 5.8: Kinetic FVM of Example 5 with $N_1 = N_2 = 400$.

GRN	FVM				SELANSI			
	100^2	200^2	300^2	400^2	100^2	200^2	300^2	400^2
Ex. 2	0.2223 s	1.6485 s	5.2159 s	11.5707 s	9.0423 s	21.5449 s	40.6726 s	71.1792 s
Ex. 3	0.2128 s	1.3679 s	4.5709 s	10.3817 s	9.0443 s	21.3982 s	40.7456 s	72.3397 s
Ex. 4	0.3241 s	1.8639 s	5.7925 s	12.3953 s	9.1355 s	22.0259 s	41.9351 s	73.4001 s
Ex. 5	0.7064 s	4.9921 s	17.0973 s	45.0809 s	–	–	–	–

Table 5.3: Average runtime of 100 simulations of several two-dimensional GRNs with various mesh sizes.

5.5.1 Memory requirement of the kinetic FVM

A notable technical challenge in our method is the efficient assembly and storage of the coefficient matrix $\Gamma^{(N)}$. For $n \geq 2$ one should store $\Gamma^{(N)}$ in a sparse representation, but even then the memory requirement can grow quickly. However, we can explicitly calculate the number of nonzero elements of the matrix to aid the design of the simulation. To be precise, the number of nonzero elements of the coefficient matrix corresponding to an n-dimensional PIDE discretized on a grid of size $\prod_{i=1}^{n} N_i$ is as follows:

$$\begin{aligned}
&\underbrace{\sum_{i=1}^{n}\left(\sum_{k=1}^{N_i}(N_i-k)\right)\prod_{\substack{j=1\\ j\neq i}}^{n}N_j}_{\text{bursting of protein } X_i}+\underbrace{\sum_{i=1}^{n}(N_i-1)\prod_{\substack{j=1\\ j\neq i}}^{n}N_j}_{\text{degradation of } X_i}+\underbrace{\prod_{i=1}^{n}N_i}_{\text{diagonal}}\\
&=\sum_{i=1}^{n}\frac{1}{2}\left(N_i^2-N_i\right)\prod_{\substack{j=1\\ j\neq i}}^{n}N_j+n\prod_{i=1}^{n}N_i-\sum_{i=1}^{n}\prod_{\substack{j=1\\ j\neq i}}^{n}N_j+\prod_{i=1}^{n}N_i\\
&=-\frac{1}{2}n\prod_{i=1}^{n}N_i+\frac{1}{2}\left(\sum_{i=1}^{n}N_i\right)\left(\prod_{i=1}^{n}N_i\right)+(n+1)\prod_{i=1}^{n}N_i-\left(\sum_{i=1}^{n}\frac{1}{N_i}\right)\left(\prod_{i=1}^{n}N_i\right)
\end{aligned}$$

$$= \frac{1}{2}\left(n + 2 + \sum_{i=1}^{n} N_i - \sum_{i=1}^{n} \frac{2}{N_i}\right)\left(\prod_{i=1}^{n} N_i\right).$$

Figure 5.9 shows the number of nonzero elements on an equidistant grid for a matrix corresponding to a mesh of size $N = 10^{10}$ (that is, the matrix has 10^{20} total elements) as a function of n. The logarithmic scaling suggests that as the dimension of the PIDE is increased, we can increase the number of finite volume cells on the grid even without exceeding the memory limits.

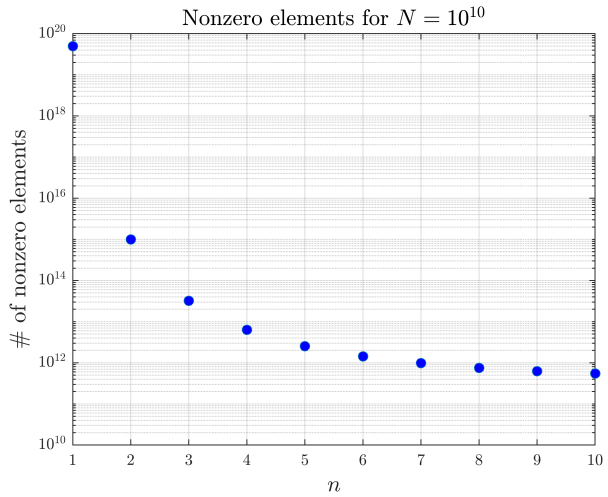

Figure 5.9: Memory requirement of an n-dimensional GRN with $N = 10^{10}$ total number of cells.

5.6 Control of a genetic toggle switch

In this section we introduce a version of the kinetic FVM, modified to be suitable for control design. We wish to employ an exogenous control on the population level through appropriate inducers affecting protein bursts; that is, we assume that $c_i(\boldsymbol{x}) = c_i(\boldsymbol{x}, \boldsymbol{I})$ in (5.1), where $\boldsymbol{I}$ denotes the concentration vector of the inducers. In order to adhere certain biological constraints we assume that the range of c_i remains in $\in (0, 1)$. For the sake of simplicity we assume that $\boldsymbol{I} \in \mathbb{R}^n$ and note that we set $I_i \equiv 0$ if we do not control the production of protein P_i.

We slightly modify the kinetic FVM in the case of the functions c_i and instead of computing their average over the cells, we use their midpoint values; that is, we set $c_\alpha^i(\boldsymbol{I}) = c_i(x_\alpha, \boldsymbol{I})$. Let us collect the degradation coefficients γ_α^i, burst coefficients $b_{\alpha,j}^i$ and controlled coefficients $c_\alpha^i(\boldsymbol{I})$ into the matrices G, B and $C(\boldsymbol{I})$, respectively. Then (5.6) can be rewritten as

$$\dot{p}(t) = Gp(t) + \big(B \odot C(\boldsymbol{I})\big)p(t),$$

where $\odot$ denotes the Hadamard (or elementwise) product.

We note that the Lyapunov function given in (5.7) simplifies to the well-known Kullback-Leibler divergence in a mass-conservative setting, given as follows

$$V(p,p^*)=\sum_{j=1}^{N}\left(p_j\log\frac{p_j}{p_j^*}+p_j^*-p_j\right)=\sum_{j=1}^{N}p_j\log\frac{p_j}{p_j^*}=D_{KL}(p\|p^*).$$

While the Kullback-Leibler divergence is not a metric as it is not symmetric and fails to satisfy the triangle inequality, it is a nonnegative measure and it is often used to estimate the difference of discrete probability distributions [139].

As described before, the mesh size directly determines the number of variables of the system (5.6). We consider an explicit Euler scheme on (5.5) and denote the approximation of $p_\alpha(t_k)$ as p_α^k. Clearly we have that $\sum_\alpha p_\alpha^{k+1}=\sum_\alpha p_\alpha^k$ for each $k\geq 0$ since (5.5) is governed by a linear conservation law. An elementary computation shows that if the step sizes satisfy the following Courant-Friedrichs-Lewy (CFL) condition, then $p_\alpha^k\geq 0$ holds for any $k\geq 0$ and α:

$$\Delta t\sum_{i=1}^{n}\max_{\substack{\boldsymbol{x}\in\Omega\\ \boldsymbol{I}\in\mathbb{R}^n}}\left(\frac{1}{h_i}\gamma_x^i(\boldsymbol{x})x_i+k_m^i\exp\left(-\frac{h_i}{2b_i}\right)c_i(\boldsymbol{x},\boldsymbol{I})\right)\leq 1.$$

We note that the c_i functions are usually Hill-type saturating functions with the property $c_i(\boldsymbol{x},\boldsymbol{I})\leq 1$ and that $\exp\left(-\frac{h_i}{2b_i}\right)\leq 1$, thus the second term is bounded by k_m^i. This shows that the degradation terms are often more dominant, hence in applications of biological relevance the CFL condition can be estimated as

$$\Delta t\sum_{i=1}^{n}\frac{1}{h_i}\max_{\boldsymbol{x}\in\Omega}\gamma_x^i(\boldsymbol{x})x_i\leq 1.$$

Of course we can normally set larger Δt values when applying a more sophisticated time discretization method. However, this demonstrates a further benefit of the FVM-based population level control, since our investigation shows that usually one can resort to very coarse grids leading to smaller systems and larger admissible temporal steps. The computed control trajectory (or the steady-state constant control) can then be applied to a system with a finer mesh.

A crucial question is what kinds of probability distributions can be reached from an initial one. The considered control structure is strictly positive and bounded from below and above, thus it is anticipated that we cannot reach arbitrarily low and high expected values. However, relying on the above observations we can estimate the reachability set of the system numerically by computing the considered statistical measures of the unique equilibrium for a simple scan of control configurations. The continuous dependence on

parameters (see, [170, Chapter V]) shows that the reachability set should be a connected set in $\mathbb{R}^n$, thus we could even interpolate control values based on an appropriately fine scan.

A natural design principle of PID controllers can be to use as few control terms as possible. In many applications a well tuned proportional controller may suffice. This is not the case for semi-discretized gene regulatory networks as the above discussions show that in general we need nonzero steady-state control; that is, the steady-state error of the controlled system will be proportional to the required control value. While integral control has proven to be reliable for biomolecular networks [171], we found that its performance can be inferior to proportional-integral control. In certain cases introducing a derivative term could further increase the convergence speed or reduce overshoots and oscillations, but it does not seem to be necessary.

We consider the classical toggle switch configuration consisting of two repressible promoters in a mutually inhibitory network. We introduce two corresponding inducers, each affecting one of the promoters. Our goal is to shift the expected values of the stationary probability density to some prescribed values. Figure 5.10 shows the structure of the controlled gene regulatory network.

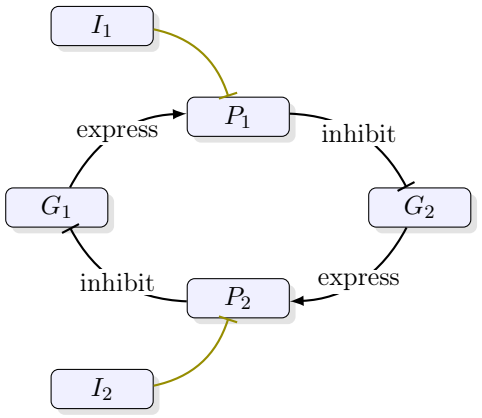

Figure 5.10: Structure of the gene toggle switch.

Following [172] we introduce the parameters $\theta_{I_i}, \theta_{X_i}$ and μ_{I_i} associated with the inducers' effects in the protein regulation. The burst coefficients are given by the following Hill-type functions

$$c_1(\boldsymbol{x}, \boldsymbol{I}) = c_1(x_2, I_1) = \frac{K_{12}(I_1)^H + \epsilon_1 x_2^H}{K_{12}(I_1)^H + x_2^H},$$
$$c_2(\boldsymbol{x}, \boldsymbol{I}) = c_2(x_1, I_2) = \frac{K_{21}(I_2)^H + \epsilon_2 x_1^H}{K_{21}(I_2)^H + x_1^H},$$

with

$$K_{12}(I_1) = \theta_{X_2}\left(1 + \left(\frac{I_1}{\theta_{I_1}}\right)^{\mu_{I_1}}\right),$$
$$K_{21}(I_2) = \theta_{X_1}\left(1 + \left(\frac{I_2}{\theta_{I_2}}\right)^{\mu_{I_2}}\right).$$

We consider $H = 4$ and Table 5.4 shows the rest of the parameters of the system.

γ_x^i	k_m^i	b_i	ϵ_i	θ_{X_i}	θ_{I_i}	μ_{I_i}
1	12	6	0.1	31.94	11.65	2
1	7	$\frac{78}{7}$	0.1	30	9.06×10^{-2}	2

Table 5.4: PIDE parameters of the gene toggle switch.

First, we compute the equilibrium of the open-loop system (that is, when $I_1 = I_2 = 0$) and then apply a PI controller to shape the protein density function. We consider a simple population level controller based on the expected values of the number of proteins. The desired and actual expected values are denoted as m_1^*, m_2^* and $m_1(t)$, $m_2(t)$, respectively. We note, that we may use other statistical measures, for example the modes of the marginal probability density functions as in [159]. Defining the errors $e_1(t) = m_1^* - m_1(t)$ and $e_2(t) = m_2^* - m_2(t)$ the dynamics of the PI controller is of the form

$$I_1(t) = I_1^0 + K_P^1 e_1(t) + K_I^1 \int_0^t e_1(s)\,\mathrm{d}s\,,$$
$$I_2(t) = I_2^0 + K_P^2 e_2(t) + K_I^2 \int_0^t e_2(s)\,\mathrm{d}s\,,$$

where we assume based on biological constraints that $I_1 \in [0, 50]$ and $I_2 \in [0, 1]$. The initial values are set as $I_1^0 = 20$, $I_2^1 = 0.25$ and the feedback gains, based on [172, 159], as $K_P^1 = 60$, $K_I^1 = 20$, $K_P^2 = 2.5$ and $K_I^2 = 6.94 \cdot 10^{-1}$. We note that for a new model these values could be obtained through the linearization of a coarse discretization. Figure 5.11a shows the open-loop equilibrium, while Figures 5.11b and 5.11c show the closed-loop equilibrium for $m_1^* = 41$ and $m_2^* = 55$ on a 300×300 and a 50×50 mesh, respectively. Table 5.5 shows the performance of the FVM with an explicit Euler discretization on different mesh-sizes with the same CFL ratio.

50×50	100×100	200×200	300×300
0.2087 s	2.4426 s	20.7634 s	90.4794 s

Table 5.5: Average runtime of 100 simulations

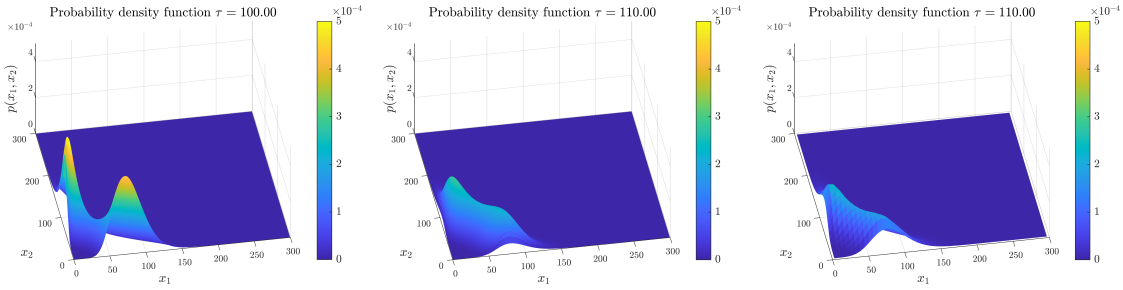

(a) Open-loop system on 300×300 mesh.

(b) Closed-loop system on 300×300 mesh.

(c) Closed-loop system on 50×50 mesh.

Figure 5.11: PI control of the genetic toggle switch on various mesh sizes with prescribed expected values $m_1^* = 41$ and $m_2^* = 55$.

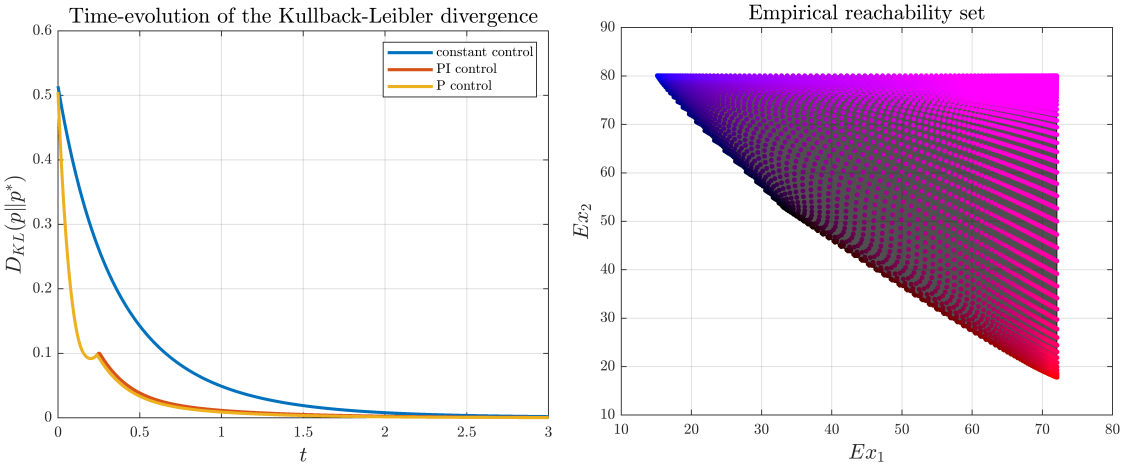

(a) Time-evolution of the Kullback-Leibler divergence of the PI control and the constant control.

(b) Empirical reachability set computed on a mesh of size 50×50 for 200 equidistant control values $I_1 \in [0, 50]$ and $I_2 \in [0, 1]$.

Figure 5.12: Self-regulated single gene network with parameters $H_{11} = -4$, $K_1 = 45$, $\epsilon_1 = 0.15$, $k_m^1 = 3.2 \times 10^{-3}$, $b_1 = 16$ and $\gamma_x^1(x) = 4 \times 10^{-4}$. The simulations are performed with $N_1 = 2000$, $\tau = t\gamma_x^1 = 50$ and $\Delta t = 0.002$.

Figure 5.12a shows the performance of the PI control and the constant control measured as the time-evolution of the Kullback-Leibler divergence of the state and the equilibrium. While in this case the PI control outperforms the constant control, it is clear that the monotonicity cannot be guaranteed, while in a constant control setting $D_{KL}(.\|p^*)$ is known to be a Lyapunov function, thus it is strictly decreasing. We emphasize that the control is based on the error of the expected values, not on the Kullback-Leibler divergence. Figure 5.12b shows the estimated reachability set of the system discretized on a 50×50 mesh. For 200 evenly spaced control values $I_1 \in [0, 50]$ and $I_2 \in [0, 1]$ we compute

and plot the expected values of the protein molecules. Each point has color represented with an RGB triplet, where the green channel is constant and the red and blue channels correspond to I_1 and I_2, respectively. The black polygon in the background is the filled boundary polygon of the computed points.

5.7 Conclusions

A novel discretization scheme was proposed in this chapter for the simulation and analysis of multidimensional PIDE models used in the stochastic dynamical description of gene regulatory networks. It was shown that using an appropriate finite volume scheme, a fully conservative linear compartmental dynamics is obtained in ODE form. The interconnection structure of the discretized system was studied in detail, and it was shown that the associated directed graph is always strongly connected. Therefore, the theory of kinetic and compartmental systems can be used to conclude that the equilibrium of the discretized dynamics representing the stationary distribution of molecules is unique and globally stable for any biologically meaningful parameter values in the PIDE model. Moreover, the stationary distribution can be obtained by solving a set of linear equations without performing the time-domain simulation. The memory requirement of the method can be precisely pre-computed based on which the applicable resolution can be determined. Five illustrative examples were presented to show the operation and performance of the method. Whenever possible, the obtained solutions and running times were compared with those given by the SELANSI toolbox, and these comparisons clearly justified the advantageous properties of the proposed approach both in terms of precision and performance. The compartmental description can be a basis of further dynamical analysis or controller design for stochastic gene regulatory network models.

The networks obtained by discretization of nonlocal models thus far can be interpreted as compartmental models, where each node represents a distinct spatial or functional unit. In the final chapter, we extend this perspective further by introducing quantum graphs, a framework in which compartments are connected by partial differential equations that model continuous transitions along edges.

Chapter 6

Domain decomposition for elliptic problems on metric graphs

In this chapter we develop a Neumann-Neumann type domain decomposition method for elliptic problems on metric graphs. We describe the iteration in the continuous and discrete setting and rewrite the latter as a preconditioner for the Schur complement system. Then we formulate the discrete iteration as an abstract additive Schwarz iteration and prove that it converges to the finite element solution with a rate that is independent of the finite element mesh size. We also show that the condition number of the Schur complement is uniformly bounded with respect to the finite element mesh size. We provide an implementation and test it on various examples of interest and compare it to other preconditioners.

6.1 Introduction

We consider a quantum graph; that is, a metric graph G equipped with an elliptic differential operator on each edge and certain standard vertex conditions. The graph consists of a finite set V of vertices and a finite set E of edges connecting pairs of vertices. We assume that the graph is simple and does not contain parallel edges or loops. Let $n = |\mathsf{V}|$ denote the number of vertices and $m = |\mathsf{E}|$ the number of edges. We assume that the graph is directed; that is, each edge has a specified (but otherwise arbitrary) orientation, and thus an origin and a terminal vertex. Each edge $\mathsf{e} \in \mathsf{E}$ is assigned a length $\ell_{\mathsf{e}} \in (0, \infty)$ and a local coordinate $x \in [0, \ell_{\mathsf{e}}]$.

A function u on a metric graph G can be defined as a vector of functions and we write $u = (u_{\mathsf{e}})_{\mathsf{e}\in\mathsf{E}}$, and consider it to be an element of a product function space, to be specified

later. Let $u_{\mathsf{e}}(\mathsf{v})$ denote the value of u at $\mathsf{v} \in \mathsf{V}$ along the edge $\mathsf{e} \in \mathsf{E}$.

To define the vertex conditions, let us denote by E_v the set of edges incident to the vertex $\mathsf{v} \in \mathsf{V}$, and by $d_\mathsf{v} = |\mathsf{E}_\mathsf{v}|$ the degree of $\mathsf{v} \in \mathsf{V}$. We denote by $\mathrm{int}(\mathsf{G})$ the set of vertices with degree $d_\mathsf{v} > 1$ and by $\partial\mathsf{G}$ the set $\mathsf{V}\backslash\mathrm{int}(\mathsf{G})$. We seek solutions that are continuous on G and satisfy the Neumann-Kirchhoff (often called standard) condition, given as

$$\sum_{\mathsf{e}\in\mathsf{E}_\mathsf{v}} u'_{\mathsf{e}}(\mathsf{v}) = 0, \qquad \mathsf{v} \in \mathsf{V},$$

where the derivatives are assumed to be taken in the directions away from the vertex. When there are (variable) diffusion coefficients or conductances present, represented by the function $c = (c_\mathsf{e})_{\mathsf{e}\in\mathsf{E}}$ defined on the graph, the Neumann-Kirchhoff condition is defined as

$$\sum_{\mathsf{e}\in\mathsf{E}_\mathsf{v}} c_{\mathsf{e}}(\mathsf{v})u'_{\mathsf{e}}(\mathsf{v}) = 0, \qquad \mathsf{v} \in \mathsf{V}.$$

If $d_\mathsf{v} = 1$, then this reduces to the classical zero Neumann boundary condition.

In order to write the vertex conditions more compactly, let us define the vector of function values at $\mathsf{v} \in \mathsf{V}$ as

$$U(\mathsf{v}) = \big(u_e(\mathsf{v})\big)_{\mathsf{e}\in\mathsf{E}_\mathsf{v}} \in \mathbb{R}^{d_\mathsf{v}}$$

and the bi-diagonal matrix

$$I_\mathsf{v} = \begin{bmatrix} 1 & -1 & & \\ & \ddots & \ddots & \\ & & 1 & -1 \end{bmatrix} \in \mathbb{R}^{(d_\mathsf{v}-1)\times d_\mathsf{v}}.$$

Then $I_\mathsf{v}U(\mathsf{v}) = 0 \in \mathbb{R}^{d_\mathsf{v}-1}$ implies that the function values along the edges in E_v coincide at $\mathsf{v} \in \mathsf{V}$. Similarly, we define

$$U'(\mathsf{v}) = \big(u'_e(\mathsf{v})\big)_{\mathsf{e}\in\mathsf{E}_\mathsf{v}} \in \mathbb{R}^{d_\mathsf{v}},$$

the vector of function derivative at $\mathsf{v} \in \mathsf{V}$ and the row vector

$$C(\mathsf{v})^\top = \Big(c_{\mathsf{e}_1}(\mathsf{v})\ c_{\mathsf{e}_2}(\mathsf{v})\ \ldots\ c_{\mathsf{e}_{d_\mathsf{v}}}(\mathsf{v})\Big) \in \mathbb{R}^{1\times d_\mathsf{v}}.$$

Then $C(\mathsf{v})^\top U'(\mathsf{v}) = 0$ implies that the function u satisfies the Neumann-Kirchhoff conditions at $\mathsf{v} \in \mathsf{V}$.

Then a quantum graph can be formally written as

$$\begin{cases} -(c_\mathsf{e}u'_\mathsf{e})'(x) + p_\mathsf{e}(x)u_\mathsf{e}(x) = f_\mathsf{e}(x), & x \in (0,\ell_\mathsf{e}),\ \mathsf{e} \in \mathsf{E}, \quad (a) \\ 0 = I_\mathsf{v}U(\mathsf{v}), & \mathsf{v} \in \mathrm{int}(\mathsf{G}), \quad (b) \\ 0 = C(\mathsf{v})^\top U'(\mathsf{v}), & \mathsf{v} \in \mathsf{V}, \quad (c) \end{cases} \tag{6.1}$$

where the function $p = (p_{\mathsf{e}})_{\mathsf{e}\in\mathsf{E}}$ represents a potential. The exact assumptions on the functions u, c, p and $f = (f_{\mathsf{e}})_{\mathsf{e}\in\mathsf{E}}$ are to be defined later in 6.2.1.

We wish to approximate the solution of (6.1) in the finite element framework. In [173] a special finite element is assigned to the vertices that have a star shaped support on the neighbouring edges ensuring the continuity of solutions, and use standard finite elements on the edges. Then the authors prove usual error estimates and an upper bound for the Neumann-Kirchhoff residual of the discrete solution. However, the size of the corresponding stiffness matrix can grow quickly and it loses its banded (tridiagonal) nature compared to one-dimensional problems.

To overcome such issues, we investigate a Neumann-Neumann type nonoverlapping domain decomposition method. The mathematical background of overlapping domain decomposition methods originate from [174], which was further developed in [175, 176, 177]. Later nonoverlapping methods gained attention due to their natural parallelism and efficiency in numerical applications along with the growth of high performance computing [178, 179, 180]. Many variants have been developed since, such as Lagrange multiplier based Finite Element Tearing and Interconnecting (FETI) methods [181, 182], least squares-control methods [183, 184], and multilevel or multigrid methods [185, 186, 187]. In particular, Neumann-Neumann methods can be traced back to [188, 189, 190, 191]. For introductory surveys we refer to [192, 193], see also [194, Chapter 7], while more thorough theoretical background and historical overview can be found in [195, 196, 197]. While certain domain decomposition methods have been successfully designed and applied for optimal control on networks [198, 199, 200, 201] and its theory was established in [202], to the authors knowledge, the performance and the convergence of Neumann-Neumann type iterative substructuring methods was never addressed. First, we rewrite the method as a preconditioner for the Schur complement system, then rigorously show via the abstract additive Schwarz framework that the iteration converges to the finite element solution with a geometric rate that is independent of the finite element mesh size, see Theorem 6.3.6. While preparing for this proof we show in Corollary 6.3.4 that the condition number of the underlying Schur complement is uniformly bounded with respect to the finite element mesh size. The chapter is organized as follows. Section 6.2 contains a brief overview of the abstract problem, the corresponding weak formulation and its FEM solution, and the abstract additive Schwarz framework. In Section 6.3 we introduce the Neumann-Neumann method and prove its convergence to the FEM solution through the Schwarz framework. We also formulate the method as a preconditioner to

the Schur complement system. We note because of the quasi-one-dimensional nature of the problem we can use powerful tools like Sobolev's embedding, and thus our proofs are much simpler and more transparent then that of classical domain decomposition methods in two or more dimensions. Finally, in Section 6.4, we demonstrate the strength of our approach through various examples and compare it to other preconditioners.

6.2 Preliminaries

Let $L^2(a,b)$ be the Hilbert space of real-valued square-integrable functions equipped with the norm

$$\|f\|^2_{L^2(a,b)} = \int_a^b \big|f(x)\big|^2 \,\mathrm{d}x\,, \qquad f \in L^2(a,b),$$

and $L^\infty(a,b)$ be the Banach space of real-valued essentially bounded functions equipped with the norm

$$\|f\|_{L^\infty(a,b)} = \operatorname*{ess\,sup}_{x\in(a,b)} \big|f(x)\big|, \qquad f \in L^\infty(a,b).$$

Let $H^k(a,b)$ be the Sobolev space of real-valued square-integrable functions whose generalized derivatives up to the kth order are also square-integrable, equipped with the norm

$$\|f\|^2_{H^k(a,b)} = \sum_{j=0}^{k} \Big\|f^{(j)}\Big\|^2_{L^2(a,b)}, \qquad f \in H^k(a,b).$$

Finally, let $C[a,b]$ be the Banach space of real-valued continuous functions equipped with the supremum norm. Using these, we define the Banach spaces

$$L^2(\mathsf{G}) = \bigoplus_{\mathsf{e}\in\mathsf{E}} L^2(0,\ell_\mathsf{e}), \qquad L^\infty(\mathsf{G}) = \bigoplus_{\mathsf{e}\in\mathsf{E}} L^\infty(0,\ell_\mathsf{e}), \qquad H^k(\mathsf{G}) = \bigoplus_{\mathsf{e}\in\mathsf{E}} H^k(0,\ell_\mathsf{e}).$$

endowed with the natural norms

$$\begin{aligned}
\|u\|^2_{L^2(\mathsf{G})} &:= \sum_{\mathsf{e}\in\mathsf{E}} \|u_\mathsf{e}\|^2_{L^2(0,\ell_\mathsf{e})}, && u = (u_\mathsf{e})_{\mathsf{e}\in\mathsf{E}} \in L^2(\mathsf{G}),\\
\|u\|^2_{L^\infty(\mathsf{G})} &:= \max_{\mathsf{e}\in\mathsf{E}} \|u_\mathsf{e}\|_{L^\infty(0,\ell_\mathsf{e})}, && u = (u_\mathsf{e})_{\mathsf{e}\in\mathsf{E}} \in L^\infty(\mathsf{G}),\\
\|u\|^2_{H^k(\mathsf{G})} &:= \sum_{\mathsf{e}\in\mathsf{E}} \|u_\mathsf{e}\|^2_{H^k(0,\ell_\mathsf{e})}, && u = (u_\mathsf{e})_{\mathsf{e}\in\mathsf{E}} \in H^k(\mathsf{G}).
\end{aligned}$$

We note that the spaces $L^2(\mathsf{G})$ and $H^k(\mathsf{G})$ are Hilbert spaces with the natural inner products. Finally, we define the space of continuous functions defined on G as

$$C(\mathsf{G}) := \Big\{ u = (u_\mathsf{e})_{\mathsf{e}\in\mathsf{E}} \Big| I_\mathsf{v} U(\mathsf{v}) = 0,\ \forall \mathsf{e} \in \mathsf{E} : u_\mathsf{e} \in C[0,\ell_\mathsf{e}] \Big\}.$$

6.2.1 The abstract problem

On $L^2(\mathsf{G})$ we define the elliptic operator

$$\mathcal{A}_{\max} := \operatorname{diag}\left(-\frac{\mathrm{d}}{\mathrm{d}x}\left(c_{\mathsf{e}}\frac{\mathrm{d}}{\mathrm{d}x}\right) + p_{\mathsf{e}}\right)_{\mathsf{e}\in\mathsf{E}}, \qquad D(\mathcal{A}_{\max}) = H^2(\mathsf{G}).$$

We further define the boundary operator $\mathcal{B} : D(\mathcal{A}_{\max}) \mapsto \mathcal{Y}$ by

$$\mathcal{B}u = \begin{bmatrix} \big(I_{\mathsf{v}}U(\mathsf{v})\big)_{\mathsf{v}\in\mathsf{V}} \\ \big(C(\mathsf{v})^\top U'(\mathsf{v})\big)_{\mathsf{v}\in\mathsf{V}} \end{bmatrix}, \qquad D(\mathcal{B}) = D(\mathcal{A}_{\max}),$$

where the boundary space $\mathcal{Y}$ is isomorphic to $\mathbb{R}^{2n}$ endowed with the standard inner product. Finally, we define

$$\mathcal{A} := \mathcal{A}_{\max}, \qquad D(\mathcal{A}) := \big\{u \in D(\mathcal{A}_{\max}) :\ \mathcal{B}u = 0_{\mathcal{Y}}\big\}.$$

Throughout the chapter we assume that $c = \big(c_{\mathsf{e}}\big)_{\mathsf{e}\in\mathsf{E}} : \mathsf{G} \mapsto \mathbb{R}$ is a positive Lipschitz function, that the function $p = \big(p_{\mathsf{e}}\big)_{\mathsf{e}\in\mathsf{E}} \in L^\infty(\mathsf{G})$ satisfies $\operatorname{ess\,inf}_{x\in\mathsf{G}}\ p(x) \geq p_0$ for some $p_0 > 0$, and that $f = \big(f_{\mathsf{e}}\big)_{\mathsf{e}\in\mathsf{E}} \in L^2(\mathsf{G})$. Using this, we can reformulate (6.1) as follows: find $u \in D(\mathcal{A})$ such that

$$\mathcal{A}u = f. \tag{6.2}$$

While (6.2) is well-posed w.r.t. a classical solution [203, Proposition 3.1], for our purposes it is convenient to introduce a weak formulation of (6.1).

6.2.2 Weak formulation and FEM

The corresponding bilinear form $\mathfrak{a}$ is defined as

$$\begin{aligned} \mathfrak{a}(u,v) &= \sum_{\mathsf{e}\in\mathsf{E}} \left(\int_{\mathsf{e}} c_{\mathsf{e}}(x) u'_{\mathsf{e}}(x) v'_{\mathsf{e}}(x)\,\mathrm{d}x + \int_{\mathsf{e}} p_{\mathsf{e}}(x) u_{\mathsf{e}}(x) v_{\mathsf{e}}(x)\,\mathrm{d}x \right), \\ D(\mathfrak{a}) &= H^1(\mathsf{G}) \cap C(\mathsf{G}), \end{aligned}$$

see [204, Lemma 3.3] and [205, Lemma 3.4]. We highlight that the Neumann-Kirchhoff condition do not appear in this bilinear form or in its domain. Thus, we seek a solution $u \in D(\mathfrak{a})$ such that

$$\mathfrak{a}(u,v) = f(v), \qquad v \in D(\mathfrak{a}), \tag{6.3}$$

where $f(v) := \langle f, v\rangle_{L^2(\mathsf{G})}$. It is well-known that under our assumptions the symmetric bilinear form $\mathfrak{a}(\cdot,\cdot)$ is bounded and coercive, and thus (6.3) is well-posed in light of the Riesz representation theorem. Moreover, the unique solution of (6.3) is the unique solution of (6.2).

Following [173] for the sake of notational simplicity we consider an equidistant discretization on the edges. This approach and our subsequent analysis can be trivially generalized to the nonequidistant case. We divide each edge $\mathsf{e} = (\mathsf{v}_a^\mathsf{e}, \mathsf{v}_b^\mathsf{e})$ into $n_\mathsf{e} \geq 2$ intervals of length $h_\mathsf{e} \in (0,1)$. For the resulting $\left\{x_j^\mathsf{e}\right\}_{j=1,2,\dots,n_\mathsf{e}-1}$ nodes we introduce the standard basis $\left\{\psi_j^\mathsf{e}\right\}_{j=1,2,\dots,n_\mathsf{e}-1}$ of hat functions

$$\psi_j^\mathsf{e}(x) = \begin{cases} 1 - \frac{|x_j^\mathsf{e} - x|}{h_\mathsf{e}}, & \text{if } x \in \left[x_{j-1}^\mathsf{e}, x_{j+1}^\mathsf{e}\right], \\ 0, & \text{otherwise,} \end{cases}$$

where $x_0^\mathsf{e} = \mathsf{v}_a^\mathsf{e}$ and $x_{n_\mathsf{e}}^\mathsf{e} = \mathsf{v}_b^\mathsf{e}$. These functions are a basis of the finite-dimensional space $V_h^\mathsf{e} \subset H_0^1(0, \ell_\mathsf{e}) \cap C[0, \ell_\mathsf{e}]$ of piecewise linear functions.

To each v we assign a special hat function ϕ_v supported on the neighbouring set W_v of the vertex defined as

$$W_\mathsf{v} = \left(\bigcup_{\mathsf{e}\in\mathsf{E}:\mathsf{v}_a^\mathsf{e}=\mathsf{v}} \left[\mathsf{v}, x_1^\mathsf{e}\right] \right) \cup \left(\bigcup_{\mathsf{e}\in\mathsf{E}:\mathsf{v}_b^\mathsf{e}=\mathsf{v}} \left[x_{n_\mathsf{e}-1}^\mathsf{e}, \mathsf{v}\right] \right).$$

Then ϕ_v is defined as

$$\phi_\mathsf{v}(x^\mathsf{e}) = \begin{cases} 1 - \frac{|x_\mathsf{v}^\mathsf{e} - x^\mathsf{e}|}{h_\mathsf{e}}, & \text{if } x^\mathsf{e} \in W_\mathsf{v}, \\ 0, & \text{otherwise,} \end{cases}$$

where x_v^e is either 0 or ℓ_e depending on the orientation of the edge.

We define the space

$$V_h(\mathsf{G}) = \left(\bigoplus_{\mathsf{e}\in\mathsf{E}} V_h^\mathsf{e} \right) \oplus \operatorname{span}\{\phi_\mathsf{v}\}_{\mathsf{v}\in\mathsf{V}}$$

of piecewise linear functions. Note, that $V_h(\mathsf{G}) \subset H^1(\mathsf{G}) \cap C(\mathsf{G})$ by construction. Any function $w_h \in V_h(\mathsf{G})$ is a linear combination of the basis functions:

$$w_h(x) = \sum_{\mathsf{e}\in\mathsf{E}} \sum_{j=1}^{n_\mathsf{e}-1} \alpha_j^\mathsf{e} \phi_j^\mathsf{e}(x) + \sum_{\mathsf{v}\in\mathsf{V}} \beta_\mathsf{v} \phi_\mathsf{v}(x).$$

Thus the solution of (6.3) can be approximated by finding $u_h \in V_h(\mathsf{G})$ such that

$$\mathfrak{a}(u_h, v_h) = f(v_h), \qquad v_h \in V_h(\mathsf{G}). \tag{6.4}$$

Equivalently, we can test only on the basis functions. Since the neighbouring set of

distinct vertices are disjoint we have that

$$\begin{aligned}
\mathfrak{a}(w_h, \psi_k^{\mathsf{e}}) &= \sum_{\mathsf{e}\in\mathsf{E}} \sum_{j=1}^{n_{\mathsf{e}}-1} \alpha_j^{\mathsf{e}} \int_{\mathsf{e}} \left(c_{\mathsf{e}} \psi_j^{\mathsf{e}\prime} \psi_k^{\mathsf{e}\prime} + p_{\mathsf{e}} \psi_j^{\mathsf{e}} \psi_k^{\mathsf{e}}\right) \mathrm{d}x \\
&\quad + \sum_{\mathsf{v}\in\mathsf{V}} \beta_{\mathsf{v}} \int_{\mathsf{e}} \left(c_{\mathsf{e}} \phi_{\mathsf{v}}{}' \psi_k^{\mathsf{e}\prime} + p_{\mathsf{e}} \phi_{\mathsf{v}} \psi_k^{\mathsf{e}}\right) \mathrm{d}x = f(\psi_k^{\mathsf{e}}), \quad k = 1, 2, \ldots, n_{\mathsf{e}-1},\ \mathsf{e} \in \mathsf{E}, \\
\mathfrak{a}(w_h, \phi_{\mathsf{v}}) &= \sum_{\mathsf{e}\in\mathsf{E}} \sum_{j=1}^{n_{\mathsf{e}}-1} \alpha_j^{\mathsf{e}} \int_{\mathsf{e}} \left(c_{\mathsf{e}} \psi_j^{\mathsf{e}\prime} \phi_{\mathsf{v}}{}' + p_{\mathsf{e}} \psi_j^{\mathsf{e}} \phi_{\mathsf{v}}\right) \mathrm{d}x \\
&\quad + \sum_{\mathsf{v}\in\mathsf{V}} \beta_{\mathsf{v}} \int_{\mathsf{e}} \left(c_{\mathsf{e}} \phi_{\mathsf{v}}{}' \phi_{\mathsf{v}}{}' + p_{\mathsf{e}} \phi_{\mathsf{v}} \phi_{\mathsf{v}}\right) \mathrm{d}x = f(\psi_k^{\mathsf{e}}), \quad \mathsf{v} \in \mathsf{V}.
\end{aligned} \tag{6.5}$$

Let us denote by

$$\boldsymbol{u} = \begin{bmatrix} u_{\mathsf{E}} \\ u_{\mathsf{V}} \end{bmatrix}, \qquad u_{\mathsf{E}} = \begin{bmatrix} u^{\mathsf{e}_1} \\ u^{\mathsf{e}_2} \\ \vdots \\ u^{\mathsf{e}_m} \end{bmatrix}, \qquad u^{\mathsf{e}} = \begin{bmatrix} u_1^{\mathsf{e}} \\ u_2^{\mathsf{e}} \\ \vdots \\ u_{n_e-1}^{\mathsf{e}} \end{bmatrix}, \qquad u_{\mathsf{V}} = \begin{bmatrix} u_{\mathsf{v}_1} \\ u_{\mathsf{v}_2} \\ \vdots \\ u_{\mathsf{v}_n} \end{bmatrix}$$

the vector of values that define the finite element function

$$u_h(x) = \sum_{\mathsf{e}\in\mathsf{E}} \sum_{j=1}^{n_{\mathsf{e}}-1} u_j^{\mathsf{e}} \phi_j^{\mathsf{e}}(x) + \sum_{\mathsf{v}\in\mathsf{V}} u_{\mathsf{v}} \phi_{\mathsf{v}}(x),$$

and by

$$\boldsymbol{f} = \begin{bmatrix} f_{\mathsf{E}} \\ f_{\mathsf{V}} \end{bmatrix}, \qquad f_{\mathsf{E}} = \begin{bmatrix} f^{\mathsf{e}_1} \\ f^{\mathsf{e}_2} \\ \vdots \\ f^{\mathsf{e}_m} \end{bmatrix}, \qquad f^{\mathsf{e}} = \begin{bmatrix} f_1^{\mathsf{e}} \\ f_2^{\mathsf{e}} \\ \vdots \\ f_{n_e-1}^{\mathsf{e}} \end{bmatrix}, \qquad f_{\mathsf{V}} = \begin{bmatrix} f_{\mathsf{v}_1} \\ f_{\mathsf{v}_2} \\ \vdots \\ f_{\mathsf{v}_n} \end{bmatrix}$$

the vector of values

$$f_k^{\mathsf{e}} = \int_{\mathsf{e}} f \psi_k^{\mathsf{e}} \, \mathrm{d}x\,, \qquad f_{\mathsf{v}} = \int_{W_{\mathsf{v}}} f \phi_{\mathsf{v}} \, \mathrm{d}x\,.$$

Then (6.5) can be rewritten as

$$A\boldsymbol{u} = \boldsymbol{f}, \tag{6.6}$$

where the stiffness matrix A has a block structure as follows:

$$A = \begin{bmatrix} A_{\mathsf{E}} & A_{\mathsf{EV}} \\ A_{\mathsf{VE}} & A_{\mathsf{V}} \end{bmatrix} + \begin{bmatrix} B_{\mathsf{E}} & B_{\mathsf{EV}} \\ B_{\mathsf{VE}} & B_{\mathsf{V}} \end{bmatrix}.$$

Here

1. the matrix $A_{\mathsf{E}} = \mathrm{diag}(A_{\mathsf{e}})_{\mathsf{e}\in\mathsf{E}}$ is block diagonal and the entries of the tridiagonal matrix A_{e} are given by

$$[A_{\mathsf{e}}]_{jk} = \int_{\mathsf{e}} c_{\mathsf{e}} \psi_j^{\mathsf{e}\prime} \psi_k^{\mathsf{e}\prime} \, \mathrm{d}x\,, \qquad j, k = 1, 2, \ldots, n_{\mathsf{e}} - 1$$

2. the entries of the blocks of $A_{\mathsf{EV}}^{\top} = A_{\mathsf{VE}} = (A_{\mathsf{e}})_{\mathsf{e}\in\mathsf{E}}$ are given by

$$[A_{\mathsf{e}}]_{\mathsf{v}k} = \int_{W_{\mathsf{v}}} c_{\mathsf{e}}\phi_{\mathsf{v}}{}'\psi_k^{\mathsf{e}\prime}\,\mathrm{d}x\,, \qquad k = 1, 2, \ldots, n_{\mathsf{e}} - 1,\ \mathsf{v}\in\mathsf{V},$$

3. the entries of the diagonal matrix $A_{\mathsf{V}} = \mathrm{diag}(A_{\mathsf{v}})_{\mathsf{v}\in\mathsf{V}}$ are given by

$$A_{\mathsf{v}} = \int_{W_{\mathsf{v}}} c_{\mathsf{e}}\phi_{\mathsf{v}}{}'\phi_{\mathsf{v}}{}'\,\mathrm{d}x\,,$$

4. the matrix $B_{\mathsf{E}} = \mathrm{diag}(B_{\mathsf{e}})_{\mathsf{e}\in\mathsf{E}}$ is block diagonal and the entries of the tridiagonal matrix B_{e} are given by

$$[B_{\mathsf{e}}]_{jk} = \int_{\mathsf{e}} p_{\mathsf{e}}\psi_j^{\mathsf{e}}\psi_k^{\mathsf{e}}\,\mathrm{d}x\,, \qquad j, k = 1, 2, \ldots, n_{\mathsf{e}} - 1$$

5. the entries of the blocks of $B_{\mathsf{EV}}^{\top} = B_{\mathsf{VE}} = (B_{\mathsf{e}})_{\mathsf{e}\in\mathsf{E}}$ are given by

$$[B_{\mathsf{e}}]_{\mathsf{v}k} = \int_{W_{\mathsf{v}}} p_{\mathsf{e}}\phi_{\mathsf{v}}\psi_k^{\mathsf{e}}\,\mathrm{d}x\,, \qquad k = 1, 2, \ldots, n_{\mathsf{e}} - 1,\ \mathsf{v}\in\mathsf{V},$$

6. the entries of the diagonal matrix $B_{\mathsf{V}} = \mathrm{diag}(B_{\mathsf{v}})_{\mathsf{v}\in\mathsf{V}}$ are given by

$$B_{\mathsf{v}} = \int_{W_{\mathsf{v}}} p_{\mathsf{e}}\phi_{\mathsf{v}}\phi_{\mathsf{v}}\,\mathrm{d}x\,.$$

Similarly to standard error estimates in the FEM framework the $H^1(\mathsf{G})$ error of the finite element solution u_h and the weak solution u is $\mathcal{O}(\hat{h})$, where $\hat{h} := \max_{\mathsf{e}\in\mathsf{E}} h_{\mathsf{e}}$ and the $L^2(\mathsf{G})$ error is $\mathcal{O}(\hat{h}^2)$, see [173, Theorem 3.2] for the special case when $c \equiv 1$ and [203, Propositions 6.1-6.2] for the general case.

6.2.3 Abstract additive Schwarz framework

In this section we recall the abstract Schwarz framework based on [206, 197]. Let V be a finite dimensional space with the inner product $b(u, v)$ and consider the abstract problem

$$b(u, v) = f(v), \qquad v \in V. \tag{6.7}$$

Let

$$V = V_1 + V_2 + \cdots + V_N$$

be a not necessarily direct sum of spaces with corresponding symmetric, positive definite bilinear forms $b_i(\cdot,\cdot)$ defined on $V_i \times V_i$. Define the projection-like operators $T_i : V \mapsto V_i$ by

$$b_i(T_i u, v_i) = b(u, v_i), \qquad v_i \in V_i$$

and let

$$T = T_1 + T_2 + \cdots + T_N.$$

Note that if $b_i(u, v) = b(u, v)$ then the operator T_i is equal to the $b(\cdot, \cdot)$-orthogonal projection P_i. However, the generality of this framework allows the use of inexact local solvers.

The operator T is used to equivalently reformulate (6.7) as

$$Tu = g = \sum_{i=1}^{N} g_i = \sum_{i=1}^{N} T_i u, \tag{6.8}$$

where g_i is obtained by solving

$$b_i(g_i, v_i) = b(u, v_i) = f(v), \qquad v_i \in V_i.$$

The following theorem is the cornerstone of the abstract additive Schwarz framework [206, Theorem 1].

Theorem 6.2.1. *Assume that*

(i) *there exists a constant $C_0 > 0$ such that there exists a decomposition $u = \sum_{i=1}^{N} u_i$ for all $v \in V$, where $u_i \in V_i$, such that*

$$\sum_{i=1}^{N} b_i(u_i, u_i) \leq C_0^2 b(u, u),$$

(ii) *there exists a constant $\omega > 0$ such that the inequality*

$$b(u_i, u_i) \leq \omega b_i(u_i, u_i), \qquad u_i \in V_i$$

holds for $i = 1, 2, \ldots, N$,

(iii) *there exist constants $\epsilon_{ij} \geq 0$ such that*

$$b(u_i, u_j) \leq \epsilon_{ij} b^{\frac{1}{2}}(u_i, u_i) b^{\frac{1}{2}}(u_j, u_j), \qquad u_i \in V_i,\ u_j \in V_j,$$

for $i, j = 1, 2, \ldots, N$.

Then T is invertible and

$$C_0^{-2} b(u, u) \leq b(Tu, u) \leq \rho(\mathcal{E}) \omega b(u, u), \qquad u \in V,$$

where $\rho(\mathcal{E})$ is the spectral radius of the matrix $\mathcal{E} = \{\epsilon_{ij}\}_{i,j=1}^{N}$.

Theorem 6.2.1 ensures the existence of a unique solution of (6.8) and provides the bound $\kappa(T) \leq C_0^{-2} \rho(\mathcal{E}) \omega$ for the condition number of T w.r.t. the inner product $b(\cdot, \cdot)$, through its Rayleigh quotient. Thus, an upper bound can be computed for the geometric convergence rate of a conjugate gradient or minimal residual method applied to (6.8).

6.3 Neumann-Neumann method

In [173] the authors proposed a nonoverlapping decomposition, where each subdomain consisted of a single edge. We generalize this approach by decomposing G into arbitrary disjoint (w.r.t. its edges) subgraphs $\{\mathsf{G}_i = (\mathsf{V}_i, \mathsf{E}_i)\}_{i=1,2,\dots,N}$ with $n_i = |\mathsf{V}_i|$ and $m_i = |\mathsf{E}_i|$. We note that each subgraph is itself a metric graph and that a subgraph may consist of only one edge. The set of vertices that are shared on the boundary of multiple subgraphs will be denoted with Γ and called the interface. The corresponding function values are denoted as $u_\Gamma = \big(u(\mathsf{v})\big)_{\mathsf{v}\in\Gamma}$.

6.3.1 Continuous version

The idea of Neumann-Neumann methods is to keep track of the interface values and iteratively update these values based on the deviation from the Neumann-Kirchhoff condition. Formally, we start the algorithm from a zero (or any inexpensive) initial guess u_Γ^0. For $n \geq 0$ the new iterate is computed as follows: first we solve the Dirichlet problems

$$(D_i) \qquad \begin{cases} f_{\mathsf{e}}(x) = -(c_{\mathsf{e}} u_{\mathsf{e}}^{k+\frac{1}{2}\prime})'(x) + p_{\mathsf{e}}(x) u_{\mathsf{e}}^{k+\frac{1}{2}}(x), & x \in (0,\ell_{\mathsf{e}}),\ \mathsf{e}\in\mathsf{E}_i, \quad (a) \\ 0 = I_{\mathsf{v}} U_i^{k+\frac{1}{2}}(\mathsf{v}), & \mathsf{v}\in\mathsf{V}_i\backslash\Gamma, \quad (b) \\ u_\Gamma^k(\mathsf{v}) = U_i^{k+\frac{1}{2}}(\mathsf{v}), & \mathsf{v}\in\mathsf{V}_i\cap\Gamma, \quad (c) \\ 0 = C_i(\mathsf{v})^\top U_i^{k+\frac{1}{2}\prime}(\mathsf{v}), & \mathsf{v}\in\mathsf{V}_i\backslash\Gamma. \quad (d) \end{cases}$$

Here the function C_i is the restriction of C to G_i. Note, that we impose natural boundary conditions on the set of vertices $\partial\mathsf{G}_i \cap \partial\mathsf{G}$, but we will still refer to these problems as Dirichlet problems. Then we compute the solutions of the residual Neumann problems

$$(N_i) \qquad \begin{cases} 0 = -(c_{\mathsf{e}} w_{\mathsf{e}}^{k+1\prime})'(x) + p_{\mathsf{e}}(x) w_{\mathsf{e}}^{k+1}(x), & x\in(0,\ell_{\mathsf{e}}),\ \mathsf{e}\in\mathsf{E}_i, \quad (a) \\ 0 = I_{\mathsf{v}} W_i^{k+\frac{1}{2}}(\mathsf{v}), & \mathsf{v}\in\mathsf{V}_i\backslash\Gamma, \quad (b) \\ 0 = C_i(\mathsf{v})^\top W_i^{k+1\prime}(\mathsf{v}), & \mathsf{v}\in\mathsf{V}_i\backslash\Gamma, \quad (c) \\ \displaystyle\sum_{i:\mathsf{v}\in\mathsf{V}_i} C_i(\mathsf{v})^\top U_i^{k+\frac{1}{2}\prime}(\mathsf{v}) = C_i(\mathsf{v})^\top W_i^{k+1\prime}(\mathsf{v}), & \mathsf{v}\in\mathsf{V}_i\cap\Gamma. \quad (d) \end{cases}$$

Finally, we update the interface values as

$$u_\Gamma^{k+1}(\mathsf{v}) = u_\Gamma^k(\mathsf{v}) - \theta \sum_{\mathsf{e}\in\mathsf{E}_\mathsf{v}} w_{\mathsf{e}}^{k+1}(\mathsf{v}), \qquad \mathsf{v}\in\Gamma,$$

with an appropriate $\theta \in (0, \theta_{\max})$, for some $\theta_{\max} > 0$ [197, Chapter C.3].

6.3.2 Discrete version

In this section we briefly overview some technical tools essential for our subsequent results based on [195, 197]. While in our analysis we will mostly rely on variational notations we will introduce some of the tools in matrix form. For the sake of notational simplicity the following introduction is carried out for a decomposition into two subgraphs.

Let us consider the linear equation $A\boldsymbol{u} = \boldsymbol{f}$ arising from the finite element approximation of an elliptic problem on the quantum graph $\mathsf{G} = (\mathsf{V}, \mathsf{E})$, where A is a symmetric, positive definite matrix. We assume that G is partitioned into two nonoverlapping subgraphs $\left\{\mathsf{G}_i = (\mathsf{V}_i, \mathsf{E}_i)\right\}_{i=1,2}$; that is, we have that

$$\mathsf{E} = \mathsf{E}_1 \cup \mathsf{E}_2,\ \mathsf{E}_1 \cap \mathsf{E}_2 = \emptyset,\ \Gamma = \mathsf{V}_1 \cap \mathsf{V}_2.$$

We recall that in traditional domain decomposition methods we would require that the solution be continuous along the interface and that the normal derivatives w.r.t. the domains sum to zero; that is, they are virtually identical to the continuity and Neumann-Kirchhoff conditions at the vertices. We highlight, that while the latter condition is quite natural and has a clear interpretation for quantum graphs, it is not straightforward to define its functional meaning for problems on domains.

Subassembly and Schur complement systems

Let us partition the degrees of freedom into those internal to G_1 and to G_2, and those on Γ and introduce

$$A = \begin{bmatrix} A_{II}^{(1)} & 0 & A_{I\Gamma}^{(1)} \\ 0 & A_{II}^{(2)} & A_{I\Gamma}^{(2)} \\ A_{\Gamma I}^{(1)} & A_{\Gamma I}^{(2)} & A_{\Gamma\Gamma} \end{bmatrix},\ \boldsymbol{u} = \begin{bmatrix} u_I^{(1)} \\ u_I^{(2)} \\ u_\Gamma \end{bmatrix},\ \boldsymbol{f} = \begin{bmatrix} f_I^{(1)} \\ f_I^{(2)} \\ f_\Gamma \end{bmatrix}.$$

A crucial observation is that the stiffness matrix A and load vector f can be subassembled from the corresponding components of the (two) subgraphs. If for $i = 1, 2$ we denote by

$$f^{(i)} = \begin{bmatrix} f_I^{(i)} \\ f_\Gamma^{(i)} \end{bmatrix},\ A^{(i)} = \begin{bmatrix} A_{II}^{(i)} & A_{I\Gamma}^{(i)} \\ A_{\Gamma I}^{(i)} & A_{\Gamma\Gamma}^{(i)} \end{bmatrix}$$

the right hand sides and local stiffness matrices of the corresponding elliptic problems with Neumann conditions, then we have that

$$A_{\Gamma\Gamma} = A_{\Gamma\Gamma}^{(1)} + A_{\Gamma\Gamma}^{(2)},\ f_\Gamma = f_\Gamma^{(1)} + f_\Gamma^{(2)}.$$

We can find an approximation of the coupled problem as

$$\begin{cases} A_{II}^{(i)} u_I^{(i)} + A_{I\Gamma}^{(i)} u_\Gamma^{(i)} = f_I^{(i)}, & i = 1,2 \\ u_\Gamma^{(1)} = u_\Gamma^{(2)} =: u_\Gamma \\ A_{\Gamma I}^{(1)} u_I^{(1)} + A_{\Gamma\Gamma}^{(1)} u_\Gamma^{(1)} - f_\Gamma^{(1)} = -\big(A_{\Gamma I}^{(2)} u_I^{(2)} + A_{\Gamma\Gamma}^{(2)} u_\Gamma^{(2)} - f_\Gamma^{(2)}\big) =: \lambda_\Gamma, \end{cases} \tag{6.9}$$

which is equivalent to (6.6). Clearly if we know the boundary values u_Γ or the approximate normal derivative λ_Γ the approximate solution inside the domains can be computed by separately solving two Dirichlet or two Neumann problems, respectively. Two well-known corresponding families of domain decomposition algorithms are the Neumann-Neumann and FETI methods. In this article we focus on the former.

To prepare our formal analysis the first standard step of iterative substructuring methods is to eliminate the unknowns $u_I^{(i)}$ with a block factorization

$$A = \begin{bmatrix} I & 0 & 0 \\ 0 & I & 0 \\ A_{\Gamma I}^{(1)} A_{II}^{(1)^{-1}} & A_{\Gamma I}^{(2)} A_{II}^{(2)^{-1}} & I \end{bmatrix} \begin{bmatrix} A_{II}^{(1)} & 0 & A_{I\Gamma}^{(1)} \\ 0 & A_{II}^{(2)} & A_{I\Gamma}^{(2)} \\ 0 & 0 & S \end{bmatrix},$$

where I is the identity matrix and $S = A_{\Gamma\Gamma} - A_{\Gamma I}^{(1)} A_{II}^{(1)^{-1}} A_{I\Gamma}^{(1)} - A_{\Gamma I}^{(2)} A_{II}^{(2)^{-1}} A_{I\Gamma}^{(2)}$ is the Schur complement relative to the unknowns on Γ. The corresponding linear system is given by

$$\begin{bmatrix} A_{II}^{(1)} & 0 & A_{I\Gamma}^{(1)} \\ 0 & A_{II}^{(2)} & A_{I\Gamma}^{(2)} \\ 0 & 0 & S \end{bmatrix} u = \begin{bmatrix} f_I^{(1)} \\ f_I^{(2)} \\ g_\Gamma \end{bmatrix},$$

where $g_\Gamma = f_\Gamma - A_{\Gamma I}^{(1)} A_{II}^{(1)^{-1}} f_I^{(1)} - A_{\Gamma I}^{(2)} A_{II}^{(2)^{-1}} f_I^{(2)}$. This can be further reduced to the Schur complement system

$$S u_\Gamma = g_\Gamma. \tag{6.10}$$

The Schur complement S is a sparse matrix that has the same sparsity pattern as the graph Laplacian of the underlying graph G [173, 207]. The fact that $A_{\Gamma\Gamma}$ and f_Γ can be subassembled from local contributions shows that the same holds for S and g_Γ. Indeed, if for $i = 1, 2$ we define the local Schur complements by

$$S^{(i)} := A_{\Gamma\Gamma}^{(i)} - A_{\Gamma I}^{(i)} A_{II}^{(i)^{-1}} A_{I\Gamma}^{(i)}$$

and

$$g_\Gamma^{(i)} = f_\Gamma^{(i)} - A_{\Gamma I}^{(i)} A_{II}^{(i)^{-1}} f_I^{(i)},$$

we have that $S = S^{(1)} + S^{(2)}$ and $g_\Gamma = g_\Gamma^{(1)} + g_\Gamma^{(2)}$. We recall the elementary fact that the Schur complement of an invertible block w.r.t. a positive definite matrix is also positive definite.

Let us define the discrete version of the Neumann-Neumann iteration. Starting from a cheap initial guess u_Γ^0, in an iteration first we solve the Dirichlet problems

$$(D_i) \quad A_{II}^{(i)} u_I^{(i),k+\frac{1}{2}} + A_{I\Gamma}^{(i)} u_\Gamma^k = f_I^{(i)}, \qquad i = 1, 2,$$

then using the approximation r_Γ for the flux residual (see the third row of (6.9)) we solve the Neumann problems

$$(N_i) \quad \begin{bmatrix} A_{II}^{(i)} & A_{I\Gamma}^{(i)} \\ A_{\Gamma I}^{(i)} & A_{\Gamma\Gamma}^{(i)} \end{bmatrix} \begin{bmatrix} w_I^{(i),k+1} \\ w_\Gamma^{(i),k+1} \end{bmatrix} = \begin{bmatrix} 0 \\ r_\Gamma \end{bmatrix}, \qquad i = 1, 2.$$

Finally, we update the interface values as

$$u_\Gamma^{k+1} = u_\Gamma^k - \theta\big(w_\Gamma^{(1),k+1} + w_\Gamma^{(2),k+1}\big).$$

Eliminating the variables interior to the subdomains of both Dirichlet and Neumann problems shows that

$$u_\Gamma^{k+1} - u_\Gamma^k = \theta\Big(S^{(1)^{-1}} + S^{(2)^{-1}}\Big)(g_\Gamma - S u_\Gamma^k);$$

that is, the Neumann-Neumann algorithm is a preconditioned Richardson iteration for (6.10) using $S^{(1)^{-1}} + S^{(2)^{-2}}$ as a preconditioner. Often an improved convergence rate can be reached if a further diagonal scaling is used based on the degrees of the vertices on Γ leading to a preconditioner of the form

$$D_\Gamma^{-1}\Big(S^{(1)^{-1}} + S^{(2)^{-1}}\Big) D_\Gamma^{-1},$$

where the diagonal elements of D_Γ are d_v for $\mathsf{v} \in \Gamma$. We note that we formulate this Richardson iteration mainly for historical reasons and to avoid the inconvenience of expressing the update of u_Γ in the case of a more sophisticated iteration. However, in practice, one should instead use a preconditioned conjugate gradient (PCG) or minimal residual method. Furthermore, the $S^{(i)}$ matrices and especially their inverses should usually not be formed, unless the solver is to be reused multiples times, since we only need to know their effect when applied to a vector. Indeed, instead of multiplying with $S^{(i)}$ (and in particular with the inverse of $A_{II}^{(i)}$) we solve a Dirichlet problem and instead of multiplying with $S^{(i)^{-1}}$ we solve a Neumann problem. The complexity of each iteration is $\mathcal{O}(mn_\mathsf{E})$, where $n_\mathsf{E} = \max_{\mathsf{e}\in\mathsf{E}} n_\mathsf{e}$.

Other well-known iterative substructuring methods can similarly be characterized by finding a preconditioner for (6.10). For example, the Dirichlet-Neumann (or Neumann-Dirichlet) corresponds to multiplying the equation with $S^{(2)^{-1}}$ (or $S^{(1)^{-1}}$). Then the

preconditioned operator ${S^{(2)}}^{-1}S = I + {S^{(2)}}^{-1}S^{(1)}$ corresponds to solving a Dirichlet problem on one subgraph and then solving a Neumann problem on the other.

If we partition G into many subgraphs a region is called floating if $\partial\mathsf{G}_i \cap \partial\mathsf{G} = \emptyset$. On floating subgraphs Neumann problems of certain elliptic equations, for example if there is no potential, are not uniquely solvable. A possible solution is to use balancing Neumann-Neumann methods, in which we choose a unique solution according to some compatibility condition. In this case the subsequent proof have to be slightly modified, see [197] for more details.

Finally, the use of domain decomposition was proposed in [173], where the Schur complement system was solved with conjugate gradient method equipped with diagonal or polynomial preconditioner. These preconditioners are obtained by truncating the Neumann series expansion of

$$S^{-1} = \big(I - D_S^{-1}(D_S - S)\big)^{-1} D_S^{-1} = \sum_{k=0}^{\infty} \big(D_S^{-1}(D_S - S)\big)^k D_S^{-1}$$

to zeroth and first order, respectively, where D_S is a diagonal matrix containing the diagonal elements of S. While the assembly of S can be avoided, the diagonal D_S needs to be extracted, for example via probing techniques or approximated with randomized methods [208, 209]. This means that preparing a diagonal or polynomial preconditioner can be more expensive than the Neumann-Neumann preconditioner, but the complexity of a single iteration is the same for all of them. Alternatively, diagonal preconditioning can be performed with D_Γ^{-1} instead of D_S^{-1}. This diminishes the cost of preparing the preconditioner but yields similar results, as in certain cases the Schur complement is equal to the graph Laplacian of G, see [173, Theorem 4.3].

While usually the condition number of the stiffness matrix A is $\mathcal{O}\big(\hat{h}^{-2}\big)$ and that of the Schur complement S is $\mathcal{O}\big(\hat{h}^{-1}\big)$, the authors in [173] observed that for scale-free graphs the condition number of S seems to be independent of $\hat{h}$ and proportional to the maximum degree. Furthermore, the dependence on the degree could be rectified with diagonal or polynomial preconditioning. However, these are purely algebraic preconditioners without the formalism of subdomains and without rigorous analysis.

Discrete harmonic functions

The space of discrete harmonic functions is an important subspace of finite element functions and are directly related to the Schur complements and to the interface values u_Γ.

Let us define for $u, v \in V_h(\mathsf{G})$ the bilinear forms corresponding to the global stiffness matrix A and local stiffness matrices A_i as

$$a(u,v) = \boldsymbol{u}^\top A \boldsymbol{v} = \sum_{i=1}^{N} a^{(i)}(u,v) = \sum_{i=1}^{N} u_I^{(i)^\top} A^{(i)} v_I^{(i)}.$$

A function $u^{(i)}$ defined on G_i is said to be discrete harmonic on G_i if

$$A_{II}^{(i)} u_I^{(i)} + A_{I\Gamma}^{(i)} u_\Gamma^{(i)} = 0. \tag{6.11}$$

Clearly such a function is completely defined by its values on $\mathsf{V}_i \cap \Gamma$ and it is orthogonal, in the $a_i(\cdot,\cdot)$-inner product, to the space $V_h(\mathsf{G}) \cap H_0^1(\mathsf{G}_i, \mathsf{V}_i \cap \Gamma)$, where $H_0^1(\mathsf{G}, \mathsf{V}_D) \subset H^1(\mathsf{G})$ is the Sobolev space of functions that vanish on $\mathsf{V}_D \subset \mathsf{V}$. We denote the discrete harmonic extension as $u^{(i)} =: \mathcal{H}_i\big(u_\Gamma^{(i)}\big)$.

We denote the space of global, piecewise discrete harmonic functions by $V_h(\Gamma) \subset V_h(\mathsf{G})$, which consists of functions that are discrete harmonic on each subgraph. Based on subassembly arguments a function u is in $V_h(\Gamma)$ if and only if $A_{II} u_I + A_{I\Gamma} u_\Gamma = 0$ and such a function is completely determined by its values on the interface Γ. The space $V_h(\Gamma)$ is orthogonal, in the $a(\cdot,\cdot)$-inner product, to each space $V_h \cap H_0^1(\mathsf{G}_i, \mathsf{V}_i \cap \Gamma)$. We denote the piecewise discrete harmonic extension as $u =: \mathcal{H}(u_\Gamma)$.

In the subsequent analysis we will also rely on the bilinear form defined by the Schur complement given by

$$s(u,v) = u_\Gamma^\top S v_\Gamma.$$

We recall that $s(\cdot,\cdot)$ is symmetric and coercive.

The preceding argument shows that Neumann-Neumann methods can be regarded as computing the global, piecewise discrete harmonic part of the solution of (6.4) by defining an appropriate preconditioner for the Schur complement S. Before we investigate the convergence we must show the equivalence of the interface space, the Schur complement energy and the space of piecewise discrete harmonic functions in H^1. The following Lemma shows the energy equivalence of the Schur complement systems and piecewise discrete harmonic functions.

Lemma 6.3.1. *Let $u_\Gamma^{(i)}$ be the restriction of a finite element function to $\mathsf{V}_i \cap \Gamma$. The discrete harmonic extension $u^{(i)} = \mathcal{H}_i\big(u_\Gamma^{(i)}\big)$ satisfies*

$$s_i\big(u^{(i)}, u^{(i)}\big) = a_i\big(u^{(i)}, u^{(i)}\big) = \min_{v^{(i)}|_{\mathsf{V}_i \cap \Gamma} = u_\Gamma^{(i)}} a_i\big(v^{(i)}, v^{(i)}\big).$$

Similarly, if u_Γ is the restriction of a finite element function to Γ, the piecewise discrete harmonic extension $u = \mathcal{H}(u_\Gamma)$ satisfies

$$s(u,u) = a(u,u) = \min_{v|_\Gamma = u_\Gamma} a(v,v). \tag{6.12}$$

Proof. The statement follows directly from the definition of (piecewise) discrete harmonic functions in (6.11). □

We define $d_i = \left|\mathsf{V}_i \cap \Gamma\right|$ to be the number of vertices of G_i on the interface and the norm $\|\cdot\|_{\mathsf{V}_i\cap\Gamma} = \|\cdot\|_{\mathbb{R}^{d_i}}$. Let $\mathcal{A}_{i,\max} : H^2(\mathsf{G}_i) \mapsto L^2(\mathsf{G}_i)$ be the operator corresponding to G_i inherited from G with $D(\mathcal{A}_{i,\max}) = H^2(\mathsf{G}_i)$ and define $\tilde{\mathcal{B}}_i : D(\mathcal{A}_{i,\max}) \mapsto \tilde{\mathcal{Y}}_i$ by

$$\tilde{\mathcal{B}}_i u = \begin{bmatrix} \big(I_{\mathsf{v}} U(\mathsf{v})\big)_{\mathsf{v}\in\mathsf{V}_i} \\ \big(C(\mathsf{v})^\top U'(\mathsf{v})\big)_{\mathsf{v}\in\mathsf{V}_i\setminus\Gamma} \end{bmatrix}, \qquad D(\tilde{\mathcal{B}}_i) = D(\mathcal{A}_{i,\max}),$$

where $\tilde{\mathcal{Y}}_i \eqsim \mathbb{R}^{2n_i - d_i}$. Finally, we define the continuous operator $\tilde{\mathcal{A}}_i : H^2(\mathsf{G}_i) \mapsto L^2(\mathsf{G}_i)$ as

$$\tilde{\mathcal{A}}_i := \mathcal{A}_{i,\max}, \qquad D(\tilde{\mathcal{A}}_i) := \big\{u \in D(\mathcal{A}_{i,\max}) :\ \tilde{\mathcal{B}}_i u = 0_{\tilde{\mathcal{Y}}_i}\big\}.$$

That is, a function $u \in D(\tilde{\mathcal{A}}_i)$ is continuous and satisfies the Neumann-Kirchhoff condition at the vertices but not necessarily on the interface Γ. A function $u \in D(\tilde{\mathcal{A}}_i)$ is said to be harmonic on G_i if $u \in \operatorname{Ker}(\tilde{\mathcal{A}}_i)$. A function $u \in H^2(\mathsf{G})\cap C(\mathsf{G})$ is said to be piecewise harmonic if $u\big|_{\mathsf{G}_i} \in D(\tilde{\mathcal{A}}_i) \cap \operatorname{Ker}(\tilde{\mathcal{A}}_i)$. Similarly to the discrete case, such a function is expected to be completely determined by the values at $\mathsf{V}_i \cap \Gamma$. The following lemma establishes the existence of the harmonic extension and the equivalence of the interface space and the space of piecewise harmonic functions in $H^2(\mathsf{G}_i)$.

Lemma 6.3.2. *For given boundary data u_Γ there exists a unique harmonic extension into G_i, and consequently a unique piecewise harmonic extension u into G. Moreover, there exist positive constants c and C such that*

$$c\|u_\Gamma\|^2_{\mathsf{V}_i\cap\Gamma} \le \|u\|^2_{H^2(\mathsf{G}_i)} \le C\|u_\Gamma\|^2_{\mathsf{V}_i\cap\Gamma}.$$

Proof. Let us define the $L : H^2(\mathsf{G}_i) \mapsto \mathbb{R}^{d_i}$ trace operator. Then for any $v \in H^2(\mathsf{G}_i)$ we have that

$$\|Lv\|_{\mathsf{V}_i\cap\Gamma} \le \|v\|_{L^\infty(\mathsf{G}_i)} \le c\|v\|_{H^1(\mathsf{G}_i)} \le c\|v\|_{H^2(\mathsf{G}_i)}. \tag{6.13}$$

Clearly $\mathcal{A}_0 := \tilde{\mathcal{A}}_i\big|_{\operatorname{Ker}(L)}$ is the generator of a strongly continuous semigroup [205], see also [210, Section 6.5.1]. We have that 0 is in the resolvent set of $\mathcal{A}_0$ since $\mathcal{A}_0$ is invertible, and thus [211, Lemma 1.2] shows that $L\big|_{\operatorname{Ker}(\tilde{\mathcal{A}}_i)}$ is an isomorphism of $\operatorname{Ker}(\tilde{\mathcal{A}}_i)$ onto $\mathbb{R}^{d_i}$; that is, the following inequality holds

$$\|u\|_{H^2(\mathsf{G}_i)} \le C\|Lu\|_{\mathsf{V}_i\cap\Gamma},$$

and the proof is finished. □

Finally, the following lemma shows that a similar statement holds for discrete harmonic functions.

Lemma 6.3.3. *Let u be a piecewise discrete harmonic function on G. Then there exist positive constants c and C independent of $\hat{h}$ such that*

$$c\|u_\Gamma\|^2_{\mathsf{V}_i\cap\Gamma} \leq \|u\|^2_{H^1(\mathsf{G}_i)} \leq C\|u_\Gamma\|^2_{\mathsf{V}_i\cap\Gamma}.$$

Consequently, for some positive constants $\tilde{c}$ and $\tilde{C}$ independent of $\hat{h}$, we have that

$$\tilde{c}\sum_{i=1}^{N}\|u_\Gamma\|^2_{\mathsf{V}_i\cap\Gamma} \leq s\big(u,u\big) \leq \tilde{C}\sum_{i=1}^{N}\|u_\Gamma\|^2_{\mathsf{V}_i\cap\Gamma}. \tag{6.14}$$

Proof. Let u be piecewise discrete harmonic on G with boundary data u_Γ. The first inequality follows from (6.13). For the second inequality, let us consider the harmonic extension $v \in H^2(\mathsf{G}_i)$ of u_Γ into G_i, which uniquely exists in light of Lemma 6.3.2. Furthermore, the function v is continuous and the standard linear interpolation operator I_h can be used resulting in the finite element function $I_h v \in H^1(\mathsf{G}_i)$. Then by (6.12) we have that

$$\|u\|_{H^1(\mathsf{G}_i)} \leq Ca_i(u,u) \leq Ca_i(I_hv, I_hv) \leq C\|I_hv\|_{H^1(\mathsf{G}_i)},$$

since the $H^1(\mathsf{G}_i)$ norm is equivalent with the $a_i(\cdot,\cdot)$-norm. Furthermore,

$$\|I_hv\|_{H^1(\mathsf{G}_i)} \leq \|I_hv - v\|_{H^1(\mathsf{G}_i)} + \|v\|_{H^1(\mathsf{G}_i)} \leq (C\hat{h}+1)\|v\|_{H^2(\mathsf{G}_i)} \leq C\|u_\Gamma\|_{\mathsf{V}_i\cap\Gamma}.$$

The third inequality is shown in the proof of [173, Theorem 3.2] and in the last inequality we used Lemma 6.3.2. □

Let us define $d = |\Gamma|$, the norm $\|\cdot\|_\Gamma = \|\cdot\|_{\mathbb{R}^d}$ and $d_{\max} = \max_{\mathsf{v}\in\Gamma}\big|\{j : \mathsf{v} \in \mathsf{V}_j\}\big|$. Then (6.14) implies that

$$c\|u_\Gamma\|^2_{\mathbb{R}^d} \leq s(u,u) \leq Cd_{\max}\|u_\Gamma\|^2_{\mathbb{R}^d}.$$

The following statement is an immediate consequence.

Corollary 6.3.4. *The condition number of the Schur complement S is uniformly bounded in $\hat{h}$ and satisfies the explicit bound $\kappa(S) \leq Cd_{\max}$, for some $C > 0$ that is independent of $\hat{h}$.*

We note that this phenomenon was already observed, although not rigorously investigated, for scale-free graphs in [173].

6.3.3 Schwarz iteration

With the above auxiliary results we can reformulate the Neumann-Neumann method as an abstract additive Schwarz iteration. We choose $V = V_h(\Gamma)$ and $V_i = V_i(\Gamma)$, where $V_i(\Gamma) \subset V_h(\Gamma)$ denotes the subspace of discrete harmonic functions that vanish on $\Gamma \backslash \mathsf{V}_i$. For the bilinear forms we set $b(u,v) = s(u,v)$ on $V \times V$ and

$$b_i(u,v) = s_i\big(I_h(\nu_i u), I_h(\nu_i v)\big) = a_i\big(\mathcal{H}_i(\nu_i u), \mathcal{H}_i(\nu_i v)\big)$$

on $V_i \times V_i$. The counting functions ν_i are defined on $\Gamma \cup \partial\mathsf{G}$ by

$$\nu_i(\mathsf{v}) = \begin{cases} \big|\{j : \mathsf{v} \in \mathsf{V}_j\}\big|, & \mathsf{v} \in (\Gamma \cap \mathsf{V}_i) \cup \partial\mathsf{G}_i, \\ 0, & \mathsf{v} \in \Gamma \backslash \mathsf{V}_i. \end{cases}$$

The pseudoinverses $\nu_i^\dagger$ of the ν_i functions, given as

$$\nu_i^\dagger(v) = \begin{cases} \nu_i^{-1}(\mathsf{v}), & \mathsf{v} \in (\Gamma \cap \mathsf{V}_i) \cup \partial\mathsf{G}_i, \\ 0, & \mathsf{v} \in \Gamma \backslash \mathsf{V}_i, \end{cases}$$

define a partition of unity on $\Gamma \cup \partial\mathsf{G}$; that is,

$$\sum_{i=1}^{N} \nu_i^\dagger(\mathsf{v}) \equiv 1, \qquad \mathsf{v} \in \Gamma \cup \partial\mathsf{G}.$$

Finally, the operators $T_i : V \mapsto V_i$ are defined by

$$b_i(T_i u, v) = b(u,v), \qquad v \in V_i,$$

and the operator T by

$$T = T_1 + T_2 + \cdots + T_N. \tag{6.15}$$

Proposition 6.3.5. *The operator T defined by* (6.15) *is invertible and for all $u \in V$ the following inequality holds*

$$\gamma_0 s(u,u) \le s(Tu,u) \le \gamma_1 \rho(\mathcal{E}) s(u,u),$$

where γ_0 and γ_1 are constants independent of $\hat{h}$, where $\mathcal{E} = \{\epsilon_{ij}\}_{i,j=1}^N$ is defined element-wise by

$$\epsilon_{ij} = \begin{cases} 1, & \mathsf{V}_i \cap \mathsf{V}_j \neq \emptyset, \\ 0, & \textit{otherwise.} \end{cases}$$

Proof. We have to establish the three estimates of Theorem 6.2.1.

Assumption (i): For $u \in V$ we choose $u_i = I_h\big(\nu_i^\dagger u\big)$, $i = 1, 2, \ldots, N$. Clearly $u_i \in V_i$ and $u = \sum_{i=1}^N u_i$ holds, and

$$b_i(u_i, u_i) = a_i(\mathcal{H}_i u, \mathcal{H}_i u) = a_i(u, u).$$

By subassembly, this shows that

$$\sum_{i=1}^N b_i(u_i, u_i) = a(u, u) = s(u, u) = b(u, u).$$

Assumption (ii): For $u_i \in V_i$ we have that

$$s(u_i, u_i) = s_i(u_i, u_i) + \sum_{j:\mathsf{V}_j \cap \mathsf{V}_i \neq \emptyset} s_j(u_i, u_i).$$

Using Lemma 6.3.3 shows that $s_i(u_i, u_i) \leq C\|u_i\|_{\mathsf{V}_i \cap \Gamma}$ and that

$$s_j(u_i, u_i) \leq C\|u_i\|^2_{\mathsf{V}_j \cap \Gamma} \leq C\|u_i\|^2_{\mathsf{V}_i \cap \Gamma},$$

since $u_i \in V_i$, and thus $u_i(x) = 0$ for $x \in (\mathsf{V}_j \cap \Gamma) \backslash \mathsf{V}_i$. Using Sobolev's embedding we can further bound $\|u_i\|^2_{\mathsf{V}_i \cap \Gamma}$ as

$$\begin{aligned}\|u_i\|^2_{\mathsf{V}_i \cap \Gamma} &\leq C\|u_i\|^2_{L^\infty(\mathsf{G}_i)} \leq C\|u_i\|^2_{H^1(\mathsf{G}_i)} \leq Ca_i(u_i, u_i) \\ &= Cs_i(u_i, u_i) \leq Cs_i\big(I_h(\nu_i u_i), I_h(\nu_i u_i)\big) = Cb_i(u_i, u_i).\end{aligned}$$

Combining the above yields $b(u_i, u_i) \leq Cb_i(u_i, u_i)$ for $u_i \in V_i$ as required.

Assumption (iii): It is easy to see that

$$\epsilon_{ij} = \begin{cases} 1, & \mathsf{V}_i \cap \mathsf{V}_j \neq \emptyset, \\ 0, & \text{otherwise}, \end{cases}$$

as $V_i \cap V_j \neq \emptyset$ if and only if $\mathsf{V}_i \cap \mathsf{V}_j \neq \emptyset$. □

This shows that the condition number of the preconditioned system is independent of $\hat{h}$. We note that $\rho(\mathcal{E}) \leq d_{\max}$ via Gershgorin's theorem. Finally, we state our main theorem.

Theorem 6.3.6. *The Neumann-Neumann algorithm converges to the solution of* (6.6) *with a geometric rate that is independent of* $\hat{h}$.

Proof. The statement follows from Proposition 6.3.5 and Lemma 6.3.3. □

Remark 6.3.7. *We note that in a multidimensional setting one usually assumes that the substructures and the elements are shape regular, meaning that the number of neighbours*

of any subdomain, and thus $\rho(\mathcal{E})$, is bounded by a constant. Furthermore, the verification of assumption (i) and (ii) is more challenging, and accordingly the estimates on $\frac{s(Tu,u)}{s(u,u)}$ are more complicated. In particular, usually polylogarithmic bounds of the form $\tilde{h}^{-2}\Big(1+\log\frac{\tilde{h}}{\hat{h}}\Big)^2$ appear, where $\tilde{h}$ denotes the size of a typical subdomain, see [206, 197]. The main technical difficulty is the fact that the boundary spaces of the domains are equipped with the $H^{\frac{1}{2}}$ Sobolev-Slobodeckij seminorm, which cannot be so straightforwardly estimated as in our case.

6.4 Numerical experiments

In this section we introduce and discuss some numerical experiments. The C++ implementation mainly relies on Eigen 3.4.0 and is compiled with GCC 13.2.1. The graphs are generated with NetworkX 3.1 in Python 3.11.6. The experiments have been performed on a computer with Intel(R) Core(TM) i7-8565U CPU @ 1.80GHz and 16 GB of RAM. The Schur complement problems are solved respectively without preconditioning, with degree preconditioning, with diagonal preconditioning, with first-degree polynomial preconditioning and finally, with Neumann-Neumann preconditioning. While our convergence theory holds for arbitrary (nonoverlapping) decomposition, in all experiments, we completely decompose the quantum graph so that each subgraph consists of a single edge. Despite this, to anticipate more general decompositions, we solve the subproblems with Cholesky decomposition without assembling the $S^{(i)}$ matrices or their inverses. The D_S diagonal is extracted in a naive way by solving n equations where the right-hand sides are set to unit vectors of $\mathbb{R}^n$. We set the length of each edge to 1. Furthermore, the c_{e} conductances are set to sigmoid functions, the p_{e} potentials are set to double-well functions and the f_{e} forcing is set as a short shock at the start of the edges; that is, we have

$$
\begin{aligned}
c_{\mathsf{e}}(x) &= \frac{1}{1+\exp\big(-25(x-0.5)\big)} + 1,\\
p_{\mathsf{e}}(x) &= \frac{0.05}{0.2^2}\big(|x-0.5|-0.2\big)^2 + 0.05,\\
f_{\mathsf{e}}(x) &= \exp\big(-1000x^2\big).
\end{aligned}
$$

The initial guess is set to the zero vector and the iteration is stopped after the relative residual norm reduces below the square root of the machine precision $\varepsilon \approx 2.2204 \cdot 10^{-16}$.

While Corollary 6.3.4 shows that condition number of the Schur complement is independent of $\hat{h}$, it might still increase as the number of vertices, and thus the maximum

degree grows, as indicated by the results below. Interestingly, this dependence is already somewhat mitigated with a diagonal preconditioner and seemingly eliminated with a polynomial or Neumann-Neumann preconditioner. Instead, the condition number of these preconditioners seem to only scale with the average degree. In fact, without We found that for small graphs with $|\mathsf{V}| \ll 1000$ solving the Schur complement system without preconditioning is the fastest independently of $\hat{h}$, but for larger graphs preconditioning is more and more crucial as $\log_2\left(\hat{h}^{-1}\right)$ increases.

6.4.1 Dorogovtsev-Goltsev-Mendes graphs

The first set of test graphs are a family of scale-free planar graphs introduced in [212], defined iteratively as follows. The graph $\mathsf{DGM}(0)$ is the path graph with two vertices. The graph $\mathsf{DGM}(k+1)$ is generated from $\mathsf{DGM}(k)$ by adding a new vertex for each edge and connecting it with the endpoint of the edge. The graph $\mathsf{DGM}(k)$ has $|\mathsf{V}| = \frac{3}{2}\left(3^k + 1\right)$ and $|\mathsf{E}| = 3^k$. Figure 6.1 shows the first few graphs of this iteration. First we set $\log_2\left(\hat{h}^{-1}\right) = 6$ and apply PCG to the Schur complement system of DGM graphs of increasing size. Table 6.1 shows the number of necessary iterations without preconditioning and with degree, diagonal, polynomial and Neumann-Neumann preconditioning. Table 6.2 shows the same for $\mathsf{DGM}(7)$ with increasing $\log_2\left(\hat{h}^{-1}\right)$.

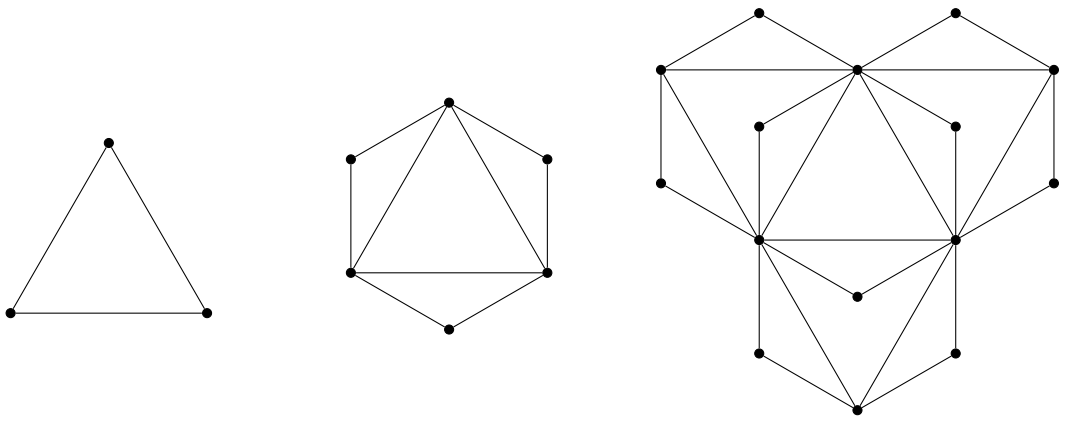

Figure 6.1: The graphs $\mathsf{DGM}(1)$, $\mathsf{DGM}(2)$ and $\mathsf{DGM}(3)$.

Graph	No prec.	Degree	Diagonal	Polynomial	Neumann-Neumann
DGM(5)	26	14	13	9	10
DGM(6)	35	14	13	11	11
DGM(7)	53	15	15	12	12
DGM(8)	73	19	16	13	14
DGM(9)	90	20	19	13	14

Table 6.1: Number of PCG iterations for the Schur complement systems of Dorogovtsev-Goltsev-Mendes graphs of increasing size with $\log_2\left(\hat{h}^{-1}\right) = 6$.

$\log_2\left(\hat{h}^{-1}\right)$	No prec.	Degree	Diagonal	Polynomial	Neumann-Neumann
4	53	15	15	12	12
6	53	15	15	12	12
8	53	15	15	12	12
10	53	15	15	12	12
12	59	15	15	12	12

Table 6.2: Number of PCG iterations for the Schur complement system of DGM(7) with increasingly finer meshes.

6.4.2 Barabási-Albert model

Next, we test our method on scale-free graphs with $|\mathsf{E}| \approx 2|\mathsf{V}|$ generated using the Barabási-Albert model [213]. Unlike the DGM graphs, which are generated deterministically, the Barabási-Albert model has randomness involved, and thus the following results have to be understood in a probabilistic sense.

Again, we set $\log_2\left(\hat{h}^{-1}\right) = 6$ and apply PCG to the Schur complement system of scale-free graphs of increasing size. Table 6.3 shows the number of necessary iterations without preconditioning and with degree, diagonal, polynomial and Neumann-Neumann preconditioning. Table 6.4 shows the same for SF(1000) with increasing $\log_2\left(\hat{h}^{-1}\right)$.

Graph	No prec.	Degree	Diagonal	Polynomial	Neumann-Neumann
SF(100)	39	25	25	13	13
SF(500)	63	28	28	15	15
SF(1000)	74	29	29	15	15
SF(2000)	90	28	28	15	15
SF(5000)	106	28	28	14	14

Table 6.3: Number of PCG iterations for the Schur complement systems of scale-free graphs of increasing size with $\log_2\left(\hat{h}^{-1}\right) = 6$.

$\log_2\left(\hat{h}^{-1}\right)$	No prec.	Degree	Diagonal	Polynomial	Neumann-Neumann
4	73	29	29	15	15
6	74	29	29	15	15
8	74	29	29	15	15
10	75	29	29	15	15
12	74	29	29	15	15

Table 6.4: Number of PCG iterations for the Schur complement system of $\mathsf{SF}(100)$ with increasingly finer meshes.

6.5 Conclusions

A Neumann-Neumann type domain decomposition method was developed for elliptic problems on metric graphs. We have defined the iteration in the continuous and discrete setting and rewritten the latter as a preconditioner for the Schur complement system. The discrete iteration was then formulated as an abstract additive Schwarz iteration and we proved that it converges to the finite element solution with a rate that is independent of the finite element mesh size. Moreover, we have shown that the condition number of the Schur complement is also independent of the finite element mesh size and depends on the maximum degree. We implemented the algorithm along with a diagonal and polynomial preconditioners and tested them on various examples. The numerical results confirm our theoretical results regarding the condition number of the Schur complement and that of the Neumann-Neumann preconditioner. Moreover, the numerical results suggest that the condition number of the Schur complement scales with the maximum degree, while the polynomial and Neumann-Neumann preconditioners seem to scale with the average degree.

Chapter 7

Conclusions

7.1 New scientific results

Thesis I.

I have shown that a class of multidimensional nonlocal conservation laws are well-posed for a broad class of flux functions and initial data, using the theory of nonlinear operator semigroups. I have also shown that the unique mild solution satisfies a Kruẑkov-type nonlocal entropy inequality, along with several desirable qualitative properties.

The results are described in detail in Chapter 3.

Related publication: [221].

Thesis II.

I have proven new results regarding two important classes of kinetic dynamical systems.

Thesis II.a

I have introduced generalized ribosome flows (GRFs) by generalizing the graph structure and the transition rate functions of existing ribosome flow models in the literature. I have shown that GRFs can be interpreted as finite volume approximations of nonlocal conservation laws. I have proven that GRFs with a strongly connected compartmental structure are asymptotically stable relative to the level sets of the linear conserved quantity. I have proven that strongly connected GRFs with time-varying transition rates are persistent and input-to-state stable.

The results are described in detail in Chapter 4.

Related publications: [216, 129, 218, 219, 220].

Thesis II.b

I have shown that delayed complex balanced reaction networks with non-mass action kinetics are quasi-thermostatic; that is, each positive stoichiometric compatibility class contains a unique equilibrium points. I have shown that delayed complex balanced reaction networks with non-mass action kinetics are quasi-thermodynamic; that is, each positive equilibrium is asymptotically stable relative to its compatibility class.

The results are described in detail in Chapter 2.

Related publication: [226].

Thesis III.

I have proposed an efficient finite volume discretization of the multidimensional PIDE model of gene regulatory networks that result in a kinetic system. I have shown that the semidiscretized model has a unique steady-state, which is globally asymptotically stable. I have used the semidiscretized model to design novel population level exogenous controllers that can drive the expected value of the system to desired values.

The results are described in detail in Chapter 5.

Related publications: [222, 225, 228].

Thesis IV.

I have developed a Neumann-Neumann type nonoverlapping domain decomposition method for elliptic problems on metric graphs. I have proven that the iteration converges to the finite element solution with a geometric rate that is independent of the mesh size, via the theory of abstract additive Schwarz methods.

The results are described in detail in Chapter 6.

Related publication: [224].

7.2 Future plans

The above results can serve as the bases for several further research directions, including:

- The results of Chapter 2 can be used to investigate the stability of complex balanced systems with distributed delays. A major shortcoming of the model class is that a given species has a fixed reaction rate function associated with it. Thus, it is not possible, for example, that a species is involved in a reaction with mass-action kinetics and involved in an other reaction with Hill kinetics. To our knowledge, this is not handled in the literature yet, thus it would be an important extension.

- The results of Chapter 4 can be used to investigate ribosome flow models with not strongly connected compartmental structure, or with discrete delays or distributed delays. Flows open to the environment can also be investigated and used to solve control problems motivated by real-world examples.

- The results of Chapter 5 can be used to implement the finite volume discretization for gene regulatory networks with more than two proteins. The discretization can also be used for model reduction and further control.

- The results of Chapter 6 can be used to implement the Neumann-Neumann iteration for decomposition where the domains are not edges. The theoretical results can be used to prove the convergence of overlapping decompositions. These iterations can be used to solve further problems, for example, the efficient generation of Gaussian Whittle-Matérn fields on metric graphs. The key problem there is white noise realization, since that requires the assembly of the mass matrix and its Cholesky decomposition. This could be mitigated with the lumped mass method, where a diagonal approximation of the mass matrix is used, in which case white noise generation can be performed domain-wise.

Bibliography

[1] W. M. Haddad, V. Chellaboina, and Q. Hui, *Nonnegative and Compartmental Dynamical Systems*. Princeton University Press, 2010.

[2] D. H. Anderson, *Compartmental modeling and tracer kinetics*. Springer Science & Business Media, 2013, vol. 50.

[3] F. Brauer, "Compartmental models in epidemiology," in *Mathematical epidemiology*. Springer, 2008, pp. 19–79.

[4] K. Godfrey, *Compartmental models and their application*. Academic Press, 1983.

[5] L. Farina and S. Rinaldi, *Positive Linear Systems: Theory and Applications*. Wiley, 2000.

[6] A. Rantzer and M. E. Valcher, "A tutorial on positive systems and large scale control," in *2018 IEEE Conference on Decision and Control (CDC)*. IEEE, 2018, pp. 3686–3697.

[7] R. F. Brown, "Compartmental system analysis: State of the art," *IEEE Transactions on Biomedical Engineering*, vol. BME-27, no. 1, pp. 1–11, jan 1980.

[8] F. Garcia-Sevilla, M. Garcia-Moreno, M. Molina-Alarcon, M. Garcia-Meseguer, J. M. Villalba, E. Arribas, and R. Varon, "Linear compartmental systems. i. kinetic analysis and derivation of their optimized symbolic equations," *Journal of Mathematical Chemistry*, vol. 50, no. 6, pp. 1598–1624, 2012.

[9] J. A. Jacquez and C. P. Simon, "Qualitative theory of compartmental systems," *SIAM Review*, vol. 35, no. 1, pp. 43–79, 1993.

[10] P. E. Rapp, "Oscillations and chaos in cellular metabolism and physiological systems," in *Chaos*, A. V. Holden, Ed. Princeton University Press, 1986, chapter 9., pp. 179–208.

[11] C. Cobelli and G. Romanin-Jacur, "Controllability, observability and structural identifiability of multi input and multi output biological compartmental systems," *IEEE Transactions on Biomedical Engineering*, vol. BME-23, no. 2, pp. 93–100, mar 1976.

[12] A. Berman and R. J. Plemmons, *Nonnegative matrices in the mathematical sciences*. SIAM, 1994.

[13] N. Meshkat, S. Sullivant, and M. Eisenberg, "Identifiability results for several classes of linear compartment models," *Bulletin of Mathematical Biology*, vol. 77, no. 8, pp. 1620–1651, aug 2015.

[14] C. Bortner and N. Meshkat, "Identifiable paths and cycles in linear compartmental models," *Bulletin of Mathematical Biology*, vol. 84, no. 5, mar 2022.

[15] M. Feinberg, *Foundations of Chemical Reaction Network Theory*. Springer, 2019.

[16] V. Chellaboina, S. P. Bhat, W. M. Haddad, and D. S. Bernstein, "Modeling and analysis of mass-action kinetics – nonnegativity, realizability, reducibility, and semistability," *IEEE Control Systems Magazine*, vol. 29, pp. 60–78, 2009.

[17] S. Müller and G. Regensburger, "Generalized mass action systems: Complex balancing equilibria and sign vectors of the stoichiometric and kinetic-order subspaces," *SIAM Journal on Applied Mathematics*, vol. 72, no. 6, pp. 1926–1947, 2012.

[18] D. F. Anderson, J. D. Brunner, G. Craciun, and M. D. Johnston, "On classes of reaction networks and their associated polynomial dynamical systems," *Journal of Mathematical Chemistry*, vol. 58, no. 9, pp. 1895–1925, 2020.

[19] B. S. Hernandez and E. R. Mendoza, "Positive equilibria of Hill-type kinetic systems," *Journal of Mathematical Chemistry*, vol. 59, no. 3, pp. 840–870, 2021.

[20] P. Érdi and J. Tóth, *Mathematical Models of Chemical Reactions. Theory and Applications of Deterministic and Stochastic Models*. Manchester, Princeton: Manchester University Press, Princeton University Press, 1989.

[21] N. Samardzija, L. D. Greller, and E. Wassermann, "Nonlinear chemical kinetic schemes derived from mechanical and electrical dynamical systems," *Journal of Chemical Physics*, vol. 90 (4), pp. 2296–2304, 1989.

[22] G. Craciun, M. D. Johnston, G. Szederkényi, E. Tonello, J. Tóth, and P. Y. Yu, "Realizations of kinetic differential equations," *Mathematical Biosciences and Engineering*, vol. 17, no. 1, pp. 862–892, 2019.

[23] D. Angeli, "A tutorial on chemical reaction network dynamics," *European Journal of Control*, vol. 15, no. 3-4, pp. 398–406, Jan. 2009.

[24] D. F. Anderson, "A proof of the Global Attractor Conjecture in the single linkage class case," *SIAM Journal on Applied Mathematics*, vol. 71, pp. 1487–1508, 2011.

[25] G. Craciun, F. Nazarov, and C. Pantea, "Persistence and permanence of mass-action and power-law dynamical systems," *SIAM Journal on Applied Mathematics*, vol. 73, no. 1, pp. 305–329, 2013.

[26] G. Craciun, "Toric differential inclusions and a proof of the global attractor conjecture," *arXiv preprint arXiv:1501.02860*, 2015.

[27] F. Horn and R. Jackson, "General mass action kinetics," *Archive for Rational Mechanics and Analysis*, vol. 47, no. 2, p. 81–116, 1972.

[28] M. Chaves, "Input-to-state stability of rate-controlled biochemical networks," *SIAM Journal on Control and Optimization*, vol. 44, pp. 704–727, 2005.

[29] M. Margaliot and T. Tuller, "Stability analysis of the ribosome flow model," *IEEE/ACM Transactions on Computational Biology and Bioinformatics*, vol. 9, no. 5, pp. 1545–1551, 2012.

[30] M. Ali Al-Radhawi, D. Angeli, and E. D. Sontag, "A computational framework for a Lyapunov-enabled analysis of biochemical reaction networks," *PLoS Computational Biology*, vol. 16, no. 2, p. e1007681, Feb. 2020.

[31] R. J. LeVeque, *Numerical Methods for Conservation Laws.* Basel: Birkhäuser, 1991, vol. 57.

[32] F. A. Chiarello and P. Goatin, "Global entropy weak solutions for general non-local traffic flow models with anisotropic kernel," *ESAIM: Mathematical Modelling and Numerical Analysis*, vol. 52, pp. 163–180, 2018.

[33] F. Kessels, *Traffic Flow Modelling: Introduction to Traffic Flow Theory Through a Genealogy of Models.* Springer International Publishing, 2019.

[34] M. Schreckenberg and S. D. Sharma, Eds., *Pedestrian and evacuation Dynamics*. Berlin Heidelberg: Springer-Verlag, 2002.

[35] A. Raveh, Y. Zarai, M. Margaliot, and T. Tuller, "Ribosome Flow Model on a Ring," *IEEE/ACM Transactions on Computational Biology and Bioinformatics*, vol. 12, no. 6, pp. 1429–1439, 2015.

[36] A. Keimer and L. Pflug, "Existence, uniqueness and regularity results on nonlocal balance laws," *Journal of Differential Equations*, vol. 263, no. 7, pp. 4023–4069, Oct. 2017.

[37] A. Keimer, G. Leugering, and T. Sarkar, "Analysis of a system of nonlocal balance laws with weighted work in progress," *Journal of Hyperbolic Differential Equations*, vol. 15, no. 3, pp. 375–406, 2018.

[38] P. Shang and Z. Wang, "Analysis and control of a scalar conservation law modeling a highly re-entrant manufacturing system," *Journal of Differential Equations*, vol. 250, no. 2, pp. 949–982, 2011.

[39] P. Goatin and S. Scialanga, "Well-posedness and finite volume approximations of the LWR traffic flow model with non-local velocity," *Networks and Heterogeneous Media*, vol. 11, no. 1, pp. 107–121, 2016.

[40] Q. Du, J. R. Kamm, R. B. Lehoucq, and M. L. Parks, "A new approach for a non-local, nonlinear conservation law," *SIAM Journal on Applied Mathematics*, vol. 72, no. 1, pp. 464–487, Jan. 2012.

[41] A. Bayen, J. Friedrich, A. Keimer, L. Pflug, and T. Veeravalli, "Modeling multilane traffic with moving obstacles by nonlocal balance laws," *SIAM Journal on Applied Dynamical Systems*, vol. 21, no. 2, pp. 1495–1538, 2022.

[42] A. Keimer and L. Pflug, "On approximation of local conservation laws by nonlocal conservation laws," *Journal of Mathematical Analysis and Applications*, vol. 475, no. 2, pp. 1927–1955, 2019.

[43] F. Bobaru, J. T. Foster, P. H. Geubelle, and S. A. Silling, Eds., *Handbook of Peridynamic Modeling*. Chapman and Hall/CRC, 2016.

[44] A. Katiyar, J. T. Foster, H. Ouchi, and M. M. Sharma, "A peridynamic formulation of pressure driven convective fluid transport in porous media," *Journal of Computational Physics*, vol. 261, pp. 209–229, 2014.

[45] D. Bothe, "Nonlinear evolutions in banach spaces – existence and qualitative theory with applications to reaction-diffusion-systems," habilitation, Paderborn University, 1999.

[46] Q. Du and Z. Huang, "Numerical solution of a scalar one–dimensional monotonicity–preserving nonlocal nonlinear conservation law," *Journal of Mathematical Research with Applications*, vol. 36, no. 1, pp. 1–18, 2017.

[47] M. Colombo, G. Crippa, and L. V. Spinolo, "On the Singular Local Limit for Conservation Laws with Nonlocal Fluxes," *Archive for Rational Mechanics and Analysis*, vol. 233, no. 3, pp. 1131–1167, 2019.

[48] S. Alimov and A. Yuldasheva, "Solvability of Singular Equations of Peridynamics on Two-Dimensional Periodic Structures," *Journal of Peridynamics and Nonlocal Modeling*, vol. 5, no. 2, pp. 241–259, 2021.

[49] J. Zhao, A. Larios, and F. Bobaru, "Construction of a peridynamic model for viscous flow," *Journal of Computational Physics*, vol. 468, p. 111509, 2022.

[50] C. Yao, H. Fan, Y. Zhao, Y. Shi, and F. Wang, "Fast algorithm for nonlocal allen–cahn equation with scalar auxiliary variable approach," *Applied Mathematics Letters*, vol. 126, p. 107805, 2022.

[51] S. Alexander, "Superconductivity of networks. A percolation approach to the effects of disorder," *Physical Review B*, vol. 27, no. 3, p. 1541–1557, 1983.

[52] C. Flesia, R. Johnston, and H. Kunz, "Strong Localization of Classical Waves: A Numerical Study," *Europhysics Letters (EPL)*, vol. 3, no. 4, p. 497–502, 1987.

[53] ——, "Localization of classical waves in a simple model," *Physical Review A*, vol. 40, no. 7, p. 4011–4018, 1989.

[54] G. Kallianpur and R. Wolpert, "Infinite dimensional stochastic differential equation models for spatially distributed neurons," *Applied Mathematics & Optimization*, vol. 12, pp. 125–172, 1984.

[55] H. Cho, K. Ayers, L. de Pills, Y.-H. Kuo, J. Park, A. Ranudskaya, and R. Rockne, "Modelling acute myeloid leukaemia in a continuum of differentiation states," *Letters in Biomathematics*, vol. 5, pp. 69–98, 2018.

[56] S. Avdonin, J. Edward, and G. Leugering, "Controllability for the wave equation on graph with cycle and delta-prime vertex conditions," *Evolution Equations and Control Theory*, vol. 12, no. 6, p. 1542–1558, 2023.

[57] S. Avdonin and Y. Zhao, "Exact Controllability of the 1-D Wave Equation on Finite Metric Tre e graphs," *Applied Mathematics & Optimization*, vol. 83, no. 3, p. 2303–2326, 2019.

[58] V. Mehandiratta, M. Mehra, and G. Leugering, "Optimal Control Problems Driven by Time-Fractional Diffusion Equations on Metric Graphs: Optimality System and Finite Difference Approximation," *SIAM Journal on Control and Optimization*, vol. 59, no. 6, p. 4216–4242, 2021.

[59] M. Stoll and M. Winkler, "Optimal Dirichlet control of partial differential equations on networks," *Electronic Transactions on Numerical Analysis*, vol. 54, p. 392–419, 2021.

[60] Q. Du, Z. Huang, and P. G. LeFloch, "Nonlocal conservation laws. A new class of monotonicity-preserving models," *SIAM Journal on Numerical Analysis*, vol. 55, no. 5, pp. 2465–2489, 2017.

[61] M. Feinberg, "Chemical reaction network structure and the stability of complex isothermal reactors - I. The deficiency zero and deficiency one theorems," *Chemical Engineering Science*, vol. 42 (10), pp. 2229–2268, 1987.

[62] E. Sontag, "Structure and stability of certain chemical networks and applications to the kinetic proofreading model of T-cell receptor signal transduction," *IEEE Transactions on Automatic Control*, vol. 46, no. 7, p. 1028–1047, 2001.

[63] G. Stépán, *Retarded dynamical systems: stability and characteristic functions*. Longman Scientific & Technical, 1989.

[64] Z. Zhu, Y. Xu, X. Liu, and S. Ruan, "Modeling the p53-Mdm2 dynamics triggered by DNA damage," *Journal of Nonlinear Science*, vol. 34, no. 3, p. 47, 2024.

[65] A. Ruiz-Herrera, "Attraction to equilibria in stage-structured predator prey models and bio-control problems," *Journal of Dynamics and Differential Equations*, vol. 31, no. 1, pp. 435–450, 2019.

[66] G. Orosz, R. E. Wilson, R. Szalai, and G. St épán, "Exciting traffic jams: Nonlinear phenomena behind traffic jam formation on highways," *Physical review E*, vol. 80, no. 4, p. 046205, 2009.

[67] Y. Wang, M. Lu, and D. Jiang, "Dynamic behavior of a general stochastic hiv model with virus-to-cell infection, cell-to-cell transmission, immune response and distributed delays," *Journal of Nonlinear Science*, vol. 33, no. 5, p. 97, 2023.

[68] L. Zhu, M. Zhou, and Z. Zhang, "Dynamical analysis and control strategies of rumor spreading models in both homogeneous and heterogeneous networks," *Journal of Nonlinear Science*, vol. 30, pp. 2545–2576, 2020.

[69] E. Fridman, *Introduction to time-delay systems: Analysis and control*. Springer, 2014.

[70] M. R. Roussel, "The use of delay differential equations in chemical kinetics," *The Journal of Physical Chemistry*, vol. 100, no. 20, pp. 8323–8330, 1996.

[71] G. Lipták, K. M. Hangos, M. Pituk, and G. Szederkényi, "Semistability of complex balanced kinetic systems with arbitrary time delays," *Systems & Control Letters*, vol. 114, p. 38–43, 2018.

[72] G. Lipták, M. Pituk, and K. M. Hangos, "Modelling and stability analysis of complex balanced kinetic systems with distributed time delays," *Journal of Process control*, vol. 84, pp. 13–23, 2019.

[73] H. Komatsu and H. Nakajima, "Persistence In Chemical Reaction Networks With Arbitrary Time Delays ," *SIAM Journal on Applied Mathematics*, vol. 79, no. 1, p. 305–320, 2019.

[74] D. Angeli, P. De Leenheer, and E. D. Sontag, "A petri net approach to the study of persistence in chemical reaction networks," *Mathematical Biosciences*, vol. 210, no. 2, p. 598–618, 2007.

[75] ——, "Persistence results for chemical reaction networks with time-dependent kinetics and no global conservation laws," *SIAM Journal on Applied Mathematics*, vol. 71, no. 1, p. 128–146, 2011.

[76] H. Komatsu and H. Nakajima, "The Deficiency Zero Theorem and global asymptotic stability for a class of chemical reaction networks with arbitrary time delays," *Systems & Control Letters*, vol. 136, p. 104601, 2020.

[77] X. Zhang and C. Gao, "Persistence of Delayed Complex Balanced Chemical Reaction Networks," *IEEE Transactions on Automatic Control*, vol. 66, no. 4, p. 1658–1669, 2021.

[78] X. Zhang, C. Gao, and D. Dochain, "Capturing Persistence of High-Dimensional Delayed Complex Balanced Chemical Reaction Systems via Decomposition of Semilocking Sets," in *2023 62nd IEEE Conference on Decision and Control (CDC)*. IEEE, 2023.

[79] M. Feinberg, "The existence and uniqueness of steady states for a class of chemical reaction networks," *Archive for Rational Mechanics and Analysis*, vol. 132, no. 4, p. 311–370, 1995.

[80] S. Müller, "A new decomposition of the graph Laplacian and the binomial structure of mass-action systems," *Journal of Nonlinear Science*, vol. 33, no. 5, p. 91, 2023.

[81] J. Stoer and C. Witzgall, *Convexity and Optimization in Finite Dimensions I*. Springer Berlin Heidelberg, 1970.

[82] A. N. Gorban, "Universal Lyapunov functions for non-linear reaction networks," *Communications in Nonlinear Science and Numerical Simulation*, vol. 79, p. 104910, 2019.

[83] I. Györi, "Two approximation techniques for functional differential equations," *Computers & Mathematics with Applications*, vol. 16, no. 3, p. 195–214, 1988.

[84] I. Györi and J. Turi, "Uniform approximation of a nonlinear delay equation on infinite intervals," *Nonlinear Analysis: Theory, Methods & Applications*, vol. 17, no. 1, p. 21–29, 1991.

[85] G. Lipták, K. M. Hangos, and G. Szederkényi, "Approximation of delayed chemical reaction networks," *Reaction Kinetics, Mechanisms and Catalysis*, vol. 123, no. 2, p. 403–419, 2018.

[86] G. Szederkényi and K. M. Hangos, "Finding complex balanced and detailed balanced realizations of chemical reaction networks," *Journal of Mathematical Chemistry*, vol. 49, no. 6, p. 1163–1179, 2011.

[87] Q. Du, M. Gunzburger, R. B. Lehoucq, and K. Zhou, "A nonlocal vector calculus, nonlocal volume-constrained problems, and nonlocal balance laws," *Mathematical Models and Methods in Applied Sciences*, vol. 23, no. 3, pp. 493–540, 2013.

[88] M. Gunzburger and R. B. Lehoucq, "A nonlocal vector calculus with application to nonlocal boundary value problems," *Multiscale Model. Simul.*, vol. 8, no. 5, pp. 1581–1598, 2010.

[89] S. Kružkov, "First order quasilinear equations in several independent variables," *Mat. Sb.*, vol. 81, no. 2, pp. 228–255, 1970.

[90] M. G. Crandall and A. Majda, "Monotone Difference Approximations for Scalar Conservation Laws," *Mathematics of Computation*, vol. 34, no. 149, pp. 1–21, 1980.

[91] R. Sanders, "On Convergence of Monotone Finite Difference Schemes with Variable Spatial Differencing," *Mathematics of Computation*, vol. 40, no. 161, p. 91, 1983.

[92] E. Conway and J. Smoller, "Global solutions of the cauchy problem for quasi-linear first-order eqautions in several space variables," *communication on Pure and Applied Mathematics*, vol. 19, pp. 95–105, 1966.

[93] A. Douglis, "On calculating weak solutions of quasi-linear, first-order partial differential equations," *Contributions to Differential Equations*, vol. 1, pp. 59–94, 1963.

[94] M. G. Crandall and T. M. Liggett, "Generation of Semi-Groups of Nonlinear Transformations on General Banach Spaces," *American Journal of Mathematics*, vol. 93, no. 2, pp. 265–298, 1971.

[95] M. G. Crandall, "The semigroup approach to first order quasilinear equations in several space variables," *Israel Journal of Mathematics*, vol. 12, no. 2, pp. 108–132, 1972.

[96] I. Miyadera, *Nonlinear Semigroups.* Providence, R.I.: American Mathematical Society, 1992.

[97] D. Bothe, "Nonlinear evolutions with Carathéodory forcing," *Journal of Evolution Equations*, vol. 3, no. 3, pp. 375–394, 2003.

[98] R. H. Nochetto and G. Savaré, "Nonlinear governed by accretive operators in banach spaces: Error control and applications," *Mathematical Models and Methods in Applied Sciences*, vol. 16, no. 03, pp. 439–477, 2006.

[99] L. C. Evans, *Partial Differential Equations.* Providence, R.I.: American Mathematical Society, 2010.

[100] Y. Kobayashi and K. Kobayasi, "On Perturbation of Non-Linear Equations in Banach Spaces," *Publications of the Research Institute for Mathematical Sciences*, vol. 12, no. 3, pp. 709–725, 1977.

[101] P.-L. Lions, *Generalized solutions of Hamilton-Jacobi equations.* London: Pitman, 1982.

[102] M. G. Crandall and P.-L. Lions, "Viscosity Solutions of Hamilton-Jacobi Equations," *Transactions of the American Mathematical Society*, vol. 277, no. 1, p. 1, 1983.

[103] D. Bothe, "Nonlinear evolutions in banach spaces – existence and qualitative theory with applications to reaction-diffusion-systems," habilitation, Paderborn University, 1999.

[104] M. G. Crandall and P. Benilan, "Regularizing effects of homogeneous evolution equations," WISCONSIN UNIV-MADISON MATHEMATICS RESEARCH CENTER, Tech. Rep., 1980.

[105] U. S. Fjordholm and A. M. Ruf, "Second-Order Accurate TVD Numerical Methods for Nonlocal Nonlinear Conservation Laws," *SIAM Journal on Numerical Analysis*, vol. 59, no. 3, pp. 1920–1945, 2021.

[106] H. Brezis, *Functional Analysis, Sobolev Spaces and Partial Differential Equations.* New York: Springer-Verlag, 2010.

[107] A.-P. Calderón, "Lebesgue spaces of differentiable functions and distributions," in *Proc. Sympos. Pure Math.* Providence, R.I.: American Mathematical Society, 1961, vol. IV, pp. 33–49.

[108] K. Deimling, *Nonlinear Functional Analysis.* Berlin Heidelberg: Springer-Verlag, 1985.

[109] C. T. MacDonald, J. H. Gibbs, and A. C. Pipkin, "Kinetics of biopolymerization on nucleic acid templates," *Biopolymers*, vol. 6, no. 1, pp. 1–25, 1968.

[110] R. Heinrich and T. A. Rapoport, "Mathematical modelling of translation of mRNA in eucaryotes; steady states, time-dependent processes and application to reticulocytest," *Journal of Theoretical Biology*, vol. 86, no. 2, pp. 279–313, 1980.

[111] T. von der Haar, "Mathematical and computational modelling of ribosomal movement and protein synthesis: an overview," *Computational and Structural Biotechnology Journal*, vol. 1, no. 1, p. e201204002, 2012.

[112] S. Reuveni, I. Meilijson, M. Kupiec, E. Ruppin, and T. Tuller, "Genome-Scale Analysis of Translation Elongation with a Ribosome Flow Model," *PLoS Computational Biology*, vol. 7, no. 9, p. e1002127, 2011.

[113] L. B. Shaw, R. K. P. Zia, and K. H. Lee, "Totally asymmetric exclusion process with extended objects: A model for protein synthesis," *Physical Review E*, vol. 68, no. 2, 2003.

[114] M. Margaliot and T. Tuller, "Ribosome flow model with positive feedback," *Journal of The Royal Society Interface*, vol. 10, no. 85, p. 20130267, 2013.

[115] A. Raveh, M. Margaliot, E. D. Sontag, and T. Tuller, "A model for competition for ribosomes in the cell," *Journal of The Royal Society Interface*, vol. 13, no. 116, p. 20151062, 2016.

[116] E. Bar-Shalom, A. Ovseevich, and M. Margaliot, "Ribosome flow model with different site sizes," *SIAM Journal on Applied Dynamical Systems*, vol. 19, no. 1, pp. 541–576, 2020.

[117] A. Jain, M. Margaliot, and A. K. Gupta, "Large-scale mRNA translation and the intricate effects of competition for the finite pool of ribosomes," *Journal of The Royal Society Interface*, vol. 19, no. 188, 2022.

[118] M. Pereira, B. Kulcsár, G. Lipták, M. Kovács, and G. Szederkényi, "The traffic reaction model: A kinetic compartmental approach to road traffic modeling," *Transportation Research Part C: Emerging Technologies*, vol. 158, p. 104435, 2024.

[119] R. J. LeVeque, *Finite Volume Methods for Hyperbolic Problems*. Cambridge: Cambridge University Press, 2002.

[120] R. Eymard, T. Gallouët, and R. l. Herbin, *Finite Volume Methods*. Elsevier, 2000.

[121] S. Godunov, "Finite difference method for numerical computation of discontinuous solutions of the equations of fluid dynamics," *Matematicheskii Sbornik*, vol. 47(89), no. 3, pp. 271–306, 1959.

[122] I. Neri, N. Kern, and A. Parmeggiani, "Totally asymmetric simple exclusion process on networks," *Physical Review Letters*, vol. 107, no. 6, 2011.

[123] S. Muhuri, "Scale-invariant density profiles of a dynamically extending TASEP," *EPL (Europhysics Letters)*, vol. 101, no. 3, p. 38001, 2013.

[124] I. Neri, N. Kern, and A. Parmeggiani, "Exclusion processes on networks as models for cytoskeletal transport," *New Journal of Physics*, vol. 15, no. 8, p. 085005, 2013.

[125] A. K. Gupta, "Collective dynamics on a two-lane asymmetrically coupled TASEP with mutually interactive langmuir kinetics," *Journal of Statistical Physics*, vol. 162, no. 6, pp. 1571–1586, 2016.

[126] D. Botto, A. Pelizzola, M. Pretti, and M. Zamparo, "Unbalanced langmuir kinetics affects TASEP dynamical transitions: mean-field theory," *Journal of Physics A: Mathematical and Theoretical*, vol. 53, no. 34, p. 345001, 2020.

[127] M. J. Lighthill and G. B. Whitham, "On Kinematic Waves . II . A Theory of Traffic Flow on Long Crowded Roads," *Proceedings of the Royal Society of London A: Mathematical and Physical Sciences*, vol. 229, no. 1178, pp. 317–345, 1955.

[128] P. I. Richards, "Shock Waves on the Highway," *Operations Research*, vol. 4, no. 1, pp. 42–51, 1956.

[129] G. Szederkényi, B. Ács, G. Lipták, and **M. A. Vághy**, "Persistence and stability of a class of kinetic compartmental models," *Journal of Mathematical Chemistry*, vol. 60, no. 4, pp. 1001–1020, 2022.

[130] J. Mierczyński, "Cooperative irreducible systems of ordinary differential equations with first integral," in *Proceedings of the Second Marrakesh International Conference on Differential Equations*, 1995.

[131] M. Vidyasagar, *Nonlinear Systems Analysis*. Prentice Hall, 1978.

[132] G. Russo, M. di Bernardo, and E. D. Sontag, "Global entrainment of transcriptional systems to periodic inputs," *PLoS Computational Biology*, vol. 6, no. 4, 2010.

[133] M. Margaliot, E. D. Sontag, and T. Tuller, "Entrainment to periodic initiation and transition rates in a computational model for gene translation," *PLoS ONE*, vol. 9, no. 5, p. e96039, 2014.

[134] B. Tang, Y. Kuang, and H. Smith, "Strictly nonautonomous cooperative system with a first integral," *SIAM Journal on Mathematical Analysis*, vol. 24, no. 5, pp. 1331–1339, 1993.

[135] J. Ji-Fa, "Periodic monotone systems with an invariant function," *SIAM Journal on Mathematical Analysis*, vol. 27, no. 6, pp. 1738–1744, 1996.

[136] Y. Zarai, M. Margaliot, E. D. Sontag, and T. Tuller, "Controllability analysis and control synthesis for the ribosome flow model," *IEEE/ACM Transactions on Computational Biology and Bioinformatics*, vol. 15, no. 4, pp. 1351–1364, Jul. 2018.

[137] E. D. Sontag, "Smooth stabilization implies coprime factorization," *IEEE Transactions on Automatic Control*, vol. 34, no. 4, pp. 435–443, 1989.

[138] A. N. Gorban, "Universal Lyapunov functions for non-linear reaction networks," *Communications in Nonlinear Science and Numerical Simulation*, vol. 79, 2019.

[139] D. J. C. MacKay, *Information Theory, Inference and Learning Algorithms.* Cambridge University Press, 2003.

[140] P. Smolen, D. A. Baxter, and J. H. Byrne, "Mathematical modeling of gene networks," *Neuron*, vol. 26, no. 3, pp. 567–580, 2000.

[141] A. Ay and D. N. Arnosti, "Mathematical modeling of gene expression: a guide for the perplexed biologist," *Critical reviews in biochemistry and molecular biology*, vol. 46, no. 2, pp. 137–151, 2011.

[142] I. S. Peter and E. H. Davidson, *Genomic control process: development and evolution.* Academic Press, 2015.

[143] H. De Jong, "Modeling and simulation of genetic regulatory systems: a literature review," *Journal of computational biology*, vol. 9, no. 1, pp. 67–103, 2002.

[144] G. Karlebach and R. Shamir, "Modelling and analysis of gene regulatory networks," *Nature Reviews Molecular Cell Biology*, vol. 9, no. 10, pp. 770–780, sep 2008.

[145] R. Barbuti, R. Gori, P. Milazzo, and L. Nasti, "A survey of gene regulatory networks modelling methods: from differential equations, to boolean and qualitative bioinspired models," *J Membr Comput*, vol. 2, no. 3, pp. 207–226, Oct. 2020.

[146] O. G. Berg, "A model for the statistical fluctuations of protein numbers in a microbial population," *Journal of Theoretical Biology*, vol. 71, no. 4, pp. 587–603, apr 1978.

[147] M. Kaern, T. C. Elston, W. J. Blake, and J. J. Collins, "Stochasticity in gene expression: from theories to phenotypes," *Nature Reviews Genetics*, vol. 6, no. 6, pp. 451–464, 2005.

[148] R. D. Dar, B. S. Razooky, L. S. Weinberger, C. D. Cox, and M. L. Simpson, "The low noise limit in gene expression," *PLoS ONE*, vol. 10, no. 10, p. e0140969, 2015.

[149] L. T. MacNeil and A. J. Walhout, "Gene regulatory networks and the role of robustness and stochasticity in the control of gene expression," *Genome Research*, vol. 21, no. 5, pp. 645–657, 2011.

[150] N. Friedman, L. Cai, and X. S. Xie, "Linking stochastic dynamics to population distribution: An analytical framework of gene expression," *Physical Review Letters*, vol. 97, no. 16, oct 2006.

[151] V. Elgart, T. Jia, A. T. Fenley, and R. Kulkarni, "Connecting protein and mRNA burst distributions for stochastic models of gene expression," *Physical Biology*, vol. 8, no. 4, p. 046001, apr 2011.

[152] R. D. Dar, B. S. Razooky, A. Singh, T. V. Trimeloni, J. M. McCollum, C. D. Cox, M. L. Simpson, and L. S. Weinberger, "Transcriptional burst frequency and burst size are equally modulated across the human genome," *Proceedings of the National Academy of Sciences*, vol. 109, no. 43, pp. 17 454–17 459, oct 2012.

[153] M. Pájaro, A. A. Alonso, and C. V. zquez, "Shaping protein distributions in stochastic self-regulated gene expression networks," *Physical Review E*, vol. 92, no. 3, sep 2015.

[154] M. Pájaro, A. A. Alonso, I. Otero-Muras, and C. Vázquez, "Stochastic modeling and numerical simulation of gene regulatory networks with protein bursting," *Journal of Theoretical Biology*, vol. 421, pp. 51–70, may 2017.

[155] M. Pájaro, I. Otero-Muras, C. V. zquez, and A. A. Alonso, "SELANSI: a toolbox for simulation of stochastic gene regulatory networks," *Bioinformatics*, vol. 34, no. 5, pp. 893–895, 2017.

[156] C. Sequeiros, C. Vázquez, J. R. Banga, and I. Otero-Muras, "Automated design of synthetic biocircuits in the stochastic regime," *IFAC-PapersOnLine*, vol. 55, no. 20, pp. 630–634, 2022.

[157] C. Sequeiros, I. Otero-Muras, C. Vazquez, and J. R. Banga, "Global optimization approach for parameter estimation in stochastic dynamic models of biosystems," *IEEE/ACM Transactions on Computational Biology and Bioinformatics*, pp. 1–12, 2022.

[158] P. Bokes and A. Singh, "Controlling noisy expression through auto regulation of burst frequency and protein stability," in *Hybrid Systems Biology*, M. Češka and N. Paoletti, Eds. Cham: Springer International Publishing, 2019, pp. 80–97.

[159] C. Fernández, H. Faquir, M. P. jaro, and I. Otero-Muras, "Feedback control of stochastic gene switches using PIDE models," *IFAC-PapersOnLine*, vol. 55, no. 18, pp. 62–67, 2022.

[160] M. Pájaro, I. Otero-Muras, C. Vázquez, and A. A. Alonso, "Transient hysteresis and inherent stochasticity in gene regulatory networks," *Nature Communications*, vol. 10, no. 1, Oct. 2019.

[161] J. A. Cañizo, J. A. Carrillo, and M. Pájaro, "Exponential equilibration of genetic circuits using entropy methods," *Journal of Mathematical Biology*, vol. 78, pp. 373–411, 1 2019.

[162] M. Feinberg, *Foundations of chemical reaction network theory.* Springer, 2019.

[163] H. Maeda, S. Kodama, and Y. Ohta, "Asymptotic behavior of nonlinear compartmental systems: Nonoscillation and stability," *IEEE Transactions on Circuits and Systems*, vol. 25, no. 6, pp. 372–378, Jun. 1978.

[164] D. F. Anderson, "A proof of the global attractor conjecture in the single linkage class case," *SIAM Journal on Applied Mathematics*, vol. 71, no. 4, pp. 1487–1508, 2011.

[165] H. Maeda and S. Kodama, "Some results on nonlinear compartmental systems," *IEEE Transactions on Circuits and Systems*, vol. 26, no. 3, pp. 203–204, 1979.

[166] D. M. Foster and J. A. Jacquez, "Multiple zeros for eigenvalues and the multiplicity of traps of a linear compartmental system," *Mathematical Biosciences*, vol. 26, no. 1–2, pp. 89–97, 1975.

[167] G. M. Süel, R. P. Kulkarni, J. Dworkin, J. Garcia-Ojalvo, and M. B. Elowitz, "Tunability and noise dependence in differentiation dynamics," *Science*, vol. 315, no. 5819, pp. 1716–1719, Mar. 2007.

[168] G. M. Süel, J. Garcia-Ojalvo, L. M. Liberman, and M. B. Elowitz, "An excitable gene regulatory circuit induces transient cellular differentiation," *Nature*, vol. 440, no. 7083, pp. 545–550, Mar. 2006.

[169] S. H. Dandach and M. Khammash, "Analysis of stochastic strategies in bacterial competence: A master equation approach," *PLoS Computational Biology*, vol. 6, no. 11, p. e1000985, Nov. 2010.

[170] P. Hartman, *Ordinary Differential Equations*. Society for Industrial and Applied Mathematics, 2002.

[171] C. Briat, A. Gupta, and M. Khammash, "Antithetic Integral Feedback Ensures Robust Perfect Adaptation in Noisy Biomolecular Networks," *Cell Systems*, vol. 2, no. 1, pp. 14–26, 2016.

[172] J.-B. Lugagne, S. S. Carrillo, M. Kirch, A. Köhler, G. Batt, and P. Hersen, "Balancing a genetic toggle switch by real-time feedback control and periodic forcing," *Nature Communications*, vol. 8, no. 1, 2017.

[173] M. Arioli and M. Benzi, "A finite element method for quantum graphs," *IMA Journal of Numerical Analysis*, vol. 38, no. 3, p. 1119–1163, 2018.

[174] H. A. Schwarz, *Gesammelte Mathematische Abhandlungen*. Berlin: Springer Berlin Heidelberg, 1870, vol. 2, first published in *Vierteljahrsschrift der Naturforschenden Gesellschaft* in Zürich, 1870.

[175] I. Babuska, "Über Schwarzsche algorithmen in partielle differentialgleichungen der mathematischen physik," *ZAMM*, vol. 37, no. 7/8, pp. 243–245, 1957.

[176] D. Morgenstern, "Begründung des alternierenden verfahrens durch otrhogonalprojektion," *ZAMM*, vol. 36, pp. 7–8, 1956.

[177] S. L. Sobolev, "L'algorithme de Schwarz dans la théorie de l'elasticité," *Comptes rendus doklady de l'académie des sciences de l'URSS*, vol. 4, no. 13, pp. 243–246, 1936.

[178] M. Dryja and O. Widlund, *An additive variant of the Schwarz alternating method for the case of many subregions*, ser. Technical Report 339, Ultracomputer Note 131. New York: Department of Computer Science, Courant Institute, 1987.

[179] P.-L. Lions, "On the Schwarz alternating method. I," in *First international symposium on domain decomposition methods for partial differential equations.* SIAM, 1988.

[180] ——, "On the Schwarz alternating method. II," in *Second international symposium on domain decomposition methods for partial differential equations.* SIAM, 1989.

[181] C. Farhat and F. Roux, "A method of finite element tearing and interconnecting and its parallel solution algorithm," *International Journal for Numerical Methods in Engineering*, vol. 32, no. 6, p. 1205–1227, 1991.

[182] A. Klawonn and O. Widlund, "FETI and Neumann-Neumann iterative substructuring methods: Connections and new results," *Communications on Pure and Applied Mathematics*, vol. 54, no. 1, p. 57–90, 2001.

[183] M. D. Gunzburger, M. Heinkenschloss, and H. Kwon Lee, "Solution of elliptic partial differential equations by an optimization-based domain decomposition method," *Applied Mathematics and Computation*, vol. 113, no. 2–3, p. 111–139, 2000.

[184] J. L. Lions, *Some methods in the mathematical analysis of systems and their control.* Beijing: Science Press, 1981.

[185] R. E. Bank, T. F. Dupont, and H. Yserentant, "The hierarchical basis multigrid method," *Numerische Mathematik*, vol. 52, no. 4, p. 427–458, 1988.

[186] A. Brandt, "Multilevel adaptive solutions to boundary-value problems," *Mathematics of Computation*, vol. 31, no. 138, p. 333–390, 1977.

[187] W. L. Briggs, V. E. Henson, and S. F. McCormick, *A Multigrid Tutorial, Second Edition*, 2nd ed. Philadelphia: SIAM, 2000.

[188] J.-F. Bourgat, R. Glowinski, P. Tallec, and M. Vidrascu, "Variational formulation and algorithm for trace operator in domain decomposition calculations," in *Second international symposium on domain decomposition methods for partial differential equations.* SIAM, 1989.

[189] ——, "Analysis and test of a local domain decomposition preconditioner," in *Fourth international symposium on domain decomposition methods for partial differential equations*. SIAM, 1991.

[190] Q. Dihn, R. Glowinski, and J. Périaux, *Solving elliptic problems by domain decomposition methods with applications*. Cambridge: Academic Press, 1984, p. 395–426.

[191] P. Tallec, Y. Roeck, and M. Vidrascu, "Domain decomposition methods for large linearly elliptic three-dimensional problems," *Journal of Computational and Applied Mathematics*, vol. 34, no. 1, p. 93–117, February 1991.

[192] T. F. Chan and T. P. Mathew, "Domain decomposition algorithms," *Acta Numerica*, vol. 3, p. 61–143, 1994.

[193] J. Xu, "Iterative Methods by Space Decomposition and Subspace Correction," *SIAM Review*, vol. 34, no. 4, p. 581–613, 1992.

[194] S. C. Brenner and L. R. Scott, *The Mathematical Theory of Finite Element Methods*. New York: Springer, 2007.

[195] T. P. A. Mathew, *Domain Decomposition Methods for the Numerical Solution of Partial Differential Equations*. Berlin: Springer Berlin Heidelberg, 2008.

[196] B. Smith, P. E. Bjorstad, and W. Gropp, *Domain decomposition*. Cambridge: Cambridge University Press, 1996.

[197] A. Toselli and O. B. Widlund, *Domain Decomposition Methods - Algorithms and Theory*. Berlin: Springer Berlin Heidelberg, 2005.

[198] G. Leugering, "Dynamic domain decomposition of optimal control problems for networks of Euler-Bernoulli beams," *ESAIM: Proceedings*, vol. 4, p. 223–233, 1998.

[199] ——, "Domain decomposition of optimal control problems for dynamic networks of elastic strings," *Computational Optimization and Applications*, vol. 16, no. 1, p. 5–27, 2000.

[200] ——, "Domain Decomposition of an Optimal Control Problem for Semi-Linear Elliptic Equations on Metric Graphs with Application to Gas Networks," *Applied Mathematics*, vol. 8, no. 8, p. 1074–1099, 2017.

[201] ——, *Nonoverlapping domain decomposition and virtual controls for optimal control problems of p-type on metric graphs*. Amsterdam: Elsevier, 2023, p. 217–260.

[202] J. E. Lagnese and G. Leugering, *Domain Decomposition Methods in Optimal Control of Partial Differential Equations*. Basel: Birkhäuser Basel, 2004.

[203] D. Bolin, M. Kovács, V. Kumar, and A. Simas, "Regularity and numerical approximation of fractional elliptic differential equations on compact metric graphs," *Mathematics of Computation*, vol. 93, pp. 2439–2472, 2023.

[204] D. Mugnolo and S. Romanelli, "Dynamic and generalized Wentzell node conditions for network equations," *Mathematical Methods in the Applied Sciences*, vol. 30, no. 6, p. 681–706, November 2006.

[205] D. Mugnolo, "Gaussian estimates for a heat equation on a network," *Networks and Heterogeneous Media*, vol. 2, no. 1, p. 55–79, 2007.

[206] M. Dryja and O. B. Widlund, "Schwarz methods of Neumann-Neumann type for three-dimensional elliptic finite element problems," *Communications on Pure and Applied Mathematics*, vol. 48, no. 2, p. 121–155, 1995.

[207] A. Weller, "Numerical Methods for Parabolic Partial Differential Equations on Metric Graphs," Ph.D. dissertation, Universität zu Köln, 2024.

[208] J. M. Tang and Y. Saad, "A probing method for computing the diagonal of a matrix inverse," *Numerical Linear Algebra with Applications*, vol. 19, no. 3, p. 485–501, 2011.

[209] E. Hallman, I. C. F. Ipsen, and A. K. Saibaba, "Monte Carlo Methods for Estimating the Diagonal of a Real Symmetric Matrix," *SIAM Journal on Matrix Analysis and Applications*, vol. 44, no. 1, p. 240–269, 2023.

[210] D. Mugnolo, *Semigroup Methods for Evolution Equations on Networks*. Cham: Springer International Publishing, 2014.

[211] G. Greiner, "Perturbing the boundary-conditions of a generator," *Houston Journal of Mathematics*, vol. 13, no. 2, pp. 213–229, 1987.

[212] S. N. Dorogovtsev, A. V. Goltsev, and J. F. F. Mendes, "Pseudofractal scale-free web," *Physical Review E*, vol. 65, no. 6, June 2002.

[213] A.-L. Barabási and R. Albert, "Emergence of Scaling in Random Networks," *Science*, vol. 286, no. 5439, pp. 509–512, October 1999.

The author's publications

[214] **M. A. Vághy**, G. Szlobodnyik, and G. Szederkényi, "Kinetic realization of delayed polynomial dynamical models," *IFAC-PapersOnLine*, vol. 52, pp. 45–50, 2019.

[215] **M. A. Vághy** and G. Szederkényi, "Realization of linearly conjugate and uncertain kinetic systems with time delay," *MATCH Commun. Math. Comput. Chem*, vol. 85, pp. 635–668, 2021.

[216] **M. A. Vághy**, M. Kovács, and G. bor Szederkényi, "Kinetic discretization of one-dimensional nonlocal flow models," *IFAC-PapersOnLine*, vol. 55, no. 20, pp. 67–72, 2022.

[217] G. Szederkényi, B. Ács, G. Lipták, and **M. A. Vághy**, "Persistence and stability of a class of kinetic compartmental models," *Journal of Mathematical Chemistry*, vol. 60, no. 4, pp. 1001–1020, 2022.

[218] **M. A. Vághy** and G. Szederkényi, "Hamiltonian representation of generalized ribosome flow models," in *European Control Conference - ECC*, 2022.

[219] ——, "Lyapunov stability of generalized ribosome flows," *IFAC-PapersOnLine*, vol. 55, pp. 56–61, 2022, presented at TFMST 2022.

[220] ——, "Persistence and stability of generalized ribosome flow models with time-varying transition rates," *PLoS ONE*, vol. 18, no. 7, 2023.

[221] **M. A. Vághy** and M. Kovács, "Nonlinear semigroups for nonlocal conservation laws," *Partial Differential Equations and Applications*, vol. 4, no. 32, 2023.

[222] **M. A. Vághy**, I. Otero-Muras, M. Pájaro, and G. Szederkényi, "A Kinetic Finite Volume Discretization of the Multidimensional PIDE Model for Gene Regulatory Networks," *Bulletin of Mathematical Biology*, vol. 86, no. 2, 2024.

[223] G. Szederkényi, D. Kocsis, **M. A. Vághy**, D. Czárán, P. Sasvári, M. Lengyel, M. B. Naszlady, F. Kreis, I. Antal, R. Csépányi-Kömi, and F. Erdő, "Mathematical modeling of transdermal delivery of topical drug formulations in a dynamic microfluidic diffusion chamber in health and disease," *PLoS ONE*, vol. 19, no. 4, p. e0299501, 2024.

[224] **M. A. Vághy** and M. Kovács, "Neumann-Neumann type domain decomposition of elliptic problems on metric graphs," *BIT Numerical Mathematics*, vol. 65, no. 2, 2025.

[225] **M. A. Vághy**, I. Otero-Muras, and G. Szederkényi, "Analysis and control of gene regulation network models using kinetic semi-discretization," in *European Control Conference - ECC*, 2024.

[226] **M. A. Vághy** and G. Szederkényi, "Asymptotic stability of delayed complex balanced reaction networks with non-mass action kinetics," *Journal of Nonlinear Science*, vol. 35, no. 1, p. 20, 2025.

[227] C. L. Laczkó, **M. A. Vághy**, and M. Kovács, "A transferable PINN-based method for quantum graphs with unseen structure," *IFAC-PapersOnLine*, vol. 59, no. 1, p. 67–72, 2025.

[228] C. Fernández, H. Faquir, **M. A. Vághy**, M. Pájaro, G. Szederkényi, and I. Otero-Muras, "PIDE models for efficient control of stochastic gene regulatory circuits," *IFAC-PapersOnLine*, 2025, to appear.

[229] G. Molnár, **M. A. Vághy**, and G. Szederkényi, "Stability of biochemical reaction networks with general kinetics and distributed time delays," *Journal of Mathematical Chemistry*, 2025.